UNIVERSIDADE DE SÃO PAULO
FACULDADE DE CIÊNCIAS FARMACÊUTICAS DE RIBEIRÃO PRETO

Development of a comprehensive study on base-controlled regioselective functionalization and Iridium-catalysed borylation of indolizines

Camila Rodrigues de Souza Bertallo

Ribeirão Preto, Brazil
2020

UNIVERSIDADE DE SÃO PAULO

FACULDADE DE CIÊNCIAS FARMACÊUTICAS DE RIBEIRÃO PRETO

Camila Rodrigues de Souza Bertallo

Development of a comprehensive study on base-controlled regioselective functionalization and Iridium-catalysed borylation of indolizines.

Desenvolvimento de um estudo abrangente sobre a funcionalização regiosseletiva base-dependente e reações de borilações catalisadas pelo irídio em indolizinas.

Doctoral thesis presented to the Graduate Program of School of Pharmaceutical Sciences of Ribeirão Preto/USP for the degree of Doctor in Sciences.

Concentration Area: Natural and Synthetic Products

PhD student: Camila Rodrigues de Souza Bertallo

Supervisor: Prof. Dr. Giuliano Cesar Clososki

Co-supervisor: Dr. Patrick G. Steel

Ribeirão Preto, Brazil
2020

APPROVAL PAGE

Camila Rodrigues de Souza Bertallo

Development of a comprehensive study on base-controlled regioselective functionalization and Iridium-Catalysed Borylation of indolizines

> Doctoral thesis presented to the Graduate Program of School of Pharmaceutical Sciences of Ribeirão Preto/USP for the degree of Doctor in Sciences.
>
> Concentration Area: Natural and Synthetic products
>
> **Supervisor:** Prof. Dr. Giuliano Cesar Clososki
>
> **Co-supervisor:** Dr. Patrick G. Steel

Approved on:

Examiners

Prof. Dr. _____

Institution: _____ Signature:_____

Prof. Dr. _____

Institution: _____ Signature:_____

Prof. Dr. _____

Institution: _____ Signature:_____

Aos meus pais amados Jane e Ademir e minhas irmãs Pâmela e Isabelle pelo amor, apoio e incentivo para que eu crescesse e lutasse pelos meus sonhos. Obrigada, por todos os sacrifícios que vocês fizeram ao longo de suas vidas para que eu pudesse voar e atingir os meus sonhos. Sem a dedicação e o suporte de vocês eu com certeza jamais teria alcançado essa conquista.

Acknowledgments

Primeiramente eu gostaria de agradecer a Deus por iluminar o meu caminho, estar sempre ao meu lado e me permitir realizar os meus sonhos.

Muito obrigada Giuliano pela orientação, amizade e empenho em me fazer crescer academicamente e por me desafiar a sempre dar o meu melhor durante esses anos de trabalho. Jamais me esquecerei de seus ensinamentos e tenha certeza de que todo sucesso que eu alcançar durante a minha jornada será devido a sólida base profissional que você me proporcionou.

I would like to thank you Patrick for all support during my time in England and for convince me that I was capable of develop this work. Thank you for the opportunity of work in such a great research group and for inspire me to overcome my personal and scientific limitations and for motivated me to continue my journey in this field.

Gostaria de agradecer ao meu marido Marcus Vinicius por toda paciência, suporte e disposição em embarcar em todas as minhas loucuras (que não são poucas). Obrigada por partilhar minhas alegrias e sofrimentos e nunca me deixar desistir dos meus objetivos. Eu te amo

Maria Luiza, obrigada por ser minha melhor amiga e sempre me apoiar nunca vou me esquecer dessa frase: "Camila, o mar não está para peixe pequeno, vai estudar". Te amo, obrigada por me ouvir, me inspirar e nunca me deixar desistir.

Graziella, minha primeira orientadora, obrigada por acreditar em mim e me apresentar esse fascinante mundo da síntese orgânica. Obrigada, pela amizade e por todos os ensinamentos.
Mônica, muito obrigada por tudo que você me ensinou durante minha iniciação cientifica, por acreditar em mim e me fazer ser uma profissional melhor.
Aos meus colegas de laboratório Thais, Valter, Vitor, Rodolfo, Franco, Leandro, Carol, muito obrigada pela amizade, por me ajudarem a ser uma profissional melhor e fazerem os meus dias mais leves.

Thais Arroio, foi um prazer poder de alguma forma contribuir com o seu crescimento científico e saiba que ao te ensinar eu também aprendi muito.

Gostaria de agradecer a Faculdade de Ciências Farmacêuticas de Ribeirão Preto-USP e ao Programa de Pós-graduação em Ciências Farmacêuticas pela infraestrutura e apoio durante todo o desenvolvimento desse trabalho.

" A mind that opens to a new idea never returns to its original size "

Albert Einstein

Resumo

Bertallo, C. R. S. **Desenvolvimento de um estudo abrangente sobre a funcionalização regiosseletiva base-dependente e reações de borilações catalisadas pelo irídio em indolizinas. 2020, 228f.** Doutorado. Faculdade de Ciências Farmacêuticas de Ribeirão Preto – Universidade de São Paulo, Ribeirão Preto, 2020.

Indolizina é um importante bioisótero do indol, sendo considerada uma estrutura privilegiada, com aplicações nas áreas farmacêutica, agroquímica e de ciências de materiais. Nesse contexto, o foco desta tese foi o desenvolvimento de novas metodologias para a preparação de derivados indolizínicos mais complexos, utilizando diferentes estratégias, como (a) metalação dirigida utilizando bases de lítio e bases mistas Mg complexadas com LiCl e (b) borilações C-H usando [Ir(OMe)(COD)]$_2$ como catalisador. Este trabalho permitiu o isolamento de 39 novos derivados funcionalizados nas posições C-2, C-3 ou C-5 em rendimentos de 48 a 95%, através de uma abordagem regiosseletiva controlada por base, utilizando amidetos de lítio e TMPMgCl·LiCl. Nos últimos anos, a borilação direta de arenos e heteroarenos vem se destacando como uma abordagem eficiente para a preparação de derivados funcionalizados que dificilmente poderiam ser preparados empregando métodos tradicionais. No entanto, embora muitos compostos heterocíclicos como indol, azaindóis, piridinas, pirróis e quinolinas tenham sido investigados, essa é a primeira vez que um estudo foi realizado para o núcleo indolizínico. Sete indolizinas inéditas puderam ser sintetizadas através deste protocolo.

Keywords: *N*-heterocíclicos, indolizinas, metalação, ativação C-H, C-H borilação, acoplamento cruzado de Negishi, acoplamento cruzado de Suzuki.

Abstract

Bertallo, C. R. S. **Development of a comprehensive study on base-controlled regioselective functionalization and Iridium-Catalysed Borylation of indolizines. 2020, 228f.** PhD Thesis. Faculdade de Ciências Farmacêuticas de Ribeirão Preto – Universidade de São Paulo, Ribeirão Preto, 2020.

Indolizines is an important bioisostere of indole being considered as privileged structure with application in pharmaceutical, agrochemical and material sciences field. In this context, the focus of this thesis was to develop new methodologies for the preparation of more complex indolizine scaffolds using different strategies such as (a) directed metalation using lithium bases and Mg bases complexed with LiCl and (b) C-H borylation using $[Ir(OMe)(COD)]_2$ as catalyst. This work allowed the isolation of 39 new indolizine derivatives functionalized at C-2, C-3 or C-5 position in 48-95% yields through a base-controlled regioselective approach using lithium amides and TMPMgCl·LiCl. Over the last years, the direct C-H borylation of arenes and heteroarenes has become an attractive method for the preparation of functionalized derivatives that could be hardly to prepare through the traditional methods. However, whilst many heterocycles such as indole, azaindoles, pyridines, pyrroles and quinolines have been investigated, to the best of our knowledge this is the first time that a study has been conducted for indolizine. Seven new modified indolizines could be synthetized using this protocol.

Keywords: *N*-heterocycles, indolizines, metalation, C-H activation, C-H borylation, Negishi cross-coupling, Suzuki cross-coupling.

Abbreviations and Symbols

Ac	Acetyl
Ar	Aryl
ATR	Attenuated total reflection
Bu	Butyl
(Bpin)$_2$bpy	4,4'-Bis(4,4,5,5-tetramethyl-1,3,2-dioxaborolan-2-yl)-2,2'-bipyridine
B$_2$pin$_2$	Bis(pinacolato)diboron
Bt	Benzotriazole
CIPE	Complex-Induced Proximity Effect
COD	1,5-Cyclooctadiene
conc.	Concentrated
COSY	Correlation spectroscopy
δ	Chemical shift
DCM	Dichloromethane
DFT	*Density Functional Theory*
DMA	*N,N*-dimethylacetamide
DMG	Directed metalation group
DMAP	4-Dimethylaminopyridine
DMF	*N,N*-dimethylformamide
DMSO	Dimethyl sulphoxide
D*o*M	Directed ortho Metalation
EI	Electron Ionisation
eq.	Equivalents
ES	Electrospray
Et	Ethyl
EtOAc	Ethyl acetate
EWG	Electron-withdrawing group
GCMS	Gas Chromatography–Mass Spectrometry
HMBC	Heteronuclear Multiple-bond Correlation Spectroscopy
HRMS	High-Resolution Mass Spectrometry
HSQC	Heteronuclear Single Quantum Coherence Spectroscopy
iPrMgCl·LiCl	Turbo Grignard
IR	Infrared

J	Coupling constant
LDA	Lithium diisopropylamide
Me	Methyl
mtbe	Methyl Tert-Butyl Ether
NOESY	Nuclear Overhauser Effect Spectroscopy
OTf	Triflate
Phen	1,10-Phenanthroline
PPh_3	Triphenylphosphine
ppm	Parts per million
Rt	Room Temperature/Ambient Temperature
SEAr	Electrophilic Aromatic Substitution
SNAr	Nucleophilic aromatic substitution
THF	Tetrahydrofuran
TLC	Thin Layer Chromatography
tmphen	3,4,7,8-Tetramethyl-1,10-phenanthroline
TMPH	2,2,6,6-tetramethypiperidine
$TMPMgCl \cdot LiCl$	Magnesium2,2,6,6-tetramethylpiperidide complexed with lithium chloride
$TMP_2Mg \cdot 2LiCl$	Magnesium bis(2,2,6,6-tetrametilpiperidide) complexed with lithium chloride
TMPLi	Lithium tetramethylpiperidide
TMS	Tetramethylsilane
TQD	Tandem Quadrupole Detector
UV	Ultraviolet

List of Figures

List of Tables

List of Schemes

Table of Contents

1. Introduction

1.1 Thesis Overview

This thesis is divided in two chapters and discusses new approaches for the regioselective functionalization of indolizines using (a) directed metalation reactions and (b) C-H activation/borylation reactions.

Chapter 1 provides a brief introduction to indolizine ring (synthesis and regioselectivity) and directed metalation strategy using lithium and mixed lithium/magnesium amides. The work presented in this chapter is focused on the development of a base-controlled regioselective approach to prepare a library of functionalized indolizines derivatives with different groups such as halogens, esters, carboxylic acids, amides, aryl, heteroaryl and formyl groups. Some of these derivatives displayed an interesting fluorescence property and consequently the photochemical and photophysical properties of these compounds were evaluated (Figure 1).
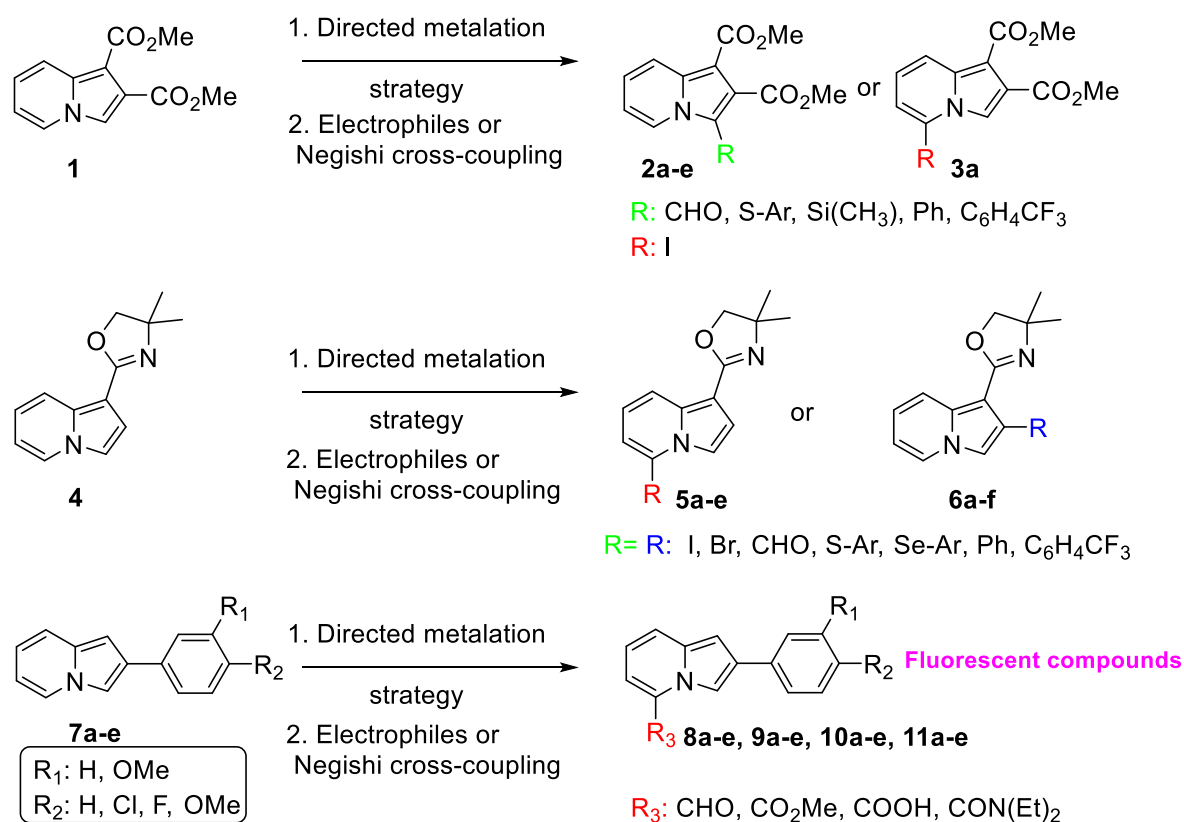
Figure 1. Directed metalation strategy to prepare functionalized indolizine derivatives.

Chapter 2 provides a brief introduction to C-H activation and C-H borylation of *N*-heterocycles. A comprehensive study was conducted focusing on the application of Ir-catalysed C-H activation/borylation of indolizines aiming the preparation of a small library of indolizines derivatives, which would be hardly to obtain by traditional methods (Figure 2).
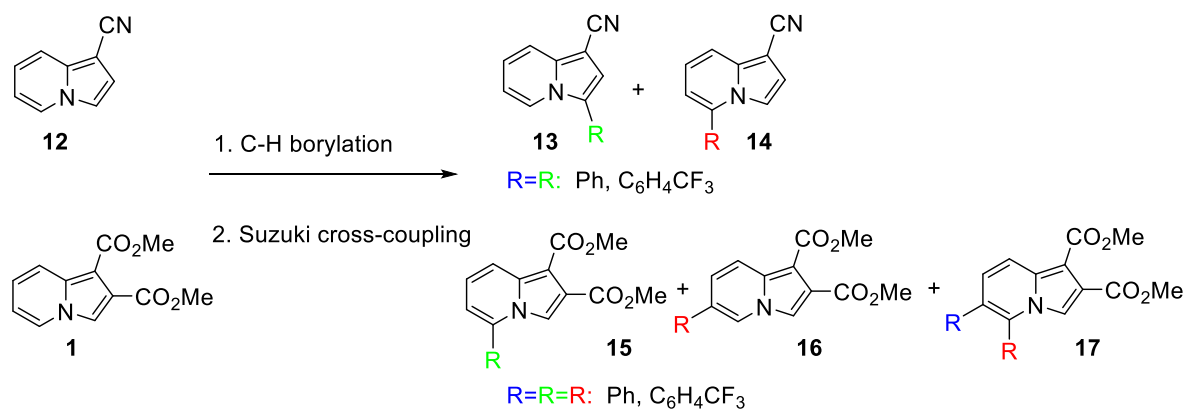
Figure 2. C-H borylation strategy to prepare functionalized indolizines derivatives.

1.2 *N*-heterocycles

N-heterocyclic compounds are the most abundant scaffolds found in nature and play an important role in the biochemical process that maintain life in different organisms. For example, they are important buildings blocks of vital vitamins, hormones, amino acids, DNA and RNA (Figure 3) (BALABAN; ONICIU; KATRITZKY, 2004; BARREIRO; FRAGA, 2001; VITAKU; SMITH; NJARDARSON, 2014).

L- tryptophan   *L*- histidine   *L*- proline   Vitamin B6
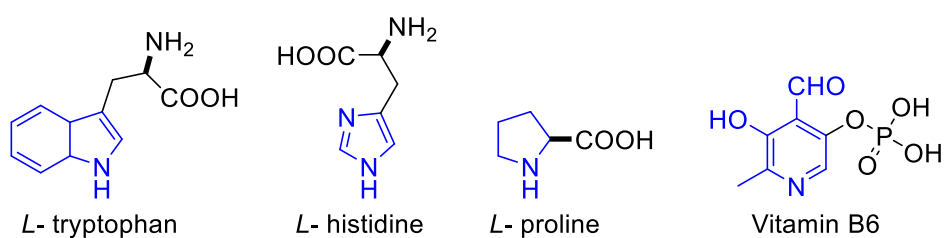
Figure 3. Examples of vital molecules that contain a *N*-heterocycle in their structures.

Their subunits can also be found in important pharmaceutical drugs such antibiotics, anticancer, antifungal, central nervous system depressant, antilipidemic, antihistaminic, proton pump inhibitor, antipsychotic and others (Figure 4) (SANDEEP et al., 2017).
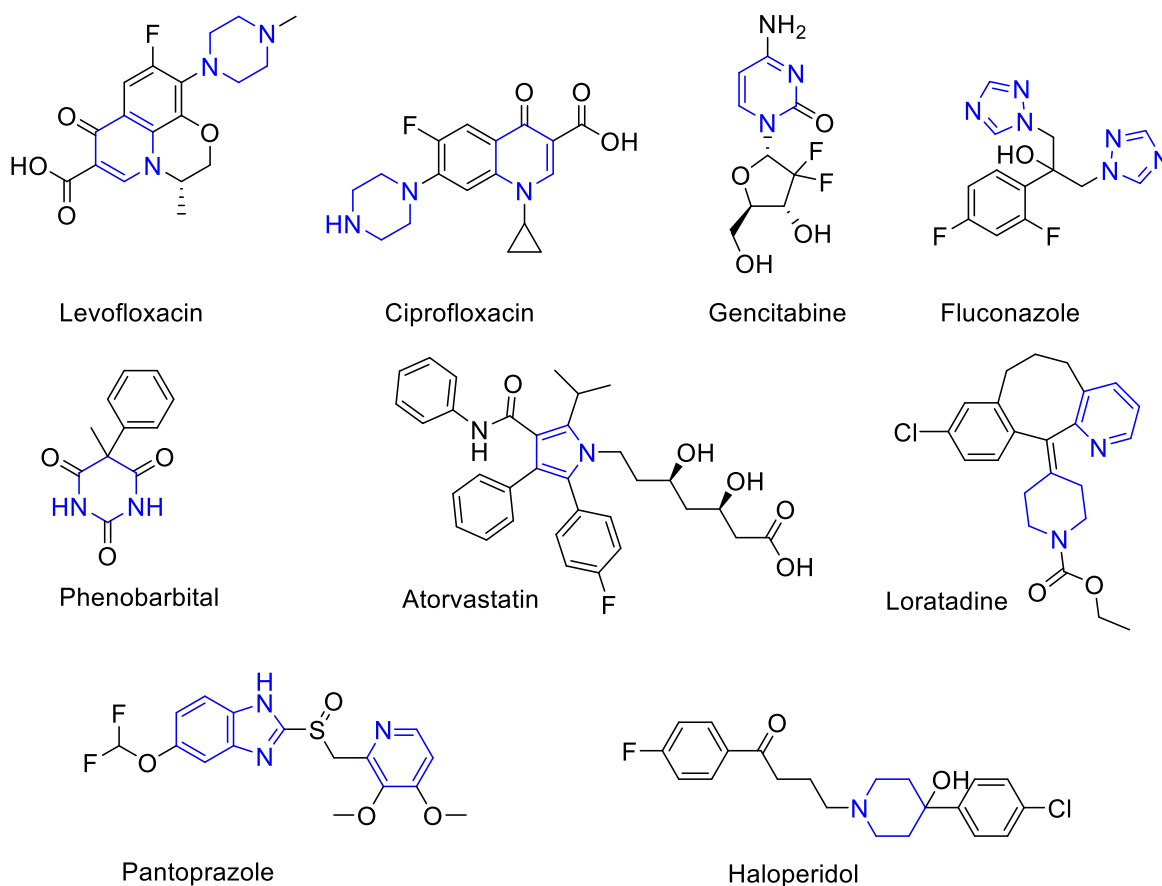
Figure 4. Pharmaceutical drugs containing N-heterocycles in their structures.

Another important class of molecules that contain *N*-heterocyclic core in their structures are alkaloids. Alkaloids such as those which contain an indole core are mainly found in plants *Apocynaceae* (genera *Alstonia*, *Aspidosperma*, *Rauvolfia* and *Catharanthus*), *Rubiaceae* (*Corynanthe*), *Loganiaceae* (*Strychnos*) and some fungi (*Psilocybe cubensis*, *Ergot* and *Bufo alvarius*)(HESSE, 2002) . The biological activity of many of these compounds has been well understood for centuries.

For example, reserpine, an alkaloid first isolated from *Rauvolfia serpentine* it was largely used as medicine to treat snake bites and insanity in India around 1000 B.C. Nowadays, it is known that this substance has an antihypertensive effect and more recently some studies have showed that it can also be used for relief of psychotic symptoms associated to schizophrenia (Figure 5) (HOENDERS et al., 2018).

Ibogaine, present in the roots of the perennial rainforest shrub Iboga was commonly used for medicinal and ritual purposes within African spiritual traditions of the Bwiti. A recent research conducted by Brazilians researchers at Federal University of São Paulo (UNIFESP) has showed that this drug can help in drug addiction (cocaine,

crack and others) (CHAGAS et al., 2014). However, its efficacy has been hard to prove, since negative side effects have been reported on administration of this drugs, which has led to it being prohibited for use in certain countries (Figure 5) (BROWN, 2013).

Reserpine   Ibugaine
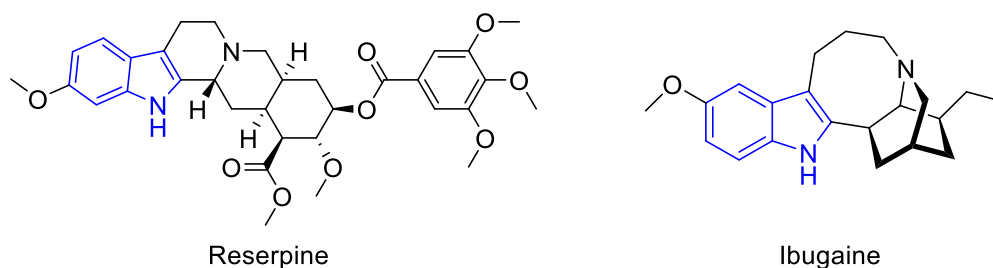
Figure 5. Examples of alkaloids with biological activity.

1.3 Indolizines

Among the most important *N*-heterocyclic compounds in drug development field are the indolizines (JOULE; MILLES; SMITH, 2000).

Indolizine is a *N*-fused bicyclic compound which is the combination of a 6-membered ring (π-deficient) and 5-membered ring (π-excessive) (Figure 6).
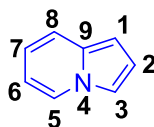
Figure 6. Indolizine ring.

It possesses a delocalized 10π-electron system and nitrogen atom has influence in both rings. The 5-membered ring resembles the reactivity of a pyrrole being suitable to electrophilic substitutions reactions while the 6-membered ring resembles the reactivity of a pyridine ring. Despite this mixture of properties, indolizines are considered a π-excessive ring and promptly undergo electrophilic substitutions (KATRITZKY, A. R.; RAMSDEN, C. A.; JOULE, J. A.; ZHDANKIN, 2010).

Indolizine is also an important bioisostere analogue of indole being considered as privileged structure with application in pharmaceutical, agrochemical and material sciences field. In addition to the natural products, in the last few years several research groups have been reported synthetic derivatives with different biological activities (against tuberculosis, leishmaniasis, antifungal, antiviral, antibacterial, antitumor properties, analgesics, anti-inflammatory agents, calcium channel blockers and inhibitors of 15-lipoxygenase) (MEDDA et al., 2003; DE BOLLE et al., 2004; TEKLU et

al., 2005; JAMES et al., 2006; DARWISH, 2008; SHEN et al., 2010; HAZRA et al., 2011; LINGALA et al., 2011; SHARMA; KUMAR, 2014) (Figure 7).

Antibacterial

calcium channel blockers

Antitumor

activity against *Mycobacterium tuberculosis*

Inhibitor sPLA2

Inhibitor of 15-Lipoxigenase

Indoxam: Antiinflamatory

Fantofarone: Antihypertensive

5-HTA-Ligant receptor
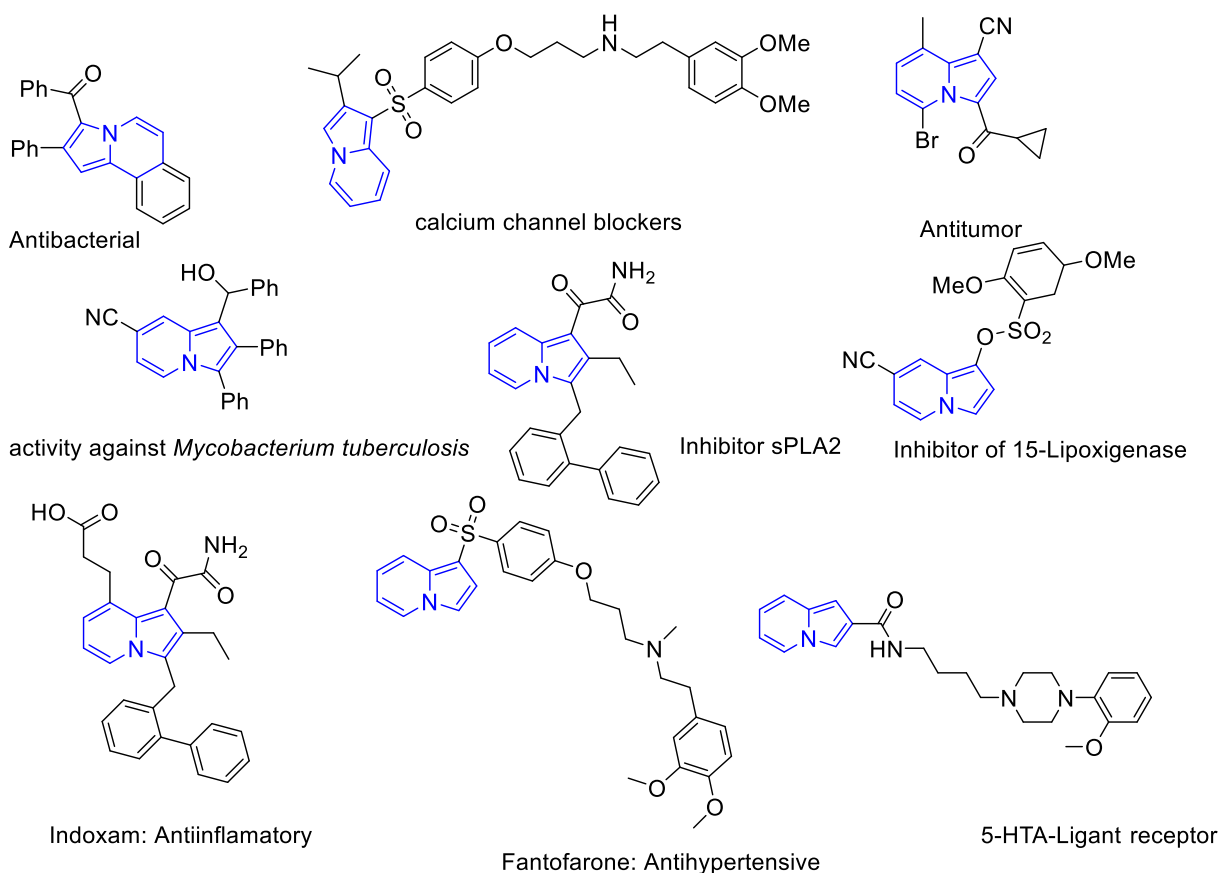
Figure 7. Examples of bioactive indolizines.

Although the occurrence of the indolizine ring system in natural products is quite rare, its partially and fully hydrogenated derivatives are common in nature and some of them present interesting biological activities. For example, Camptothecin is a natural product isolated from a Chinese tree *Camptotheca acuminate* (BUTA; NOVAK, 1978) which selectivity inhibits DNA tropomerase I (HERTZBERG; CARANFA; HECHT, 1989) (Figure 8). (+)-Castanorpermum, (+)-lentiginosine and (+)-swainsonine are examples of fully saturated indolizines (known as indolizidinone alkaloids) which are potent glycosidase inhibitors (Figure 8) (WATSON et al., 2001).

(+)-Camptothecin

(+)-Castanorpermum

(+)-Lentiginosine

(+)-Swainsonine
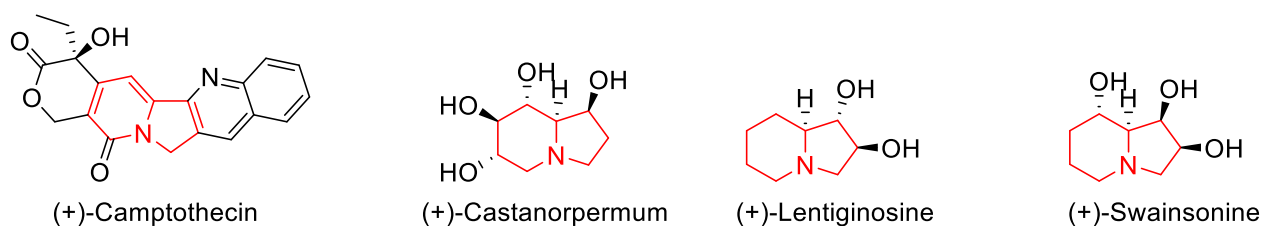
Figure 8. Examples of partially and fully indolizine derivatives found in nature.

Despite of all medicinal chemistry relevance, recently many research groups have been dedicated to the synthesis of fluorescent π-conjugated indolizines derivatives due to their application as dyes (KUMAR et al., 2013; OOYAMA et al., 2013), bioprobes (KIM; LEE; PARK, 2011; JEONG et al., 2012; CHOI et al., 2014), electroluminescent material for optoelectronic (WAN et al., 2012; WANG et al., 2013), biomarkers (OLIVEIRA et al., 2010; LIU et al., 2012) and sensors (DELATTRE et al., 2005; LUNGU et al., 2005; MORO et al., 2013).

For example, Sung and co-workers (SUNG et al., 2017) have developed a new fluorescent mitochondrial probe for monitoring mitochondrial integrity under the live cell condition (Figure 9). It is known that cancer cells have different patterns in mitochondrial morphology and because of that the design of probes which can cross the cellular membrane of a cancerous cell can help in cancer phenotype identification and in the measurement of the drug, due to the accumulation of the probe at the mitochondrial membrane (ALIROL; MARTINOU, 2006; BLANCHET et al., 2015; GIEDT et al., 2016).

In this study they were able to show that simple changes in the chemical structure of organic fluorophores can cause a significant difference in the cellular staining ability as well as photophysical properties of organic fluorochromes. For example, the introduction of an olefin spacer between pyridinium moiety and indolizine fluorophore caused significant differences in the absorption, emission wavelength and mitochondrial staining ability of bioprobes.

Mitochondria targeting probe

Sensitizer compound for DSCs

Bioimaging fluorescent probe
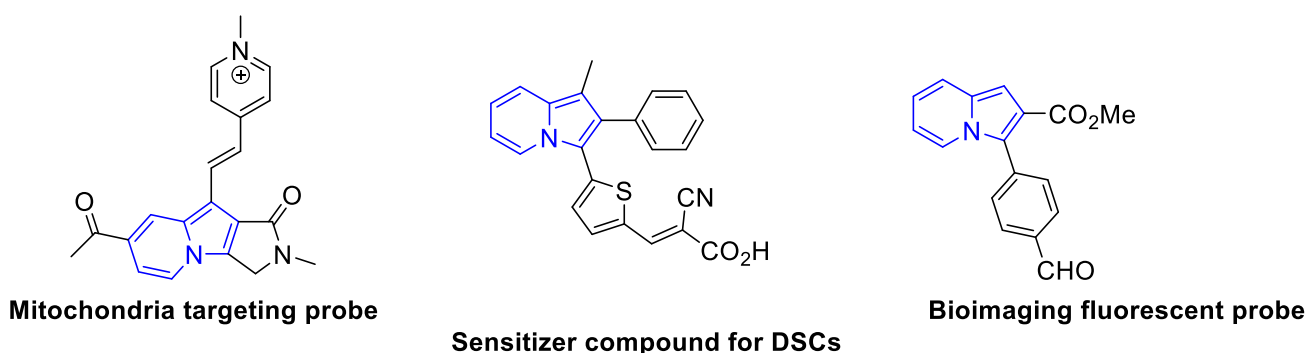
Figure 9. Examples of fluorescent π-conjugated indolizines derivatives.

1.4 Indolizine: Synthesis

Indolizine scaffold can be synthetized through several different approaches (SADOWSKI; KLAJN; GRYKO, 2016), however, most of used protocols are based in the annulation of pyridine or pyrrole-based substrates to indolizines (Figure 10).

pyrrole-based substrate
annulation strategy

pyridine-based substrate
annulation strategy
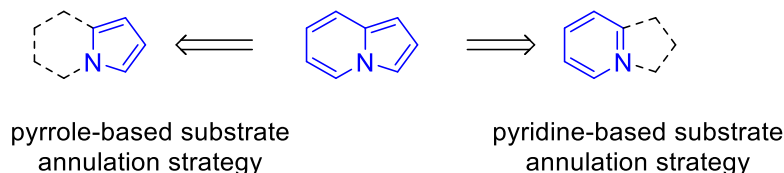
Figure 10. Approaches to indolizine framework.

The annulation of pyridines is the most used strategy for the synthesis of indolizines, being relevant to highlight two approaches: (a) intramolecular cyclization of 2-akylpyridines with anhydrides (Scholtz reaction) or α-haloketones (Tschitschibabin or Chichibabin reaction) and (b) 1,3-dipolar cycloadditions of pyridinium salts with alkenes or alkynes (SINGH; MMATLI, 2011; VEMULA; VURUKONDA; BAIRI, 2011; SHARMA; KUMAR, 2014; KIM et al., 2015) (Figure 11).

1,3-dipolar cycloaddition

Scholtz and Tschitschibabin
reaction
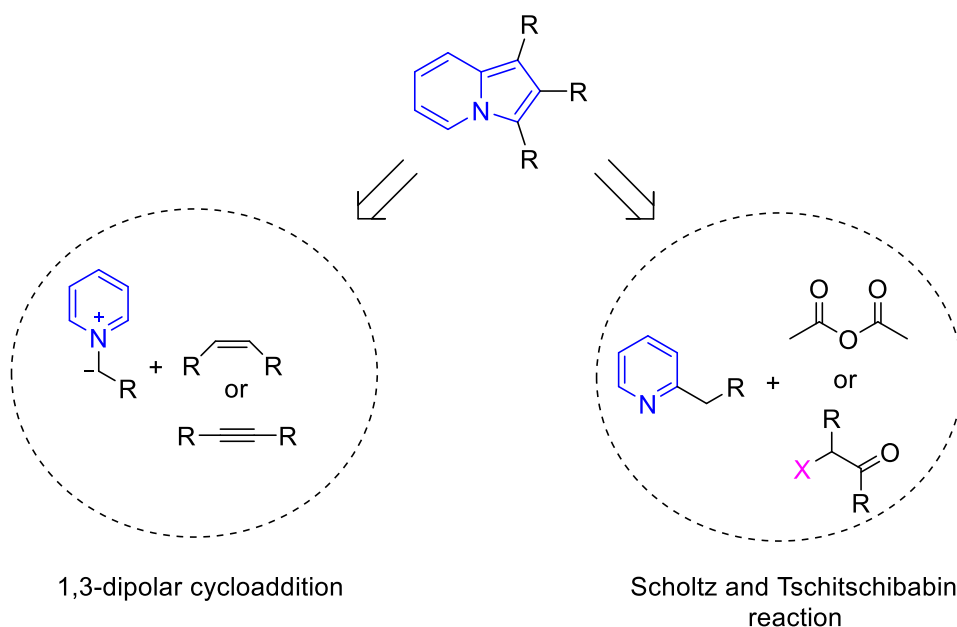
Figure 11. Traditional synthesis of indolizine using pyridines.

In 1912 Scholtz described for the first time the synthesis of indolizine **20** through reaction between 2-methyl-pyridine **18** and acetic anhydride at 220 °C followed by a hydrolysis step. However, this approach is no longer used because of the low yield,

the difficulty in preparing functionalized derivatives and the requirement of high temperatures (SCHOLTZ, 1912) (Scheme 1).
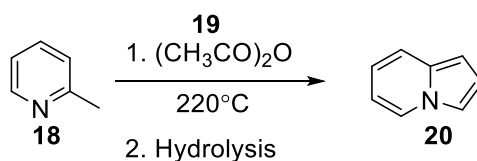
Scheme 1. Scholtz reaction.

On the other hand, Tschitschibabin's strategy was first reported in 1927 and remain the simplest and most efficient way to prepare 2-alkyl or aryl indolizines. In this approach, pyridine is converted into its corresponding quaternary salt **23** by reaction with α-haloketones **22**. Then, after an intermolecular cyclization mediated by base (K_2CO_3), 2-alkyl or aryl indolizines were obtained in good yield. Chai and co-workers have demonstrated the efficiency of this approach through the synthesis of novel 2-arylated indolizines of type **24** using several pyridinium ylides in a chromatography-free protocol (TSCHITSCHIBABIN, 1927; CHAI et al., 2003).

Different kind of bases can be used including inorganic salts such as carbonates and bicarbonates in aqueous medium. The yield for this reaction are reasonable, however, the electron-withdrawing nature of the α-haloketone and the presence of bulky substituents in the pyridine ring (R_1 and R_2) may slower the intramolecular cyclization or leave the nitrogen less accessible to the *N*-alkylation (Scheme 2, compound **21** to **23**) leading to low yield (CHAI et al., 2003) (Scheme 2).
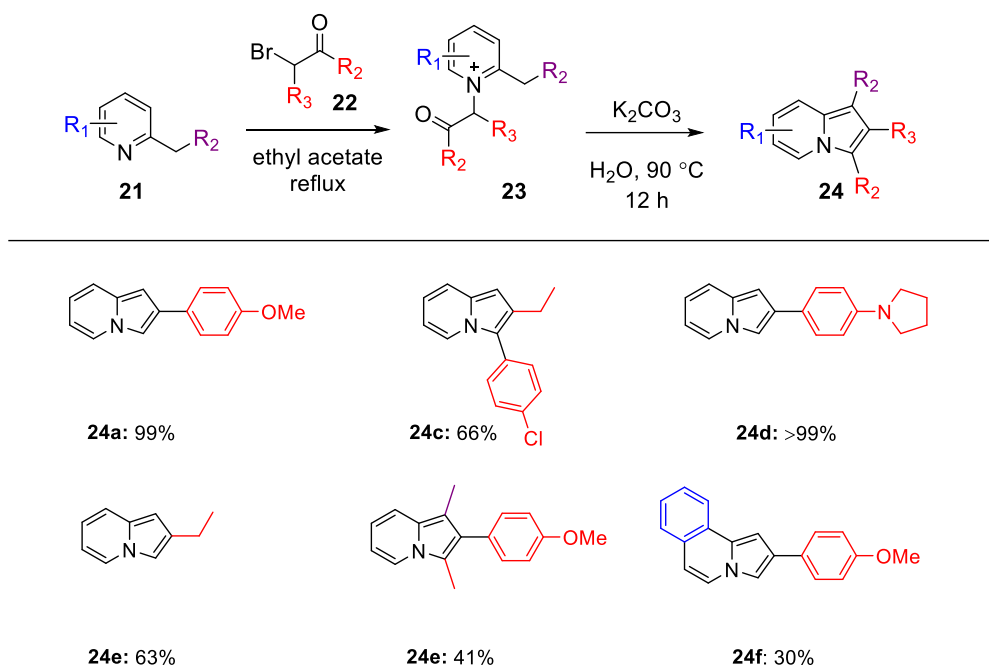
Scheme 2. Tschitschibabin approach adapted by Chai and co-workers.

In 2007, Przewloka and co-workers reported the synthesis of an array of 3-acylindolizines in the presence of DMF·Me$_2$SO$_4$. This methodology exploits the use of pyridines and α-haloketones substituted with several functional groups such as methoxy, cyano, nitro, halogens and heteroaryl (PRZEWLOKA et al., 2007) (Scheme 3).
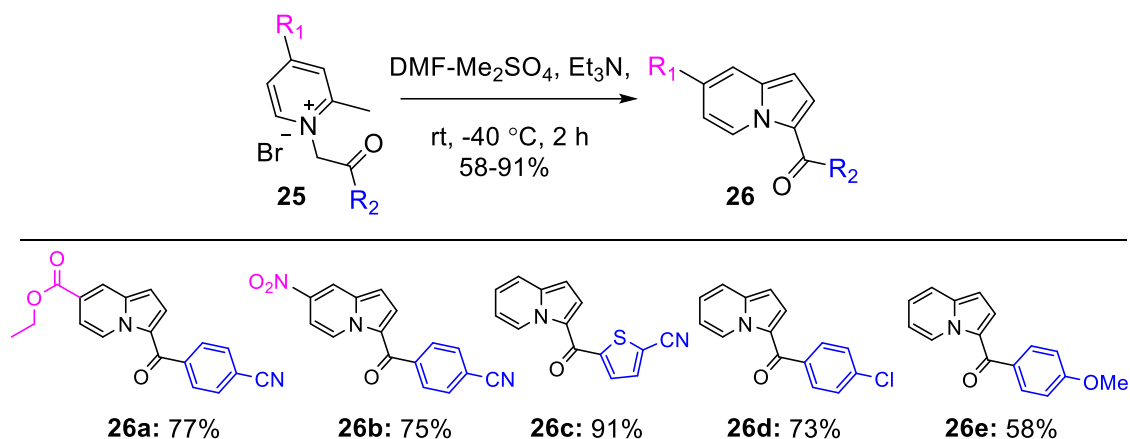
Scheme 3. Synthesis of 3-acylindolizines.

Another stablished approach for the preparation of functionalized indolizines is 1,3-dipolar cycloaddition of pyridinium ylides with electron-deficient dipolarophiles. In 1961 Boekelheide demonstrated the preparation of 1,2,3-trisubstituted indolizines **29**

by reaction between pyridinium ylide type **27** with an activated alkyne **28**, using toluene as solvent in the presence of Pd/C (GALBRAITH et al., 1961) (Scheme 4).
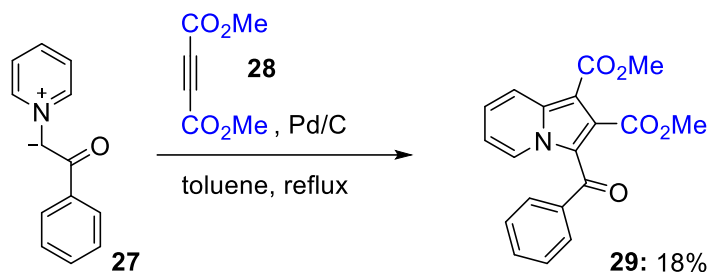
Scheme 4. Synthesis of 1,2,3-trisubstituted indolizines.

Since then, numerous methodologies using different kind of activated alkynes and alkenes as dipolarophiles have been reported. According to the cycloaddition mechanism, there is formation of an unstable tetrahydro-adduct intermediate **31** which decomposes to form ring opened compound called betaines or starting materials (Scheme 5) (TSUGE; KANEMASA; TAKENAKA, 1985).
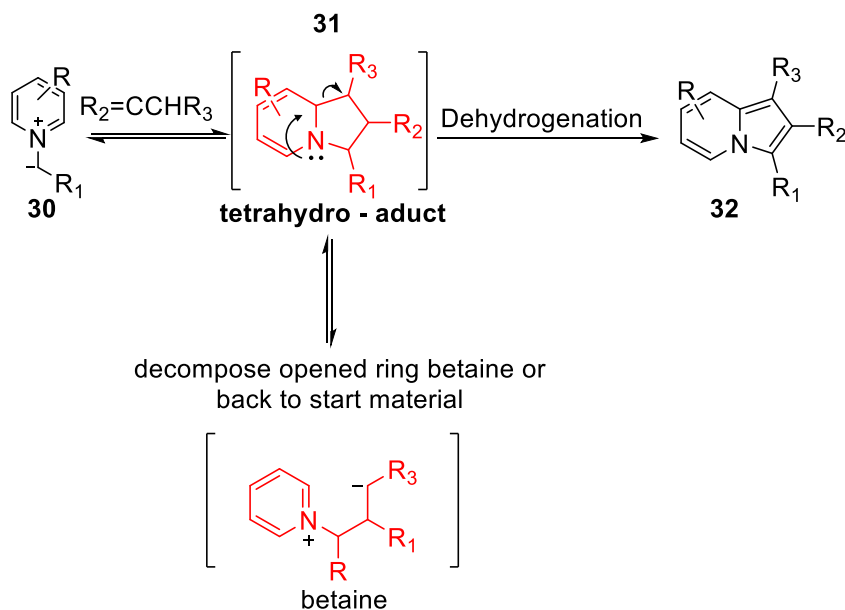
Scheme 5. Decomposition of tetrahydro-adduct intermediate to betaine or starting material.

Because of the formation of this instable intermediate **31** when activated methylenes are used as dipolarophiles, it is necessary that they contain in their structure a good leaving group or the use of an oxidizing reagent during the reaction. Katritzky and co-workers have used α-bromo-α,β-unsaturated esters or nitrile as

dipolarophiles to prepare indolizines of type **35**. Through a base-assisted elimination of bromo substituents or benzotriazole (Bt) from the corresponding cycloadduct they were able to prepare C-1 substituted indolizines with different groups (Scheme 6) (KATRITZKY et al., 1999).
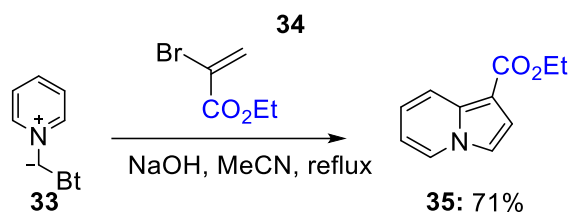
Scheme 6. Synthesis of ethyl indolizine-1-caboxylate.

In 2000, Zhang and co-workers reported the synthesis of 3-unsubstituted indolizines through a 1,3-cycloadditon/oxidation step between activated alkenes and carboxylic acid substituted pyridinium salts **36**. In the absence of good leaving groups in the alkene structure, it was necessary the use of an oxidant in order to promote *in-situ* dehydrogenation of the unstable tetrahydro-adduct. After trying several commercial oxidizing agents, they achieve best results when using MnO_2. For example, by using this strategy they were able to prepare indolizine **1** in 92% yield (Scheme 7) (ZHANG et al., 2000).
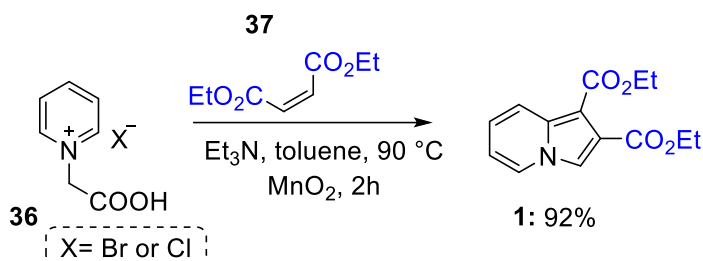
Scheme 7. Synthesis of dimethyl indolizine-1,2-dicarboxylate.

Furthermore, another interesting strategy to prepare indolizines bearing groups at pyrrole ring is using Morita-Baylis-Hillman acetates (MBHAs). In this context, Zhu and co-workers were able to react MBHAs with ethyl 2-pyridylacetate and 2-pyridylacetonitrile to obtain several trisubstituted indolizines in moderate to good yield **40** (Scheme 8) (ZHU et al., 2013).
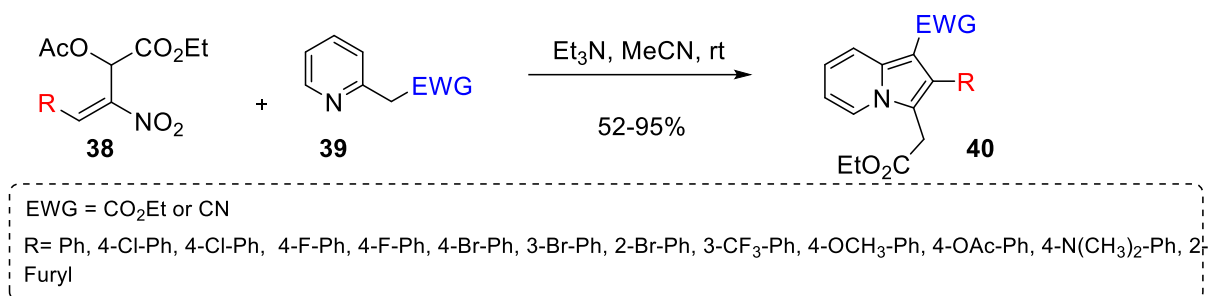
Scheme 8. Synthesis of trisubstituted indolizines from MBHA adduct.

However, these are not the only strategies that can be used to prepare indolizines using pyridine-like substrates. There are also multi-components reactions, cyclodimerizations catalysed by metals or metal free reactions, iodine-mediated direct oxidative cyclization between 2-alkylpyridines and enolizable aldehydes, annulation of propargylic alcohols with pyridine derivatives and others (GOFF, 1999; KIM et al., 2007; CUNHA; DE OLIVEIRA; VASCONCELLOS, 2013).

Despite of the majority strategies to prepare indolizines have been based on pyridine derivatives, recently have been a rising number of approaches using pyrrole-like substrates. In 2013, Kim and co-workers proposed an annulation process that involved a Knoevenagel reaction followed by an intramolecular aldol cyclization which make possible the construction of much more diversified molecules bearing a variety of substituents groups in both rings (KIM; JUNG; KIM, 2013) (Scheme 9).
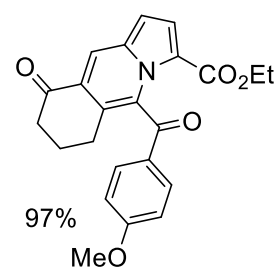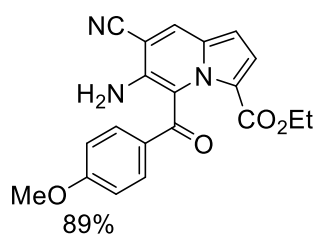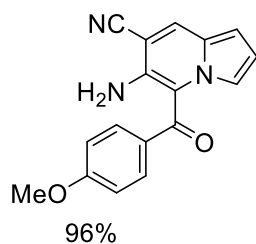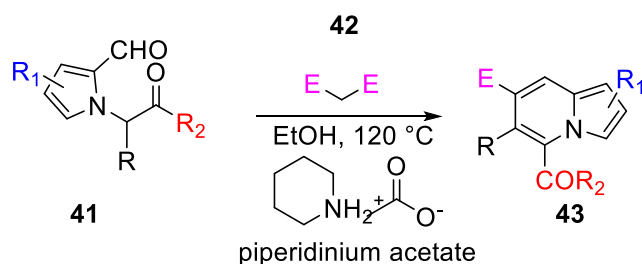
Scheme 9. Synthesis of polysubstituted indolizines involving Knoevenagel approach.

Later, Kucukdisli and Opatz through an one-pot conjugated addition / cyclodehydration / dehydrocyanation sequence involving α,β-unsaturated ketones or aldehydes **44** and 2-(1H-pyrrol-1-yl)nitriles **45** have prepared a number of indolizines fully substituted at pyridine ring (Scheme 10). (KUCUKDISLI; OPATZ, 2012).
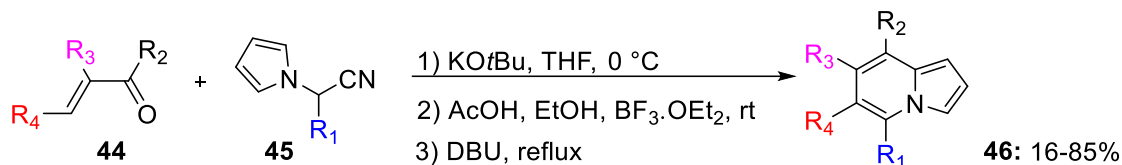
Scheme 10. Synthesis of indolizines fully substituted at pyridine ring.

At the same time, Kim and co-workers have demonstrated preparation of 6,8-dissubtituted indolizines through a based-mediated cyclodimerization of 2-acetylpyrrole derivatives. In this approach, they were able to isolate valuable synthetic intermediates such as *O*-triflate and *O*-acetate indolizines which after undergone Suzuki-Miyaura cross-coupling, Heck coupling, Friedel-Crafts acylation and Vielsmeier-Haack formylation led to the preparation of more complex indolizine derivatives (**Error! Reference source not found.**) (LEE; KIM, 2013).
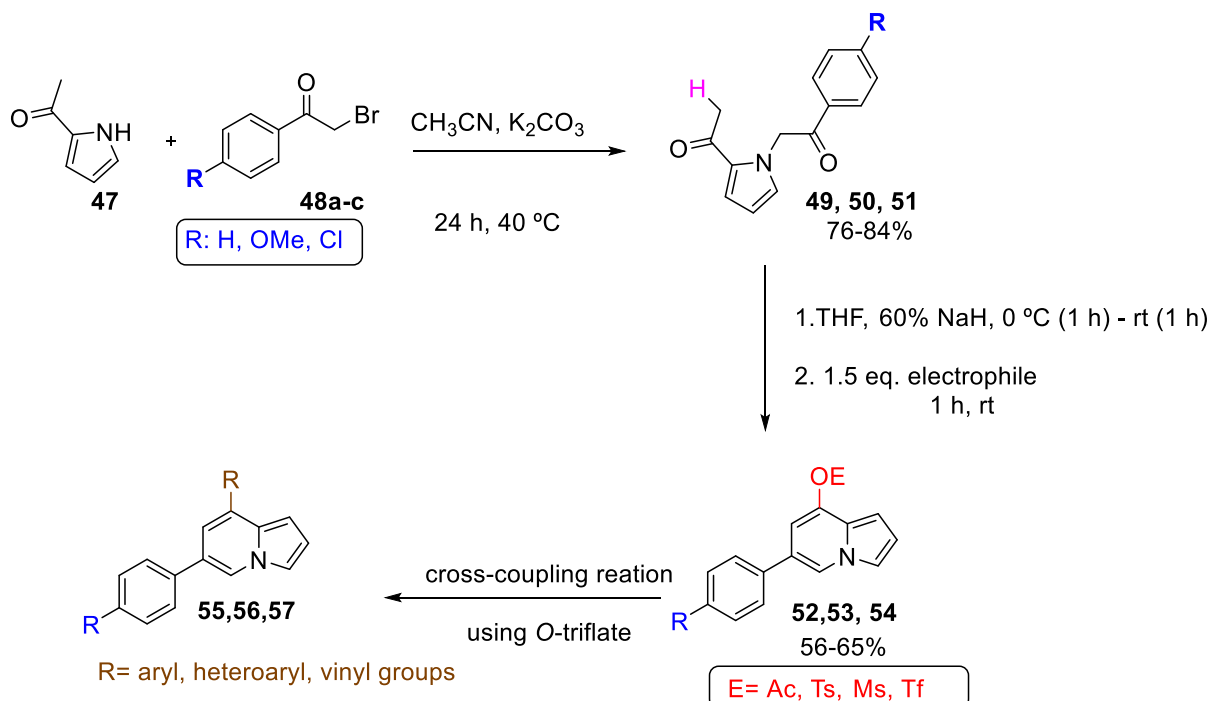
Scheme 11. Synthesis of 6,8-dissubtituted indolizines through a based-mediated cyclodimerization of 2-acetylpyrrole derivatives.

More recently, Liu and co-workers have reported the synthesis of polysubstituted indolizines type **60** using gold catalyst to promote an efficient hydroarylation /

cycloaromatization. In this work they used α-(*N*-pyrrolyl)ketones **58** and terminal or activated alkynes **59** in the presence of 5 mol% of Ph₃PAuNTf₂ (Scheme 12) (LI; XIE; LIU, 2016).
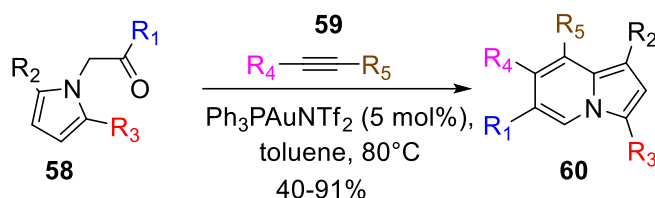
Scheme 12. Synthesis of polysubstituted indolizines through hydroarylation / cycloaromatization catalysed by gold.

1.5 Reactivity of Indolizines

Indolizines belong to the class of *N*-fused heterocyclic π-electron-rich type and because of that promptly undergo electrophilic substitution, but in specific cases they can suffer nucleophilic attacks. For example, Babaev and co-workers have shown a protocol were indolizines bearing electron-drawing groups at C-6 position are susceptible to nucleophilic attacks. In this work, firstly, they were able to convert 2-aryl-6-cyano-7-methyl-5-indolizinones **67** to 2-aryl-5-chloro-6-cyano-7-methylindolizines **61**. Then, reacting these 5-chlorinated derivatives with several nucleophiles indolizines type **62-66** were synthetized in good yield (Scheme 13) (BABAEV; VASILEVICH; IVUSHKINA, 2005).
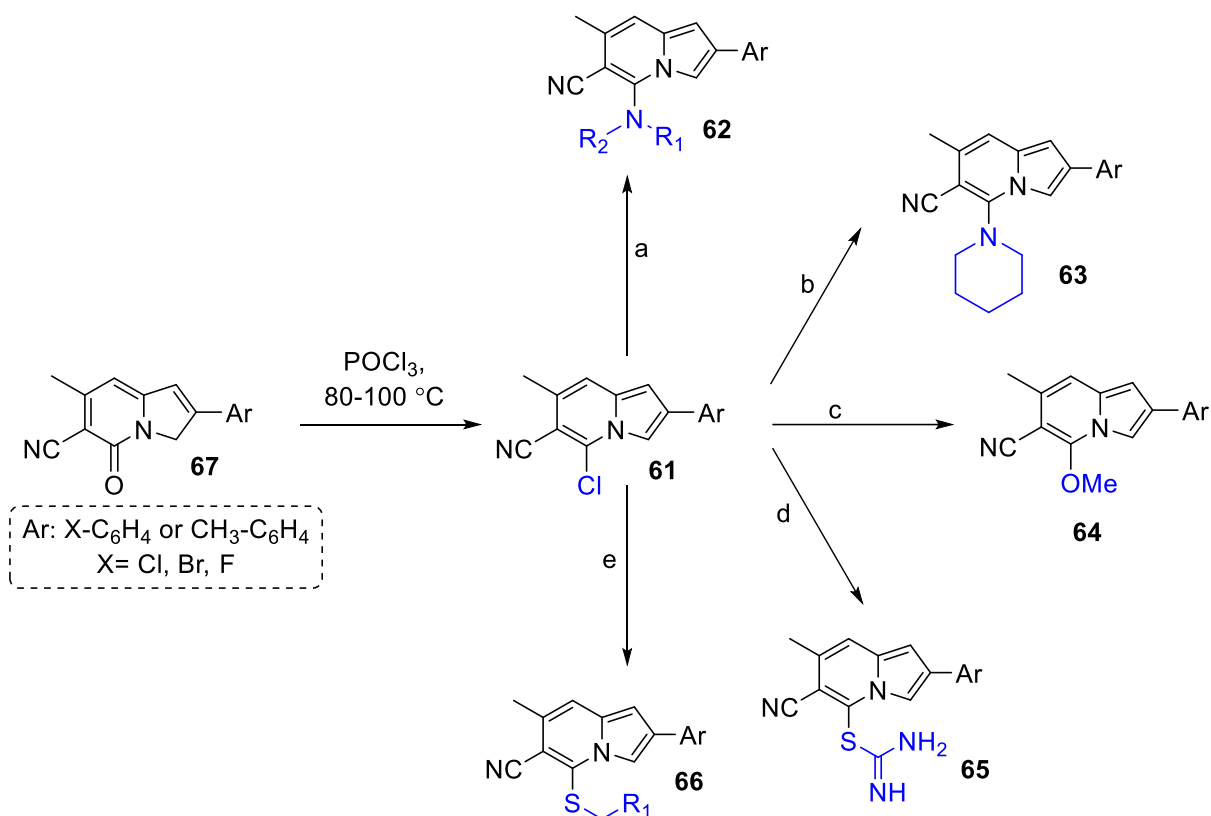
a) NHR$_1$R$_2$, rt. b)piperidyl,rt. c)MeONa;MeOH. d) (NH$_2$)$_2$CS. e) HSCH$_2$CO$_2$Et, EtOH, NaOH, rt.

Scheme 13. Nucleophilic attack in indolizines bearing electron-drawing groups at C-6 position.

Regarding to electrophilic substitution attack the most reactivity position at indolizine ring is C-3 followed by C-1. C-3 position is more reactive due to two factors: (a) C-3 position holds electronic density and (b) After a nucleophilic attack the C-3 isomer formed can display conjugation over carbon atom (better orbital overlap for conjugation purpose) (Scheme 14, I) while C-1 isomer displays over nitrogen atom (Scheme 14, II) (FRASER; MCKENZIE; REID, 1966a).

energy required for charge separation → **b > c**
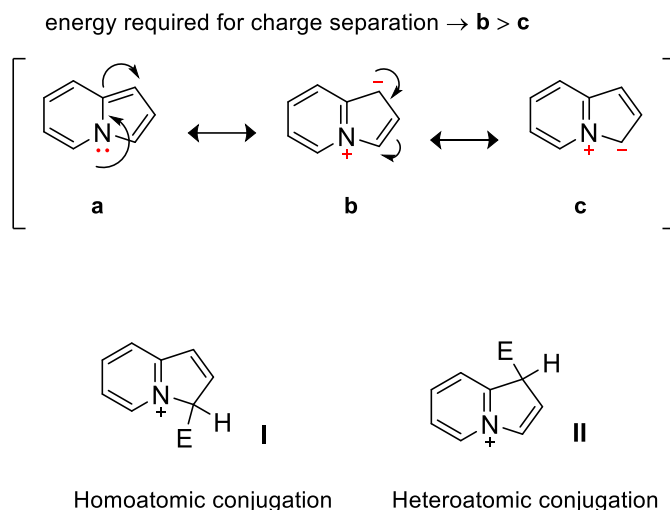
Scheme 14. Resonance structures for indolizine moiety.

Furthermore, indolizines can be protonated at C-1 and C-3 position, alkylated through a Mannich-type reaction, acylated at C-3 position through a Friedel-Crafts reaction, C-1 or C-2 halogenated using *N*-bromosuccinimide or C-5 halogenated (when C-1 and C-2 positions are blocked) via regioselective lithiation and can suffer nitration, nitrosation and diazo coupling or oxidation leading to derivatives with or without nucleus cleavage (BORROWS; HOLLAND; KENYON, 1946a, 1946b; ARMAREGO, 1966; FRASER; MCKENZIE; REID, 1966; HARRELL, 1970; GRECI; RIDD, 1979; LINS; BLOCK; DOERGE, 1982; KATRITZKY; REES, 1984; ROSEMARY, 1994; MULVEY et al., 2007; KUZNETSOV; BUSH; BABAEV, 2008; MATVIIUK et al., 2014).

In addition, more complex structure or fluorescent compounds can be prepared through directed metalation approach or palladium-catalysed coupling strategies (AMARAL et al., 2014a, 2015).

1.6 Directed Metalation reaction

The regiocontrolled insertion of different groups into an aromatic and hetroaromatic ring is one of the biggest challenges in organic chemistry. In this kind of manipulation, it is required to have the ability to find the best reactional condition in the presence of frequently sensitive or reactive groups. Besides, even if it is possible to manage these inconvenient in some cases the challenge is pushing the insertion into the desired ring position.

In 1939 and 1940, Gilman and Wittig independently reported the *ortho*-metalation of anisole using PhLi or *n*-BuLi, respectively. As consequence of these studies, the new concept that some functional groups (called directed metalation groups - DMG) could promote metalation to specific positions (usually ortho DMG) started to be investigated (Scheme 15) (GILMAN; BEBB, 1939; WITTIG; PIEPER; FUHRMANN, 1940).
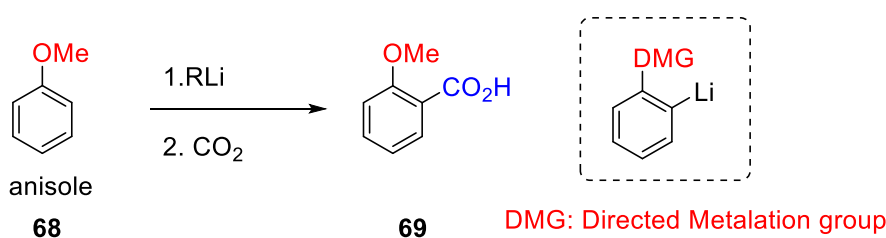
Scheme 15. *Ortho*-metalation of anisole using lithium bases by Gilman and Wittig.

Over the subsequent years researchers such as Hauser (1964), Gronowitz (1968), Gschwend (1976), Meyers (1975), Comins (1983), Beak (1977), Snieckus (1989 and 1999) and others showed that amides, sulfonamides, ozaxolinyl groups, carbamates, esters and oxide phosphines groups can act as good DMGs leading to successful regioselective functionalization of numerous aromatic and heteroaromatic compounds (GREEN; CHAUDER; SNIECKUS, 1999; SCHLOSSER, 2005).

DMGs can direct the metalation to the *ortho* position due to (a) the ability of the heteroatom present in the DMG be able to effectively coordinate with the metal (lithium) in other to settle a complex-induced proximity effect (CIPE) and promote the directed deprotonation of the substrate or (b) through a inductive effect that lower the pKa value of the adjacent proton (Figure 12) (MONGIN; QUÉGUINER, 2001; CHEVALLIER et al., 2012). It is also important that the DMG group does not react with the base by a nucleophilic attack.

DMG: Directed metalation group

Chelation in the transition state   Acid-base (inductive) mechanism

Figure 12. CIPE effect.

The most common base used in DoM (directed ortho metalation) are the alkyl lithium such as *s*-BuLi, *n*-BuLi and *t*-BuLi. Best results were observed using dry THF or Et$_2$O as solvents in the presence of TMEDA.

As TMEDA is a good ligand for metals, when in presence of lithium bases the nitrogen present in its structure can coordinate to lithium, forming a cluster of higher reactivity than the normal tetramer and hexamer forms of these bases.

Despite the success of this methodology, the use of lithium bases has some inconvenient such as (a) it is necessary work at low temperatures to achieve regioselectivity, (b) organolithium intermediate formed are very reactive and can led to the formation of undesired side products, (c) lithium bases normally do not tolerate sensitives groups such esters, cyano, ketones, aldehyde, amides, thus it is difficult to apply DoM in substrates bearing these functional groups without previously protection, (d) due to the low stability of this bases in THF at room temperature, they needed to be generated *in-situ* (EATON; MARTIN, 1988; RAPPOPORT; MAREK, 2008). These drawbacks are especially critical in the industry environment, where robust synthetic protocols are needed for process developments.

In 1947, Hauser and Walker reported the preparation of magnesium dialkyl-(R$_2$NMgX) and bisdialkylamides (R$_2$N)$_2$Mg as an alternative to lithium bases. Later, Eaton and co-workers described the *ortho*-metalation of the methyl benzoate **70** using the magnesium diamide TMP$_2$Mg. In this approach they used excess of TMP$_2$Mg to form the intermediate **71** which was reacted with carbon dioxide followed by

diazomethane leading to the preparation of **72** in 81% (Scheme 16) (HAUSER; WALKER, 1947; EATON; LEE; XIONG, 1989).
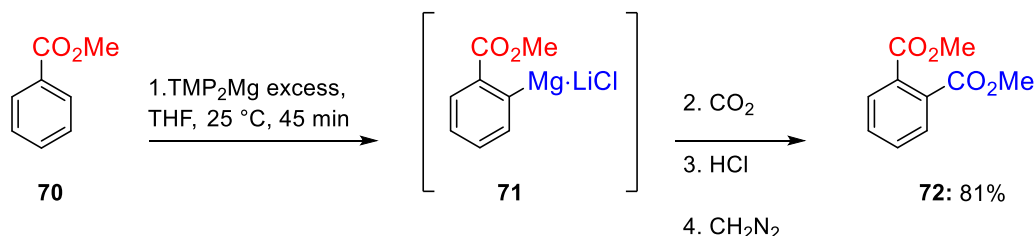
Scheme 16. *Ortho*-metalation of methyl benzoate **70** using TMP$_2$Mg.

In the following years, the reactivity of these magnesium amides was investigated in the metalation of indoles, thiazoles and pyridines. Despite appearing as an interesting strategy for the functionalization of those substrates, these bases tend to form clusters in organic solvents and because of this the use of large amounts of base was crucial for the reaction success.

In 2006, Knochel and co-workers announced a new class of mixed Mg/Li, Zn/Li and Zn/Mg/Li bases (KRASOVSKIY; KRASOVSKAYA; KNOCHEL, 2006; CLOSOSKI; ROHBOGNER; KNOCHEL, 2007; CLOSOSKI, G. C.; ROHBOGNER, C. J.; KNOCHEL, P. KRASOVSKIY, A., KRASOVISKAYA, 2008; WUNDERLICH et al., 2010) (Figure 13). This combination of hindered bases (less nucleophilic) with LiCl allow the preparation of more soluble and stable bases in THF (standard solvent used in metalation reactions). Besides, selectivity can be achieve working at higher temperatures (25-45 °C) when compared with alkyl lithium bases.
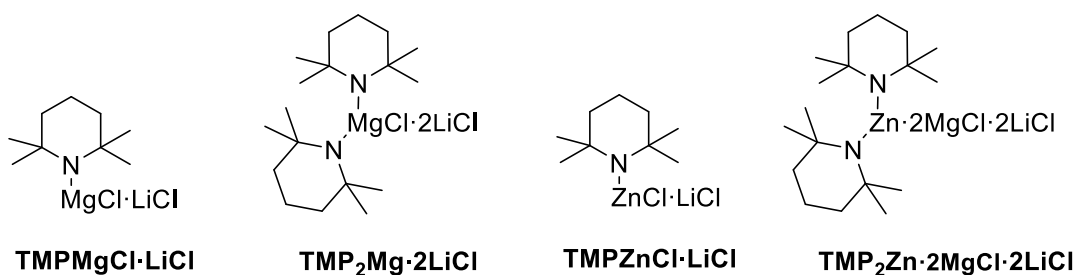
Figure 13. Mixed Mg/Li, Zn/Li and Zn/Mg/Li bases.

Boudet and co-workers have demonstrated the applicability of this approach in the synthesis of Talnetant, a selective antagonist of NK3 receptor produced by GlaxoSmithKline. In this work, quinoline **73** bearing a sensitive group (ester) was selectively deprotonated using 1.1 equivalent of TMPMgCl·LiCl. After deprotonation,

the intermediate **74** was reacted with 2-ethoxy-4,4,5,5-tetramethyl-1,3,2-dioxaborolane led to the key compound **71** in 71% isolated yield (Scheme 17) (BOUDET; LACHS; KNOCHEL, 2007).

Scheme 17. Synthesis of Talnetant.
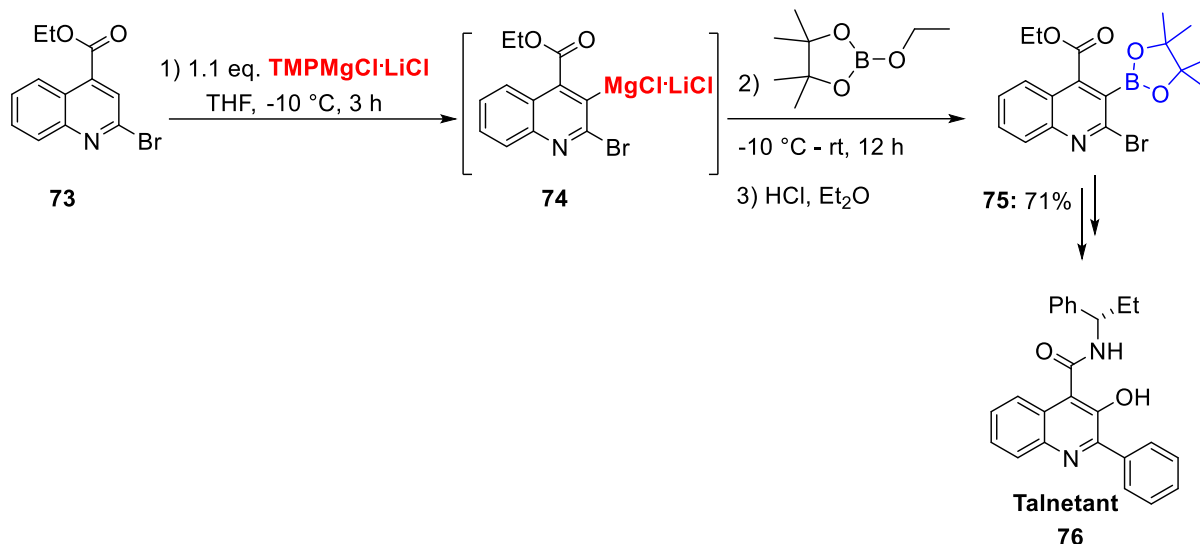
Even though, the relevance of this new kind of mixed Li/Mg bases in the metalation of a range of unsaturated substrates and the advantages over alkyl lithium bases, some moderately activated substrates gave unsatisfactory results. This is the case of tert-butyl benzoate **77** in which when reacting with TMPMgCl·LiCl followed by quench with iodine gave *tert*-butyl 2-iodobenzoate **78** in 7% yield only. On the other hand, using the new magnesium bisamide complexed with LiCl, first reported by Clososki and co-workers, the desired product **78** was obtained in 80% yield (Scheme 18) (CLOSOSKI; ROHBOGNER; KNOCHEL, 2007).

Scheme 18. TMPMgCl·LiCl versus TMP$_2$Mg·2LiCl in the metalation reaction of *tert*-butyl 2-iodobenzoate.
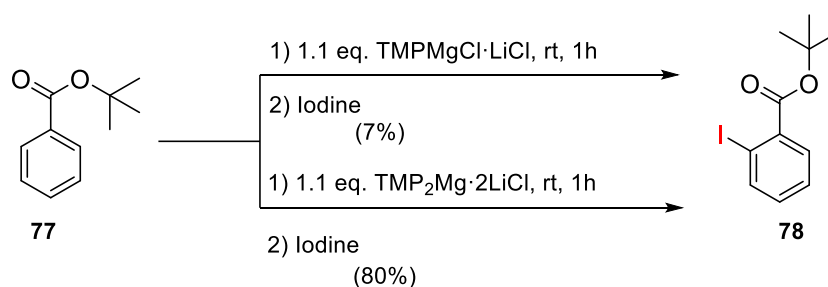
In this same work the authors prepared another two magnesium bisamides complexed with LiCl (Scheme 19). They also were able to conclude that (a) these new bases can tolerate sensitive functional groups (ketones, cyano, carbonates and

bis(dimethylamino) phosphonate groups) (b) they are more powerful then magnesium amide mixed with LiCl and (c) they were capable of promote regioselective metalation of ester-substituted pyridines.

Magnesium bisamides complexed with LiCl

Substrates

| 70-94% | 66% | 70% | 81-83% | 78-93% | 71-77% | 77% |

X= CH or N, R= Et, *t*Bu, *i*Pr, E= I, PhCOCl, EtCOCl, *p*-C$_6$H$_4$CO$_2$Et, *p*-IC$_6$H$_4$CN, (BrCl$_2$C)$_2$
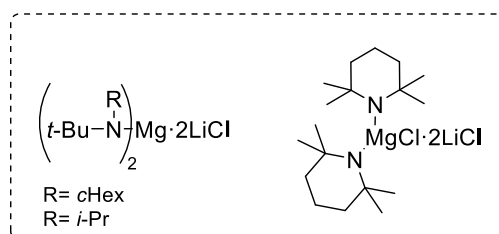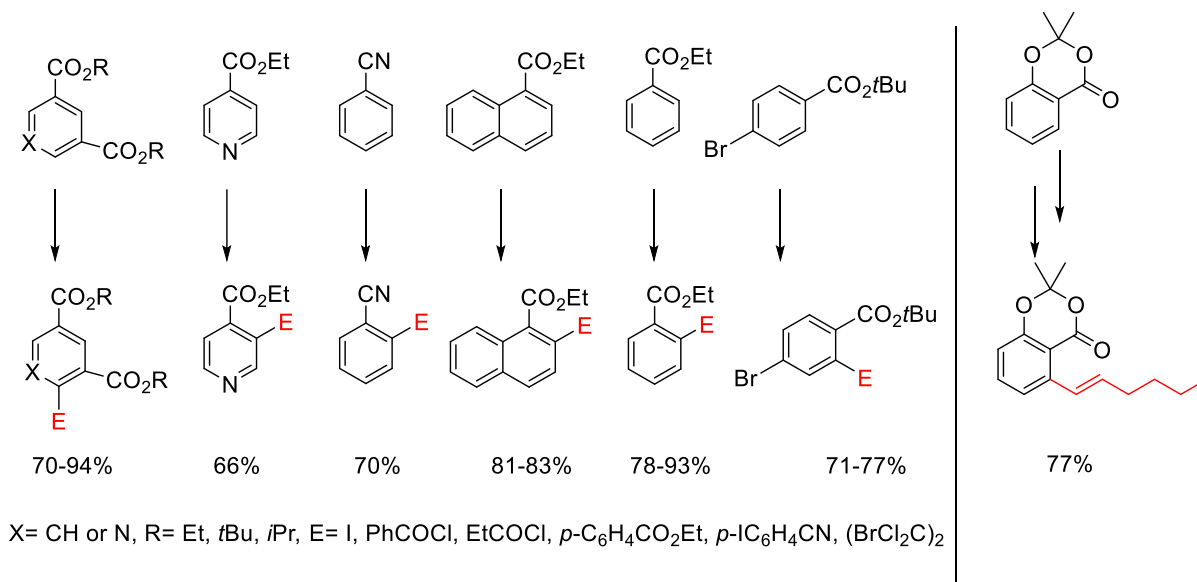
Scheme 19. Examples of substrates that were capable of being reacted with magnesium bisamides complexed with LiCl.

1.7 Metalation of indolizine

In 1992 Renard and Gubin reported for the first time, the regioselective lithiation of 2-phenylindolizine using *n*-BuLi. In this work, they were able to react the C-5 lithiated indolizine intermediate **79** with some electrophiles such as CO$_2$, benzaldehyde, iodomethane, HCl, D$_2$O and (CH$_3$)$_3$SiCl to obtain C-5 derivatives **80** in good yield (Scheme 20) (RENARD; GUBIN, 1992).
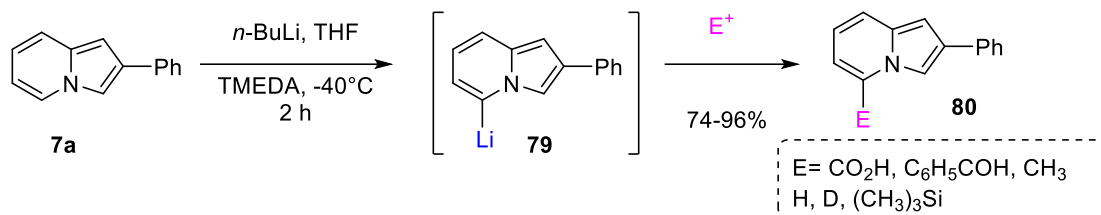
Scheme 20. Regioselective lithiation of 2-phenylindolizine.

Then, in 2005 Kuznetsov and co-workers, based in the Renard and Gubin work, demonstrated that 2-substituted indolizines bearing alkyl and phenyl groups, after undergo directed metalation can led to the preparation of iodine and formyl derivatives in good yield (Scheme 21) (KUZNETSOV et al., 2005).
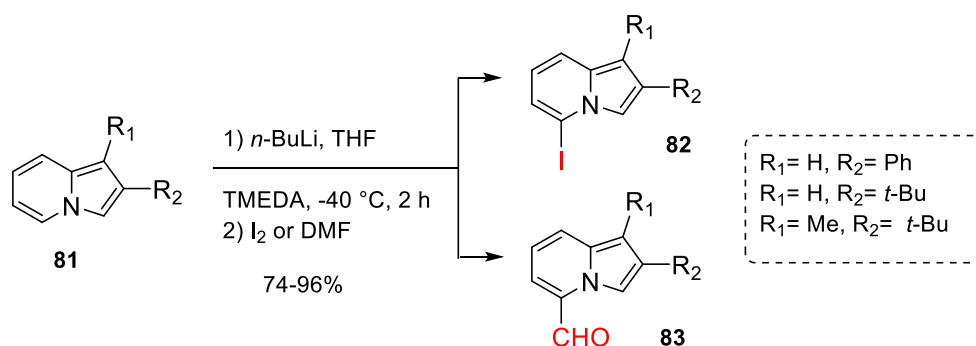
Scheme 21. Lithiation of 2-substituted indolizines followed by reaction with iodine and DMF.

Later, Amaral and co-workers have developed a new base-controlled protocol in which 1-sustituted indolizines were successfully functionalized through reaction with LDA and Mg amides complexed with LiCl, followed by reaction with different electrophiles. In this study, they showed that seems to be a dynamic equilibrium between C-2 and C-5 positions when using TMPMgCl·LiCl and the nature of the electrophiles appears to carry out regioselectivity. More reactive electrophiles afforded C-2 substitution **85** while less reactive electrophiles conduct to C-5 derivatives **86** (Scheme 22) (AMARAL et al., 2015).

They also synthetized aryl and heteroaryl derivatives using Negishi cross-coupling strategy.
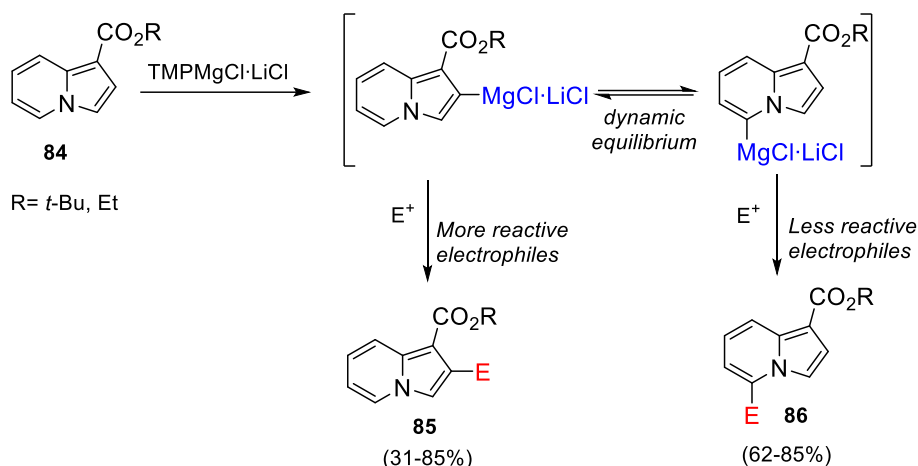
Scheme 22. Base controlled approach for 1-substituted indolizines using Li/Mg amides complexed with LiCl.

In another work, Amaral and co-workers have demonstrated the efficiency of Palladium-catalysed cross-coupling reaction between aromatic halides and 2-arylindolizines. In the first step, 2-arylindolizines **7a-e** were lithiated using *n*-BuLi. Then, they promoted an lithium/ZnCl$_2$ exchange and the 2-aryl-5-organozinc intermediate **87** could be coupled with aryl halides using catalytic amounts of Pd(Ph$_3$)$_4$ (Scheme 23) (AMARAL et al., 2014).
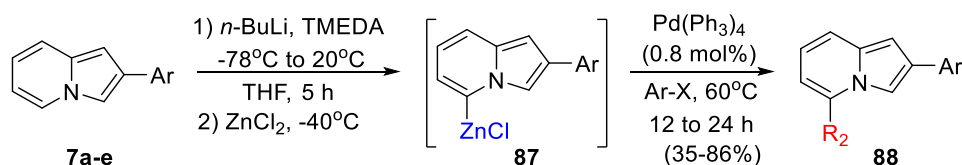
Scheme 23. Lithiation of 2-arylindolizines followed by Negishi cross-coupling reaction.

Given the importance of indolizine scaffold in different fields, in this thesis we will discuss strategies to prepare functionalized indolizines with potential application in medicinal chemistry and material science.

2. Aim

The main goal of this work was to investigate the development of synthetic methodologies for the regioselective functionalization of indolizines bearing different *ortho*-metalation groups (DMG). Further reaction of the reaction intermediates with different electrophiles would afford a library of highly functionalized derivatives which would be hard to synthetize through the conventional approaches. For that, two strategies were studied during this work (a) directed metalation using lithium and magnesium bases complexed with LiCl and (b) C-H activation/ borylation using [Ir(OMe)(COD)]$_2$ as catalyst.

Chapter I – **Comprehensive study on directed metalation using lithium amides and magnesium amides complexed with LiCl followed by reactions with electrophiles**

3. Results and Discussion

Specific goals

1. Preparation of indolizines bearing *ortho*-metalation groups with the purpose of explore their reactivity face alkyl lithium and Mg complexed with LiCl bases.
2. Preparation of Mg bases complexed with LiCl.
3. Reaction of the intermediates formed after metalation step with several electrophiles.

3.1 Preparation of Indolizines

Following literature procedure (ZHANG et al., 2000), dimethyl indolizine-1,2-dicarboxylate **1** was synthetized in two steps (Scheme 24). In the first step, pyridinium salt **36** was formed by reaction between pyridine **89** and 2-chloroacetic acid **90** in EtOAc after reflux for 12 hours. Then, through 1,3-cycloadditon/oxidation step using pyridinium salt **36** and dimethyl maleate **91** as dipolarophile in the presence of Et_3N and MnO_2, the desired indolizine **1** was achieve in 90% isolated yield.

In the 1,3-dipolar cycloaddition pyridinium salts react with dipolarophiles in a concerted, often asynchronous and symmetry-allowed $_\pi 4s + _\pi 2s$ fashion through a thermal six-electron Hückel aromatic transition state leading to a tetrahydro-adduct intermediate type **92**.

MnO_2 prove to be a good and cheap option of oxidizing agent which is responsible for *in-situ* dehydrogenation of this unstable tetrahydro-adduct **92** (Scheme 24). The presence of **92** could be detected by CG-MS analysis during the first hours of reaction and it was also possible to see a deep red colour during the formation of this intermediate in the reaction flask that disappears after **92** undergoes dehydrogenation to afford indolizine **1**.
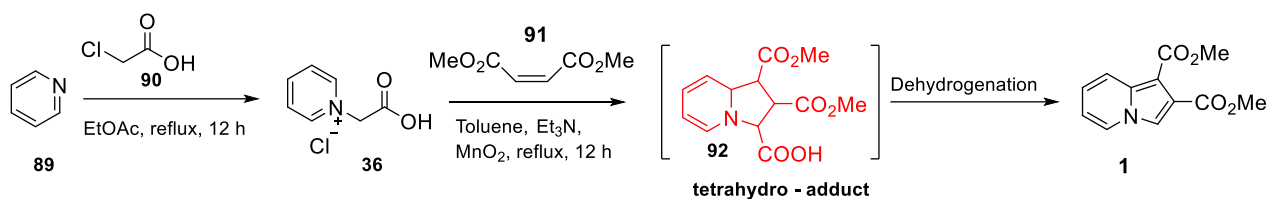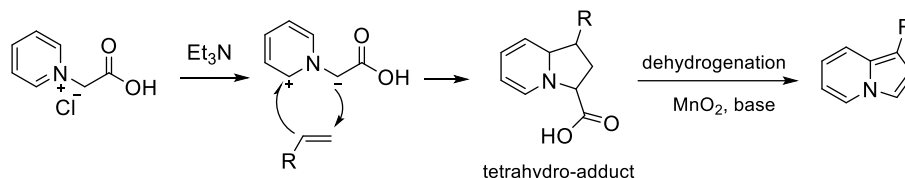
Scheme 24. 1.3-dipolar addition approach used to synthetize 1-substituted indolizines.

Aiming to synthetize 2-(indolizin-1-yl)-4,4-dimethyl-4,5-dihydrooxazole **4**, indolizine-1-carbonitrile **12** was first prepared. The same methodology used in the preparation of indolizine **1** was applied here. Acrylonitrile **93** was used as dipolarophile and indolizine **87** was obtained in 63% isolated yield (Scheme 25).
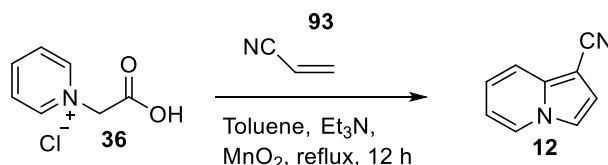
Scheme 25. Synthesis of 1-cyano indolizine.

Then, following Schumacher and co-workers protocol (SCHUMACHER et al., 1990), K_2CO_3 and 2-amino-2-methylpropan-1-ol **92** were dissolved in glycerol and heated at 120 °C for 10 minutes. Subsequently, indolizine-1-carbonitrile **12** were added. This reaction was monitored by TLC for 72 hours upon complete consumption of the starting material. However, after work-up and chromatographic purification, indolizine **4** was obtained only in 40% yield. The modest yield was attributed to poor partitioning. Unfortunately, after testing different solvents we could not remove all product from water/glycerol layer.

In order to overcome this problem, some modifications in the protocol were tested and the results are summarized in Table 1.
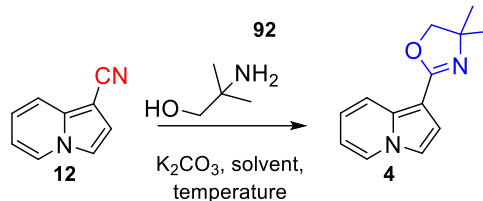
Table 1. Study of reactional condition to prepare indolizine **4**.

Entry	Solvent	Additive	Temperature (°C)	Time (h)	Conversion* (%)
a	ethylene glycol	-	120 [a]	72	52[c]
b	ethylene glycol		150 [b]	4	35[c]
b	-	-	150 [b]	1	-
c	-	-	180 [b]	1	25[d]
d	-	-	240 [b]	1	-
e	THF/glycerol	ZnCl$_2$	150 [b]	4	98
f	THF	ZnCl$_2$	150 [b]	4	-

*CG-MS conversion between start material and product.
[a] traditional heating
[b] microwave irradiation
[c] product desired **4** and starting material without presence of other molecules
[d] 25% product **4** and a complex mixture of other molecules.

Using traditional heating and ethylene glycol as solvent (Table 1, entry a), after 72 hours, only 52% of indolizine-1-carbonitrile **12** was converted into the desired product **4**. Other attempts (Table 1, entry b-d and f) were made in absence of solvent and using microwave irradiation, but it appears that glycerol play an important role in the formation of **4**. Adding a solution of ZnCl$_2$ 1 M in THF using a microwave-assisted protocol (Table 1, entry e) it was observed 98% conversion of the starting material into the desired product. The amount of glycerol used in this protocol was smaller (0.1 mL/mmol of starting material) than in the Schumacher and co-workers (3.6 mL/mmol of starting material), because of that the work-up were easily performed using ethyl

acetate and saturated solution of NaCl. After, chromatographic purification (using reverse phase column-C18) indolizine **4** was obtained in 80% yield.

3.2 Preparation of mixed Li/ Mg bases and lithium bases

TMPMgCl·LiCl **96** was prepared by reaction between 2,2,6,6-tetramethylpiperidine **95** and *i*-PrMgCl·LiCl **94** in THF for 48 hours at room temperature (KRASOVSKIY; KRASOVSKAYA; KNOCHEL, 2006; LIN; BARON; KNOCHEL, 2006). *i*-PrMgCl·LiCl (turbo Grignard) can be purchased or prepared through reaction of isopropyl chloride **93** with metallic magnesium in the presence of LiCl in THF. This procedure allowed the preparation of stock solution of TMPMgCl·LiCl **96** that could be storage over one month (Figure 14).

Titration was performed using a known amount of benzoic acid and 4-(Phenylazo)diphenylamine (PDA) as colorimetric indicator in THF (BLUMBERG; MARTIN, 2015).

TMPMg·2LiCl **97** were generate *in-situ* through reaction between TMPMgCl·LiCl **96** (stock solution) and TMPLi (BOUDET; LACHS; KNOCHEL, 2007; CLOSOSKI; ROHBOGNER; KNOCHEL, 2007) (Figure 14).
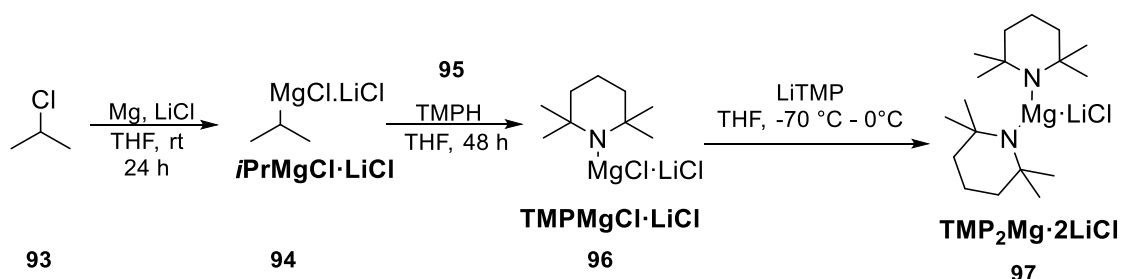
Figure 14. Mixed Mg/Li bases.

LDA **100** and TMPLi **99** were prepared *in-situ* and used in the same day of the experiment. They were synthetized treating a cooled (-70 °C) solution of fresh distilled diisopropylamine **98** or 2,2,6,6-tetramethylpiperidine (TMPH) **95** in THF with *n*-BuLi (Figure 15).
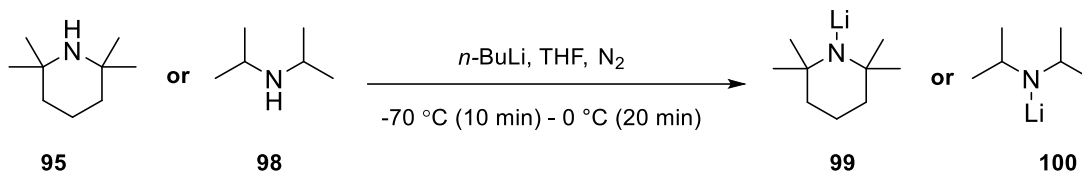
Figure 15. Lithium bases.

3.3 Metalation study of dimethyl indolizine-1,2-dicarboxylate 1 using lithium amides and Mg amides complexed with LiCl.

Aiming understand the reactivity of dimethyl indolizine-1,2-dicarboxylate **1** face lithium amides and Mg amides complexed with LiCl, we started this study by evaluating each base and varying some parameters as loading of base, temperature, time and presence of additive. The results are summarized in Table 2.
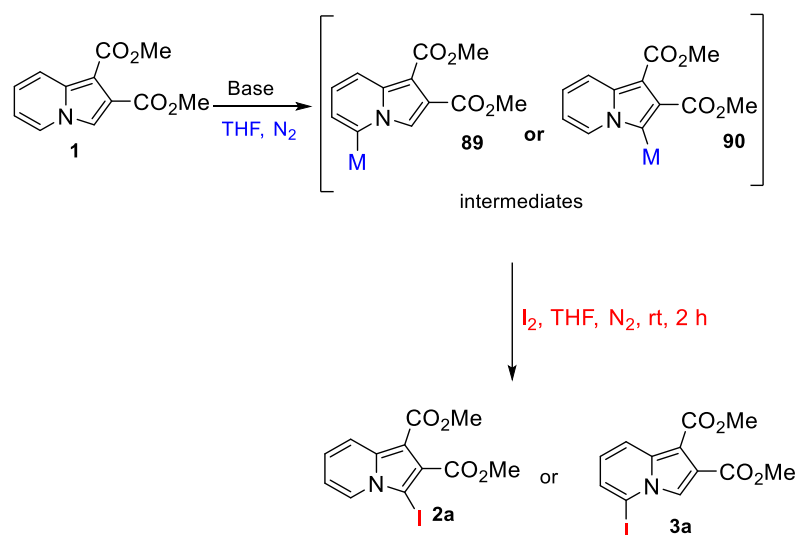
Table 2. Evaluation of the best condition to promote a regioselective metalation of **1**.

Entry	Base	Additive	Nº de Eq.	Temp. (ºC)	Time (h)	3a (%)*	2a (%)*
a	TMPLi		1.5	0	1	-[a]	-
b	TMPLi		1.8	0	1	37	-
c	TMPLi		2.0	0	2	40	-

	Base	Additive	Equiv.	T (°C)		Conversion*	
d	LDA		1.5	0	1	Complex mixture	-
e	LDA		1.8	-20	1	-	-
f	TMPMgCl·LiCl		1.5	25	1	-[a]	-
g	TMPMgCl·LiCl		1.5	25	2	-[a]	-
h	TMPMgCl·LiCl		1.8	25	1	30%	-
i	TMPMgCl·LiCl		1.8	25	2	40%	-
j	TMPMgCl·LiCl	ZnCl$_2$ (1,2 eq.)	1.8	0	1		-
k	TMPMgCl·LiCl	ZnCl$_2$ (0,6 eq.)	1.8	0	1		-
l	TMPMgCl·LiCl		2.0	25	1	49%	-
m	TMPMgCl·LiCl		2.0	25	2	98%	-

*Conversion determinate by GC-MS between starting material and product.
[a]NR – reaction not observed – only starting material found.

All tests were made using 0.5 mmol of indolizine **1** dissolved in THF (2 mL) followed by dropwise addition of the respective base or when using TMPLi or LDA the solution of indolizine **1** was dropwise to the *in-situ* prepared base.

Surprisingly, indolizine **1** was not suitable to regioselective metalation using TMPLi and LDA amides (Table 2, entries a-e). When 1.5 equivalents of TMPLi (Table 2, entry a) were used, no product was found and by increasing the equivalents up to 1.8 (Table 2, entry b) only 37% of conversion into product **3a** (C-5 functionalized) was observed. Thereby, taking inspiration in the Amaral and co-workers study (AMARAL et al., 2015) that showed LDA as a good base to drive a base-controlled regioselective approach in indolizines decorated with esters, some experiments using LDA were performed. However, using 1.5 equivalents at 0 °C (Table 2, entry c) a complex mixture of unidentified products was noted in the GC/MS. By decreasing temperature to -20 °C

and using 1.8 equivalents of base (Table 2, entry d) no product was detected, remaining only starting materials.

After those unsatisfactory results we decided explore another kind of base. The Mg amide complexed with LiCl (TMPMgCl·LiCl) first reported by Knochel and co-workers has been the subject of study in our research group for a while (AMARAL et al., 2015; BATISTA et al., 2015; SANTOS et al., 2015; BOZZINI et al., 2017; MURIE et al., 2018; BERTALLO et al., 2019). This new class of base has some advantages over lithium amides, such as greater solubility in organic solvents, higher stability allowing good regioselectivity at room temperature and the possibility of design new aromatic or heteroaromatic reagents containing sensitive functional groups (nitrile, ester, ketone, amide, aldehyde).

In the first test, 1.5 equivalents of TMPMgCl·LiCl (Table 2, entry f) were reacted with indolizine **1** at room temperature for 1 hour followed by addition of 1.8 equivalents of iodine. However, no product was observed. The same result was obtained when the reactional time was increased to 2 hours (Table 2, entry g). For this reason, in the subsequent experiments, influence of the number of equivalents of base, temperature and presence of coordinating additives were evaluated. Using 1.8 equivalents of base at room temperature for 1 or 2 hours (Table 2, entries h and i) a small conversion into product **3a** was observed in 30% and 40%, respectively.

Based on Nishimura work (NISHIMURA, 2019) in which addition of $ZnCl_2$ or $ZnCl_2 \cdot 2LiCl$ enable regioselective functionalization of 5-bromoisoquinolines, we decided test the addition of $ZnCl_2$ to our system. Nishimura explained that the complexation of these additives with their substrate promoted a decrease of the pKa values for the neighbouring hydrogens which led to a regioselective approach. Nevertheless, in our experiments no product was detected, remaining only starting material in the end of reaction (Table 2, entries j and k). It was hypothesised that the complexation of indolizine **1** with this coordinating agent ($ZnCl_2$) preclude the access of this bulky base (TMPMgCl·LiCl) to the neighbouring hydrogens which have become really blocked after the complexation and because of that the deprotonation was thwarted.

New attempts were made and using 2.0 equivalents of TMPMgCl·LiCl at 25 ºC for 1 hour (Table 2, entry l) it was observed by GC-MS analyse 49% conversion into the desired product. In order to improve the formation of product, the number of equivalents employed was kept in 2.0 equivalents and the reaction time was increased

to 2 hours (Table 2, entry m) leading to 98% conversion of the starting material. Product **3a** was further isolated in 87% yield and the assignments were made with the support of the ^{13}C NMR, ^{1}H NMR, techniques confirming that iodine was inserted at C-5 position of the indolizine ring. The key points that helped to identify this compound as C-5 iodine derivative were the disappearing of the signal in 7.93 *ppm* (H-5) and a shift to lower field observed for hydrogen H-3 (7.97 *ppm*) (Figure 16).
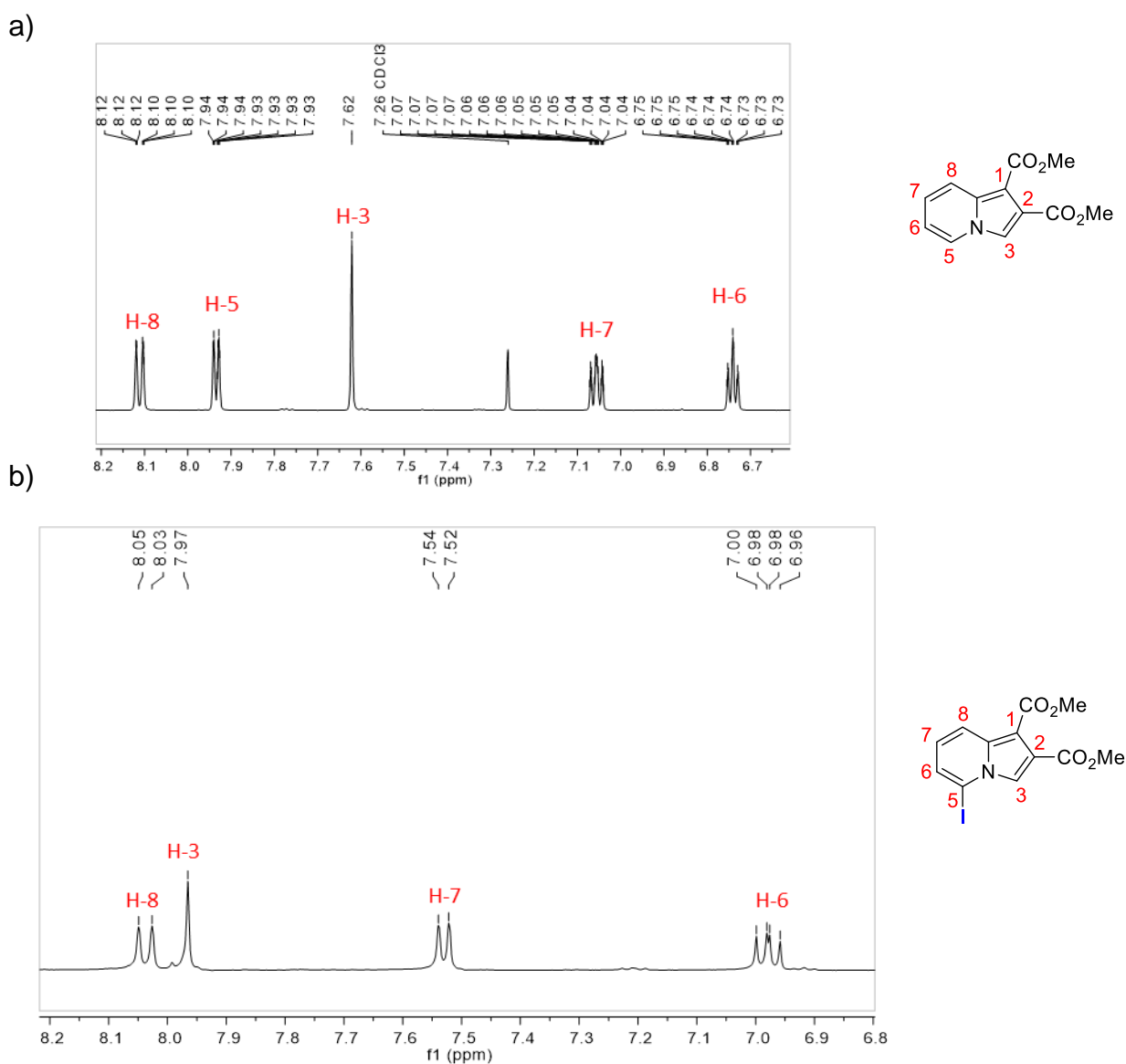
Figure 16. a) ^{1}H NMR spectrum of indolizine **1** (400 MHz, CDCl$_3$). b) ^{1}H NMR spectrum of indolizine **3a** (400 MHz, DMSO-d$_6$).

In order to investigate the scope and versatility of this methodology other electrophiles, such as DMF, diphenyl disulphide, diphenyl diselenide, hexachloroethane, benzaldehyde and others, were evaluated. However, it was only possible to obtain products **3b** and **2b** since in the other attempts either start material or a complex mixture of unidentified products were recovered. (Scheme 26).

After characterization of the obtained products, we could conclude that functionalization has occurred at C-3 or C-5 position depending on the electrophile used.
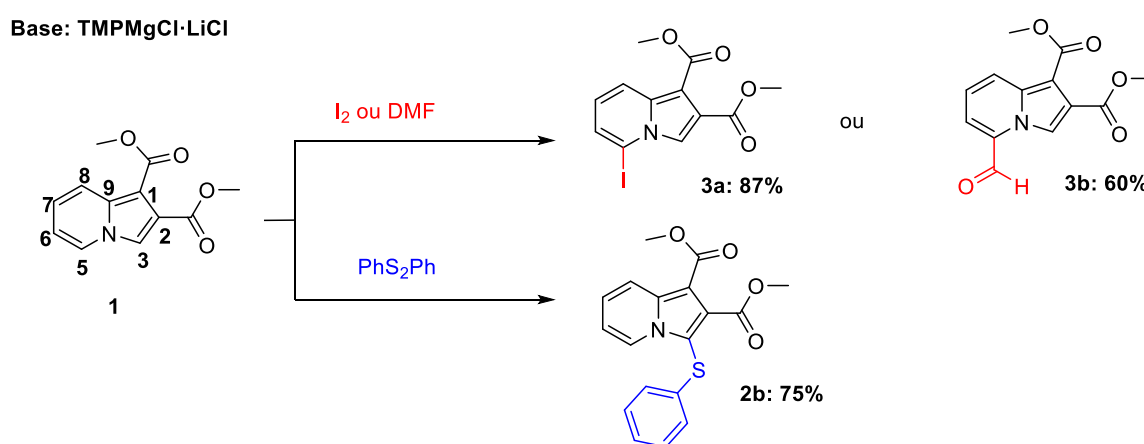
Scheme 26. C-3 or C-5 dimethyl-1,2-indolizine carboxylate derivatives obtained through the metalation approach using TMPMgCl·LiCl.

For compound **3b** we can see in the ^{1}H NMR spectrum the disappearing of the signal referring to H-5 in 7.93 *ppm* and a shift to lower field for the H-3 (9.01 *ppm*). This can be explained by a *peri-effect* caused by magnetic anisotropy of the 5-formyl group located at the *peri-position* with proton H-3 (Figure 17). The same can be noted for parent indolizines that contain ester groups attached to C-1 or C-1/C-2, C-3 and C-8 position. In these molecules it is observed a downfield shift for the hydrogens H-8, H-5 or H-1 respectively (Figure 17).

On the other hand, in the ^{1}H NMR spectrum of compound **2b** there is the disappearing of the singlet signal referring to H-3 (in the starting material located at 7.62 *ppm*) confirming the substitution at this position (Figure 17).
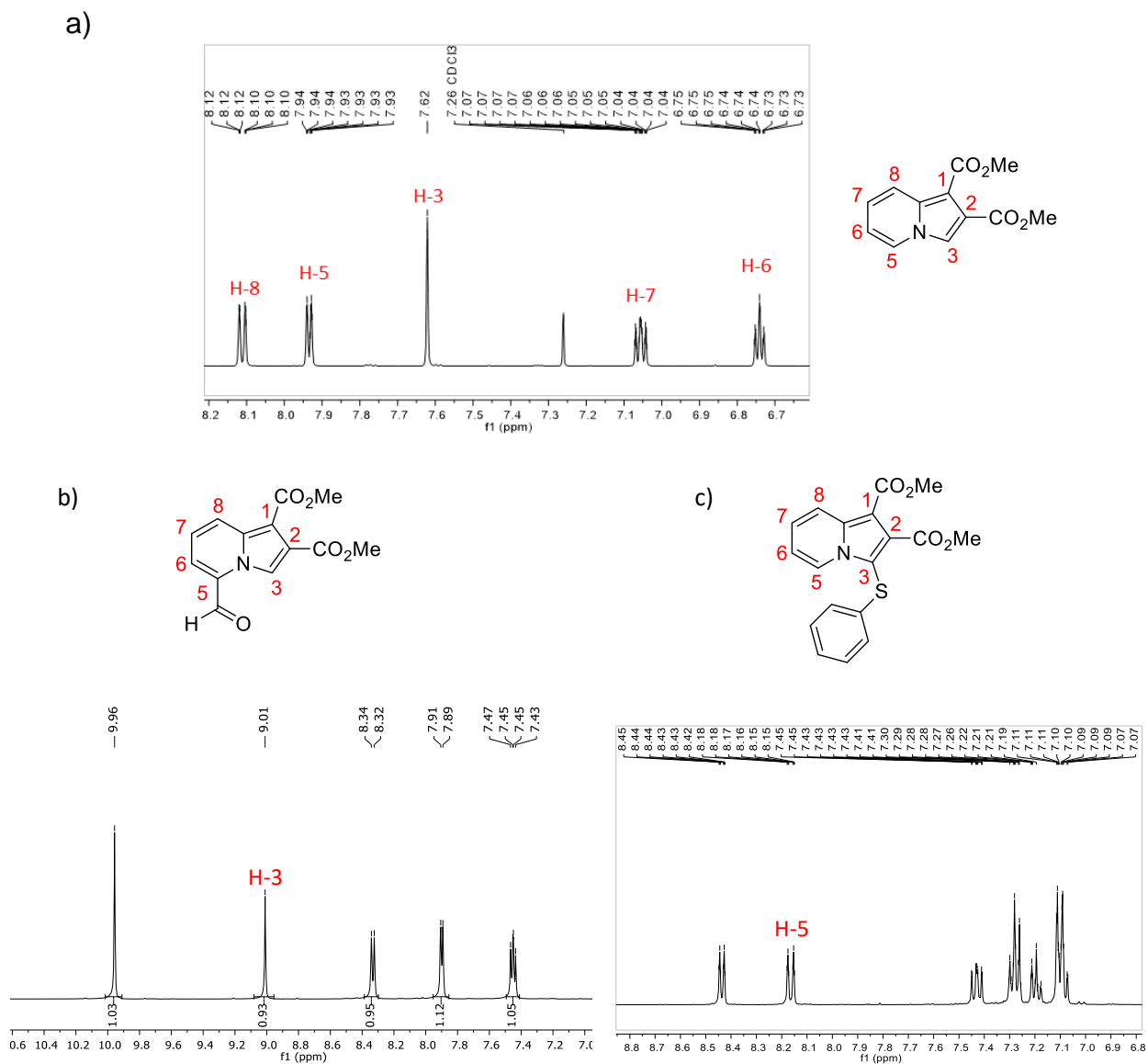
Figure 17. a) ^{1}H NMR spectrum of indolizine **1** (400 MHz, CDCl$_3$). b) ^{1}H NMR spectrum of indolizine **3b** (400 MHz, DMSO-d$_6$). c) ^{1}H NMR spectrum of indolizine **2b** (400 MHz, DMSO-d$_6$).

To better understand this electrophile-dependent selectivity, two experiments were carried out using TMSCl. The literature (BRIKCI-NIGASSA et al., 2018) show the possibility of trapping organometallic intermediates with TMSCl as soon they are formed and this may help to understand which regioisomer is formed first when the substrate has more than one proton that can be deprotonated.

In the first experiment, TMSCl was added (4 equivalents) to the reaction vial containing dimethyl indolizine-1,2-dicarboxylate **1** prior to the addition of 2 equivalents of TMPMgCl·LiCl. This order of addition was rationalized so that the first organometallic intermediate formed was trapped with TMSCl immediately after its formation (see scheme in Table 3). Aliquots of this reaction were taken at 10 min, 30 min, 1 h, 2 h, 3 h 4 h and 5 h. In the second experiment, after 5 hours of reaction at room temperature with TMPMgCl·LiCl (2 equivalents; this is the standard protocol used in directed metalation reactions with other electrophiles), TMSCl (4 equivalents) was added as electrophile. All aliquots were analysed using GC-MS. Results obtained are summarized in Table 3.
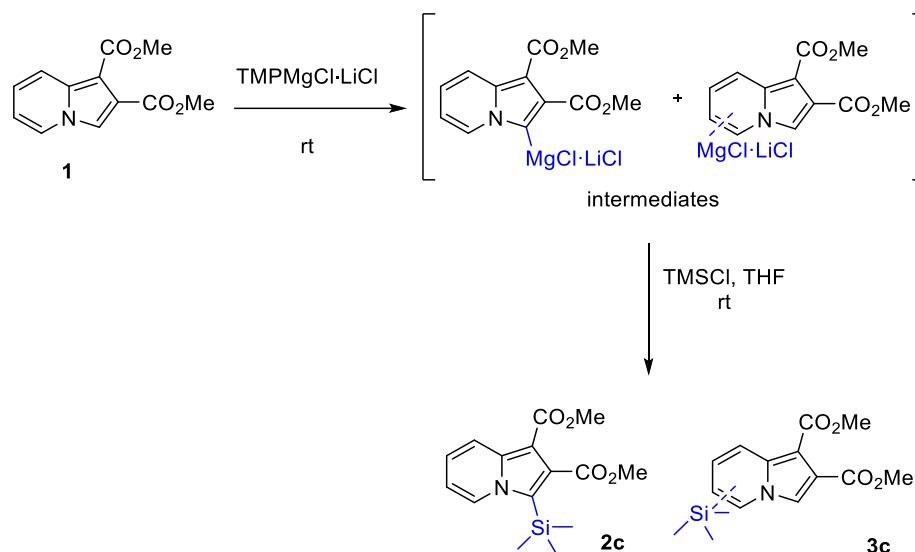
Table 3. *In-situ* tapping test with TMSCl.

Entry	Time (min)[a]	2c (%)[b]	3c (%)[c]
a	10	40	-
b	30	50	1
c	60	63	2
d	120	68	4
e	180	75	5
f	240	80	6
g	300	85	7
H[d]	300	88	7

[a] Time: aliquots were colected whrn TMSCl was added in the begining of the reaction.
[b] Conversion determined by CG-MS.
[c] another regioisomer found by CG-MS analyse
[d] TMSCl added after 5 hours reaction.

We could observe the presence of a silylated product (40% conversion) within 10 minutes reaction (Table 3, entry a). This quickly formation of product was not observed when the rection was carried out without the addition of TMSCl (usually the first products start being detected within 40 minutes reaction, before that time it was detected only start material). In the subsequent experiments, where the reactional time was always increased, an unidentified regioisomer (**2c**) started being detected by GC/MS (Table 3, entries b-h). During these tests we observed the presence of only two regioisomers and after purification and characterization through NMR analyses it was proven that the major product observed in the GC/MS data was the C-3 silylated product **2c**. In the ^{1}H NMR spectrum there is the loss of the singlet signal referring to

hydrogen H-3 (7.62 *ppm*) which confirm the pattern of substitution at C-3 position (Figure 18).

Unfortunately, it was not possible to obtain an enough quantity of the other regioisomer for to do the proper characterization. However, we believe that this may be the C-5 silylated, according to what was observed in reactions with different electrophiles.
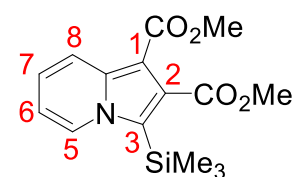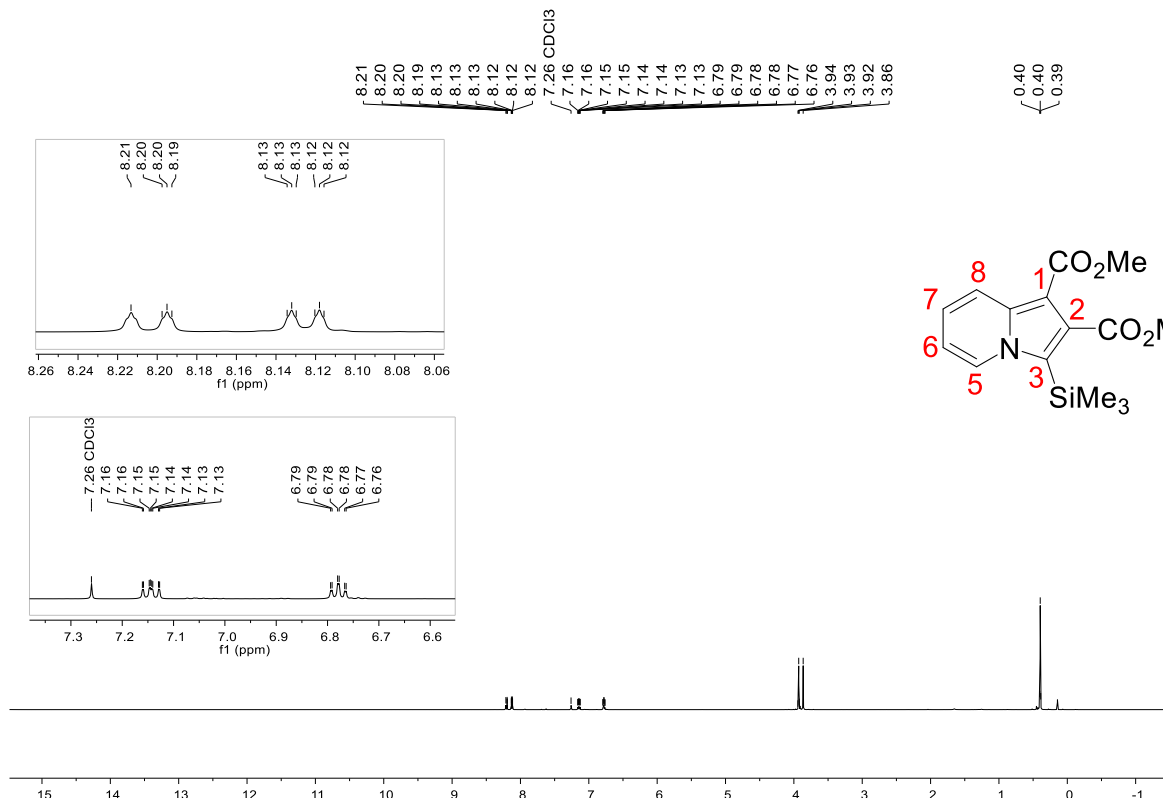
a)
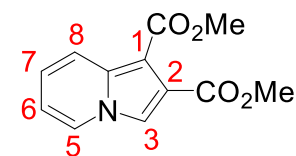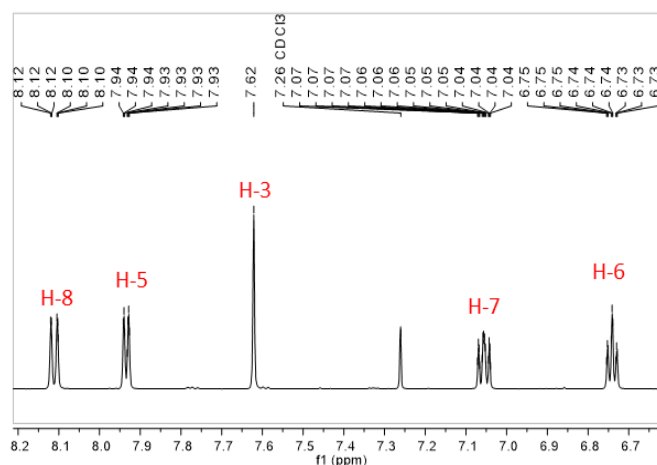
b)

Figure 18. a) ^{1}H NMR spectrum indolizine **1** (400 MHz, CDCl$_3$). b) ^{1}H NMR spectrum indolizine **2c** (400 MHz, CDCl$_3$).

It is known that TMPMgCl·LiCl can promote *ortho*-metalation in substrates that contain a DMG group. This effect can be explained by CIPE complex theory (Complex-Induced Proximity Effect) (MONGIN; QUÉGUINER, 2001; WHISLER et al., 2004). According to CIPE effect, DMG groups may push to *ortho*-metalation in two ways: (1) by chelation (a) stabilizing the metal in the *ortho* position or (b) by chelation in the transition state or (2) by inductive effect (c) stabilizing the negative charge in the *ortho* position and/or (d) decreasing the pKa of the hydrogen atom adjacent to it (Figure 19).
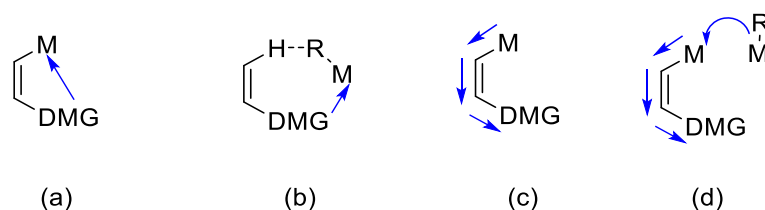

Figure 19. Efeito do Complexo CIPE.

With the data obtained in the experiments described above and with the pKa values of the dimethyl indolizine-1,2-dicarboxylate hydrogens (calculated using the software B3LYP / 6-31 + G (d, p) level in Gaussian 03 software) we weave some possible explanations for the selectivity observed in these reaction (Figure 20).
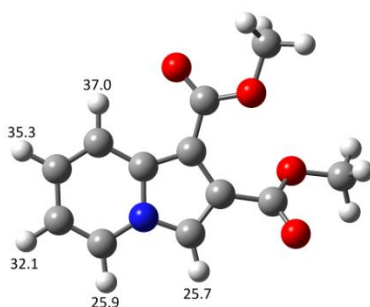
dimethyl indolizine-1,2-dicarboxylate **1**

Figure 20. pKa values for indolizine **1**.

According to the pKa values, it is observed that the hydrogens H-5 (pKa 25.9) and H-3 (pKa 25.7) have approximately equal acidity values and because of that we believe that there may be a dynamic equilibrium between anionic species **89** and **90** (Scheme 27). We hypothesized that the generation of intermediate C-3 is preferred due to a chelating effect of the magnesium counter ion from TMPMgCl·LiCl with the indolizine **1** ester group (Figure 21).
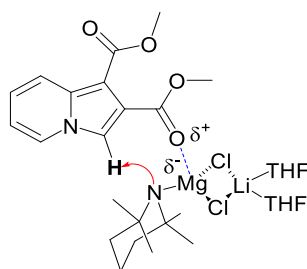
Figure 21. Chelation of indolizine **1** with TMPMgCl·LiCl.

This hypothesis is corroborated with the data observed in the trapping experiment with TMSCl, where the majority product obtained is the silylated C-3 **2c**. However, we believe that coordinating electrophiles such as I_2 can break the chelation, which may lead to an equilibrium for species type 5 (less sterically hindered) that continue towards the formation of the substituted C-5 product. In this case, we also cannot rule out that a halogen dance is taking place since an excess of TMPMgCl·LiCl is used (MILLER et al., 2010).

On the other hand, we observed that when non-coordinating reagents such as $ZnCl_2$ (used in Negishi cross-coupling reactions) are used, the C-3 arylated derivative is the only formed product. We speculate that it happens due to the quick reaction between the first organometallic species formed (ionic species C-3) with the non-coordinating reagent. Therefore, there is no time for equilibration to form with ionic species C-5, leading exclusively to arylated C-3 products (compounds **2c** and **2d** in Scheme 27).
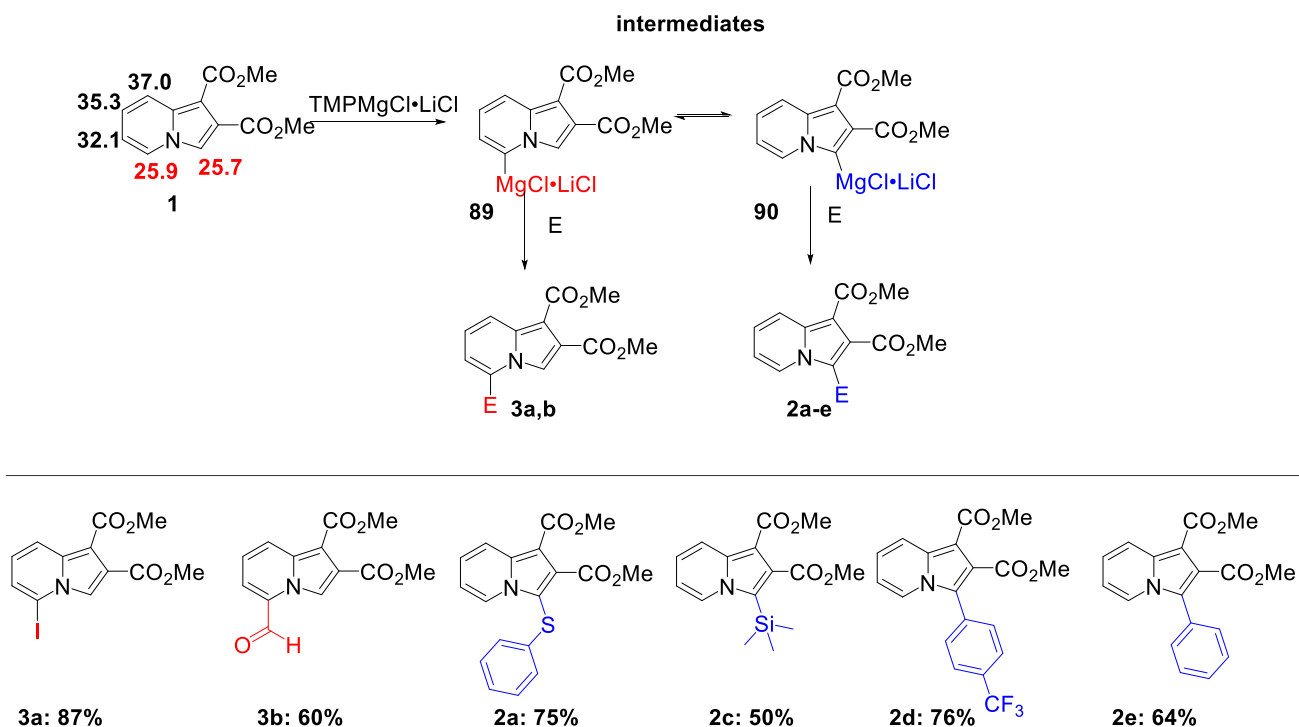
Scheme 27. Proposed equilibrium between C-3 and C-5 magnesium intermediates leading to C-3 or C-5 substituted indolizine derivatives.

Two arylated C-3 derivatives (**2d** and **2e**, Scheme 27) were synthesized through Negishi cross-coupling approach.

Negishi cross-coupling mechanism proceed via standard Pd catalysed cross-coupling pathway (Figure 22). In the first step of the catalytic cycle Pd(0) is oxidised to Pd(II) through an oxidative addition involving organohalides species. These organohalides can be aryl, vinyl, alkynyl, and acyl halides, acetates, or triflates reagents. Next, an organozinc specie exchanges its organic substituent with the halide in the Pd(II) complex, generating the trans-Pd(II) complex and a zinc halide salt. In the final step, there is a reductive elimination yielding the coupled organic product and regenerating the Pd(0) catalyst (Figure 22).
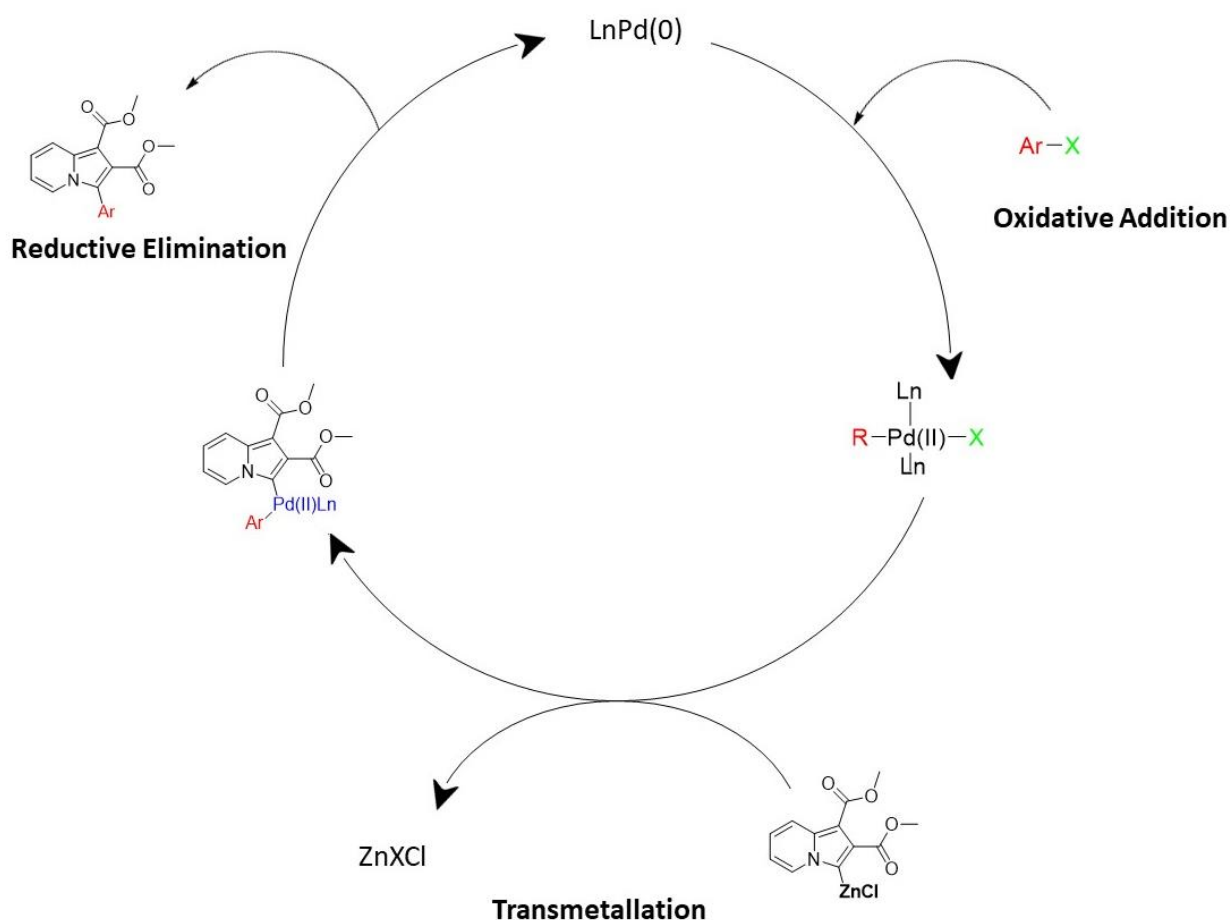
Figure 22. Palladium catalysed cross-coupling pathway.

In the first attempt, after metalation reaction with TMPMgCl·LiCl, a solution of ZnCl$_2$ 1 M was added to the reactional medium and the temperature was kept in -40 °C for 20 minutes. Subsequently, 10 mol% of Pd(PPh$_3$)$_4$ was added followed by the respective aryl halide and the reaction remained under reflux for 12 hours. However, only starting materials were detected by CG/MS analysis.

Being the trasmetallation reaction of organomagnesium with solution of ZnCl$_2$ the key step for the success of this type of coupling, we decided to carry out a more detailed study on the reaction conditions for this step, which involved variations in temperature, reaction time and the number of equivalents of ZnCl$_2$ used. The performed experiments are described in Table 4.
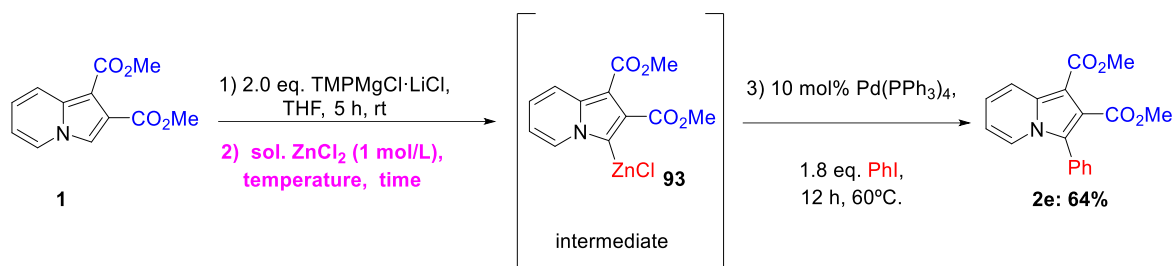
Table 4. Evaluation of the best conditions to promote transmetallation in **1**.

Entry	Eq. ZnCl$_2$[a]	Time (min)[b]	Temperature (°C)	2e (%)[c]
a	1	20	-20	-
b	1	30	-20	-
c	2	30	-40	-
d	1	30	-40	-
e	2	30	0	80
f	1	30	0	65
g	1	30	rt	70
h	2	30	rt	82 (64)[d]

[a] Solution of ZnCl$_2$ in THF (1 mol/L).
[b] Time for trasmetallation step.
[c] Conversion determinated by CG-MS.
[d] Isolated yield.

As it was not possible to isolate the organozinc intermediate **93** formed after the trasmetallation step (see scheme in table 4) the success of that step was monitored by CG/MS based on the presence of the desired arylated product **2e** after the work-up of the reaction.

During the first experiments (Table 4, entries a-d) it was observed that, regardless of the number of equivalents of ZnCl$_2$ used and the reaction time when this reaction was carried out under low temperatures (-40 °C or -20 °C) there was no formation of the desired product **2e** since only the starting material **1** was detected.

Nonetheless, when the experiments were carried out at room temperature or at 0 °C the formation of the arylated product **2d** was observed in conversions varying from 65% to 80% (Table 4, entries e-h). Best results were achieved when 2.0 equivalents of ZnCl$_2$ in THF were used. Due to practical reasons, we have adopted room temperature as the standard procedure. By using this reaction condition, the use of BrC$_6$H$_4$CF$_3$ as aryl halide allowed the preparation of **2d** in 76% yield (see Scheme 27).

The expanded ^{1}H NMR spectrum for compound **1** and **2d** are shown below. All assignments presented here were confirmed with the aid of bidimensional techniques such as HSQC, HMBC, COZY and NOESY. Only the relevant aspects which led to the characterization of compound **2d** as a C-3 derivative were highlighted.

In Figure 23a (^{1}H NMR spectrum of the indolizine **1**) it is possible to observe the presence of a singlet at 7.62 ppm referring to the H-3 hydrogen. Figure 23b shows the loss of this signal indicating a substitution at this carbon.
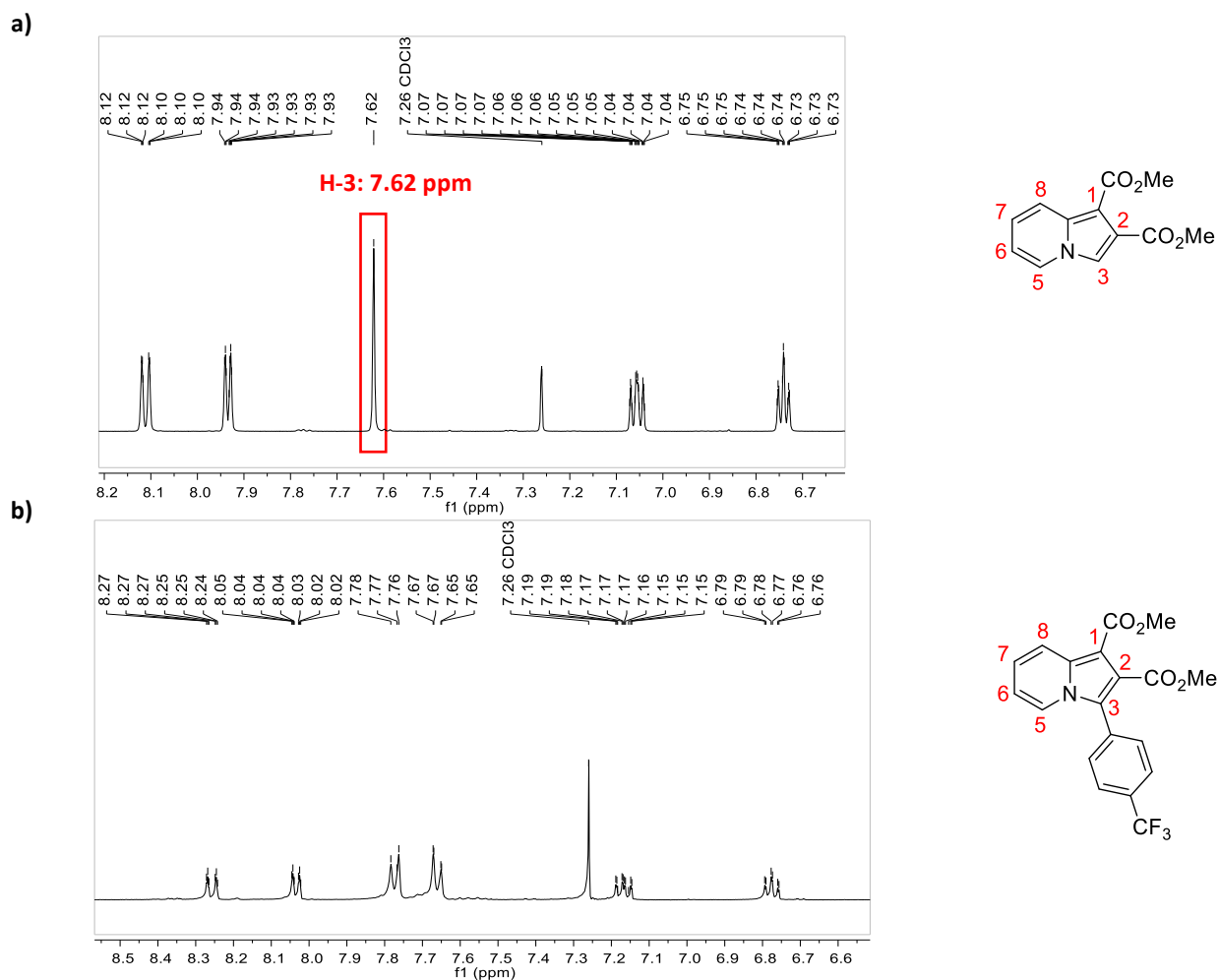
Figure 23. a) ^{1}H NMR spectrum of indolizine **1** (400 MHz, CDCl$_3$). b) ^{1}H NMR spectrum of indolizine **2d** (400 MHz, CDCl$_3$).

In addition, through the analysis of the NOESY spectrum of compound **2d**, it was possible to assemble the correlations between hydrogens H-5 (δ 8.33 ppm) and H-6' (δ 7.66 *ppm*), H-5 (δ 8.33 ppm) and H-6 (δ 6.98 ppm) which confirm that the substitution occurred in hydrogen H-3 and not in H-5 (Figure 24).
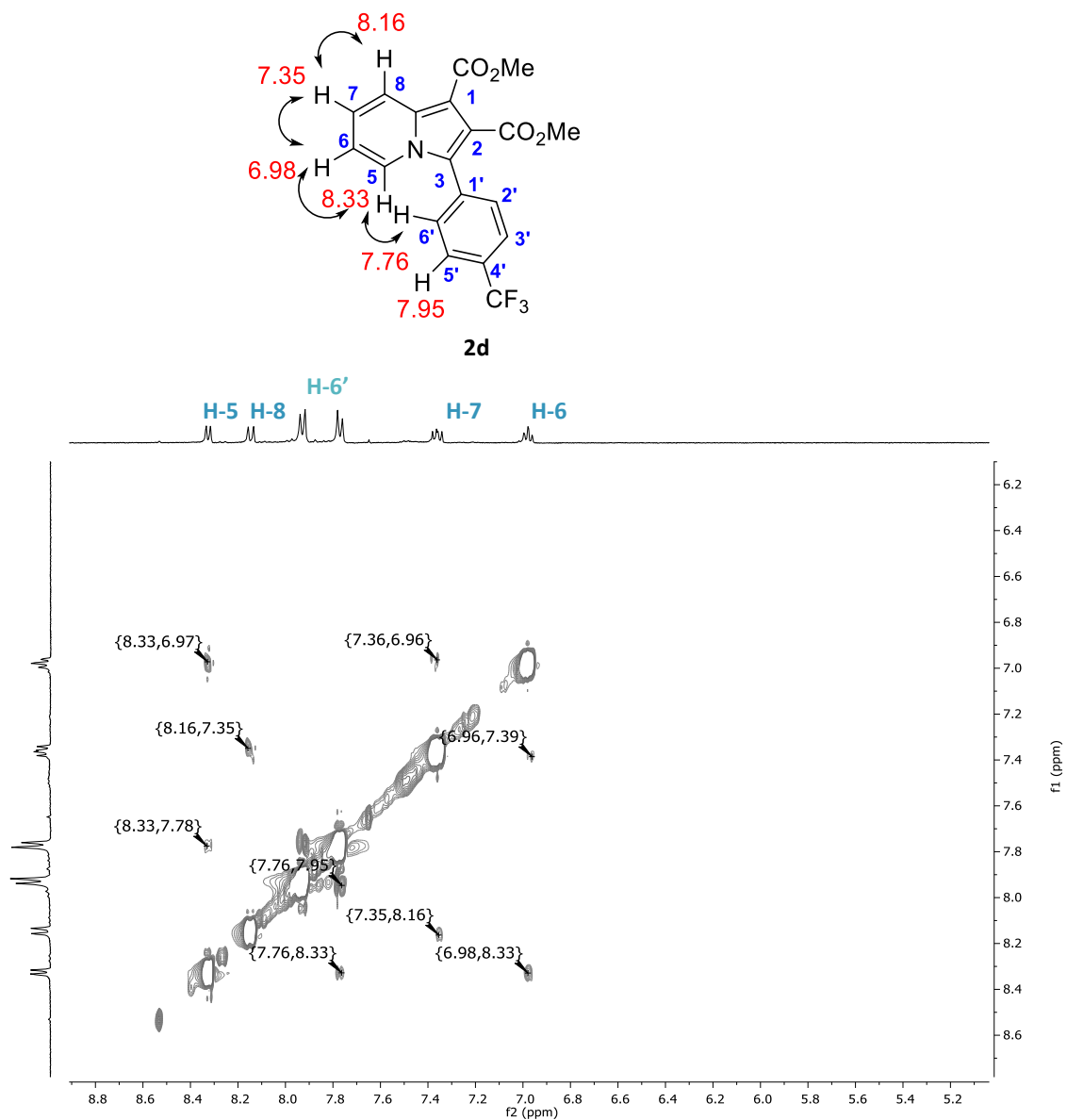
Figure 24. NOESY spectrum for molecule **2d** (DMSOd$_6$, 400MHz).

3.4 Metalation study of 2-(indolizin-1-yl)-4,4-dimethyl-4,5-dihydrooxazole 4 using lithium amides and Mg amides complexed with LiCl

Moving forward with the metalation studies, indolizine **4** was reacted with different organometallic bases in order to find the best base capable to promote successful regioselective deprotonation. For that, different reaction conditions were tested, and the results obtained are shown in Table 5.
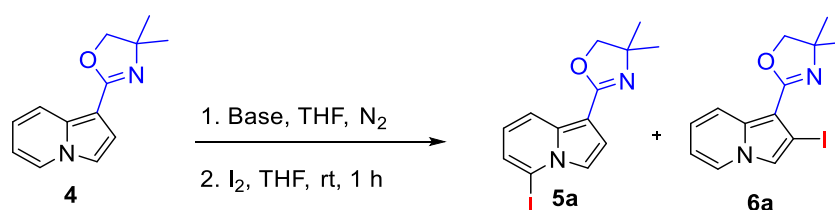
Table 5. Evaluation of reaction conditions to promote a regioselective metalation of **4**.

Entry	Base	Eq.	Time (h)	Temp. (°C)	Conversion[a] (%)	Product	Yield* (%)
a	TMPMg·LiCl	1.8	2	rt	51	**6a**	
b	TMPMg·LiCl	2.0	1	rt	83	**6a**	**78**
c	TMPMg·LiCl	2.0	2	rt	85	**6a**	79
d	LDA	1.4	0.5	0	35	**5a**	
e	LDA	1.4	1	0	53:3[b]	**5a/6a**	
f	TMPLi	1.4	0.5	0	42	**5a**	
g	TMPLi	1.4	1	0	55:25[b]	**5a/6a**	
h	TMPLi	1.5	0.5	0	60:23[b]	**5a/6a**	
i	TMPLi	1.5	1	0	81:12[b]	**5a/6a**	
j	*n*-BuLi	1.1	1	-70	30	**5a**	
k	*n*-BuLi	1.5	2	-70	57	**5a**	
l	*n*-BuLi	1.7	2	-70	97	**5a**	**88**

[a] Conversion determined by CG-MS.
[b] regioisomer iodine product was detected.
*Isolated yield.

All tests were made using 0.3 mmol of indolizine **4** dissolved in THF (1.5 mL) followed by dropwise addition of the respective base. When using TMPLi or LDA the solution of indolizine **4** in THF was dropwise to the *in-situ* prepared base.

Based on the metalation results found for indolizine **1**, we start the screening by using 1.8 equivalents of TMPMg·LiCl at room temperature for 2 hours (Table 5, entry a). However, after the reaction quench with iodine, only 51% of an iodide derivative was detected by CG/MS analysis. After purification, the C-2 substituted indolizine **6a** was confirmed by NMR analysis. Subsequently, the amount of base was increased to 2.0 equivalents and the reaction was analysed over 1 and 2 hours (Table 5, entries b and c). In these experiments, the iodide derivative **6b** was detected in 83 and 85%

yields, respectively. It is important to highlight that tests using 2.5 and 3.0 equivalents of base were made and no increase in the conversions into the desired product were observed.

When using 1.4 equivalents of TMPLi or LDA for 30 minutes at 0°C (Table 5, entries d and f) we could observe the formation of a different iodide derivative **5a** (regioisomer) in 35 and 42% yields, respectively. Attempts performed with increased reaction time and equivalents of base (Table 5, entries e, g-i) led to a mixture of isomers **5a** and **6a** being **5a** the major product (C-5 substituted). The isomers were characterized by 1D and 2D NMR techniques.

After analysing the pKa values for indolizine **4** (calculated using the software B3LYP / 6-31 + G (d, p) level in Gaussian 03 software), we decided use *n*-BuLi to try to promote the selective deprotonation at C-5 position (H-5 pKa 28.9 – Kinect product). In the first attempt 1.1 equivalents of *n*-BuLi were reacted with indolizine **4** at -70°C for 1 hour (Table 5, entry j) and only 30% of product **5a** was detected by CG/MS. Increasing the number of equivalents up to 1.7 equivalents (Table 5, entries k and l) and leaving the reaction for 2 hours it was possible to observe a chromatographic conversion into the desired product of 57% and 97% respectively, without the presence of isomer **6a**.
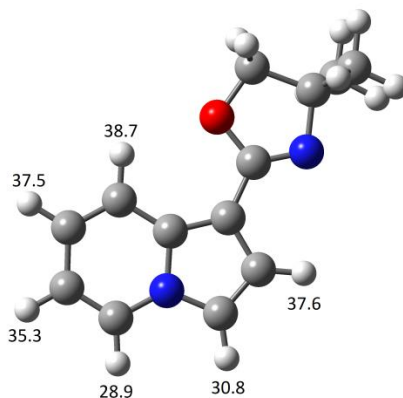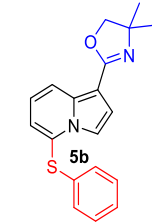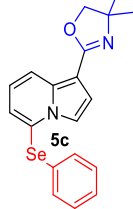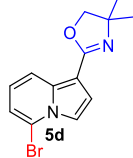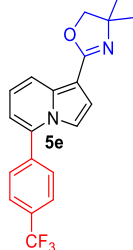

Figure 25. pKa Values for indolizine **4**.

With this base-controlled regioselective method in hands we decided to expand the scope of that methodology using different electrophiles in order to show its versatility and synthetic applicability. Thus, a small library of functionalized indolizines was built, results are shown in Table 6.
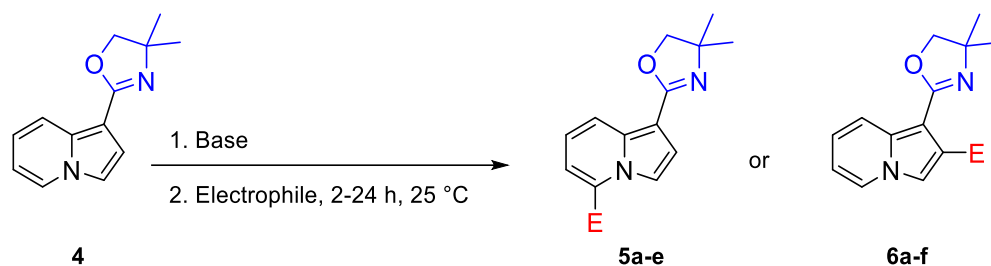
Table 6. Directed metalation of indolizine **4** followed by reaction with different electrophiles.

Entry	Base	Equiv.	Temp. (°C)	Time (h)	Electrophile	Product	Yield
a	TMPMgCl·LiCl	2.0	rt	1	I_2	6a	78
b	TMPMgCl·LiCl	2.0	rt	1	DMF	6b	63
c	TMPMgCl·LiCl	2.0	rt	1	$(C_6H_5S)_2$	6c	77
d	TMPMgCl·LiCl	2.0	rt	1	$(C_6H_5Se)_2$	6d	91
e	TMPMgCl·LiCl	2.0	rt	1	$(BrCCl_2)_2$	6e	79
f	TMPMgCl·LiCl	2.0	rt	1	$Br(C_6H_4)CF_3$[a]	6f	82
g	*n*-BuLi	1.7	-70	2	I_2	5a	80

h	*n*-BuLi	1.7	-70	2	$(C_6H_5S)_2$		60
i	*n*-BuLi	1.7	-70	2	$(C_6H_5Se)_2$		70
j	*n*-BuLi	1.7	-70	2	$(BrCCl_2)_2$		75
k	*n*-BuLi	1.7	-70	2	$Br(C_6H_4)CF_3$[b]		74

[a] Negishi cross-coupling (trasmetallation with $ZnCl_2$ 1M at rt followed by addition of 10 mol% of $Pd(PPh_4)_3$).
[b] Negishi cross-coupling (trasmetallation with $ZnCl_2$ 1M at -70°C-ta (30min) followed by addition of 10 mol% of $Pd(PPh_4)_3$) and $Br(C_6H_4)CF_3$.

We observed that in all experiments using TMPMgCl·LiCl exclusively C-2 derivatives were synthetized in good to excellent yields (63-91%) (Table 6, entries a-e). We believe that despite the H-5 (see Figure 25) be the most acidic hydrogen (pKa 28.9) the C-2 deprotonation (H-2 pKa 37.3) was favoured due to the chelation effect between magnesium counter ion from base and nitrogen present in the oxazoline ring in substrate **4** (Figure 26).
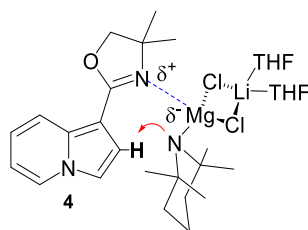

Figure 26. Chelation between indolizine **4** and TMPMgCl·LiCl.

On the other hand, using *n*-BuLi (strong and less hindered base – pKa 50) it was possible synthesize selectively the C-5 derivatives (Table 6, entries g-j). These results

agree with the knowledge that strong and less hindered bases prefers to react with the most acidic proton present in the molecule, in this case H-5 (pKa 28.9).

Regarding Negishi cross-coupling reaction (Table 6, entries f and k) we tried to use the same condition applied to indolizine **1** (1.0 equivalents $ZnCl_2$, room temperature for 30min) in both approaches (with TMPMgCl·LiCl and *n*-BuLi*)* however no coupling product was observed. Because of that, we decided to conduct a study on the best reactional conditions to promote effective trasmetallation reaction between the organometallic intermediates (**94** and **95)** and $ZnCl_2$. The results are described in   .

5e: 74%   6f: 82%
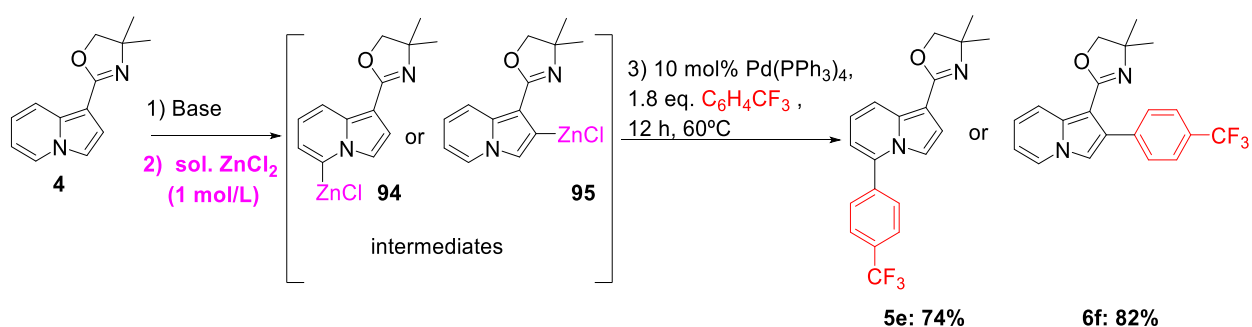
Table 7. Trasmetallation study to indolizine **4**.

Entry	Base	Equiv. $ZnCl_2$[a]	Time (min)[b]	Temp. (°C)	Product[c]	Yield
a	TMPMgCl·LiCl	2	30	ta	3d: 34%	
b	TMPMgCl·LiCl	1	30	ta	3d: 98%	82
c	TMPMgCl·LiCl	1	30	0	3d: 98%	
d	*n*-BuLi	2	30	0	3c: 10%	
e	*n*-BuLi	1	30	-20	3c: 10%	
f	*n*-BuLi	1	30	0	3c: 15%	
g	*n*-BuLi	2	30	-70-ta	3c: 95%	74

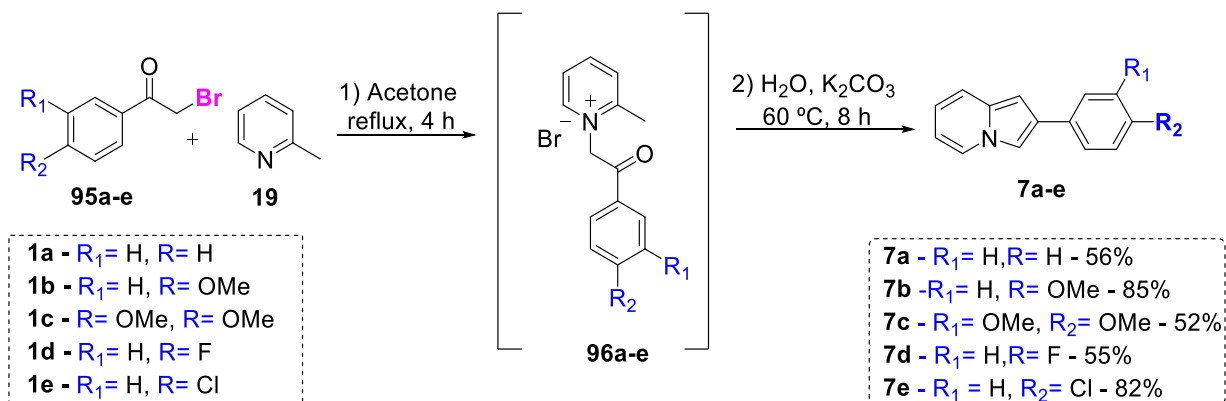[a] Solution of $ZnCl_2$ in THF (1 mol/L).
[b] Transmetallation time.
[c] GC/MS conversion.

According to the results that were based on the yields of the arylated product **6f**, the best condition for found for the Mg/Zn trasmetallation used 1.0 equivalent of $ZnCl_2$ (1 mol/L) at room temperature for 30 minutes. Moreover, the Li/Zn transmetallation using excess of $ZnCl_2$ (2 equivalents), with the solution salt addition at -70°C followed by warming up to room temperature for 30 minutes gave the best results. By using these protocols, the new arylated derivatives **5e** and **6f** could be isolated in 82% and 74% isolated yields, respectively.
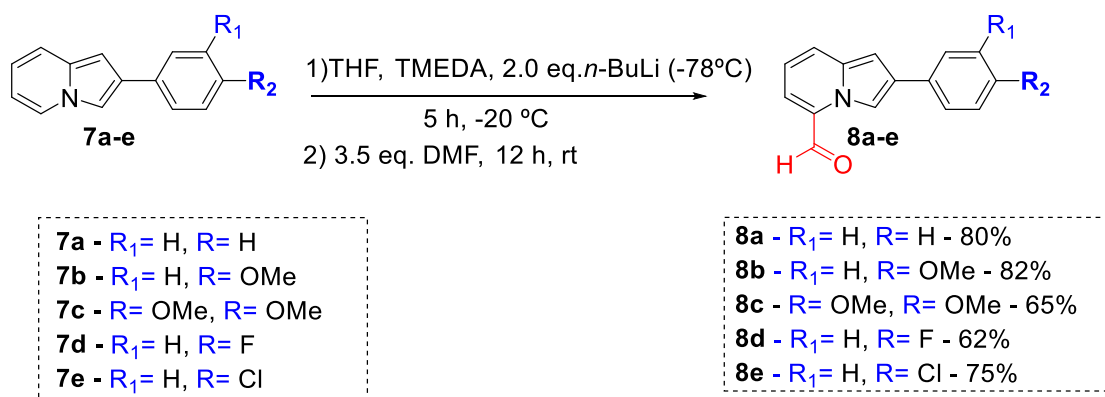
3.5 Formylation of 2-arylindolizines

In 2014, our research group reported the synthesis and photophysical properties of 2-aryl-indolizines functionalized with aryl or heteroaryl groups (AMARAL et al., 2014). In order to expand our knowledge in this area some new carbonylated 2-arylindolizines have been synthesized.

We have started our studies preparing 2-aryl-indolizines **7a-e** using the Tschitschibabin approach. In the first step, reaction between 2-picoline **19** and α-bromo-ketones type **95a-e** led to intermediary pyridinium salts **96a-e**. After solubilization in water these salts have undergone an intramolecular cyclization mediated by K_2CO_3 to afford 2-arylated indolizines **7a-e** with high purity (Scheme 28).

1a - R_1= H, R= H
1b - R_1= H, R= OMe
1c - R= OMe, R= OMe
1d - R_1= H, R= F
1e - R_1= H, R= Cl

7a - R_1= H,R= H - 56%
7b - R_1= H, R= OMe - 85%
7c - R_1= OMe, R_2= OMe - 52%
7d - R_1= H,R= F - 55%
7e - R_1 = H, R_2= Cl - 82%

Scheme 28. Synthesis of 2-arylindolizines **7a-e**.

With these substrates in hands, through a directed metalation approach using 2.0 equivalents of *n*-Butyl lithium in THF (-20°C for 5 hours) followed by reaction quench with *N,N*-dimethylformamide, five new fluorescents 2-aryl-5-formyl derivatives **8a-e** were synthesized in yields varying from 62% to 82% yield (Scheme 29).

7a - R_1= H, R= H
7b - R_1= H, R= OMe
7c - R= OMe, R= OMe
7d - R_1= H, R= F
7e - R_1= H, R= Cl

8a - R_1= H, R= H - 80%
8b - R_1= H, R= OMe - 82%
8c - R= OMe, R= OMe - 65%
8d - R_1= H, R= F - 62%
8e - R_1= H, R= Cl - 75%

**Scheme 29.** Synthesis of 5-formyl-2aryl indolizine derivatives **8a-e**.

The photochemical and photophysical properties of compounds **8a-e** were preliminary evaluated in collaboration with the group of Prof. Amando Siuiti Ito, from the Physics Department of University of São Paulo, Ribeirão Preto. Based on those results, a number of 2-arylindolizines bearing ester, carboxylic acid and amide groups at C-5 position were synthesized.

Thus, after the metalation step of compounds **7a-e** with *n*-BuLi, the reactional mixture was quenched with dry CO_2. The gas was bubbled into the reaction for 15 minutes at -20°C. After that, reaction was stirred for 12 h at room temperature to give derivatives **9a-e** in moderate to good yields (Scheme 30). Then, by reacting the 5-carboxilic acids derivatives **9a-e** with 1.5 equivalents of MeI in the presence of K_2CO_3 for 24 hours at room temperature using DMF as solvent the 5-ester derivatives **10a-e** were easily prepared in good yields (Scheme 30).

The 5-amides derivatives **11a-e** were synthetized by reaction of **9a-e** with the coupling reagents HBTU/HBOt in the presence of Et_3N and diethylamine at room temperature for 12 hours using DMF as solvent (Scheme 30).
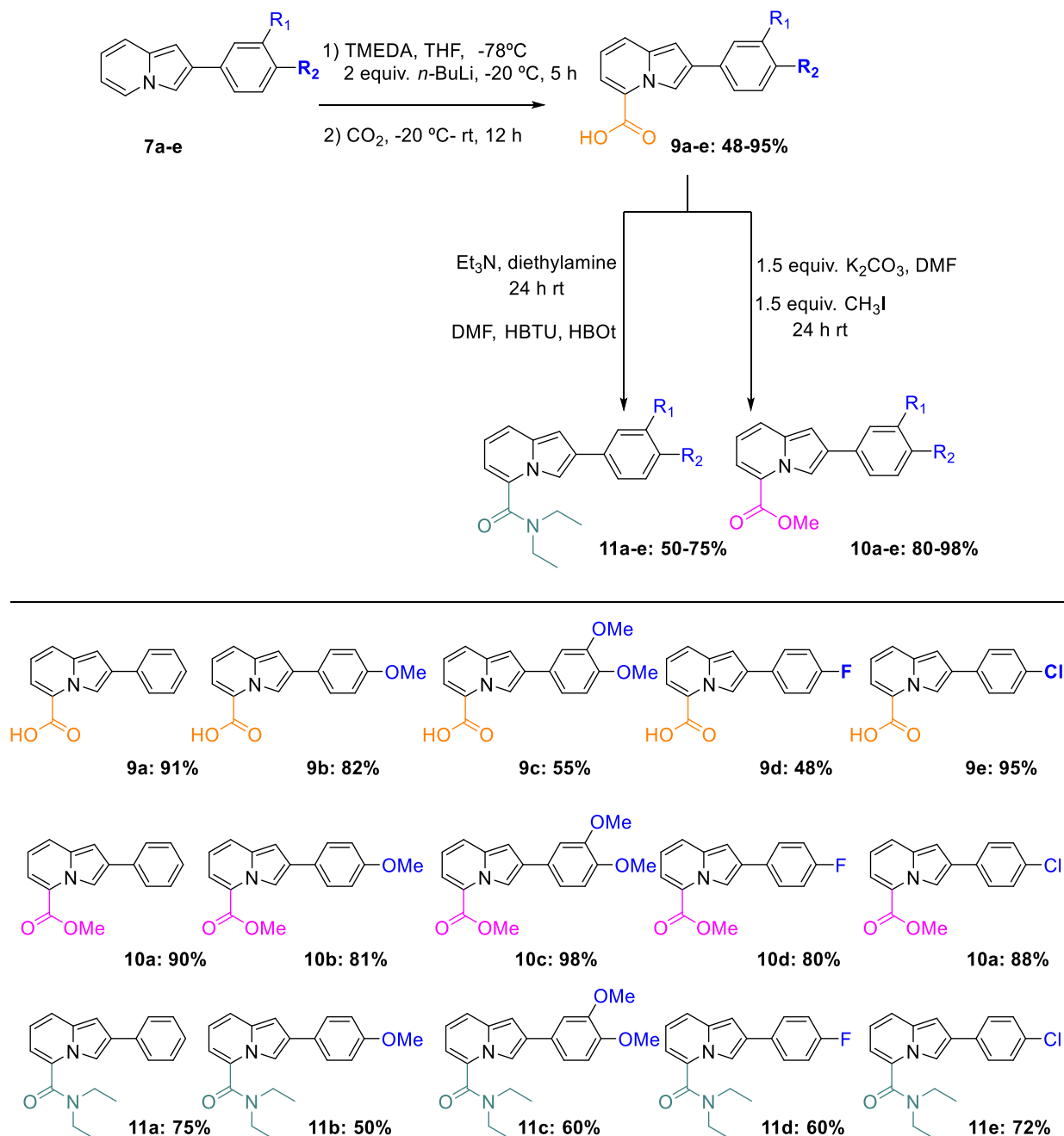
Scheme 30. Synthesis of indolizine derivatives **9a-e – 11a-e**.

Once prepared, these new twenty fluorescent compounds had their absorbance, fluorescence, stokes shifts and quantum yields values evaluated. The results are shown below.

Absorption and emission spectral position

For these experiments all compounds **8(a-e)-11(a-e)** were solubilized in DMSO and methanol. The compounds were separated in four groups according to their functional groups (aldehyde, ester, carboxylic acid and amide).

Absorbance measurements showed maximum absorption in the UV-vis region, ranging from approximately 257 *nm* to 457 *nm*, in both solvents. The maximum fluorescence emission ranges were from 485 *nm* to 549 *nm* (Table 8).

Using the Lippert model, that describes general solvent effects on the absorption and emission, it should be expected lower Stokes shift values for molecules in DMSO compared to the values in methanol. However, the experimental results presented the opposite trend: larger Stokes shift in DMSO than in methanol (Table 8). As the Stokes shift depends on the difference between the electric dipole moment of ground and excited states, these contradictory results may be associated to different distribution of the charges of the compounds in DMSO and methanol. It was also possible to observe higher Stokes shift values inside the amide derivatives group **11a-e**. Fluorescent molecules which showed large Stoke shift (>80nm) and high photostability has been reported as good candidates to dyes (DA SILVEIRA NETO et al., 2005; GAO et al., 2017).

The quantum yield of fluorescence characterizes the emission efficiency of a fluorophore (calculated by the ratio of emitted photons and absorbed photons). In both solvents higher quantum yield values were observed for the ester derivatives **9a-e** (Table 8). Relatively lower values were observed for the aldehyde derivatives **8a-e**, possibly because the dissipation of excited state energy is favoured by vibrational modes in the CHO group, increasing the non-radiative rate of deexcitations.

Table 8. Wavelengths of maximum absorbance and maximum emission and Stokes shift for the compounds in DMSO and methanol.

	Absrobance (*nm*)		Fluorescence (*nm*)		Stokes shift (10^3cm^{-1})		Quantum Yield	
Molecule	**DMSO**	**MeOH**	**DMSO**	**MeOH**	**DMSO**	**MeOH**	**DMSO**	**MeOH**
8a	322	452	529	546	12.2	3.81	0.269	0.067
8b	270	457	536	549	18.4	3.67	0.073	0.079
8c	258	454	540	548	20.2	3.78	0.041	0.031

8d	346	453	534	544	10.2	3.69	0.089	0.075
8e	342	449	535	542	10.6	3.82	0.099	0.124
9a	261	400	524	495	19.2	4.80	--	0.251
9b	304	338	485	502	12.3	9.67	0.066	0.060
9c	258	403	485	495	18.1	4.61	0.099	0.221
9d	259	391	488	488	18.2	5.08	--	0.101
9e	223	275	505	505	25.0	16.6	--	0.065
10a	325	426	510	510	11.2	3.87	0.165	0.315
10b	330	428	510	513	10.7	3.87	0.143	0.289
10c	335	426	511	511	10.3	3.90	0.220	0.292
10d	329	431	510	510	10.8	3.59	0.172	0.331
10e	324	422	508	510	11.2	4.09	0.146	0.389
11a	257	364	505	516	19.1	8.09	0.124	0.111
11b	304	368	527	527	13.9	8.20	-	0.042
11c	264	360	510	526	18.3	8.77	0.096	0.101
11d	256	363	512	524	19.5	8.46	-	0.159

Time resolved fluorescence

The emission decay profiles were fitted to one or two exponential curves depending on the functional group studied (Table 9).

Inside the aldehyde group, compounds **8a**, **8d** and **8e** showed a monoexponential decay curves with lifetime around 5.0 ns in methanol and 9.0 ns in DMSO while compounds **8b** and **8c** showed biexponential curves with short lifetime (values from 1.0 to 2.0 ns, and pre-exponential factor 0.36 in methanol and 0.12 in DMSO).

Carboxylic acid derivatives **9a-e** presented a decay curve profile with two lifetime components with predominance of a long lifetime, around 10.0 ns, and contributions (generally with normalized pre-exponential factor below 0.30) from a short lifetime, around 1.0 to 2.0 ns. In this group the average lifetimes were higher when compared with other groups (around 10.0 ns) (Table 9).

The ester group derivatives **10a-e** mostly presented monoexponential decay curves with lifetimes above 10.0 ns in DMSO and around 8.0 ns in methanol. On the other hand, amide derivatives **11a-e** showed fluorescence decay profile which were

best fitted to biexponential curves with predominance of long lifetime components, around 8.0 ns in methanol and 10.0 ns in DMSO and minor contribution from shorter lifetime components (1.0 to 2.0 ns).

In general, compounds in DMSO showed higher Stokes shift values, quantum yield and lifetime, compared to results in methanol. Among the groups, lower values were registered for aldehyde compounds **8a-e**. Interestingly, it is also noticed that in all groups, the compounds containing 2-phenyl group (**8a**, **9a**, **10a**, and **11a**) presented higher efficiency for fluorescence emission with longer average lifetime.

Table 9. Lifetime normalized pre-exponential factor and average lifetime in methanol and DMSO.

Molecule	Methanol					DMSO				
	T_1 (ns)	T_2 (ns)	An_1	An_2	T_{ave} (ns)	T_1 (ns)	T_2 (ns)	An_1	An_2	T_{ave} (ns)
8a	4.03	-	1	-	4.03	10.2	-	1	-	10.2
8b	7.97	2.27	0.64	0.36	7.18	6.54	1.8	0.88	0.12	6.37
8c	5.38	0.93	0.64	0.36	4.98	5.05	1.23	0.88	0.12	4.93
8d	5.13	-	1	-	5.13	9.57	-	1	-	9.57
8e	4.88	-	1	-	4.88	9.28	-	1	-	9.28
9a	11.3	2.55	0.75	0.25	10.69	9.7	1.78	0.90	0.10	9.54
9b	7.60	1.51	0.67	0.33	7.06	8.2	1.65	0.33	0.67	6.27
9c	10.2	1.52	0.91	0.09	10.11	11.8	0.94	0.75	0.25	11.52
9d	11.2	1.62	0.92	0.08	11.10	11.3	1.45	0.74	0.26	10.86
9e	8.00	1.58	0.70	0.30	7.49	5.5	1.29	0.50	0.50	4.71
10a	8.45	-	1	-	8.45	11.2	-	1	-	11.20
10b	8.04	-	1	-	8.04	10.6	1.32	0.89	0.11	10.46
10c	7.83	-	1	-	7.83	10.8	1.45	0.89	0.11	10.64
10d	7.43	1.48	0.72	0.28	7.01	11.8	-	1	-	11.80
10e	8.59	-	1	-	8.59	12.0	-	1	-	12.00
11a	7.14	1.77	0.81	0.19	6.85	11.8	1.15	0.93	0.07	11.72
11b	6.01	1.64	0.76	0.24	5.66	9.1	1.45	0.72	0.28	8.65
11c	6.06	-	1	-	6.06	10.1	1.3	0.85	0.15	9.90
11d	7.09	1.93	0.84	0.16	6.84	11.4	1.44	0.93	0.07	11.30

Theoretical calculations

The calculations of the electronic transition were performed for the molecules without a substituent in the 2-phenyl ring (**8a**, **9a**, **10a** and **11a**). The calculated energies among these molecules were very close each other, with energy values in the interval from 2.82 to 2.88 eV. Despite the structural differences HOMO energies among them were close to –7.5 eV (Table 10).

On the other hand, LUMO energies were distinct, generating different values for the energy gap of each molecule. However, in all cases the predominant transitions were observed from HOMO → LUMO (Table 10).

The **11a** molecule presented values of transition energy and orbital energies slightly different from the others. Its HOMO energy is –7.21 eV. The transition energy also presented higher value when compared to the other molecules (3.07 eV), resulting in a lower wavelength for the absorption, 404 nm (Table 10). There is good agreement between calculated and measured absorption wavelength, with differences around 10 to 20 nm. The larger difference was observed for **11a** approximately 10%.

Table 10. Molecule classes with their experimental absorption wavelength in comparison with theoretical calculations: electronic transitions, HOMO and LUMO energies, harmonic oscillators frequencies and absorption wavelength.

Molecule	λ_{exp} (nm)	E_{HOMO} (eV)	E_{LUMO} (eV)	λ_{calc} (nm)	E (eV)	f_{osc}	Transitions
8a	452	–7.54	–1.06	439	2.82	0.236	H → L = 0.97
9a	401	–7.49	–0.96	436	2.85	0.230	H → L = 0.96
10a	422	–7.44	–0.87	431	2.88	0.227	H → L = 0.96
11a	365	–7.21	–0.33	404	3.07	0.153	H → L = 0.96

Chapter II - Comprehensive study on C-H activation / borylation of indolizines followed by Suzuki-Miyaura cross-coupling

This work has been developed in partnership with Prof. Dr. Patrick G. Steel at Durham University, United Kingdom, during an internship of research, funded by FAPESP (**BEPE Process: 2018/02855-7**).

1. C-H borylation

The direct functionalization of C–H bonds catalysed by transition metals has emerged as an important and versatile strategy for the synthesis/functionalization of heterocyclic compounds. The ability of transition metals such as Copper (DO; DAUGULIS, 2007; DO; KHAN; DAUGULIS, 2008; YOSHIZUMI et al., 2008; KLEIN et al., 2010; RAO; SHI, 2016; DANG et al., 2018; JALA; PALAKODETY, 2019; KANTAM et al., 2019), Ruthenium (CHATANI et al., 2001; KAKIUCHI; MURAI, 2002; YI; YUN; GUZEI, 2005; NAREDDY; JORDAN; SZOSTAK, 2017; WU et al., 2019), Iridium (IVERSON; SMITH, 1999; CHO, 2002; PAN; SHIBATA, 2013; LARSEN; HARTWIG, 2014; FERNÁNDEZ et al., 2017; KERR et al., 2018; BERTALLO et al., 2019), Rhodium (O'MALLEY et al., 2005; WITULSKI; SCHWEIKERT, 2005; LOU et al., 2018; REJ; CHATANI, 2019; YAMADA; IWASAWA; TAKAYA, 2019), Palladium (SHIBAHARA; YAMAGUCHI; MURAI, 2010, 2011; WANG et al., 2015; JIAO et al., 2017), Platinum (JOHNSON; SAMES, 2000; JOHNSON; LI; SAMES, 2002; LABINGER, 2017; SATTLER et al., 2020) to activate C–H bonds has been used extensively to construct C–heteroatom and C–C bonds in organic synthesis.

In 2002, Miyara and co-workers (ISHIYAMA et al., 2002) described a new approach for the direct conversion of aryl C–H bonds to aryl C–B bonds by using an Ir(I) catalyst and B_2pin_2 (Scheme 31). This interesting protocol leads to the rapid synthesis of highly useful arylboronic esters that in many cases were previously hard to synthesize. In addition, this methodology is tolerant to several functional groups and can display excellent regioselectivity, largely defined by steric factors.
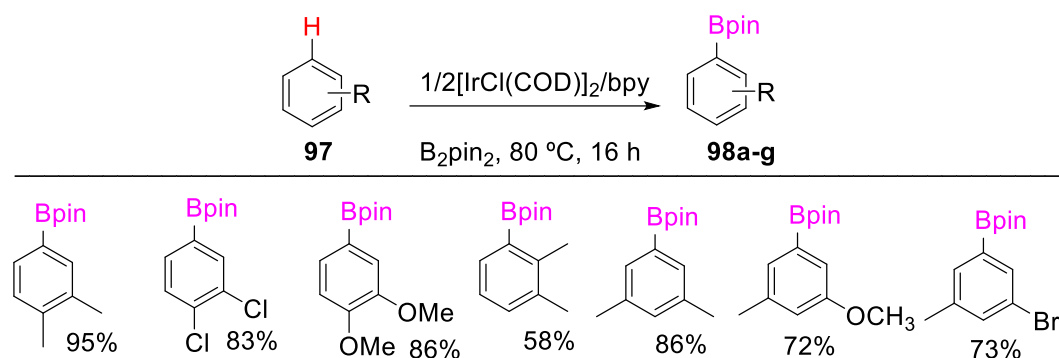
Scheme 31. Synthesis of arylboronic esters.

In the same year, Ishiyama and co-workers (ISHIYAMA et al., 2002) reported the borylation of arenes and heteroarenes catalysed by iridium complexes of di-*tert*-butylbipyridine (dtbpy) and bipyridine (bpy) under mild conditions. After that, aromatic borylation using other pre-catalyst/ligand combinations were reported by several authors (TAGATA; NISHIDA, 2004; MURATA et al., 2006; ROBBINS; HARTWIG, 2013; LARSEN; HARTWIG, 2014; SADLER et al., 2014, 2015).

Due to the high efficiency and selectivity of the C-H activation/borylation protocol, it has been applied in the functionalization of several arenes and heteroarenes and in the total synthesis of bioactive targets, such as rhazinicine **102**, a drug that mimics the cellular effects of paclitaxel (BECK; HATLEY; GAUNT, 2008) (Scheme 32). In the key step of the preparation of rhazinicine **102** the TMS-protected pyrrole **99** underwent a one-pot Ir-catalysed borylation and Suzuki coupling to form the target pyrrole isomer **101** arylated at C-3 position in 78% yield (Scheme 32).

More recently, this approach has allowed further reactions of the crude boronate esters without removal of the residual catalysts in one-pot cross-coupling reactions, halogenations and oxidation reactions (MALECZKA, et al., 2003; MURPHY; LIAO; HARTWIG, 2007; MURPHY; TZSCHUCKE; HARTWIG, 2007; TZSCHUCKE; MURPHY; HARTWIG, 2007; E. MALECZKA et al., 2010).
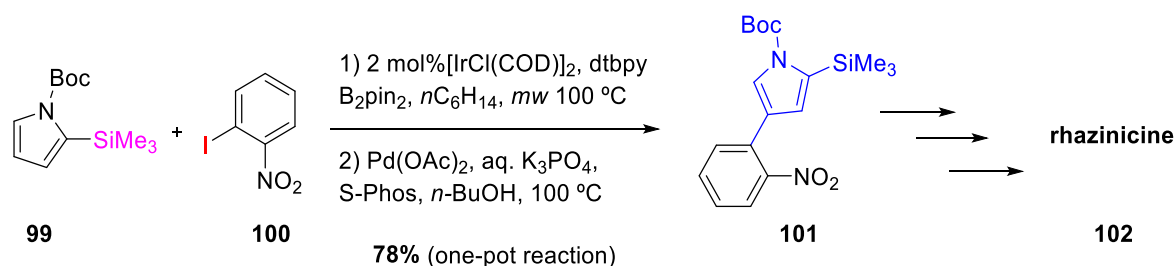
Scheme 32. Synthesis of rhazinicine.

1.1 Proposed mechanism for bipyridyl Ir(III) complexes

The most accepted mechanism for this process is described in Figure 27. Ishiyama, Hartwig, Miyaura and co-workers have proposed a mechanism that involves an iridium catalytic cycle. They showed that when the catalyst was generated from [Ir(COD)X]$_2$/dtbpy there is the initial formation of a stable [Ir(COE)(dtbpy)(Bpin)$_3$] **103**.

This hexacoordinate Ir(III)trisboryl complex **103** is formed during the induction period which cod is reduced to coe and boron reagent permit the oxidation of the Ir(I) catalyst. Subsequently, coe dissociates to form **104** with a vacant coordination site allowing the oxidative addition of an aryl C-H bond leading to the Ir(V) heptacoordinate complex **105**. Then, after a reductive elimination of the arylBpin fragment, Ir(III) complex **106** is generated. Finally, through the oxidative addition of B$_2$pin$_2$ or HBpin **107** is formed and followed by reductive eliminantion of HBpin or H$_2$ the cycle is completed (ISHIYAMA et al., 2002; TAMURA et al., 2003; BOLLER et al., 2005; LISKEY et al., 2009; TAJUDDIN et al., 2012).
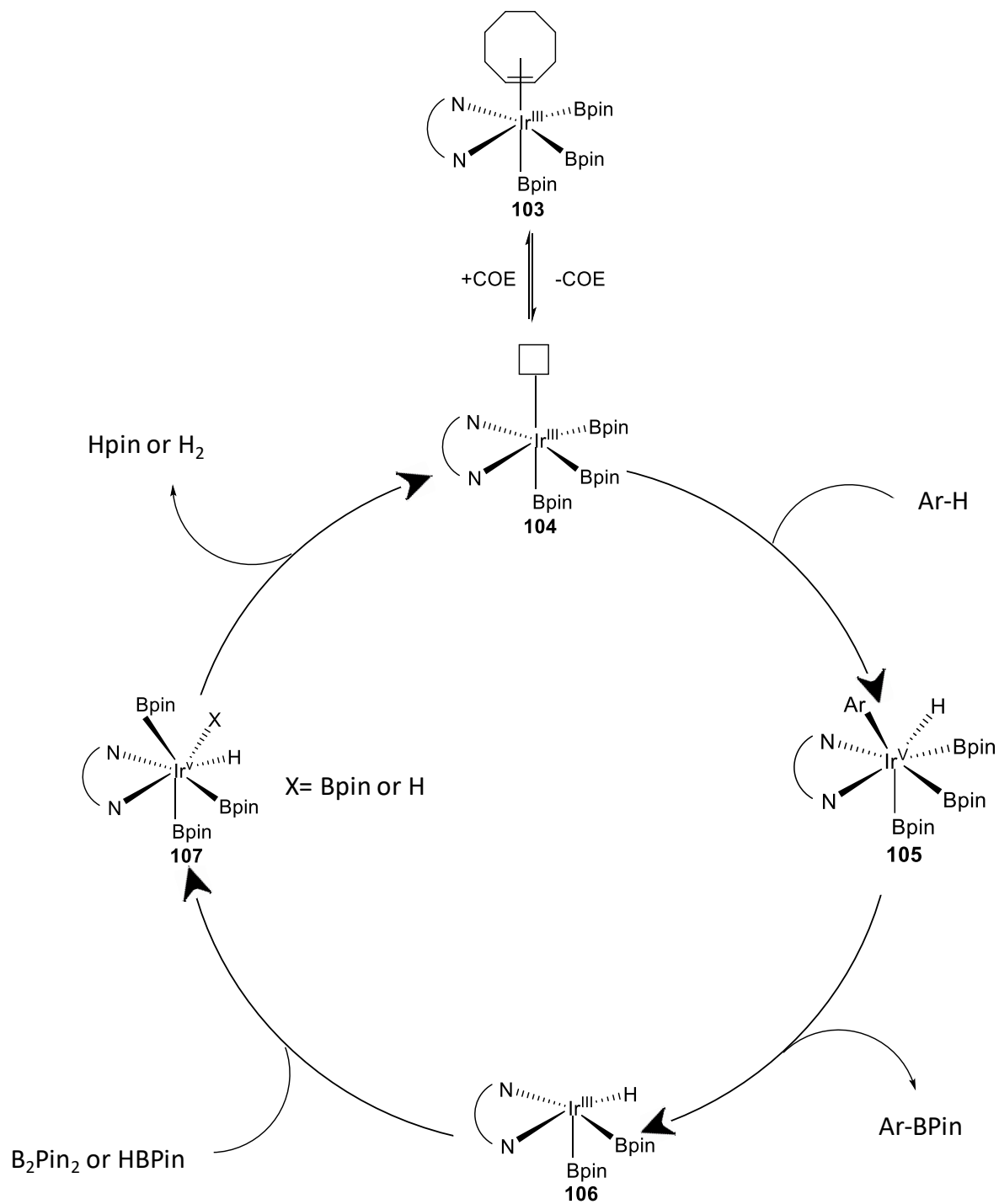
Figure 27. Iridium Catalytic cycle.

1.2 Reactivity and Scope

The C-H borylation using [Ir(OMe)cod]$_2$ showed reasonable selectivity for aromatic C-H bonds in arenes and heteroarenes containing sensitive functional groups such as ketones, nitriles, amine, esters and silyl groups. However, substrates containing alkenes, alkynes, enolizable protons, nitro and sulphonyl groups showed be problematic. Moreover, electron-deficient arenes showed be more reactive than electron-rich arenes (MKHALID et al., 2010).

Regarding the solvents, the reaction can be successfully carried out in a variety of solvents such as MTBE, hexane, THF and NMP. Nonetheless, solvents with acidic hydrogens such as alcohols can react with the Ir−Bpin bonds to form ROBpin and Ir hydrides, being not eligible as solvents (MKHALID et al., 2010).

In addition, the reactivity of the acetyl methyl protons in isopropyl acetates and the C-H acidity of acetonitrile may account for the poor results observed using these solvents. Side reaction between active catalyst and solvents were reported in some cases using DCM and DMSO (PRESHLOCK et al., 2013).

1.3 Regiochemistry

The regioselectivity of the C-H borylation employing bipyridyl ligands in arenes is largely controlled by steric effects, with boryl groups being incorporated to the most sterically accessible C-H position. Often, mixture of borylation products are observed in monosubstituted arenes (Scheme 33a).

In symmetrically 1,2-dissubstituted arenes borylation occurs leading to exclusively to a single product (Scheme 33b). However, when the substituents are different a mixture of products were observed. The rule of selectivity showed that in 1,3-dissubstituted or 1,2,3 trisubstituted arenes the borylation will occur at C-5 position no matter if the substituents are the same or not (Scheme 33c-d).

On the other hand, 1,4-dissubstituted arenes showed patters of borylation at the *ortho* position when substituents are symmetrically (Scheme 33e). Although, when the steric properties of the two substituents are distinct it was observed that the borylation occurs preferentially *ortho* to the smaller substituent (Scheme 33f) (ISHIYAMA et al., 2002b, 2002a; MKHALID et al., 2010; HARTWIG, 2011)

a)

R= CF₃, OMe, Me

ratio 1:2 (80-95%)

b)

112: 82%

c)

114: 84%

d)

116: 91%

e)

118: 53%

f)

ratio 95:5
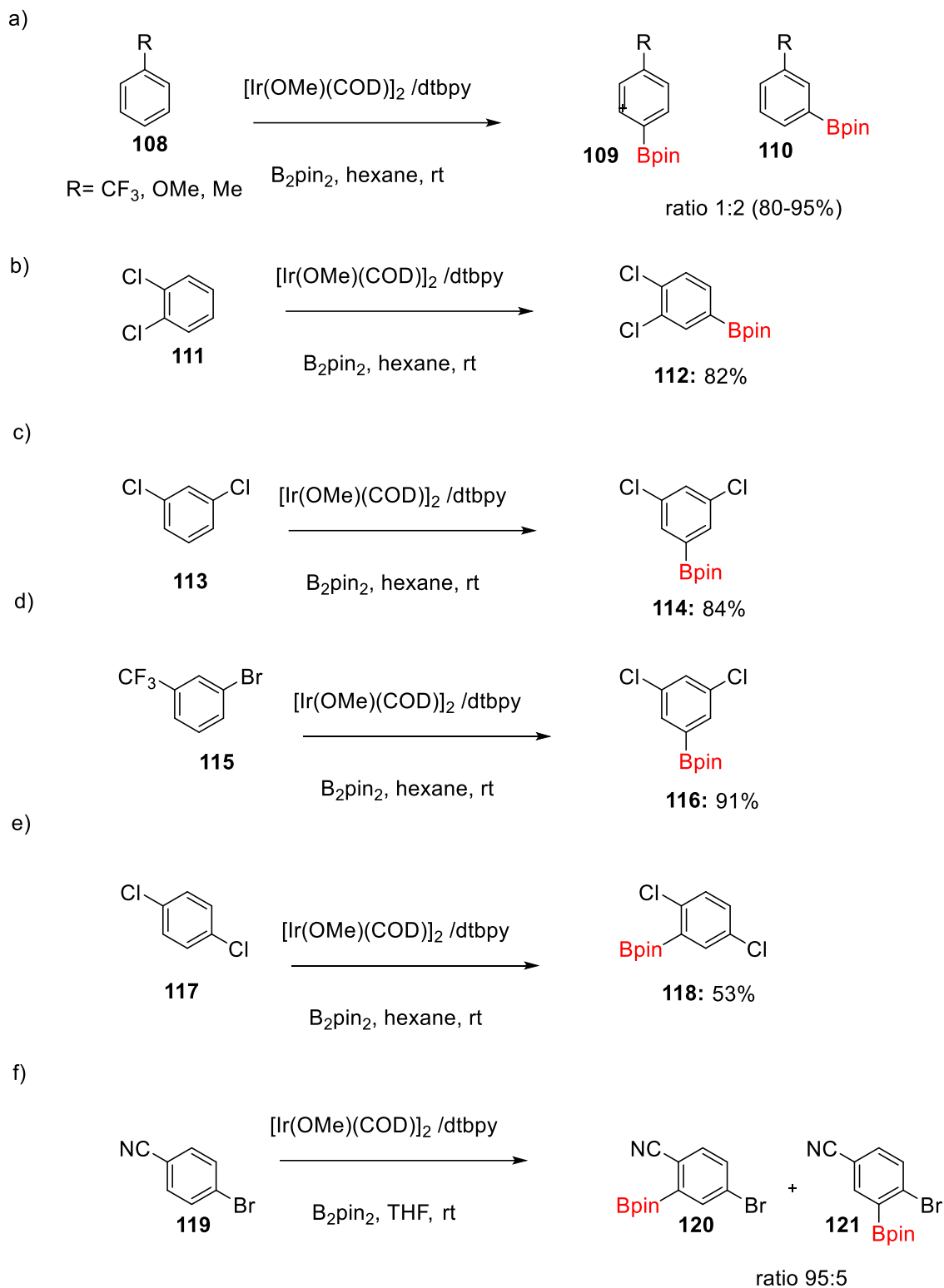
Scheme 33. Examples of borylation reaction in substituted arenes.

Despite the steric effects observed for arenes, Hartwig and co-worker have showed that it is possible to design *ortho* borylations using a directing group such as dialkyl hydrosilyl group. In this study, they successfully demonstrated the *orhto* borylation of benzylic silanes, phenols, and anilines (BOEBEL; HARTWIG, 2008). One

year later, Kawamorita and co-worker showed that arenes decorated with amides, sulfonate, ester, alkoxymetal, acetal and chloro groups can be successfully *ortho* borylated using Silica-SMAP (Silica-supported Silicon-constrained Monodentate Trialkylphosphine). This immobilised phosphine ligand can form mono-phosphine-ligated active species, allowing substrate coordination (Scheme 34) (KAWAMORITA et al., 2009).

Since then, several researches groups have been using this strategy to promote ortho borylation not only in arenes but also in quinolines, quinoxalines, indoles and others heteroarenes (KAWAMORITA; OHMIYA; SAWAMURA, 2010; ROBBINS; HARTWIG, 2013; KONISHI et al., 2014).
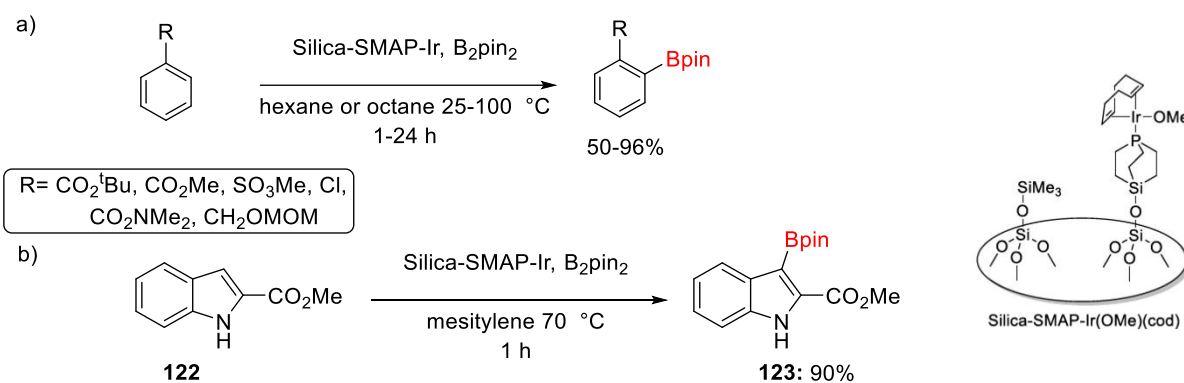
Scheme 34. Examples of *ortho*-borylation promoted by Silica-SMAP-Ir.

In contrast, the site-selectivity for the borylation of heteroarenes is mainly controlled by electronic effects. For example, borylation of five-membered heterocycles containing NH, O and S atoms occurs preferentially alpha to the heteroatom (Scheme 35a). However, Smith, Maleczka and co-workers demonstrated that the borylation of 2-substituted indoles, when the position alpha to the N-H is blocked, takes place at the C-7 position (Scheme 35b) (TAKAGI et al., 2002; ISHIYAMA et al., 2003).
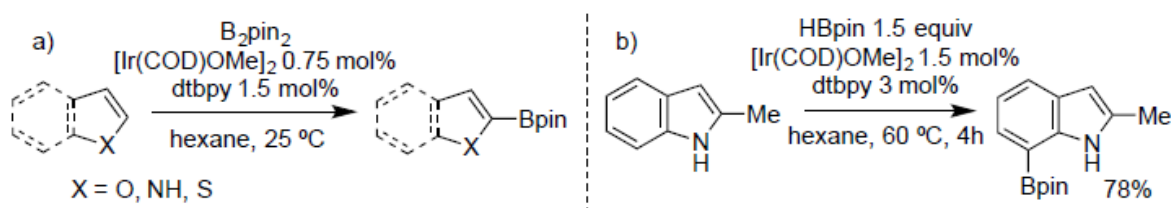
Scheme 35. Site-selectivity for the borylation in heteroarenes.

On the other hand, in pyridine system the borylation does not occurs alpha to nitrogen atom, but rather forms mixture of C-3 and C-4 borylated products (TAKAGI et al., 2002). The lower reactivity and yield can be attributed to coordination of the pyridyl nitrogen to iridium catalyst by blocking access to the required site for C-H activation (Scheme 36).
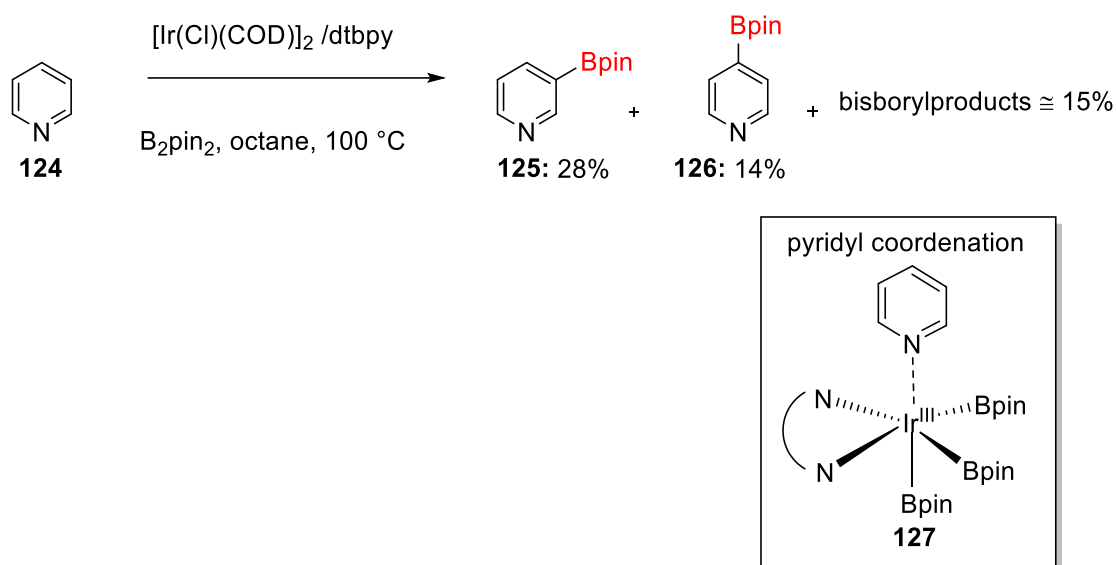
Scheme 36. Examples of borylation in pyridines - Effect of the pyridyl coordination with Ir-catalyst**.**

This pyridyl coordination with Ir-catalyst can be disrupted by insertion of one or two substituents in the pyridine moiety. For example, 2,6-dimethylpyridine **128** and 2,3-dimethylpyrazine **130** could be borylated in excellent yields (Scheme 37).
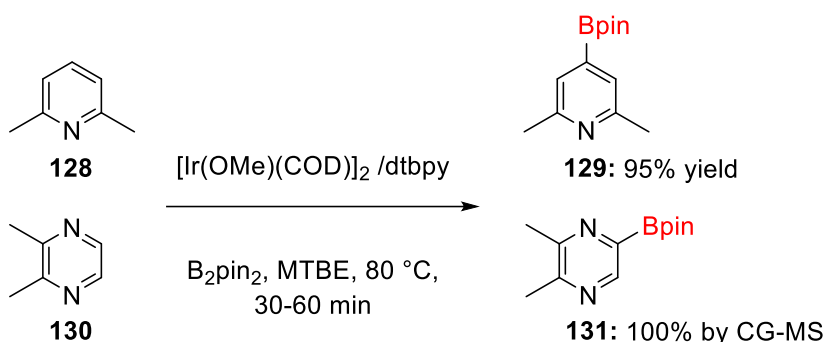
Scheme 37. Example of borylation in pyridines/pyrazine rings containing methyl groups - Disruption in the pyridyl coordination with Ir-catalyst.

Notably, despite the applicability and versatility of C-H borylation of aromatic and heterocyclic compounds, at the best of our knowledge this strategy has not been applied to the functionalization of indolizines.

2. Aim

In Chapter I, we have presented the development of a base-controlled regioselective methodology to prepare functionalized indolizines at C-2, C-3 or C-5 positions depending on the substrate. These interesting results led us to begin to wonder if it would be possible to prepare new indolizines with different substitution patterns using C-H activation approach.

Because of that, the main goal of this work it was the development of a comprehensive study on the application of Ir-catalysed C-H activation/borylation aiming the preparation of a small library of indolizines derivatives.

3. Results and Discussion

3.1 Preparation of catalyst complex

We started this study by preparing [Ir(OMe)(COD)]$_2$ catalyst **134** in two step. First, IrCl$_3$ was reacted with 1,5-cyclooctadiene in 2-propanol and water. The reaction was refluxed for 4 hours leading to [Ir(Cl)(COD)]$_2$ **133** as a red free solid. After, drying over vacuum for 12 hours [Ir(Cl)(COD)]$_2$ was dissolved in degassed MeOH and KOH was added. The reaction stayed at room temperature for 3 hours. Then, the mixture was cooled to 0 °C and water was added. After 1 hour a fine free flowing yellow powder was formed in 71% yield (Scheme 38).

IrCl$_3$ $\xrightarrow{\text{H}_2\text{O, 2-propanol}}$ [Ir(Cl)(COD)]$_2$ $\xrightarrow{\text{1. KOH, MeOH}}$ [Ir(OMe)(COD)]$_2$

132 1,5-cyclooctadiene, reflux 4h   **133:** 65%   3 h, rt   2. H$_2$O, 0 °C, 1 h   **134:** 71%
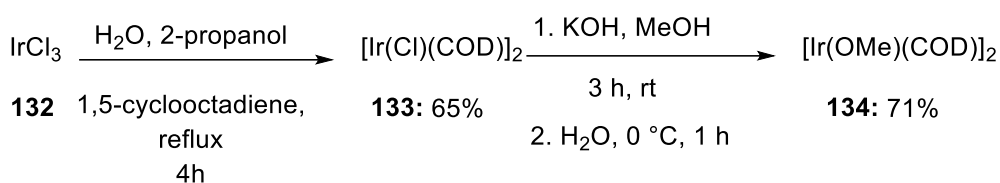
Scheme 38. Synthesis of Ir-catalyst.

3.2 C-H borylation: Methodological study

Initially, the Ir C-H borylation of indolizine-1-carbonitrile **12** was investigated. For that, a standard set of reagents (B$_2$pin$_2$ as the source of boron, [Ir(OMe)(COD)]$_2$ complex as catalyst and 4,4′-di-tert-butyl-2,2′-dipyridyl (dtbpy) as ligand) was explored varying catalysts loading, temperature and time (Table 11). All the results were analysed by CG-MS and NMR when possible.

Based on the C-H Suzuki–Miyaura-type direct C-H arylation using a palladium/copper bimetallic catalyst published by Liu and co-workers, we believed that borylation could occur at C-3 position (Scheme 39). However as shown in Table 11 we observed a different pattern of borylation.
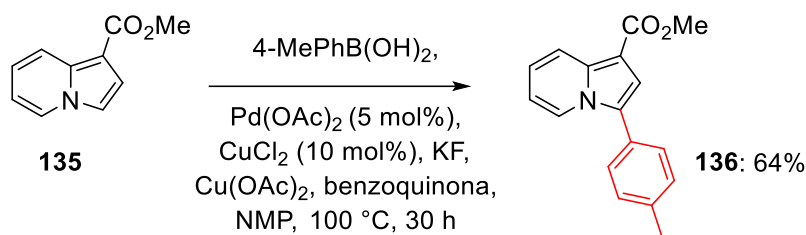
Scheme 39. C-H Suzuki–Miyaura-type direct C-H arylation of indolizine 135.
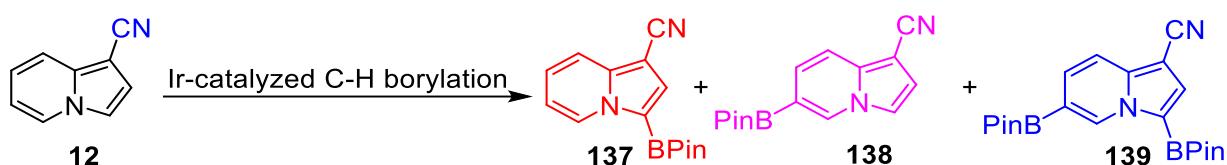
Table 11. Borylation tests using indolizine **12** as substrate.

Entry	[Ir(OMe)(COD)]₂	Ligand	B₂Pin₂ (eq.)	Temp. °C	Time (h)	Product[b]	GC-MS* (%) or NMR
a	10 mol%	20 mol% dtbpy	0.7	r.t	1-24	**137**	2
b	10 mol%	20 mol% dtbpy	1.5	r.t	1-24	**137**	5
c	10 mol%	20 mol% dtbpy	0.7	60	1	**137**	40
d	10 mol%	20 mol% dtbpy	0.7	60	5	**137/138**	35/6
e	10 mol%	20 mol% dtbpy	1.0	60[c]	2	**137/138**	43/3
f	10 mol%	20 mol% dtbpy	1.5	60[c]	1	**137/138**	53/3
g	10 mol%	20 mol% dtbpy	1.5	60[c]	3	Multiple mono- and di- borylated products	
h	10 mol%	20 mol% dtbpy	1.0	60[c]	3	**137/138/139**	45/5/5
i	10 mol%	20 mol% dtbpy	1.0	100[c]	1	Multiple mono- and di- borylated products	
j	10 mol%	20 mol% tmphen	1.0	60	24	**137**	5
k	5 mol%	10 mol% dtbpy	1.0	60	3	4 products mono- borylated	3/21/48/2

l	5 mol%	10 mol% dtbpy	1.0	60	1	**137/138**	30:10
m	10 mol%	20 mol% dtbpy	1.0	80	24	Multiple mono- and di- borylated products	
n	5 mol%	10 mol% dtbpy	1.0	60[c]	1	**137/138**	31/12

[a]GC-MS conversion calculated between starting material and borylated products. [c] Microwave
[b] mono e di-borylated products

Based on the GC-MS and NMR analyses it was possible to note the formation of four mono-borylated isomers (***m/z* 268**) and two di-borylated products (***m/z* 394**) being the C-3 mono-borylated **137** isomer the majority product formed in all experiments.

In the first attempts (Table 11, entries **a** and **b**) we chose to use dtbpy as ligand and B_2pin_2 as source of boron because these reagents had already showed good results in the borylation of other substrates studied in the Professor Steel group. During these attempts, all reactions were monitored by CG-MS. Aliquots were taken with 2 h, 4 h, 6 h, 12 h, 20 h and 24 h and it was observed the formation of one borylated product (***m/z* 268**) in a small conversion, even when 1.5 equivalents of B_2pin_2 were used (Table 11, entry **b**).

Aiming better results, the temperature of the reaction was increased to 60 °C and the number of equivalents of B_2pin_2 was kept in 0.7 equivalents (Table 11, entries **c** and **d**). After 1 hour, we could detect the presence of product **137** (mono-borylated) in 40% conversion (NMR conversion calculated using internal standard) and after 5 hours (Table 11, entry **d**), a second mono-borylated product was detected in 6% conversion (NMR conversion calculated using internal standard). Later, this product was identified as C-6 mono-borylated product **138**.

In the subsequent experiments (Table 11, entries **e-h**) the number of equivalents of B_2pin_2 were increased up to 1.5 and all reactions were carried out in microwave. Unfortunately, we observed that large amounts of B_2pin_2 combined with long time reactions led to a complex mixture of mono-and di-borylated products (Table 11, entry **g**) without significative increase in the global reaction conversion. It was also verified that heating above 60 °C favoured the formation of poly-borylated products (Table 11, entry **l** and **m**).

Because of these results and based on the study developed by Preshlock and co-workers we decided change the ligand to tmphen (3,4,7,8-tetramethyl-1,10-phenanthroline) (PRESHLOCK et al., 2013). In Preshlock study they could observed that more electron-rich ligands led to more reactive catalysts and due to this good result was achieved using this catalyst at elevated temperature. However, for indolizine moiety this catalyst was not reactive (Table 11, entry **j**).

Changes in the pre-catalysts loading [Ir(OMe)cod]$_2$ and dtbpy did not have impact in the improvement of formation of mono-borylated products (Table 11, entries **h**, **l** and **n**).

In conclusion, after all these experiments, we observed that conditions which led to high conversion (Table 11, entries **g**, **k** and **m**) also afforded a complex mixture of mono and di-borylated products and because of that we moved forward with the studies using the condition showed in Table 11, entry **l**. Despite the low conversion (40%) only 2 isomers were formed.

Unfortunately, we could not find a combination that led to high conversion in products with good selectivity. However, these preliminary results are important since that was the first time that the C-H borylation of indolizines were explored.

3.3   Deborylation

In a previous study, Kallepalli and co-workers reported the possibility of converting di-borylated products into mono-borylated derivatives in good yields (KALLEPALLI et al., 2015) (Scheme 40).

R= CN, CL, CH$_3$, Br
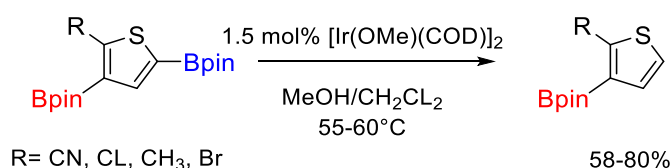
Scheme 40. Deborylation of thiophene derivative.

Based on this study, indolizine-1-carbonitrile **12** was reacted with 10 mol% [Ir(OMe)cod]$_2$, 20 mol% dtbpy and 2.0 equivalents of B$_2$Pin$_2$ in MTBE at 60 °C for 24 hours. We chose to use 2.0 equivalents of B$_2$Pin$_2$ in order to increase the amount of di-borylated formed. Then, the solvent was removed under vacuum, and 1.5 mol% of [Ir(OMe)cod]$_2$ was added, followed by a mixture of 2:1 MeOH/CH$_2$Cl$_2$.
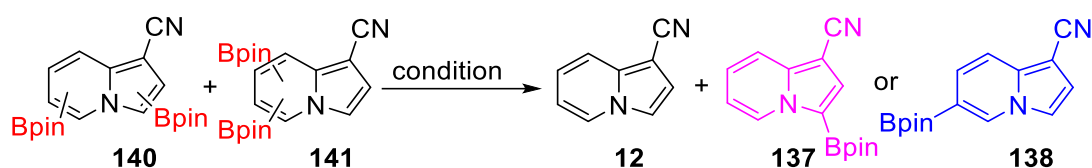
Table 12. Deborylation experiments.

Entry	[Ir(OMe)(COD)]₂	Solvent (2:1)	Temp. (°C)	Time (min)	Products	CG/MS conversion
a	1.5 mol%	MeOH/DCM	55	15	still with di-borylated products	-
b	1.5 mol%	MeOH/DCM	55	30	12/137/138	68/27/5
c	1.5 mol%	MeOH/DCM	rt	30	12/137/138	50/30/8
d	1.5 mol%	MeOH/DCM	rt	60	137/12/138	17/78/15

Despite variation in the reactional conditions the deborylation process proved not to be satisfactory for indolizine **12** leading to mixtures of mono-borylated **137** and **138** and fully deborylated product **12** as majority product in all cases (Table 12, entries **a-d**). Deborylation of substrates **140** and **141** appeared to be quick and not regioselective with both C-3 (**137**) and C-6 (**138**) mono-borylated isomers undergoing to fully deborylated product too.

3.4   Suzuki-Miyaura cross-coupling

Due to the deborylation observed during the chromatographic purification of the compounds described in section 3.1, using silica we decided to perform a one-pot C-H borylation Suzuki-Miyaura cross-coupling reaction in order to determine the borylation sites at the indolizine ring. Thus, a standard protocol well established in the Steel group, using Pd(dppf)Cl₂, K₃PO₂ and dimethylacetamide (DMAc)/H₂O (2:1) was employed. The results are shown in Table 13.
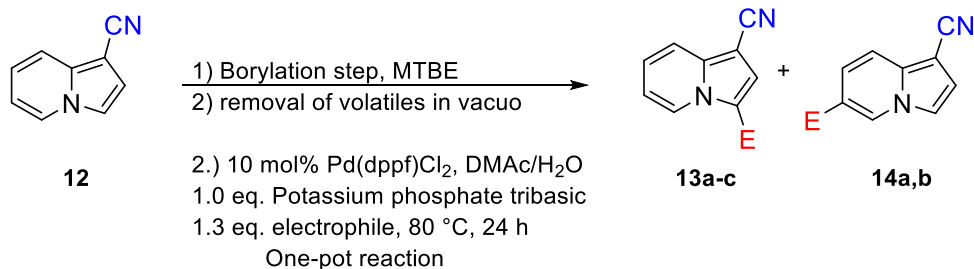
Table 13. One-pot C-H borylation Suzuki-Miyaura cross-coupling

Entry	[Ir(OMe)(COD)]₂	dtbpy	B₂Pin₂ (eq.)	Temp. °C	Time (h)	Conversion[a]	ArX	Ratio	Yield[b]	Product
a	5 mol%	10 mol%	0.7	60	1	45	Ph-I	3:1	30:10	**13a/14a**
b	5 mol%	10 mol%	0.7	60	1	40	I-PhOMe	-	20	**13b/-**
c	5 mol%	10 mol%	0.7	60[c]	1	45	Br-PhCF₃	3:1	33:12	**13c/14b**

[a]GC-MS conversion between starting material and borylated products
[b] isolated yields
[c] Microwave

The Suzuki-Miyaura cross-coupling reaction was successful in all cases. Best conversions were achieved using iodo-benzene and 1-bromo-4-(trifluoromethyl) benzene and all isomers were successfully purified and characterized. When 1-iodo-4-methoxybenzene was used the CG-MS analyses showed the presence of ≤5 % of another mono-borylated isomer (**m/z 248** - possible C-6 mono-borylated isomer), but all attempts to isolate and purify this product were ineffective.

3.5   2D NMR analyses

The isomers identities were confirmed by full assignment of ^{1}H and ^{13}C NMR spectra using NOESY, COSY, HSQC and HMBC spectroscopy techniques and comparison to the parent indolizine chemical shifts (Figure 28).
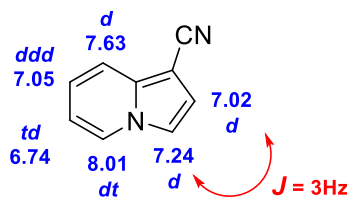
Figure 28. ^{1}H NMR chemical shifts of indolizine-1-carbonitrile (600 MHz, CDCl₃).

In the ^{1}H NMR spectrum of 3-(4-(trifluoromethyl)phenyl)indolizine-1-carbonitrile **13c** it was possible to observe the peaks corresponding to H-5 (8.29 *ppm*, *J*= 7.1, 1.1 Hz), H-6 (6.1 *ppm*, *J*= 6.9, 1.3 Hz), H-7 (7.14 *ppm*, J= 9.0, 6.6, 1.0 Hz) and H-8 (7.72 *ppm*, J= 9.0, 1.2 Hz), which confirmed that substitution occurred at the pyrrole ring instead at the pyridine ring (Figure 29). The doubt was if the substitution occurred at C-2 or C-3 position at the pyrrole ring. The ^{1}H NMR spectrum showed one peak in 7.12 *ppm* as singlet. NOESY and COSY spectrum showed correlation between peak in 7.12 *ppm* and 7.66 *ppm* (corresponding to H-13 and H-17), peak in 8.29 *ppm* (H-5) and 7.66 ppm (corresponding to H-13 and H-17) and no correlation between peak in 8.29 *ppm* (H-5) and 7.12 *ppm*, which confirmed that substitution occurred at C-3 position (Figure 29). Besides, there were correlation in the HMBC spectra among hydrogen in 7.12 *ppm* and carbons in 116.4 *ppm* (CN), 125.3 *ppm* (C-3) and 138.8 *ppm* (C-9).
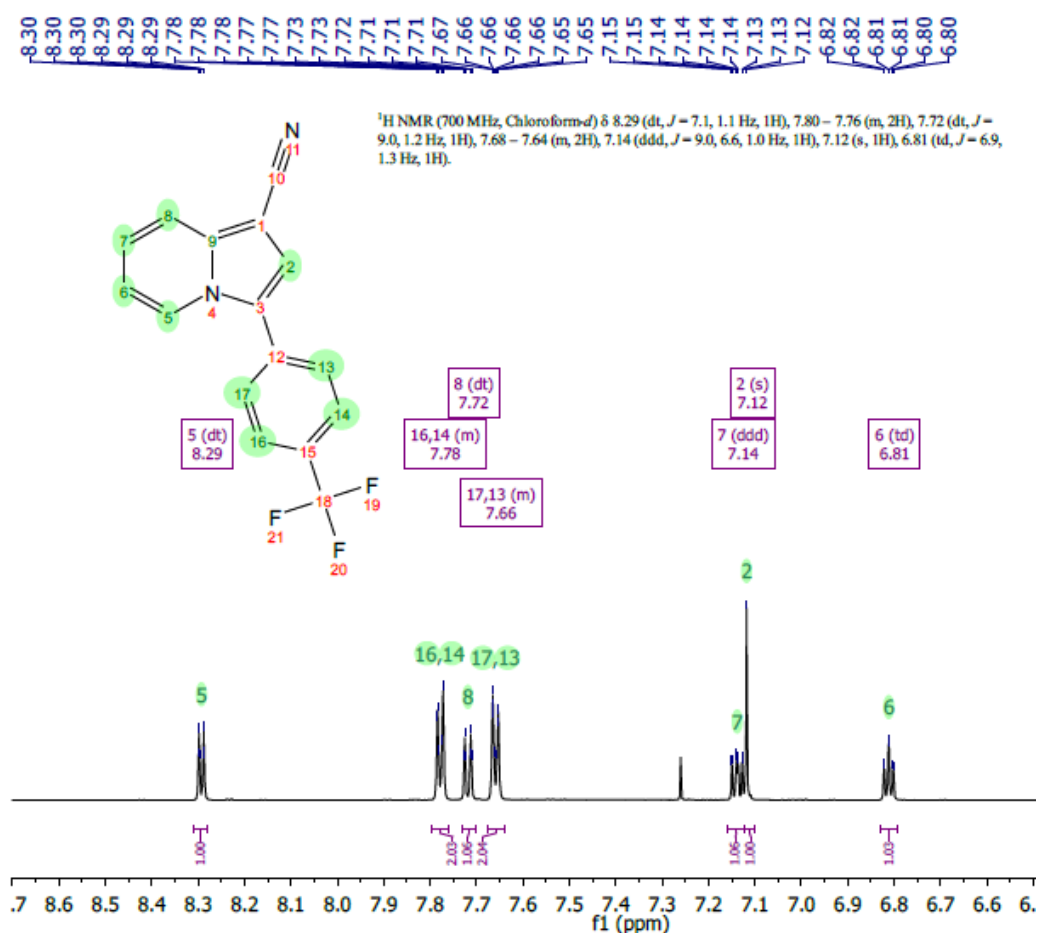
Figure 29. ^{1}H NMR expanded spectrum of aromatic peaks compound **13c.**
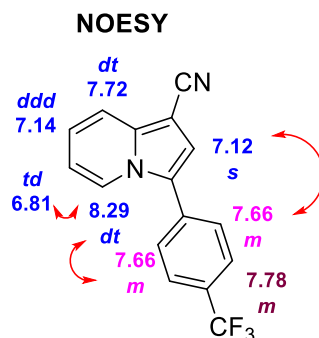
Figure 17.
Figure 30. NOESY correlation for compound **13c**.

Similarly, spectroscopic analysis was performed in order characterize the isomer arylated at C-6 position **14b**. In the ^{1}H NMR analysis of 6-phenylindolizine-1-carbonitrile the peaks corresponding to H-2 (7.06 *ppm*, *J*= 3.0 Hz) and H-3 (7.31 *ppm*, J= 3.0 Hz) were present in the spectrum, which confirmed that substitution occurred at pyridine ring instead the pyrrole ring. The signals corresponding to H-7 appeared as a doublet of doublets of doublets (*ddd)* at 7.31 *ppm* and H-8 as doublet in 7.71 *ppm*. Besides, H-5 appeared as singlet in 8,20 *ppm*, confirming that substitution occurred now at C-6 position. NOESY and COSY spectrum showed correlation among peak in 8.20 *ppm* (H-8), 7.56 *ppm* (corresponding to the *ortho*-position of the phenyl ring) and peak in 7.31 *ppm* (H-3). Correlation between hydrogen in 7.34 *ppm* (H-7) and the same peak 7.56 *ppm* was observed as well and corroborate with the aryl group was incorporated at C-6 position (Figure 18).
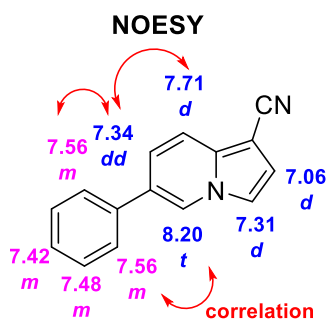
Figure 31. NOESY correlation for compound **14b**.

3.6 Methodological study using dimethyl indolizine-1,2-dicarboxylate

The same reaction screening used for indolizine-1-carbonitrile **12** was then conducted for dimethyl indolizine-1,2-dicarboxylate **4**. The results are summarized in Table 14.
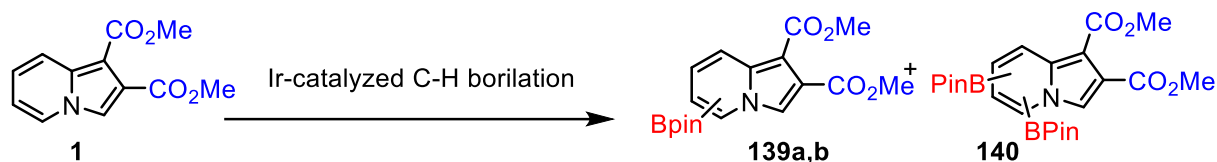
Table 14. Borylation tests using indolizine 1 as substrate.

Entry	[Ir(OMe)(COD)]₂	Ligand	B₂pin₂ (eq.)	Temp. (°C)	Time (h)	Conversion[a]	Products[b]	% GC/MS
a	5 mol%	5 mol% dtbpy	1.0	60	1	69	4 products mono- and 2 products di-borylated	21/29/12/7/7/3
b	10 mol%	20 mol% dtbpy	0.7	60	1	45	139a/ 139b/140	28/9/8
c	10 mol%	20 mol% dtbpy	1.0	rt	1	4	139a/139b	2/2
d	5 mol %	10 mol% dtbpy	1.0	80	4	87	139a/ 139b/140	53/12/12
e	10 mol%	20 mol% dtbpy	0.5	rt	2-24	0	-	0
f	10 mol%	20 mol% dtbpy	0.5	100[c]	1	18	-	0
g	10 mol%	20 mol% tris(4-methoxyphenyl)phosphane	1.0	r.t	16	0	-	0
h	10 mol%	20 mol% 4-4'-dimethoxy-2-2'-bipyridine	1.0	rt	18	29	4 mono-borylated products	2/20/4/3
i	10 mol%	20 mol% 4-4'-dimethoxy-2-2'-bipyridine	1.0	80	24	70	4 products mono- and 2 products di-borylated	10/30/13/10/3/4
j	10 mol%	20 mol% dtbpy	1.5	55	24	96	4 products mono- and 2 products di-borylated	13/4/4/22/21/32
k	10 mol%	20 mol% 4-4'-dimethoxy-2-2'-bipyridine	1.0	80	24	85	4 products mono- and 2 products di-borylated	10/32/9/12/12/10
l	10 mol%	20 mol% 4-4'-dimethoxy-2-2'-bipyridine	2.0	80	24	99	4 products mono- and 2 products di-borylated	5/1/5/12/35/46

[a] GC/MS conversion calculated between starting material and borylated products
[b] mono e di-borylated products
[c] Microwave

We started this study using the same condition used for the borylation of indolizine-1-carbonitrile **12** (Table 14, entry **a**), but despite the better conversion (69%) six borylated products were observed. Because of that, in the next experiments temperature, time, ligand and equivalents of B_2pin_2 were modified in order to achieve better conversion and selectivity.

Using 0.7 equivalents of B_2pin_2 (Table 14, entry **b**) led to the formation of 2 mono-borylated and one di-borylated compound. Later, these compounds were identified as C-5 and C-6 mono-borylated isomers and C-5, C-6 di-borylated product.

Changing temperature, reaction time and amounts of the pre-catalyst [Ir(OMe)cod]$_2$ and ligand (Table 14, entries **c-l**) it was possible to observe, in some cases, an improvement in the conversions (85%-99%, Table 14, entries **j-l**), however it was accompanied of a formation of a mixture of different mono- and di-borylated products.

Attempts using 4-4'-dimethoxy-2-2'-bipyridine as ligand (more electron-rich ligand than dtbpy) showed similar results when using dtbpy (Table 14, entries **h-l**). Deborylation protocol used for indolizine **12** was also tested but without success, since we only recovered fully deborylated products.

All these experiments led us to conclude that the best balance between the number of borylated compounds and conversion was achieved using the conditions showed in Table 14, entry **d**, where two mono-borylated isomers and one di-borylated compound were formed in a ratio 5:1:1 with 77% of GC-MS conversion.

Due to difficulty in isolating these borylated products (deborylation observed), we decided to conduct a one-pot Suzuki-Miyaura cross-coupling reaction in order to determine the borylation sites. Thus, a standard protocol well established in the Steel group, using Pd(dppf)Cl$_2$, K_3PO_2 and dimethylacetamide (DMAc)/H_2O (2:1) was employed. The results are shown in Table 15.

The identity of the 2 isomers and the di-borylated product were determined by fully assignment of ^1H and ^{13}C NMR spectra using NOESY, COSY, HSQC and HMBC spectroscopy techniques (see Spectrum section). The 2 mono-borylated isomers were identified as C-5 (**15**) and C-6 (**16**) arylated products and the di-borylated compound as C-5, C-6-di-arylated (**17**) derivative.

1) Borylation step, MTBE
2) removal of volatiles in vacuo

2.)10 mol% Pd(dppf)Cl$_2$, DMAc/H$_2$O
1.0 eq. Potassium phosphate tribasic
1.3 eq. electrophile, 80°C, 24h
One-pot reaction

15a,b + **16a,b** + **17a,b**
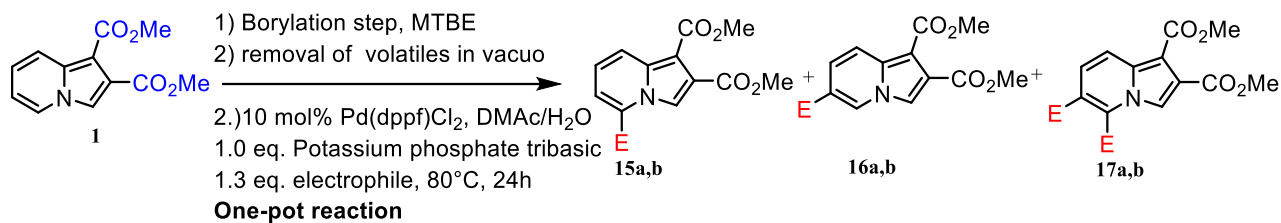
Table 15. One-pot C-H borylation Suzuki-Miyaura cross-coupling

Entry	[Ir(OMe)(COD)]$_2$	dtbpy	B$_2$Pin$_2$ (eq.)	Temp. °C	Time (h)	Conversion[a]	ArX	Yield[b]	Product
a	5 mol%	10 mol%	1.0	80	24	80	Ph-I	42:18:11	16a/17a/18a
b	5 mol%	10 mol%	1.0	80	24	83	Br-PhCF$_3$	48:12:12	16b/17b/18b

[a] GC/MS conversion calculated between starting material and borylated products
[b] isolated yields

The Suzuki-Miyaura cross-coupling reaction was successful in all cases. Best conversions were achieved using iodo-benzene and 1-bromo-4-(trifluoromethyl) benzene and all isomers were successfully purified and characterized.

4. CONCLUSION

In this work, we have performed a comprehensive study on the functionalization of the indolizine ring by using metalation and C-H borylation strategies. Based in our results, the mixed magnesium-lithium base TMPMgCl·LiCl proved to be an excellent reagent for regioselective functionalization of indolizines bearing strong directing metalation groups, such as esters and 2-oxazolines. Reaction of the organomagnesium intermediates with several electrophiles allowed the isolation of a number of functionalized derivatives in reasonable to good yields. We could also note that some electrophiles appear to be able to disrupt the chelation between DMG and the magnesium base complexed with LiCl (TMPMgCl·LiCl) leading to C-5 derivatives for substrate **1**. In the case of the 2-oxazoline substituted substrate, the highly nucleophilic reagent n-BuLi could be used as metalating agent, allowing the selective deprotonation of the most acidic hydrogen and further isolation of C-5 functionalized derivatives in good yields. This base dependent control offered by the 2-oxazoline as DMG should be highlighted and possibly will find further applications in organic synthesis.

In the second part of this work, the lithiation of 2-arylindolizines led to the synthesis of five new 5-formyl-2-aryl indolizine derivatives in good yield. This methodology allowed to the preparation of other 15 new 5-substituted derivatives containing ester, carboxylic acid and amide groups in good yield as well. Due to the fluoresce exhibited for these compounds they had their photochemical and photophysical properties evaluated.

The maximum absorption in the UV-vis region observed were in the range of 257-457 *nm* and the maximum fluorescence emission were in the range of 485-549 *nm*. These compounds were evaluated in methanol and DMSO, the values of quantum yield were higher for the 5-ester derivatives (**9a-e**) and relatively lower for the aldehydes (**8a-e**). The emission decay profiles were fitted to one or two exponential curves depending on the functional group. In general, compounds in DMSO showed higher Stokes shift values, quantum yield and lifetime, compared to results in methanol. Among the groups, lower values were registered for aldehyde compounds (**8a-e**). Interestingly, it is also noticed that in all groups, the compounds containing 2-phenyl group (**8a**, **9a**, **10a**, and **11a**) presented higher efficiency for fluorescence emission with longer average lifetime.

Regarding to the C-H borylation, we could find a reactional condition that despite low yield and less selectivity, when compared with the metalation protocol, led to C-3 and C-5 arylated derivatives for indolizine **12** and C-5, C-6 and C-5,6 arylated derivatives for indolizine **1**. We could conclude with this study that the C-H borylation reaction it is possible for substituted indolizines, however it necessary more investigation using different catalyst and ligands in order to achieve site-selectively. Nonetheless, the results achieve in this study still important since to the best of our knowledge this was the first study on C-H activation/borylation using indolizines as model substrates.

Overall, this work allowed the expansion of our knowledge in the reactive of substituted indolizines and the development of new approaches that, in the future, can help in the construction of more complex derivatives.

5. References

ALIROL, E.; MARTINOU, J. C. Mitochondria and cancer: Is there a morphological connection ? **Oncogene**, v. 25, n. 34, p. 4706–4716, 7, 2006.

AMARAL, M. F. Z. J. et al. Synthesis, photophysical, and electrochemical properties of 2,5-diaryl-indolizines. **Tetrahedron**, v. 70, n. 20, p. 3249–3258, 2014.

AMARAL, M. F. Z. J. et al. Directed Metalation of 1-Ester-Substituted Indolizines: Base/Electrophile-Controlled Regioselective Functionalization. **Organic Letters**, v. 17, n. 2, p. 238–241, 2015.

ARMAREGO, W. L. F. C-1 and C-3 protonation of indolizines. **Journal of the Chemical Society B: Physical Organic**, n. C, p. 191, 1966.

BABAEV, E. V.; VASILEVICH, N. I.; IVUSHKINA, A. S. Efficient synthesis of 5-substituted 2-aryl-6-cyanoindolizines via nucleophilic substitution reactions. **Beilstein Journal of Organic Chemistry**, v. 1, p. 5–8, 2005.

BATISTA, J. H. C. et al. Directed Functionalization of Halophenyl-2-oxazolines with TMPMgCl·LiCl. **European Journal of Organic Chemistry**, v. 2015, n. 5, p. 967–977, 2015.

BECK, E. M.; HATLEY, R.; GAUNT, M. J. Synthesis of Rhazinicine by a Metal-Catalyzed C-H Bond Functionalization Strategy. **Angewandte Chemie International Edition**, v. 47, n. 16, p. 3004–3007, 2008.

BERTALLO, C. R. d. S. et al. C-H Activation/Metalation Approaches for the Synthesis of Indolizine Derivatives. **European Journal of Organic Chemistry**, v. 2019, n. 31–32, p. 5205–5213, 2019.

BLANCHET, L. et al. Quantifying small molecule phenotypic effects using mitochondrial morpho-functional fingerprinting and machine learning. **Scientific Reports**, v. 5, n. 1, p. 8035, 2015.

BLUMBERG, S.; MARTIN, S. F. 4-(Phenylazo)diphenylamine (PDA): a universal indicator for the colorimetric titration of strong bases, Lewis acids, and hydride reducing agents. **Tetrahedron Letters**, v. 56, n. 23, p. 3674–3678, 2015.

BOEBEL, T. A.; HARTWIG, J. F. Silyl-Directed, Iridium-Catalyzed ortho-Borylation of Arenes. A One-Pot ortho-Borylation of Phenols, Arylamines, and Alkylarenes. **Journal of the American Chemical Society**, v. 130, n. 24, p. 7534–7535, 2008.

BOLLER, T. M. et al. Mechanism of the Mild Functionalization of Arenes by Diboron Reagents Catalyzed by Iridium Complexes. Intermediacy and Chemistry of Bipyridine-Ligated Iridium Trisboryl Complexes. **Journal of the American Chemical Society**, v.

127, n. 41, p. 14263–14278, 2005.

BORROWS, E. T.; HOLLAND, D. O.; KENYON, J. The chemistry of the pyrrocolines. Part II. Nitroso-derivatives of some substituted pyrrocolines. **Journal of the Chemical Society (Resumed)**, n. 111, p. 1075, 1946.

BORROWS, E. T.; HOLLAND, D. O.; KENYON, J. 238. The chemistry of the pyrrocolines. Part III. Nitration. **Journal of the Chemical Society (Resumed)**, n. I, p. 1077, 1946.

BOUDET, N.; LACHS, J. R.; KNOCHEL, P. Multiple Regioselective Functionalizations of Quinolines via Magnesiations. **Organic Letters**, v. 9, n. 26, p. 5525–5528, 2007.

BOZZINI, L. A. et al. Selective functionalization of cyano-phenyl-2-oxazolines using TMPMgCl·LiCl. **Tetrahedron Letters**, v. 58, n. 44, p. 4186–4190, 2017.

BRIKCI-NIGASSA, N. et al. In Situ 'Trans-Metal Trapping': An Efficient Way to Extend the Scope of Aromatic Deprotometalation. **Synthesis**, v. 50, n. 18, p. 3615–3633, 2018.

BROWN, T. K. Ibogaine in the treatment of substance dependence. **Current Drug Abuse Reviews**, v. 6, n. 1, p. 3–16, 2013.

BUTA, J. G.; NOVAK, M. J. Isolation of Camptothecin and 10-Methoxycamptothecin from Camptotheca Acuminata by Gel Permeation Chromatography. **Industrial and Engineering Chemistry Product Research and Development**, v. 17, n. 2, p. 160–161, 1978.

CHAGAS, M. H. N. et al. Effects of cannabidiol in the treatment of patients with Parkinson's disease: An exploratory double-blind trial. **Journal of Psychopharmacology**, v. 28, n. 11, p. 1088–1092, 2014.

CHAI, W. et al. A Practical Parallel Synthesis of 2-Substituted Indolizines. **Synlett**, n. 13, p. 2086–2088, 2003.

CHATANI, N. et al. $Ru_3(CO)_{12}$ -Catalyzed Coupling Reaction of sp^3 C−H Bonds Adjacent to a Nitrogen Atom in Alkylamines with Alkenes. **Journal of the American Chemical Society**, v. 123, n. 44, p. 10935–10941, 2001.

CHEVALLIER, F. et al. Deproto-metallation and computed CH acidity of 2-aryl-1,2,3-triazoles. **Organic & biomolecular chemistry**, v. 10, n. 25, p. 4878–85, 2012.

CHO, J.-Y. Remarkably Selective Iridium Catalysts for the Elaboration of Aromatic C-H Bonds. **Science**, v. 295, n. 5553, p. 305–308, 2002.

CHOI, E. J. et al. Rational perturbation of the fluorescence quantum yield in emission-tunable and predictable fluorophores (Seoul-Fluors) by a facile synthetic method

involving C-H activation. **Angewandte Chemie - International Edition**, v. 53, n. 5, p. 1346–1350, 2014.

CLOSOSKI, G. C.; ROHBOGNER, C. J.; KNOCHEL, P. Direct Magnesiation of Polyfunctionalized Arenes and Heteroarenes Using (tmp)$_2$Mg·2LiCl. **Angewandte Chemie International Edition**, v. 46, n. 40, p. 7681–7684, 2007.

CUNHA, S. M. D.; DE OLIVEIRA, R. G.; VASCONCELLOS, M. L. A. A. Microwave-assisted convenient syntheses of 2-indolizine derivatives from Morita-Baylis-Hillman adducts: New in silico potential ion channel modulators. **Journal of the Brazilian Chemical Society**, v. 24, n. 3, p. 432–438, 2013.

DANG, H. V. et al. Copper-catalyzed one-pot domino reactions via C–H bond activation: synthesis of 3-aroylquinolines from 2-aminobenzylalcohols and propiophenones under metal–organic framework catalysis. **RSC Advances**, v. 8, n. 55, p. 31455–31464, 2018.

DARWISH, E. S. Facile synthesis of heterocycles via 2-picolinium bromide and antimicrobial activities of the products. **Molecules**, v. 13, n. 5, p. 1066–1078, 2008.

DASILVEIRA NETO, B. A. et al. Photophysical and electrochemical properties of π-extended molecular 2,1,3-benzothiadiazoles. **Tetrahedron**, v. 61, n. 46, p. 10975–10982, 2005.

DE BOLLE, L. et al. Potent, selective and cell-mediated inhibition of human herpesvirus 6 at an early stage of viral replication by the non-nucleoside compound CMV423. **Biochemical Pharmacology**, v. 67, n. 2, p. 325–336, 2004.

DELATTRE, F. et al. 1-(4-Nitrophenoxycarbonyl)-7-pyridin-4-yl indolizine: A new versatile fluorescent building block. Application to the synthesis of a series of fluorescent β-cyclodextrins. **Tetrahedron**, v. 61, n. 16, p. 3939–3945, 2005.

DO, H.-Q.; KHAN, R. M. K.; DAUGULIS, O. A General Method for Copper-Catalyzed Arylation of Arene C−H Bonds. **Journal of the American Chemical Society**, v. 130, n. 45, p. 15185–15192, 2008.

DO, H. Q.; DAUGULIS, O. Copper-catalyzed arylation of heterocycle C-H bonds. **Journal of the American Chemical Society**, v. 129, n. 41, p. 12404–12405, 2007.

E. MALECZKA, R. et al. Divergent Synthesis of 2,3,5-Substituted Thiophenes by C-H Activation/Borylation/Suzuki Coupling. **HETEROCYCLES**, v. 80, n. 2, p. 1429, 2010.

EATON, P. E.; MARTIN, R. M. Transmetalation and reverse transmetalation on ortho-activated aromatic compounds: a direct route to o,o'-disubstituted benzenes. **The Journal of Organic Chemistry**, v. 53, n. 12, p. 2728–2732, 1988.

EATON, P. E.; LEE, C. H.; XIONG, Y. Magnesium amide bases and amido-Grignards. 1. Ortho magnesiation. **Journal of the American Chemical Society**, v. 111, n. 20, p. 8016–8018, 1989.

FERNÁNDEZ, D. F. et al. Iridium(I)-Catalyzed Intramolecular Hydrocarbonation of Alkenes: Efficient Access to Cyclic Systems Bearing Quaternary Stereocenters. **Angewandte Chemie International Edition**, v. 56, n. 32, p. 9541–9545, 2017.

FRASER, M.; MCKENZIE, S.; REID, D. H. Nuclear magnetic resonance. Part IV. The protonation of indolizines. **Journal of the Chemical Society B: Physical Organic**, n. 44, p. 44, 1966.

GALBRAITH, A. et al. The Formation of Cycl[3.2.2]azine Derivatives via the Reaction of Pyrrocoline with Dimethyl Acetylenedicarboxylate. **Journal of the American Chemical Society**, v. 83, n. 2, p. 453–458, 1961.

GAO, Z. et al. A fluorescent dye with large Stokes shift and high stability: synthesis and application to live cell imaging. **RSC Advances**, v. 7, n. 13, p. 7604–7609, 2017.

GIEDT, R. J. et al. Computational imaging reveals mitochondrial morphology as a biomarker of cancer phenotype and drug response. **Scientific Reports**, v. 6, n. 1, p. 32985, 2016.

GILMAN, H.; BEBB, R. L. Relative Reactivities of Organometallic Compounds. XX. Metalation. **Journal of the American Chemical Society**, v. 61, n. 1, p. 109–112, 1939.

GOFF, D. A. Combinatorial synthesis of indolizines on solid support. **Tetrahedron Letters**, v. 40, n. 50, p. 8741–8745, 1999.

GRECI, L.; RIDD, J. H. The kinetics of nitration and nitrosation of 1-methyl-2-phenylindolizine. **Journal of the Chemical Society, Perkin Transactions 2**, v. 1, n. 3, p. 312, 1979.

GREEN, L.; CHAUDER, B.; SNIECKUS, V. The directed ortho metalation-cross-coupling symbiosis in heteroaromatic synthesis. **Journal of Heterocyclic Chemistry**, v. 36, n. 6, p. 1453–1468, 1999.

HARRELL, W. B. Mannich bases from 1,2-diphenylindolizine: Ephedrine and methamphetamine as amine components. **Journal of Pharmaceutical Sciences**, v. 59, n. 2, p. 275–275, 1970.

HARTWIG, J. F. Regioselectivity of the borylation of alkanes and arenes. **Chemical Society Reviews**, v. 40, n. 4, p. 1992, 2011.

HAUSER, C. R.; WALKER, H. G. Condensation of Certain Esters by Means of

Diethylaminomagnesium Bromide. **Journal of the American Chemical Society**, v. 69, n. 2, p. 295–297, 1947.

HAZRA, A. et al. Amberlite-IRA-402(OH) ion exchange resin mediated synthesis of indolizines, pyrrolo[1,2-a]quinolines and isoquinolines: Antibacterial and antifungal evaluation of the products. **European Journal of Medicinal Chemistry**, v. 46, n. 6, p. 2132–2140, 2011.

HERTZBERG, R. P.; CARANFA, M. J.; HECHT, S. M. On the Mechanism of Topoisomerase I Inhibition by Camptothecin: Evidence for Binding to an Enzyme-DNA Complex. **Biochemistry**, v. 28, n. 11, p. 4629–4638, 1989.

HESSE, M. **Alkaloids**. Switzerland: Wiley-VCH, VHCA, 2002.

HOENDERS, H. J. R. et al. Natural Medicines for Psychotic Disorders: A Systematic Review. **Journal of Nervous and Mental Disease**, v. 206, n. 2, p. 81–101, 2018.

ISHIYAMA, T. et al. A Stoichiometric Aromatic C-H Borylation Catalyzed by Iridium(I)/2,2′-Bipyridine Complexes at Room Temperature. **Angewandte Chemie**, v. 114, n. 16, p. 3182–3184, 2002.

ISHIYAMA, T. et al. Mild Iridium-Catalyzed Borylation of Arenes. High Turnover Numbers, Room Temperature Reactions, and Isolation of a Potential Intermediate. **Journal of the American Chemical Society**, v. 124, n. 3, p. 390–391, 2002.

ISHIYAMA, T. et al. Iridium-Catalyzed Direct Borylation of Five-Membered Heteroarenes by Bis(pinacolato)diboron: Regioselective, Stoichiometric, and Room Temperature Reactions. **Advanced Synthesis & Catalysis**, v. 345, n. 910, p. 1103–1106, 2003.

IVERSON, C. N.; SMITH, M. R. Stoichiometric and Catalytic B−C Bond Formation from Unactivated Hydrocarbons and Boranes. **Journal of the American Chemical Society**, v. 121, n. 33, p. 7696–7697, 1999.

JALA, R.; PALAKODETY, R. K. Copper-catalyzed oxidative C-H bond functionalization of N-allylbenzamide for C-N and C-C bond formation. **Tetrahedron Letters**, v. 60, n. 21, p. 1437–1440, 2019.

JAMES, D. A. et al. Conjugated indole-imidazole derivatives displaying cytotoxicity against multidrug resistant cancer cell lines. **Bioorganic and Medicinal Chemistry Letters**, v. 16, n. 19, p. 5164–5168, 2006.

JEONG, M. S. et al. A selective Seoul-Fluor-based bioprobe, SfBP, for vaccinia H1-related phosphatase—a dual-specific protein tyrosine phosphatase. **Chemical Communications**, v. 48, p. 6553, 2012.

JIAO, K.-J. et al. Palladium catalyzed CH functionalization with electrochemical oxidation. **Tetrahedron Letters**, v. 58, n. 9, p. 797–802, mar. 2017.

JOHNSON, J. A.; LI, N.; SAMES, D. Total Synthesis of (−)-Rhazinilam: Asymmetric C−H Bond Activation via the Use of a Chiral Auxiliary. **Journal of the American Chemical Society**, v. 124, n. 24, p. 6900–6903, 2002.

JOHNSON, J. A.; SAMES, D. C−H Bond Activation of Hydrocarbon Segments in Complex Organic Molecules: Total Synthesis of the Antimitotic Rhazinilam. **Journal of the American Chemical Society**, v. 122, n. 26, p. 6321–6322, 2000.

JOULE, J. A.; MILLES, K.; SMITH, G. F. **Heterocyclic Chemistry**. 4ºed. [s.l.] Blackwell Publishing, 2000.

KAKIUCHI, F.; MURAI, S. Catalytic C−H/Olefin Coupling. **Accounts of Chemical Research**, v. 35, n. 10, p. 826–834, 2002.

KALLEPALLI, V. A. et al. Harnessing C–H Borylation/Deborylation for Selective Deuteration, Synthesis of Boronate Esters, and Late Stage Functionalization. **The Journal of Organic Chemistry**, v. 80, n. 16, p. 8341–8353, 2015.

KANTAM, M. L. et al. Copper Catalyzed C−H Activation. **The Chemical Record**, v. 19, n. 7, p. 1302–1318, 2019.

KATRITZKY, A. R.; RAMSDEN, C. A.; JOULE, J. A.; ZHDANKIN, V. V. **Handbook of Heterocyclic Chemistry**. 3ª Ed ed. [s.l.] Oxford: Elsevier, 2010.

KATRITZKY, A. R. et al. Novel syntheses of indolizines and pyrrolo[2,1-a]isoquinolines via benzotriazole methodology. **Journal of Organic Chemistry**, v. 64, n. 20, p. 7618–7621, 1999.

KATRITZKY, A. R.; REES, C. W. The Strucutre, Reactions, Synthesis and Uses of Heterocyclic Compounds. In: BIRD, C. W.; CHEESEMAN, G. W. H. **Comprehensive Heterocyclic Chemistry**. 1st ed. Oxford: Pergamon Press, 1984. p. 453–460.

KAWAMORITA, S. et al. Directed Ortho Borylation of Functionalized Arenes Catalyzed by a Silica-Supported Compact Phosphine−Iridium System. **Journal of the American Chemical Society**, v. 131, n. 14, p. 5058–5059, 2009.

KAWAMORITA, S.; OHMIYA, H.; SAWAMURA, M. Ester-Directed Regioselective Borylation of Heteroarenes Catalyzed by a Silica-Supported Iridium Complex. **The Journal of Organic Chemistry**, v. 75, n. 11, p. 3855–3858, 2010.

KERR, W. J. et al. Iridium-Catalyzed Csp 3 –H Activation for Mild and Selective Hydrogen Isotope Exchange. **ACS Catalysis**, v. 8, n. 11, p. 10895–10900, 2018.

KIM, E. et al. Discovery , Understanding , and Bioapplication of Organic Fluorophore :

A Case Study with an Indolizine-Based Novel. **Accounts of Chemical Research**, v. 48, p. 538–547, 2015.

KIM, E.; LEE, S.; PARK, S. B. 9-Aryl-1,2-dihydropyrrolo[3,4-b]indolizin-3-one (Seoul-Fluor) as a smart platform for colorful ratiometric fluorescent pH sensors. **Chemical communications (Cambridge, England)**, v. 47, n. 27, p. 7734–7736, 2011.

KIM, I. et al. Expeditious synthesis of indolizine derivatives via iodine mediated 5-endo-dig cyclization. **Tetrahedron Letters**, v. 48, n. 39, p. 6863–6867, 2007.

KIM, M.; JUNG, Y.; KIM, I.Domino Knoevenagel condensation/intramolecular aldol cyclization route to diverse indolizines with densely functionalized pyridine units. **Journal of Organic Chemistry**, v. 78, n. 20, p. 10395–10404, 2013.

KLEIN, J. E. M. N. et al. First C−H Activation Route to Oxindoles using Copper Catalysis. **Organic Letters**, v. 12, n. 15, p. 3446–3449, 2010.

KONISHI, S. et al. Site-Selective C-H Borylation of Quinolines at the C8 Position Catalyzed by a Silica-Supported Phosphane-Iridium System. **Chemistry - An Asian Journal**, v. 9, n. 2, p. 434–438, 2014.

KRASOVSKIY, A.; KRASOVSKAYA, V.; KNOCHEL, P. Mixed Mg/Li Amides of the Type R2NMgCl·LiCl as Highly Efficient Bases for the Regioselective Generation of Functionalized Aryl and Heteroaryl Magnesium Compounds. **Angewandte Chemie International Edition**, v. 45, n. 18, p. 2958–2961, 2006.

KRASOVSKIY, A.; KRASOVSKAYA, V.; KNOCHEL, P. Mixed Mg/Li Amides of the Type R_2NMgCl·LiCl as Highly Efficient Bases for the Regioselective Generation of Functionalized Aryl and Heteroaryl Magnesium Compounds. **Angewandte Chemie International Edition**, v. 45, n. 18, p. 2958–2961, 2006.

KUCUKDISLI, M.; OPATZ, T. A modular synthesis of polysubstituted indolizines. **European Journal of Organic Chemistry**, n. 24, p. 4555–4564, 2012.

KUMAR, D. et al. Synthesis, optical properties, and blue electroluminescence of fluorene derivatives containing multiple imidazoles bearing polyaromatic hydrocarbons. **Tetrahedron**, v. 69, n. 12, p. 2594–2602, 2013.

KUZNETSOV, A. G. et al. An improved synthesis of some 5-substituted indolizines using regiospecific lithiation. **Molecules**, v. 10, n. 9, p. 1074–1083, 2005.

KUZNETSOV, A. G.; BUSH, A. A.; BABAEV, E. V. Synthesis and reactivity of 5-Br(I)-indolizines and their parallel cross-coupling reactions. **Tetrahedron**, v. 64, n. 4, p. 749–756, 2008.

LABINGER, J. A. Platinum-Catalyzed C–H Functionalization. **Chemical Reviews**, v.

117, n. 13, p. 8483–8496, 2017.

LARSEN, M. A.; HARTWIG, J. F. Iridium-Catalyzed C–H Borylation of Heteroarenes: Scope, Regioselectivity, Application to Late-Stage Functionalization, and Mechanism. **Journal of the American Chemical Society**, v. 136, n. 11, p. 4287–4299, 2014.

LEE, J. H.; KIM, I. Cycloaromatization approach to polysubstituted indolizines from 2-acetylpyrroles: Decoration of the pyridine unit. **Journal of Organic Chemistry**, v. 78, n. 3, p. 1283–1288, 2013.

LI, X.; XIE, X.; LIU, Y. Gold(I)-Catalyzed Cascade Hydroarylation /Cycloaromatization to Indolizines via Pyridine Ring Construction. **The Journal of Organic Chemistry**, v. 81, n. 9, p. 3688–3699, 2016.

LIN, W.; BARON, O.; KNOCHEL, P. Highly Functionalized Benzene Syntheses by Directed Mono or Multiple Magnesiations with TMPMgCl·LiCl. **Organic Letters**, v. 8, n. 24, p. 5673–5676, 2006.

LINGALA, S. et al. Synthesis and comparative anti-tubercular activity of indolizine derivatives of Isoniazid / Pyrazinamide / Ethionamide. **International Journal of Pharmaceutical Sciences Review and Research**, v. 6, n. 2, p. 128–131, 2011.

LINS, C. L. K.; BLOCK, J. H.; DOERGE, R. F. Nitro- para- and meta- Substituted 2-Phenylindolizines as Potential Antimicrobial Agents. **Journal of Pharmaceutical Sciences**, v. 71, n. 5, p. 556–561, 1982.

LISKEY, C. W. et al. Pronounced effects of substituents on the iridium-catalyzed borylation of aryl C–H bonds. **Chemical Communications**, n. 37, p. 5603, 2009.

LIU, B. et al. Discovery of a full-color-tunable fluorescent core framework through direct C-H (hetero)arylation of N-heterocycles. **Chem. Eur. J.**, v. 18, n. 6, p. 1599–1603, 2012.

LOU, M. et al. Rhodium-catalyzed C–H bond activation alkylation and cyclization of 2-arylquinazolin-4-ones. **Organic & Biomolecular Chemistry**, v. 16, n. 11, p. 1851–1859, 2018.

LUNGU, N. C. et al. Synthesis of a new fluorinated fluorescent-cyclodextrin sensor. **Journal of Fluorine Chemistry**, v. 126, n. 3, p. 393–396, 2005.

MALECZKA, R. E. et al. C−H Activation/Borylation/Oxidation: A One-Pot Unified Route To Meta-Substituted Phenols Bearing Ortho-/Para-Directing Groups. **Journal of the American Chemical Society**, v. 125, n. 26, p. 7792–7793, 2003.

MATVIIUK, T. et al. Synthesis of 3-heteryl substituted pyrrolidine-2,5-diones via catalytic Michael reaction and evaluation of their inhibitory activity against InhA and

Mycobacterium tuberculosis. **European Journal of Medicinal Chemistry**, v. 71, p. 46–52, 2014.

MEDDA, S. et al. Phospholipid microspheres: a novel delivery mode for targeting antileishmanial agent in experimental leishmaniasis. **Journal of drug targeting**, v. 11, n. 2, p. 123–8, 2003.

MILLER, R. E. et al. Combined Directed ortho Metalation−Halogen Dance (HD) Synthetic Strategies. HD−Anionic ortho Fries Rearrangement and Double HD Sequences. **Organic Letters**, v. 12, n. 10, p. 2198–2201, 2010.

MKHALID, I. A. I. et al. C−H Activation for the Construction of C−B Bonds. **Chemical Reviews**, v. 110, n. 2, p. 890–931, 10 fev. 2010. Disponível em: <https://pubs.acs.org/doi/10.1021/cr900206p>.

MONGIN, F.; QUÉGUINER, G. Advances in the directed metallation of azines and diazines (pyridines, pyrimidines, pyrazines, pyridazines, quinolines, benzodiazines and carbolines). Part 1: Metallation of pyridines, quinolines and carbolines. **Tetrahedron**, v. 57, n. 19, p. 4059–4090, 2001.

MORO, A. V. et al. Synthesis and photophysical properties of fluorescent 2,1,3-benzothiadiazole-triazole-linked glycoconjugates: Selective chemosensors for Ni(II). **Tetrahedron**, v. 69, n. 1, p. 201–206, 2013.

MULVEY, R. E. et al. Deprotonative Metalation Using Ate Compounds: Synergy, Synthesis, and Structure Building. **Angewandte Chemie International Edition**, v. 46, n. 21, p. 3802–3824, 2007.

MURATA, M. et al. Aromatic C–H Borylation Catalyzed by Hydrotris(pyrazolyl)borate Complexes of Rhodium and Iridium. **Bulletin of the Chemical Society of Japan**, v. 79, n. 12, p. 1980–1982, 2006.

MURIE, V. E. et al. Base-Controlled Regioselective Functionalization of Chloro-Substituted Quinolines. **The Journal of Organic Chemistry**, v. 83, n. 2, p. 871–880, 2018.

MURPHY, J. M.; LIAO, X.; HARTWIG, J. F. Meta Halogenation of 1,3-Disubstituted Arenes via Iridium-Catalyzed Arene Borylation. **Journal of the American Chemical Society**, v. 129, n. 50, p. 15434–15435, 2007.

MURPHY, J. M.; TZSCHUCKE, C. C.; HARTWIG, J. F. One-Pot Synthesis of Arylboronic Acids and Aryl Trifluoroborates by Ir-Catalyzed Borylation of Arenes. **Organic Letters**, v. 9, n. 5, p. 757–760, 2007.

NAREDDY, P.; JORDAN, F.; SZOSTAK, M. Recent Developments in Ruthenium-

Catalyzed C–H Arylation: Array of Mechanistic Manifolds. **ACS Catalysis**, v. 7, n. 9, p. 5721–5745, 2017.

NISHIMURA, R. H. V. **Funcionalização de compostos N-heterocíclicos visando a síntese de substâncias bioativas.** 2019. Faculdade de Filosofia Ciências e Letras de Ribeirão Preto – Universidade de São Paulo, 2019.

O'MALLEY, S. J. et al. Total Synthesis of (+)-Lithospermic Acid by Asymmetric Intramolecular Alkylation via Catalytic C−H Bond Activation. **Journal of the American Chemical Society**, v. 127, n. 39, p. 13496–13497, 2005.

OLIVEIRA, F. F. D. et al. On the use of 2,1,3-benzothiadiazole derivatives as selective live cell fluorescence imaging probes. **Bioorganic and Medicinal Chemistry Letters**, v. 20, n. 20, p. 6001–6007, 2010.

OOYAMA, Y. et al. Solid-state fluorescence properties and mechanofluorochromism of D-π-A pyridinium dyes bearing various counter anions. **Tetrahedron**, v. 69, n. 29, p. 5818–5822, 2013.

PAN, S.; SHIBATA, T. Recent Advances in Iridium-Catalyzed Alkylation of C–H and N–H Bonds. **ACS Catalysis**, v. 3, n. 4, p. 704–712, 2013.

PRESHLOCK, S. M. et al. High-Throughput Optimization of Ir-Catalyzed C–H Borylation: A Tutorial for Practical Applications. **Journal of the American Chemical Society**, v. 135, n. 20, p. 7572–7582, 2013.

PRZEWLOKA, T. et al. Application of DMF-methyl sulfate adduct in the regioselective synthesis of 3-acylated indolizines. **Tetrahedron Letters**, v. 48, n. 33, p. 5739–5742, 2007.

RAO, W.-H.; SHI, B.-F. Recent advances in copper-mediated chelation-assisted functionalization of unactivated C–H bonds. **Organic Chemistry Frontiers**, v. 3, n. 8, p. 1028–1047, 2016.

RAPPOPORT, Z.; MAREK, I. **The Chemistry of Organomagnesium Compounds**. Chichester, UK: John Wiley & Sons, Ltd, 2008.

REJ, S.; CHATANI, N. Rhodium-Catalyzed C(sp 2)- or C(sp 3)−H Bond Functionalization Assisted by Removable Directing Groups. **Angewandte Chemie International Edition**, v. 58, n. 25, p. 8304–8329, 2019.

RENARD, M.; GUBIN, J. Metallation of 2-phenylindolizine. **Tetrahedron Letters**, v. 33, n. 31, p. 4433–4434, 1992.

ROBBINS, D. W.; HARTWIG, J. F. Sterically Controlled Alkylation of Arenes through Iridium-Catalyzed C À H Borylation. **Angew. Chem. Int. Ed.**, v. 52, p. 933–937, 2013.

ROSEMARY, G. **Synthesis and conformational studies of indolizines**. 1994. Rhodes University, Grahamstown, 1994.

SADLER, S. A. et al. Iridium-catalyzed C–H borylation of pyridines. **Organic & Biomolecular Chemistry**, v. 12, n. 37, p. 7318, 2014.

SADLER, S. A. et al. Multidirectional Synthesis of Substituted Indazoles via Iridium-Catalyzed C − H Borylation. p. 1–7, 2015.

SADOWSKI, B.; KLAJN, J.; GRYKO, D. T. Recent advances in the synthesis of indolizines and their π-expanded analogues. **Organic & Biomolecular Chemistry**, v. 14, n. 33, p. 7804–7828, 2016.

SANDEEP, C. et al. Review on Chemistry of Natural and Synthetic Indolizines with their Chemical and Pharmacological Properties. **Journal of Basic and Clinical Pharmacy**, v. 8, n. 2, p. 49–61, 2017.

SANTOS, F. M. dos et al. Directed Functionalization of Cyano-Substituted Furans and Thio- phenes with TMPMgCl·LiCl. p. 2795–2800, 2015.

SATTLER, A. et al. Platinum Catalyzed C–H Activation and the Effect of Metal–Support Interactions. **ACS Catalysis**, v. 10, n. 1, p. 710–720, 2020.

SCHLOSSER, M. The 2×3 Toolbox of Organometallic Methods for Regiochemically Exhaustive Functionalization. **Angewandte Chemie International Edition**, v. 44, n. 3, p. 376–393, 2005.

SCHOLTZ, M. **Ber.**, v. 45, p. 734, 1912.

SCHUMACHER, D. P. et al. An efficient synthesis of florfenicol. **The Journal of Organic Chemistry**, v. 55, n. 18, p. 5291–5294, 1990.

SHARMA, V.; KUMAR, V. Indolizine: A biologically active moiety. **Medicinal Chemistry Research**, v. 23, n. 8, p. 3593–3606, 2014.

SHEN, Y. et al. European Journal of Medicinal Chemistry Synthesis and antiproliferative activity of indolizine derivatives incorporating a cyclopropylcarbonyl group against Hep-G2 cancer cell line. **European Journal of Medicinal Chemistry**, v. 45, n. 7, p. 3184–3190, 2010.

SHIBAHARA, F.; YAMAGUCHI, E.; MURAI, T. Direct multiple C–H bond arylation reaction of heteroarenes catalyzed by cationic palladium complex bearing 1,10-phenanthroline. **Chemical Communications**, v. 46, n. 14, p. 2471, 2010.

SHIBAHARA, F.; YAMAGUCHI, E.; MURAI, T. Direct Arylation of Simple Azoles Catalyzed by 1,10-Phenanthroline Containing Palladium Complexes: An Investigation of C4 Arylation of Azoles and the Synthesis of Triarylated Azoles by Sequential

Arylation. **The Journal of Organic Chemistry**, v. 76, n. 8, p. 2680–2693, 2011.

SINGH, G. S.; MMATLI, E. E. Recent progress in synthesis and bioactivity studies of indolizines. **European Journal of Medicinal Chemistry**, v. 46, n. 11, p. 5237–5257, 2011.

SUNG, J. et al. Development of fluorescent mitochondria probe based on 1,2-dihydropyrrolo[3,4- b]indolizine-3-one. **Dyes and Pigments**, v. 145, p. 461–468, 2017.

TAGATA, T.; NISHIDA, M. Aromatic C-H borylation catalyzed by iridium/2,6-diisopropyl-N-(2- pyridylmethylene)aniline complex. **Advanced Synthesis and Catalysis**, v. 346, n. 13–15, p. 1655–1660, 2004.

TAJUDDIN, H. et al. Iridium-catalyzed C–H borylation of quinolines and unsymmetrical 1,2-disubstituted benzenes: insights into steric and electronic effects on selectivity. **Chemical Science**, v. 3, n. 12, p. 3505, 2012.

TAKAGI, J. et al. Iridium-catalyzed C–H coupling reaction of heteroaromatic compounds with bis(pinacolato)diboron: regioselective synthesis of heteroarylboronates. **Tetrahedron Letters**, v. 43, n. 32, p. 5649–5651, 2002.

TAMURA, H. et al. Iridium-Catalyzed Borylation of Benzene with Diboron. Theoretical Elucidation of Catalytic Cycle Including Unusual Iridium(V) Intermediate. **Journal of the American Chemical Society**, v. 125, n. 51, p. 16114–16126, 2003.

TEKLU, S. et al. Indolizine 1-sulfonates as potent inhibitors of 15-lipoxygenase from soybeans. **Bioorganic and Medicinal Chemistry**, v. 13, n. 9, p. 3127–3139, 2005.

TSCHITSCHIBABIN, A. E. **Ber. Dtsch. Chem. Ges.**, p. 1607, 1927.

TSUGE, O.; KANEMASA, S.; TAKENAKA, S. Stereochemical Study on 1,3-Dipolar Cycloaddition Reactions of Heteroaromatic N-Ylides with Symmetrically Substituted cis and trans Olefins. **Bulletin of the Chemical Society of Japan**, v. 58, n. 11, p. 3137–3157, 1985.

TZSCHUCKE, C. C.; MURPHY, J. M.; HARTWIG, J. F. Arenes to Anilines and Aryl Ethers by Sequential Iridium-Catalyzed Borylation and Copper-Catalyzed Coupling. **Organic Letters**, v. 9, n. 5, p. 761–764, 2007.

VEMULA, V. R.; VURUKONDA, S.; BAIRI, C. K. Indolizine derivatives: Recent advances and potential pharmacological activities. **International Journal of Pharmaceutical Sciences Review and Research**, v. 11, n. 1, p. 159–163, 2011.

WAN, J. et al. Multifunctional electron-transporting indolizine derivatives for highly efficient blue fluorescence, orange phosphorescence host and two-color based white OLEDs. **Journal of Materials Chemistry**, v. 22, n. 10, p. 4502, 2012.

WANG, J. et al. New emissive organic molecule based on pyrido[3,4-g]isoquinoline framework: Synthesis and fluorescence tuning as well as optical waveguide behavior. **Tetrahedron**, v. 69, n. 13, p. 2687–2692, 2013.

WANG, X.-C. et al. Ligand-enabled meta-C-H activation using a transient mediator. **Nature**, v. 519, n. 7543, p. 334–8, 2015.

WATSON, A. A. et al. Polyhydroxylated alkaloids - Natural occurrence and therapeutic applications. **Phytochemistry**, v. 56, n. 3, p. 265–295, 2001.

WHISLER, M. C. et al. Beyond Thermodynamic Acidity: A Perspective on the Complex-Induced Proximity Effect (CIPE) in Deprotonation Reactions. **Angewandte Chemie International Edition**, v. 43, n. 17, p. 2206–2225, 2004.

WITTIG, G.; PIEPER, G.; FUHRMANN, G. Über die Bildung von Diphenyl aus Fluorbenzol und Phenyl-lithium (IV. Mitteil. über Austauschreaktionen mit Phenyl-lithium). **Berichte der deutschen chemischen Gesellschaft (A and B Series)**, v. 73, n. 11, p. 1193–1197, 1940.

WITULSKI, B.; SCHWEIKERT, T. Synthesis of Indolo[2,3-a]pyrrolo[3,4-c]carbazoles by Oxidative Cyclization of Bisindolylmaleimides with a Rhodium(III)-Copper(II) Catalytic System. **Synthesis**, v. 2005, n. 12, p. 1959–1966, 2005.

WU, C. et al. Ruthenium(II)-catalyzed selective C–H bond activation of imidamides and coupling with sulfoxonium ylides: an efficient approach for the synthesis of highly functional 3-ketoindoles. **Organic Chemistry Frontiers**, v. 6, n. 8, p. 1183–1188, 2019.

WUNDERLICH, S. H. et al. Scaleable Preparation of Functionalized Organometallics via Directed Ortho Metalation Using Mg- and Zn-Amide Bases. **Organic Process Research & Development**, v. 14, n. 2, p. 339–345, 2010.

XIA, J. B.; YOU, S. L. Synthesis of 3-Haloindolizines by copper(ii) halide mediated direct functionalization of indolizines. **Organic Letters**, v. 11, n. 5, p. 1187–1190, 2009.

YAMADA, R.; IWASAWA, N.; TAKAYA, J. Rhodium-Catalyzed C−H Activation Enabled by an Indium Metalloligand. **Angewandte Chemie International Edition**, v. 58, n. 48, p. 17251–17254, 2019.

YI, C. S.; YUN, S. Y.; GUZEI, I. A. Catalytic Synthesis of Tricyclic Quinoline Derivatives from the Regioselective Hydroamination and C−H Bond Activation Reaction of Benzocyclic Amines and Alkynes. **Journal of the American Chemical Society**, v. 127, n. 16, p. 5782–5783, 2005.

YOSHIZUMI, T. et al. Copper-mediated direct arylation of benzoazoles with aryl

iodides. **Tetrahedron Letters**, v. 49, n. 10, p. 1598–1600, 2008.

ZHANG, L. et al. A Novel and Practical Synthesis of 3-Unsubstituted Indolizines. **Synthesis**, v. 2000, n. 12, p. 1733–1737, 2000.

ZHU, H. et al. Functionalized heterocyclic scaffolds derived from Morita-Baylis-Hillman Acetates. **Chemical Communications**, v. 49, n. 70, p. 7738–7740, 2013.

6. Experimental

6.1 General Considerations

Metalation reactions were carried out under dry nitrogen atmosphere using traditional flasks with rubber septum.

Borylation reactions were performed under dry nitrogen atmosphere using Schlenk techniques. Solvents used in the borylation protocols were anhydrous and degassed through several freeze-pump-thaw cycles. All solvents used for Suzuki-Miyaura cross-coupling reactions were used without drying but with several freeze-pump-thaw cycles.

Solvents

Chapter I: Tetrahydrofuran (THF) was purchased from Panreac and dried through distillation process from metallic sodium and benzophenone. After the solvent turns deep blue in colour, the amount required for reaction can be distilled off. All other reactions solvents used in this chapter were purified by standard protocols.

***n*-BuLi** was purchased from Sigma Aldrich and tritiated following standard procedure.

An oven-dried 25 mL round bottom flask under N_2 atmosphere was charged with 1.10-Phenantroline, THF (2 mL) and *n*-BuLi (1 mL). Then, the reaction mixture was cooled to 0 °C and tritiated with anhydrous isopropyl alcohol.

***i*-PrMgCl·LiCl** was purchased from Sigma Aldrich and tritiated following standard procedure.

An oven-dried 25 mL round bottom flask under N_2 atmosphere was charged with I_2 (0.5 mmol, 127 mg) and THF (1 mL). Then, the reaction mixture was tritiated with *i*-PrMgCl·LiCl.

ZnCl₂ was purchased from Sigma Aldrich. **ZnCl₂ solution 1 M** was prepared following the described procedure.

An oven-dried Schlenk tube equipped with a magnetic stirring bar was charged with $ZnCl_2$ (25 mmol, 3.4 g) and heated to 140 °C for 4 hours under vacuum. Then, Schlenk tube was cooled to room temperature under N_2 atmosphere. After, 25 mL of dry THF was added and the reactional mixture was stirred until upon solubilization.

LiCl was purchased from Sigma Aldrich. **LiCl solution 1 M** was prepared following the described procedure.

An oven-dried Schlenk tube equipped with a magnetic stirring bar was charged with LiCl (25 mmol, 1.06 g) and heated to 140 °C for 4 hours under vacuum. Then, Schlenk tube was cooled to room temperature under N_2 atmosphere. After, 25 mL of dry THF was added and the reactional mixture was stirred until upon solubilization.

Chapter II: Methyl-tert-butyl-ether (MTBE) was purchased anhydrous from Sigma Aldrich. DMF and DMAc were purchased from Sigma-Aldrich. All other reaction solvents were dried using an Innovative Technology Solvent Purification System (SPS) and kept under nitrogen.

Microwave Reactor

Chapter I: Microwave reactions were carried out in septum sealed vials in an Anton Paar GmbH - Monowave 300 (Microwave synthesis reactor).

Chapter II: Microwave reactions were carried out in septum-containing, crimp-capped, sealed vials in a monomodal EmrysTM Optimizer reactor from Personal Chemistry.

TLC

TLC analyses were performed on pre-coated aluminum-backed plates (Silica gel 60 F254, Merck). Signals were visualized with UV-light (254 nm and 365 nm) or by staining when necessary (Sulfuric Vanilla).

Flash Column Chromatography

Chapter I: Hand column using silica gel *flash* from Aldrich®, particle size 230-400 mesh, 40-63 μm and 60 Å with the stated solvent gradient.

Chapter II: Flash column chromatography was performed on a CombiFlash® System from Teledyne Isco equipped with an UV-light detector using prepacked silica RediSep® Rf cartridges with the stated solvent gradient. Crude mixtures to be purified were dry loaded onto silica prior to loading on the column. Reverse phase chromatography used pre-packed C18 silica Redisep® Rf cartridges and a 0-100% CH_3CN in H_2O gradient elution.

NMR Spectroscopy

^1H and ^{13}C chemical shifts are reported in *ppm* using the residual solvent signal of the deuterated solvents (CDCl$_3$: δ_H= 7.26 *ppm*, δC = 77.16 *ppm* and DMSO-d$_6$: δ_H =

2.50 *ppm*, δ_C= 39.51 *ppm*, Py-d$_5$: δ_H= 8.74 *ppm*, 7.58 *ppm*, 7.22 *ppm*, δ_C= 150.35 *ppm*, 135.91 *ppm*, 123.87 *ppm*). All chemical shifts are reported in parts per million relative to tetramethylsilane (δ_H = 0.00 *ppm*). All coupling constants are reported in *Hz*. Multiplicities are reported using the following abbreviations: *s* (singlet), *d* (doublet), *dd* (doublet of doublets), *ddd* (doublet of doublets of doublets), *t* (triplet), *td* (triplet of doublets), *q* (quartet), *m* (unresolved multiplet). Assignment of spectra was carried out using 2D COSY, HMBC, HSQC and NOESY techniques.

Chapter I: NMR spectra were recorded at ambient temperature on Bruker®: DPX-300 (^{1}H, ^{13}C), DRX-400 (^{1}H, ^{13}C[1H], HSQC, HMBC, COSY) and DRX-500 (^{1}H, ^{13}C[1H], HSQC, HMBC, COSY) spectrometers.

Chapter II: NMR spectra were recorded at ambient temperature on Varian Inova-600 (^{1}H, ^{13}C[1H], HSQC, HMBC, COSY) or Varian VNMRS-700 (^{1}H,^{13}C[1H], HSQC, HMBC, COSY) spectrometers.

Gas chromatography (GC/FID)

Chapter I: GC/FID were performed on Shimadzu® GC-2014 Automatic injector AOC-20i. Column used RTX-1 (100 % dimethyl polyloxane) from Restek.

Mass Spectrometry

Chapter I: GC/MS analyses were performed on Shimadzu® GC–MS-QP2010 using electron ionization (EI: 70eV). Column: DB-5-MS J&W Scientific, 30 m, Ø 0.25 mm, film 0.25 µm; carrier gas: helium (1.30 mL min^{-1}). HRMS measurements were carried out on LC-MS-Bruker Daltonics® MicroTOF QII with an electrospray ion source and time of flight analyser (TOF).

Chapter II: GC/MS analyses were performed on a Shimadzu® GC-MS-QP2010-Ultra using electron ionization (EI: 70 eV). The mass spectrometer was equipped with either a Rxi-5Sil MS column (0.15 µm × 10 m × 0.15mm) for non-polar compounds or a Rxi-17Sil MS column (0.15 µm × 10 m × 0.15 mm) for polar compounds; carrier gas: helium (1.6 mL min^{-1}). HRMS measurements were carried out on a QToF Premier mass spectrometer (Waters Ltd, UK) with an electrospray ion source.

IR Spectroscopy

Chapter I: Infrared spectra were measured on a Perkin-Elmer® 400 FT-IR spectrometer via use of a ZnSe ATR (attenuated total reflection) accessory in the range of 600-4000 cm^{-1}. Assigned peaks are reported in wavenumbers (cm^{-1}).

Chapter II: Infrared spectra were measured on a Perkin-Elmer® RX I FT-IR spectrometer via use of a Pike ATR accessory in the range of 3500 – 600 cm^{-1}. Assigned peaks are reported in wavenumbers (cm^{-1}).

Melting points

Chapter I: Melting points were measured on Buchi® M-560 equipment.

Chapter II: Melting points were measured in open capillary tubes using a Thermo Scientific™ Melting Point Apparatus.

6.2 Synthetic Procedures

General Procedure A: Preparation of pyridinium salt 36

A 100 mL round bottom flask fitted with reflux condenser and magnetic stirring was charged with pyridine (100 mmol), EtOAc (60 mL) and chloroacetic acid (100 mmol). The mixture was refluxed for 6 hours and the precipitate formed was filtered and dried under vacuum to provide a white solid in 94% yield.

1- (carboxymethyl) pyridin-1-yl chloride (36)
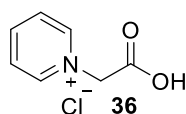
It was used without further purification due to high purity. White solid; yield 94%.CAS: 152968-00-8.^{1}H NMR (CDCl$_3$, 300 MHz) δ *(ppm)*: 9.08 (d, J= 5.4 Hz, 2H), 8.59 (t, J= 7.79 Hz, 1H), 8.13 (t, J= 6.89 Hz, 2H), 5.57 (s, 2H). ^{13}C NMR (75 MHz, CDCl$_3$) δ *(ppm)*: 167.9, 146.7 (2C), 146.6, 128.1 (2C), 61.4. HRMS (ESI) *m/z* [M + H]$^+$ calcd. for C$_7$H$_8$NO$_2$ 138.0549; found 138.0555.

General Procedure B: Preparation of 1-substituted indolizines (1 and 12)

A 200 mL 1-necked flask fitted with reflux condenser and under magnetic stirring was charged with pyridinium salt **36** (10 mmol), respective acrylate (50 mmol), Et₃N (1.5 mL) and toluene (60 mL). Next, MnO₂ (80 mmol) was added and reactional mixture was heated to 90 °C for 12 hours. Then, reaction was cooled to room temperature and the precipitate formed was filtered under vacuum and washed with acetone. The solvent was evaporated, and residue purified by flash chromatography with gradient elution of hexane and ethyl acetate (90:10 - 70:30) to provide the indolizines **1** and **12**.

Indolizine-1-carbonitile 12
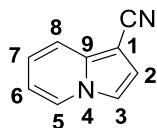
Dark green solid. Yield: 55%. mp: 58-59 ⁰C. CAS: 3352-05-4.¹H NMR (500 MHz, CDCl₃) δ 8.02 (d, *J* = 6.9, 1.1 Hz, H-5), 7.58 (dd, *J* = 9.0, 1.0 Hz, H-8), 7.25 (dd, *J* = 2.9, 0.6 Hz, H-3), 7.07 – 7.02 (m, H-7), 6.99 (d, *J* = 3.0 Hz, H-2), 6.73 (td, *J* = 6.8, 1.3 Hz, H-6).¹³C NMR (101 MHz, CDCl₃) δ 137.6 (C-9), 126.3 (C-5), 122.2 (C-7), 117.5 (C-8), 116.8 (CN), 116.6 (C-2), 113.8 (C-3), 112.7 (C-6), 81.2 (C-1). IR (KBr, ʋmáx., cm⁻¹): 3095, 2958, 2208, 1514, 1481, 1356, 1237, 1040, 740. HRMS (ESI) *m/z* [M + H]⁺ calcd. for C₁₃H₁₅NO₂ 143.0603; found 143.0592.
¹H NMR (600 MHz, Chloroform-*d*) δ 8.01 (dt, *J* = 6.9, 1.0 Hz, 1H), 7.63 (d, *J* = 9.0 Hz, 1H), 7.24 (d, *J* = 3.0 Hz, 1H), 7.05 (ddd, *J* = 8.8, 6.6, 1.0 Hz, 1H), 7.02 (d, *J* = 3.0 Hz, 1H), 6.74 (td, *J* = 6.8, 1.1 Hz, 1H). ¹³C NMR (151 MHz, cdcl₃) δ 137.80, 126.36, 122.32, 117.89, 116.91, 113.87, 112.90, 81.65.

Dimethyl indolizine-1,2-dicarboxylate 4
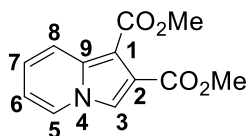
Isolated by pre-packed silica Redisep® *R*f cartridges (ethyl acetate/hexane, 2:8), brown solid, mp: 95-96 °C, yield: 90%. ¹H NMR (600 MHz, CDCl₃) δ= 8.11 (d, *J* = 9.4 Hz, 1H), 7.93 (dd, *J* = 6.9, 0.9 Hz, 1H), 7.62 (s, 1H), 7.06 (ddd, *J* = 9.2, 6.6, 1.0 Hz,

1H), 6.74 (td, J = 6.7, 1.3 Hz, 1H), 3.91 (d, J = 0.7 Hz, 3H), 3.90 (d, J = 0.7 Hz, 3H). ^{13}C NMR (151 MHz, CDCl₃) δ= 165.10, 164.25, 136.12, 125.85, 123.23, 121.59, 120.56, 116.94, 113.65, 102.71, 52.46, 51.59. HRMS (ESI) m/z [M + H]⁺ calcd. for $C_{12}H_{11}NO_4$ 233.0688; found 233.0692.

General Procedure C: Preparation of 2-(indolizin-1-yl)-4,4-dimethyl-4,5-dihydrooxazole 4

Procedure 1C: A thick-walled microwave synthesis vial was charged with indolizine-1-carbonitrile **12** (0.142 g, 1.0 mmol, 1.0 equiv.), ZnCl₂ solution in THF (1M, 0.2 mL), 2-amino-2-methylpropan-1-ol (0,178 g, 0.18 mL, 2.0 equiv.) and glycerol (0.1 mL). The vial was sealed with a crimp top septum cap and heated at 150 °C for 4 hours. After, the reaction mixture was diluted with water (10 mL) and extracted with AcOEt (3 × 10 mL). The combined organic layers were washed with brine (10 mL), dried over anhydrous MgSO₄, and concentrated in vacuo to afford the crude product. Purification was achieved by flash column chromatography using Hexane/AcOEt (1:1).

Procedure 2C: A 50 mL 1-necked flask fitted with reflux condenser and under magnetic stirring was charged with glycerine (4.9 ml), K₂CO₃ (121 mg) and 2-amino-2-methylpropanol (0.33 ml, 1.05 equiv.). After 10 minutes under heating at 120 °C, indolizine-1-carbonitrile **12** (3.29 mmol) was added. The reaction mixture remained under heating of 120 °C for 96 hours.

At the end of the reaction, the reaction mixture was diluted in H₂O and extracted with EtOAc. The combined organic layer was washed with brine (10 mL), dried over anhydrous MgSO₄, and concentrated in vacuum. The crude product was purified by flash chromatography with gradient elution of Et₃N and ethyl acetate (10:90).

2- (indolizin-1-yl) -4,4-dimethyl-4,5-dihydrooxazole 4
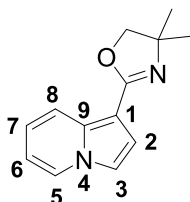
Green solid, mp: 80-81 ºC, yield: 80%. ^{1}H NMR (700 MHz, CDCl₃, 25ºC) δ= 8.10 (dt, J = 9.2, 1.4 Hz, 1H), 7.93 (dt, J = 6.9, 1.1 Hz, 1H), 7.26 – 7.23 (m, 1H), 7.22 (d, J = 2.9 Hz, 1H), 6.90 (ddd, J = 9.1, 6.6, 1.1 Hz, 1H), 6.60 (td, J = 6.7, 1.3 Hz, 1H), 4.06 (s, 2H),

1.39 (s, 6H).^{13}C NMR (176 MHz, cdcl3) δ= 160.2, 133.8, 126.0, 120.8, 120.5, 115.1, 113.7, 112.0, 101.4, 78.6, 77.5, 67.1, 29.0. HRMS (ESI) m/z ([M+H]+ calcd for $C_{13}H_{14}N_2O$: 214.1106, found 215.1112.

General Procedure D: Metalation in the presence of TMSCl
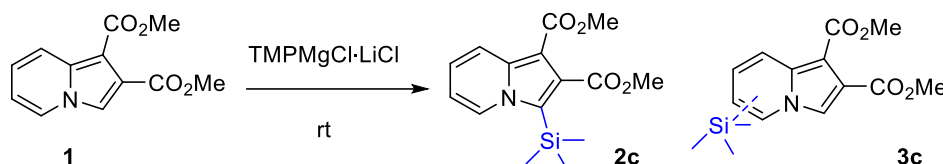
Experiment A: A dry round-bottom flask sob N_2 under magnetic stirring containing 2 mL of THF and indolizine **1** (0.3 mmol, 1.0 equiv.) was charged with TMSCl (4 equiv.) followed by dropwise addition of TMPMgCl·LiCl (0.98 M; 2 equivalents, see Error! R eference source not found.). The reaction mixture was left at room temperature for 5 hours. Aliquots were removed at 10 min, 30 min, 1 h, 2 h, 3 h, 4 h and 5 h. Then, the reaction mixture was diluted with ethyl acetate (10 mL) and washed with a saturated NH_4Cl solution (3 x 10 mL). The organic layer was washed with saturated solution of NaCl (30 mL) and dried over $MgSO_4$. The solvent was removed under reduced pressure and the residue was purified by chromatography column using a gradient of pure hexane to a hexane / ethyl acetate mixture (70:30).

Experiment B: TMSCl were added (4.0 equivalents) to reactional mixture after 5 hours of metalation reaction with TMPMgCl·LiCl (0.98 M; 2 equivalents, see Error! Reference s ource not found.).

Dimethyl 3- (trimethylsilyl) indolizine-1,2-dicarboxylate 2c
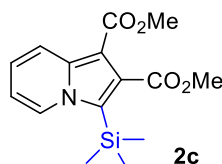
Brown oil, yield 50%. ^{1}H NMR (500 MHz, CDCl3) δ 8.20 (dt, J = 9.0; 1.3 Hz, 1H), 8.13 (dt, *J* = 7.0; 1.1 Hz, 1H), 7.14 (ddd, J = 9.1; 6.6; 1.1 Hz, 1H), 6.78 (td, J = 6.8; 1.4 Hz, 1H), 3.93 (s, 3H), 3.86 (s, 3H), 0.40 (s, 9H). ^{13}C NMR (126 MHz, CDCl3) δ 168.8; 164.1; 138.5; 133.0; 127.3; 123.8; 123.0; 120.8; 113.4; 102.5; 52.5; 51.3; -1.0. EMAR-ESI) m / z ([M + H] [+] calculated for $C_{15}H_{19}NO_4Si$ 305,1086, found 306,1157.

General Procedure E: Regioselective magnesiation of indolizines 1 and 4

In a dry round-bottom flask sob N_2 under magnetic stirring containing 2 mL of THF and starting material **1** or **4** (0.50 mmol), TMPMgCl·LiCl was added dropwise to the reaction mixture (see Error! Reference source not found. and **Table 5**). After stirring f or 1 hour to 5 hours (see Error! Reference source not found. and **Table 5**) a solution of an appropriate electrophile (1.8 equiv.) in THF (1.0 mL) was added, and the reaction mixture was kept at room temperature for 6 hours (for iodine) to 12 hours (other electrophiles). The reaction was quenched with saturated solution of NH_4Cl and products were extracted with ethyl acetate (3 × 15 mL). Organic layer was dried over $MgSO_4$ and solvent removed under reduced pressure. The residue was purified by flash column chromatography (silica gel, ethyl acetate/hexane).

Dimethyl-3-(phenylthio)indolizine-1,2-dicarboxylate 2a
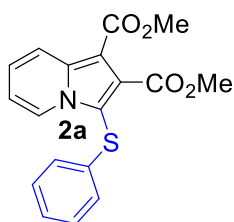
From dimethyl indolizine-1,2-dicarboxylate (116.5 mg, 0.5 mmol) and diphenylsulfane (131.0 mg, 0.6 mmol), silica gel (ethyl acetate/hexane: 3/7), yield: 128 mg (75%), orange oil. ^1H NMR (400 MHz, DMSO-d_6, 25°C) δ 8.44 (dd, J = 7.0, 1.2 Hz, 1H, H-8), 8.16 (dt, J = 9.0, 1.3 Hz, 1H, H-5), 7.43 (ddd, J = 9.1, 6.9, 1.1 Hz, 1H, H-6), 7.31 – 7.24 (m, 2H), 7.24 – 7.17 (m, 1H, H-7), 7.14 – 7.06 (m, 3H), 3.86 (s, 3H), 3.82 (s, 3H). ^{13}C NMR (101 MHz, DMSO-d_6) δ 165.6, 163.0, 136.8, 133.7, 131.6, 129.9, 127.3, 127.3, 126.7, 125.1, 119.6, 115.4, 110.1, 101.6, 53.0, 51.7. HRMS (ESI) m/z ([M+H]+ calcd for $C_{18}H_{15}NO_4S$ 342.0722, found 342.0796.

Dimethyl-5-iodoindolizine-1,2-dicarboxylate 3a
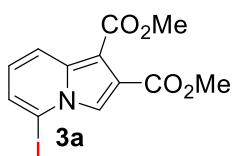
From dimethyl indolizine-1,2-dicarboxylate **1** (116.5 mg, 0.5 mmol) and I_2 (342.6.4 mg, 0.9 mmol), silica gel (ethyl acetate/hexane: 2/8), yield: 156 mg (87%), brown solid, mp: 91-93ºC. ^1H NMR (400 MHz, DMSO-d_6, 25°C) δ 8.04 (d, J = 9.1 Hz, 1H, H-8), 7.97 (s,

1H, H-3), 7.53 (dd, J = 7.1, 1.1 Hz, 1H, H-6), 6.98 (dd, J = 9.1, 7.0 Hz, 1H, H-7), 3.83 (s, 3H), 3.80 (s, 3H).^{13}C NMR (101 MHz, DMSO-d$_6$) δ 164.3, 163.4, 135.6, 125.9, 124.4, 121.0, 120.7, 118.8, 103.6, 91.5, 52.1, 51.3. HRMS (ESI) m/z ([M+H]+ calcd for C$_{12}$H$_{10}$INO$_4$ 359.9655, found 359.9729.

Dimethyl-5-formylindolizine-1,2-dicarboxylate 3b
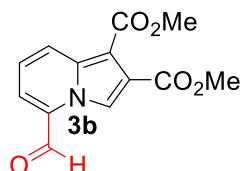
From dimethyl indolizine-1,2-dicarboxylate **1** (116.5 mg, 0.5 mmol) and DMF (0.12 mL, 1.5 mmol), silica gel (ethyl acetate/hexane: 3/7), yield: 78 mg (60%), brown oil. 1H NMR (500 MHz, DMSO-d6, 25°C) δ 9.95 (d, J = 10.5 Hz, 1H), 8.99 (s, 1H, H-3), 8.31 (d, J = 9.0 Hz, 1H, H-8), 7.95 – 7.85 (m, 1H, H-6), 7.43 (dd, J = 9.0, 7.0 Hz, 1H, H-7), 3.84 (d, J = 4.2 Hz, 6H). 13C NMR (126 MHz, DMSO-d6) δ 187.0, 163.9, 163.1, 135.0,131.0, 128.6, 125.7, 122.4, 122.1, 117.8, 104.5, 52.0, 51.5. HRMS (ESI) m/z ([M+H]+ calcd for C$_{13}$H$_{11}$NO$_5$ 262.0637, found 262.0713.

2-(2-iodoindolizin-1-yl)-4,4-dimethyl-4,5-dihydrooxazole 6a
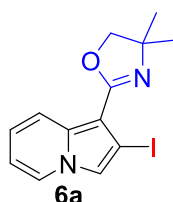
 From 2-(indolizin-1-yl)-4,4-dimethyl-4,5-dihydrooxazole (64.2 mg, 0.3 mmol) and I$_2$ (228.4 mg, 0.6 mmol); silica gel (ethyl acetate/hexane: 2/8); yield: 79.6 mg (78%); brown oil.^{1}H NMR (300 MHz, MeOD, 25°C) δ = 8.13 (dt, *J* = 7.0, 1.1 Hz, 1H), 7.95 – 7.87 (d, *J* = 7.0 Hz, 1H), 7.61 (s, 1H), 7.00 – 6.90 (m, 1H), 6.67 (td, *J* = 6.9, 1.3 Hz, 1H), 4.10 (s, 2H), 1.38 (s, 6H).^{13}C NMR (75 MHz, MeOD) δ = 161.4, 136.3, 126.3, 122.5, 121.7, 119.4, 113.3, 104.1, 79.1, 71.2, 67.8, 28.5. HRMS (ESI) m/z ([M+H]$^+$ calcd for C$_{13}$H$_{13}$IN$_2$O: 341.0073, found 341.0146.

1-(4,4-dimethyl-4,5-dihydrooxazol-2-yl)indolizine-2-carbaldehyde 6b
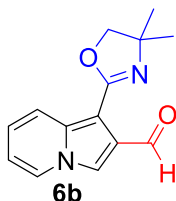
From 2-(indolizin-1-yl)-4,4-dimethyl-4,5-dihydrooxazole (64.2 mg, 0.3 mmol) and DMF (0.07 mL, 0.9 mmol); silica gel (ethyl acetate/hexane: 3/7); yield: 45.7 mg (63%); light yellow solid; mp: 153-155 °C. IR (KBr) 2888, 1665, 1491, 1173, 1153, 1042, 966, 753. ^{1}H NMR (400 MHz, CDCl$_3$, 25°C) δ = 10.71 (s, 1H), 8.20 (d, J = 9.3 Hz, 1H), 7.92 (d, J = 7.0 Hz, 1H), 7.81 (s, 1H), 6.95 (dd, J = 9.3, 6.5 Hz, 1H), 6.71 (t, J = 7.0 Hz, 1H), 4.09 (s, 2H), 1.40 (s, 6H). ^{13}C NMR (101 MHz, CDCl$_3$) δ = 190.7, 158.6, 134.8, 127.5, 126.1, 121.8, 121.7, 115.5, 114.3, 101.8, 78.4, 67.5, 28.7. HRMS (ESI) m/z ([M+H]$^+$ calcd for C$_{14}$H$_{14}$IN$_2$O$_2$: 243.1055, found 243.1129.

4,4-dimethyl-2-(2-(phenylthio)indolizin-1-yl)-4,5-dihydrooxazole 6c
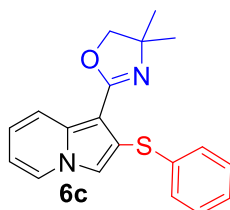
From 2-(indolizin-1-yl)-4,4-dimethyl-4,5-dihydrooxazole (64.2 mg, 0.3 mmol) and diphenylsulfane (131.0 mg, 0.6 mmol); silica gel (ethyl acetate/hexane: 3/7); yield: 74.4 mg (77%); dark yellow oil. ^{1}H NMR (400 MHz, CDCl$_3$, 25°C) δ = 8.02 (d, J = 9.1 Hz, 1H), 7.74 – 7.61 (m, 1H), 7.49 – 7.37 (m, 2H), 7.31 – 7.15 (m, 3H), 6.81 (ddd, J = 9.1, 6.7, 1.0 Hz, 1H), 6.70 (s, 1H), 6.48 (td, J = 6.8, 1.2 Hz, 1H), 3.89 (s, 2H), 1.27 (s, 6H). ^{13}C NMR (101 MHz, CDCl$_3$) δ 159.1, 135.3, 135.2, 132.0, 129.2, 127.4, 124.8, 123.8, 121.0, 119.6, 113.5, 112.0, 100.2, 78.2, 66.9, 28.7. HRMS (ESI) m/z ([M+H]$^+$ calcd for C$_{19}$H$_{18}$N$_2$OS: 322.1140, found 322.1213.

4,4-dimethyl-2-(2-(phenylselanyl)indolizin-1-yl)-4,5-dihydrooxazole 6d
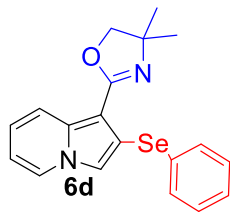
From 2-(indolizin-1-yl)-4,4-dimethyl-4,5-dihydrooxazole (64.2 mg, 0.3 mmol) and diphenylselane (187.0 mg, 0.6 mmol); silica gel (ethyl acetate/hexane: 1/9); yield: 101.0 mg (91%); dark yellow oil. ^{1}H NMR (300 MHz, CDCl$_3$, 25°C) δ = 8.02 (dd, J = 9.2, 1.3 Hz, 1H), 7.77 – 7.71 (m, 2H), 7.68 (dd, J = 6.9, 1.2 Hz, 1H), 7.40 – 7.31 (m, 3H), 6.84 (ddd, J = 9.1, 6.7, 1.1 Hz, 1H), 6.53 – 6.47 (m, 2H), 4.05 (s, 2H), 1.40 (s, 6H). ^{13}C NMR (75 MHz, CDCl$_3$) δ = 159.4, 135.8, 135.1, 129.5, 128.3, 124.6, 120.4, 120.2, 119.2, 112.7, 111.5, 100.7, 78.4, 67.1, 28.8. HRMS (ESI) m/z ([M+H]$^+$ calcd for C$_{19}$H$_{18}$N$_2$OSe: 371.0584, found 371.0658.

2-(2-bromoindolizin-1-yl)-4,4-dimethyl-4,5-dihydrooxazole 6e
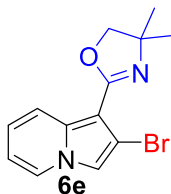
From 2-(indolizin-1-yl)-4,4-dimethyl-4,5-dihydrooxazole (64.2 mg, 0.3 mmol) and 1,2-dibromotetrachloroethane (193.0, 0.6 mmol); silica gel (ethyl acetate/hexane: 3/7); yield: 69.2 mg (79%); dark green solid; mp 78-80°C. ^{1}H NMR (400 MHz, DMSO-d_6, 25°C) δ = 8.14 (d, J= 9.5 Hz, 1H), 7.64 (d, J = 3.0 Hz, 1H), 7.21-7.16 (m, 2H), 6.97 (dd, J = 9.0, 7.1 Hz, 1H), 4.01 (s, 2H), 1.28 (s, 6H). ^{13}C NMR (101 MHz, DMSO) δ = 157.9, 134.12, 121.2, 118.4, 116.1, 115.1, 114.8, 114.3, 102.9, 77.4, 67.0, 28.5. HRMS (ESI) m/z ([M+H]$^+$ calcd for C$_{13}$H$_{13}$BrN$_2$O: 292.0211, found 292.0286.

General Procedure F: Regioselective lithiation of indolizine 4 using n-BuLi

In a dry round-bottom flask sob N$_2$ under magnetic stirring containing 2-(indolizin-1-yl)-4,4-dimethyl-4,5-dihydrooxazole (107 mg, 0.50 mmol) in THF (2.0 mL) and TMEDA (0.15 mL, 2.0 equiv.), n-BuLi (0.85 mmol, 2.35 M in hexanes, 0.34 mL, 1.7 equiv.) was added dropwise to the reaction mixture at -70 °C. After 2 hours, a solution of an appropriate electrophile (1.8 equiv.) in THF (1.0 mL) was added, and the reaction

mixture was kept under room temperature for 6 hours (for iodine) to 12 hours (other electrophiles). The reaction was quenched with saturated aqueous NH$_4$Cl and products extracted with ethyl acetate (3 × 15 mL). The organic layer was dried over MgSO$_4$ and solvent was removed under reduced pressure. The residue was purified by flash column chromatography (silica gel, hexanes/ethyl acetate).

2-(5-iodoindolizin-1-yl)-4,4-dimethyl-4,5-dihydrooxazole 5a
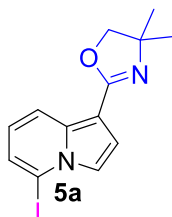
From 2-(indolizin-1-yl)-4,4-dimethyl-4,5-dihydrooxazole (64.2 mg, 0.3 mmol) and I$_2$ (228.4 mg, 0.6 mmol); silica gel (ethyl acetate/hexane: 2/8); yield: 81,6 mg (80%); brown oil.^{1}H NMR (300 MHz, CDCl$_3$, 25°C) δ = 8.17 (d, 7.54, J = 9.0 Hz, 1H), 7.54 (d, J = 3.0 Hz, 1H), 7.29 (d, J = 3.1 Hz, 1H), 7.15 (d, J = 6.4 Hz, 1H), 6.63 (dd, J = 9.0, 7.0 Hz, 1H), 4.06 (s, 2H), 1.38 (s, 6H). ^{13}C NMR (75 MHz, CDCl$_3$) δ = 159.8, 134.5, 124.4, 120.7, 120.1, 118.9, 114.7, 104.9, 87.2, 78.5, 67.1, 28.8. HRMS (ESI) *m/z* ([M+H]$^+$ calcd for C$_{13}$H$_{13}$IN$_2$O: 341.0073, found 341.0168.

4,4-dimethyl-2-(5-(phenylthio)indolizin-1-yl)-4,5-dihydrooxazole 5b
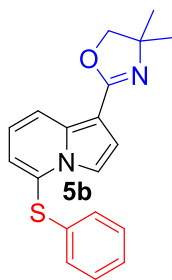
From 2-(indolizin-1-yl)-4,4-dimethyl-4,5-dihydrooxazole (64.2 mg, 0.3 mmol) and diphenylsulfane (131.0 mg, 0.6 mmol); silica gel (ethyl acetate/hexane: 3/7); yield: 74.4 mg (77%); dark brown oil. ^{1}H NMR (500 MHz, DMSO-d_6, 25°C) δ = 8.22 (d, J = 8.9 Hz, 1H), 7.47 (d, J = 3.0 Hz, 1H), 7.34 (dd, J = 8.2, 6.6 Hz, 2H), 7.32 – 7.27 (m, 1H), 7.27 – 7.19 (m, 3H), 7.10 (dd, J = 9.1, 6.9 Hz, 1H), 7.08 (d, J = 3.0 Hz, 1H), 4.00 (s, 2H), 1.27 (s, 6H). ^{13}C NMR (101 MHz, DMSO) δ = 157.9, 133.3, 130.9, 129.8, 128.7, 127.7,

120.7, 120.6, 120.3, 114.5, 113.1, 102.7, 77.3, 66.9, 28.5. HRMS (ESI) m/z ([M+H]$^+$ calcd for C$_{19}$H$_{18}$N$_2$OS: 322.1140, found 322.1213.

4,4-dimethyl-2-(5-(phenylselanyl)indolizin-1-yl)-4,5-dihydrooxazole 5c
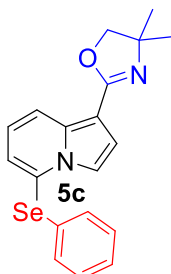
From 2-(indolizin-1-yl)-4,4-dimethyl-4,5-dihydrooxazole (64.2 mg, 0.3 mmol) and diphenylselane (187.0 mg, 0.6 mmol); silica gel (ethyl acetate/hexane: 1/9); yield: 71.2 mg (70%); dark brown oil. ^{1}H NMR (500 MHz, DMSO-d_6, 25 °C) δ = 8.19 (d, J = 8.9 Hz, 1H), 7.51 (d, J = 3.1 Hz, 1H), 7.42 – 7.37 (m, 2H), 7.31 (d, J = 4.1, 2.3 Hz, 3H), 7.20 (dd, J = 6.8, 1.2 Hz, 1H), 7.07 (d, J = 3.0 Hz, 1H), 7.03 (dd, J = 9.0, 6.8 Hz, 1H), 3.99 (s, 2H), 1.27 (s, 6H).^{13}C NMR (101 MHz, DMSO) δ = 158.0, 133.2, 131.4, 129.9, 128.1, 127.4, 125.3, 121.6, 120.6, 119.9, 114.6, 114.3, 102.5, 66.9, 28.5. HRMS (ESI) m/z ([M+H]$^+$ calcd for C$_{19}$H$_{18}$N$_2$OSe: 371.0584, found 371.0658.

2-(5-bromoindolizin-1-yl)-4,4-dimethyl-4,5-dihydrooxazole 5d
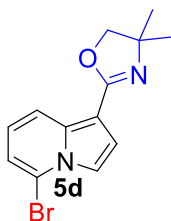
 From 2-(indolizin-1-yl)-4,4-dimethyl-4,5-dihydrooxazole (64.2 mg, 0.3 mmol) and 1,2-dibromotetrachloroethane (193.0, 0.6 mmol); silica gel (ethyl acetate/hexane: 3/7); yield: 72.1 mg (75%); yellow oil. ^{1}H NMR (400 MHz, DMSO) δ= 8.34 (d, J = 7.7 Hz, 1H), 8.08 (d, J = 9.1 Hz, 1H), 7.82 (s, 1H), 7.08 (dd, J= 9.1, 6.7 Hz, 1H), 6.82 (t, J = 6.8 Hz, 1H), 4.02 (s, 2H), 1.29 (s, 6H). HRMS (ESI) m/z ([M+H]$^+$ calcd for C$_{13}$H$_{13}$BrN$_2$O:293.0211, found 293.0286.

General Procedure F: Regioselective metalation of indolizines 1 and 4 followed by Negishi cross-coupling reaction

After metalation step (according to **General Procedure E** or **F**) temperature was warmed to 0 ⁰C or room temperature (see **Table 4** or **Table 7**) and ZnCl$_2$ (1.0 M in THF, see amounts in **Table 4** or **Table 7**) was added dropwise to the reaction mixture. The chosen temperature was kept for 30 minutes. Then, Pd(PPh$_3$)$_4$ (10 mol%) in THF (1 mL) and the appropriate electrophile (1.8 equiv. in THF) were added. The reaction mixture was kept at 60 °C for 12 hours. The reaction was quenched with saturated aqueous NH$_4$Cl, products were extracted with ethyl acetate (3 × 15 mL), and the organic layer was dried over MgSO$_4$. The solvent was removed under reduced pressure. The residue was purified by flash column chromatography (silica gel, ethyl acetate/hexanes).

Dimethyl 3- (4- (trifluoromethyl) phenyl) indolizine-1,2-dicarboxylate 2d
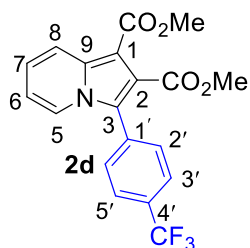
From dimethyl indolizine-1,2-dicarboxylate (116.5 mg, 0.5 mmol) and 1-bromo-4-(trifluoromethyl)benzene (0.12 mL, 0.9 mmol); green oil; silica gel (ethyl acetate/hexane: 2/8); yield: 143.7 mg (76%). ^{1}H NMR (400 MHz, CDCl$_3$) δ = 8.26 (dt, J = 9.1; 1.2 Hz, 1H, H-8), 8.03 (dt, J = 7.2; 1.1 Hz, 1H, H-5), 7.81–7.74 (m, 2H), 7.70-7.63 (m, 2H), 7.21-7.13 (m, 1H, H-7), 6.78 (td, J = 6.9, 1.3 Hz, 1H, H-6), 3.91 (s, 3H), 3.82 (s, 3H). ^{13}C NMR (101 MHz, CDCl$_3$) δ = 166.6; 164.2; 135.7; 130.4; 126.3 (q, J$_{F,C}$= 3.1; 2.7 Hz, 2C, C-3′, C5′), 124.1 (q, J$_{F,C}$= 272 Hz, CF$_3$), 120.8; 114.1; 102.7; 52.8; 51.6. EMAR-ESI m / z [M + H] $^+$ calculated for C$_{19}$H$_{14}$F$_3$NO$_4$ 378.0875, found 378.0941.

Dimethyl 3-phenylindolizine-1,2-dicarboxylate 2e

2e
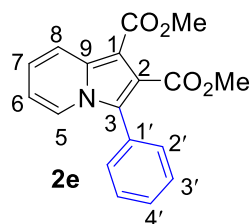
From dimethyl indolizine-1,2-dicarboxylate (116.5 mg, 0.5 mmol) and iodobenzene (0.10 mL, 0.9 mmol); silica gel (ethyl acetate/hexane 2/8), yield: 99 mg (64%), green oil.^{1}H NMR (400 MHz, CDCl$_3$, 25°C) δ 8.23 (dt, J = 9.1, 1.3 Hz, 1H), 8.05 (dt, J = 7.1, 1.1 Hz, 1H), 7.51 (dd, J = 4.2, 0.8 Hz, 4H), 7.49 – 7.45 (m, 1H), 7.13 (ddd, J = 9.2, 6.6, 1.1 Hz, 1H), 6.72 (td, J = 6.9, 1.4 Hz, 1H), 3.91 (s, 3H), 3.81 (s, 3H). ^{13}C NMR (101 MHz, CDCl$_3$) δ 167.0, 164.4, 135.4, 130.1, 129.2, 129.0, 125.2, 123.7, 122.2, 120.5, 113.6, 102.1, 52.6, 51.4. HRMS (ESI) m/z ([M+H]+ calcd for C$_{18}$H$_{15}$NO$_4$ 310.1001, found 310. 1069.

4,4-dimethyl-2-(3-(4-(trifluoromethyl)phenyl)indolizin-1-yl)-4,5-dihydrooxazole 6f
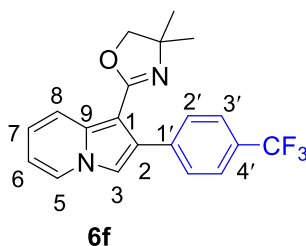
6f

From 2-(indolizin-1-yl)-4,4-dimethyl-4,5-dihydrooxazole (64.2 mg, 0.3 mmol) and 1-bromo-4-(trifluoromethyl)benzene (0.12 mL, 0.9 mmol); green oil; silica gel (ethyl acetate/hexane: 2/8); yield: 139 mg (74%). ^{1}H NMR (500 MHz, DMSO-d_6, *ppm*) δ 8.37 (d, J= 6.9 Hz, 1H), 8.08 (d, J = 9.1 Hz, 1H), 7.79 (s, 1H), 7.71 (s, 4H), 7.04 (dd, J = 9.1, 6.6 Hz, 1H), 6.79 (t, J = 6.4 Hz, 1H), 3.88 (s, 2H), 1.26 (s, 6H). ^{13}C NMR (126 MHz, DMSO, *ppm*) δ 158.0, 139.0, 134.1, 129.8, 127.8, 127.4, 127.2, 126.9, 126.7, 126.2, 125.5, 124.4, 124.4, 124.4, 124.3, 123.3, 121.3, 119.2, 113.9, 112.2, 97.8, 28.1. HRMS (ESI) m/z ([M+H]$^+$ calcd C$_{20}$H$_{17}$F$_3$N$_2$O:358.1293, found 359.1364.

4,4-dimethyl-2-(5-(4-(trifluoromethyl)phenyl)indolizin-1-yl)-4,5-dihydrooxazole

5e
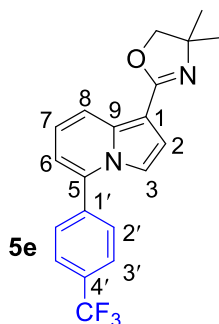
5e

From 2-(indolizin-1-yl)-4,4-dimethyl-4,5-dihydrooxazole (64.2 mg, 0.3 mmol) and 1-bromo-4-(trifluoromethyl)benzene (0.12 mL, 0.9 mmol); green oil; silica gel (ethyl acetate/hexane: 2/8); yield: 139 mg (74%). ^{1}H NMR (400 MHz, Chloroform-*d*) δ 8.20 (d, *J* = 9.1 Hz, 1H), 7.80 (dd, *J* = 8.4, 1.9 Hz, 2H), 7.77 – 7.71 (m, 2H), 7.32 (s, 1H), 7.06 (ddd, *J* = 9.0, 6.7, 1.9 Hz, 1H), 6.61 (dt, *J* = 6.8, 1.2 Hz, 1H), 4.14 (s, 2H), 1.43 (s, 6H).^{13}C NMR (101 MHz, DMSO) δ 158.1, 137.9, 135.7, 134.2, 134.1, 133.6, 131.5, 131.4, 129.4, 128.7, 128.6, 128.1, 128.1, 128.0, 128.0, 126.2, 126.2, 126.1, 126.1, 125.3, 122.6, 121.2, 119.2, 114.5, 113.5, 111.7, 101.5, 77.2, 66.9, 28.5. HRMS (ESI) m/z ([M+H]$^+$ calcd $C_{20}H_{17}F_3N_2O$:358.1293, found 359.1370.

General Procedure G: Synthesis of 2-arylindolizines

1a - R$_1$= H, R= H	**7a -** R$_1$= H,R= H - 56%
1b - R$_1$= H, R= OMe	**7b -**R$_1$= H, R= OMe - 85%
1c - R= OMe, R= OMe	**7c -** R$_1$= OMe, R$_2$= OMe - 52%
1d - R$_1$= H, R= F	**7d -** R$_1$= H,R= F - 55%
1e - R$_1$= H, R= Cl	**7e -** R$_1$ = H, R$_2$= Cl - 82%
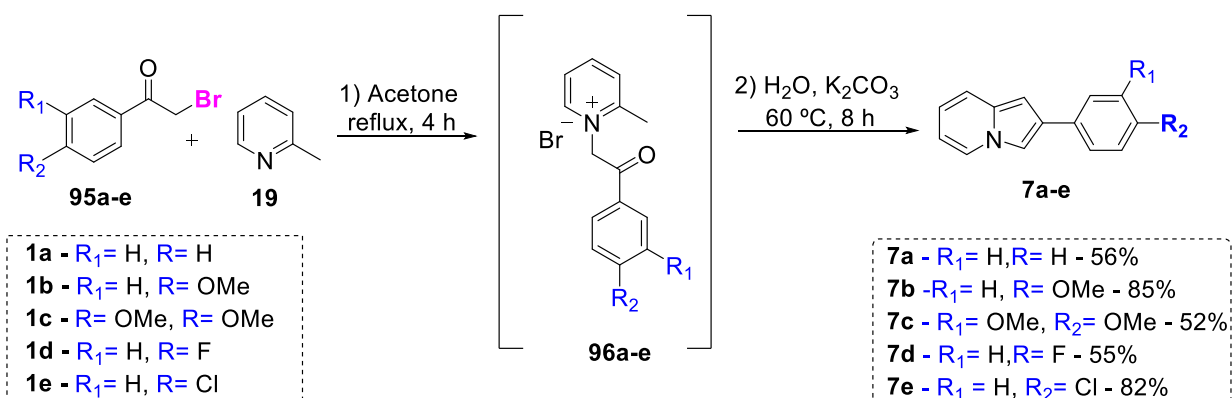
Step 1: A 250 mL dry nitrogen-flushed round-bottom flask was charged with 2-picoline (20 mmol; 1.86 g; 2 mL), acetophenone (20 mmol) and acetone (100 mL). The reactional mixture was refluxed for 4 hours leading to the formation of a precipitate (quaternary salt) which was isolated by vacuum filtration.

Step 2: The quaternary salt **96** was dissolved in water (100 mL) and K_2CO_3 (2.76 g; 20.0 mmol) was added. The reactional mixture was heated to 100 °C for 8 hours. After filtration step, the solid obtained was dried under reduced pressure for 12 hours to afford 2-arylindolizines (**7a-e**).

2-phenylindolizine 7a

7a
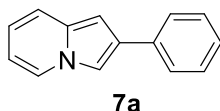
White solid; mp 212-214 °C (literature 214-215 °C); yield 56%. IR (KBr; $U_{max.}$, cm^{-1}): 3101, 3072, 3028, 1514, 1454, 759, 690; CAS: 25379-20-8. ^{1}H NMR (DMSO-d$_6$, 400 MHz) δ *(ppm)*: 8.21 (dd, 1H, J = 6.9, 0.8 Hz), 7.96 (d, 1H, J = 1.5 Hz,), 7.70 (dd, 2H, J = 8.1 Hz, 1.0 Hz), 7.43-7.35 (m,3H), 7.25-7.21 (m, 1H), 6.76 (s, 1H), 6.70 – 6.66 (m, 1H), 6.53 (td, 1H). ^{13}C NMR (100 MHz, DMSO) δ*(ppm)*: 134.90 132.9, 128.8 (2C), 128.2, 128.4, 125.7, 125.6 (2C), 118.6, 117.5, 110.4, 109.8, 96.1. HRMS (ESI) m/z ([M+H]$^+$ calcd for $C_{14}H_{11}N$: 193.0881, found 194.0885.

2-(4-methoxyphenyl)indolizine 7b

7b
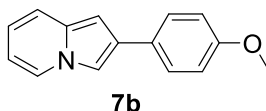
Brown solid; mp 186 °C (literature 184 °C); yield 85%. IR (KBr; $U_{max.}$, cm^{-1}): 3090, 3007, 1608, 1521, 1244, 1031, 781, 731. ^{1}H NMR (400 MHz, DMSO-d$_6$) δ 8,19 (dd, 1H, J = 6,9, 1,0 Hz); 7,87 (d, 1H, J = 1,5 Hz); 7,62 (d, 2H, J = 8,8 Hz); 7,36 (d, 1H, J = 8,9 Hz); 6,96 (d, 2H, J = 8,8 Hz); 6,68 - 6,64 (m, 2H); 6,50 (td, 1H); 3,77 (s, 3H). ^{13}C NMR (100 MHz, DMSO-d$_6$) δ 158.1, 132.8, 128.2, 127.7 (2C), 126.7, 125.5, 118.4, 117.3, 114.2 (2C), 110.1, 109.1, 95.8, 55.0. HRMS (ESI) m/z ([M+H]$^+$ calcd for $C_{15}H_{13}NO$ 223.1070, found 224.1075.

2-(3,4-dimethoxyphenyl)indolizine 7c

7c
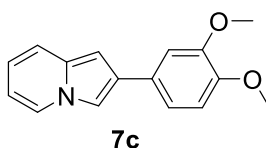
Grey solid; mp 171-173 °C (Literature 179 °C); yield 52%; CAS 169210-15-5. IR (KBr; $U_{max.}$, cm^{-1}): 3099, 2954, 2837, 1516, 1450, 1259, 1024, 775. ^{1}H NMR (500 MHz, DMSO-d$_6$, *ppm*) δ 8.18 (dd, 1H, J = 6.9 Hz, 0.8 Hz), 7.91 (d, 1H, J = 1.3 Hz), 7.36 (d,

1H, J = 9.0 Hz), 7.27 (d, 1H, J = 2.0 Hz), 7.22 (dd, 1H, J = 8.2, 2.0 Hz), 6.96 (d, 1H, J = 8.3 Hz), 6.72 (s, 1H), 6.66 (ddd, 1H, J = 8.9, 6.5, 0.7 Hz), 6.51 (td, 1H, J = 6.8, 1.1 Hz), 3.84 (s, 3H), 3.76 (s, 3H).^{13}C NMR (DMSO-d$_6$, 126 MHz, *ppm*) δ 149.6, 148.3, 133.3, 129.0, 128.4, 126.0, 118.9, 118.4, 117.8, 112.9, 110.7, 110.3, 109.9, 96.6, 56.1, 55.1. HRMS (ESI) m/z ([M+H]$^+$ calcd for C$_{16}$H$_{15}$NO$_2$ + H$^+$ 254,1176, found 254,1176.

2-(4-fluorophenyl)indolizine 7d

7d
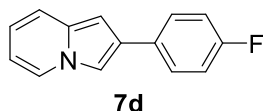
Grey solid; mp 87 °C; yield 55%. ^{1}H NMR (400 MHz, Pyr, *ppm*) δ 8.04 (d, 1H, J = 6.9 Hz), 7.84-7.76 (m,3H), 7.43 (d, 1H, J = 9.0 Hz), 7.24-7.19 (m, 2H), 6.85 (sl, 1H), 6.69-6.66 (m, 1H), 6.46-6.42 (m, 1H). ^{13}C NMR (100 MHz, Pyr, *ppm*) δ 163.8, 161.4, 134.5, 132.9, 132.9, 129.2, 128.6, 128.5, 126.2, 119.7, 118.4, 116.5, 116.3, 111.4, 110.5, 97.6. HRMS (ESI) m/z ([M+H]$^+$ calcd for C$_{14}$H$_{10}$FN 211.0797, found 212.2401.

2-(4-chlorophenyl)indolizine 7e

7e
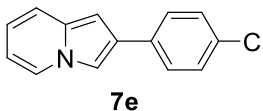
White solid; mp 246 °C; yield 82%; CAS: 7496-73-3. IR (KBr; $U_{max.}$, cm^{-1}): 3079, 3028, 1598, 1467, 1090, 780, 690.^{1}H NMR (400 MHz, Pyr, *ppm*) δ 8.04 (s, 1H), 7.83-7.75 (m, 3H), 7.46 – 7.44 (m, 3H), 6.86 (s, 1H), 6.67 (s, 1H), 6.45 (s, 1H). ^{13}C NMR (100 MHz, Pyr, *ppm*) δ 135.2, 134.6, 132.6, 129.7 (2C), 128.8, 128.3 (2C), 128.2, 119.8, 118.5, 111.5, 110.8, 97.6. HRMS (ESI) m/z ([M+H]$^+$ calcd for C$_{14}$H$_{10}$ClN 227.0575, found 228.0593.

General Procedure H: Regioselective lithiation of 2-aryl-indolizines

In a dry nitrogen-flushed round-bottom flask respective 2-aryl-indolizine **7a-e** (0.5 mmol) was dissolved in THF (5.0-20.0 mL) and *n*-butyllithium (2.48 M in hexanes, 2.0 equiv.) was added dropwise at -70 °C. After 15 min, the mixture was warmed to -20 °C and was stirred for 5 hours. Then *N, N*-dimethylformamide (3.5 equiv.) was added and the reaction was stirred at room temperature for more 24 hours. The reaction mixture

was quenched with saturated solution of NH$_4$Cl and products extracted with ethyl acetate (3 x 15 mL). The organic layer was washed with brine, dried over MgSO$_4$, and concentrated under reduced pressure. The crude product was purified by flash column chromatography (ethyl acetate/hexane).

2-phenylindolizine-5-carbaldehyde 8a
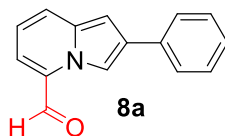
From 2-phenylindolizine **7a** (0.5 mmol, 96.5 mg). Silica gel (hexane/ethyl acetate 8:2); red solid: 98.4 mg (89%), mp 128.6-129.6 °C (lit, mp 128-130°C). ^{1}H NMR (DMSO-d$_6$, 400 MHz): d (*ppm*) = 9.91 (s, 1H), 9.19 (d, *J* = 1.2 Hz, 1H), 7.95 (d, *J* = 8.6 Hz, 1H), 7.83 – 7.73 (m, 2H), 7.71 – 7.60 (m, 1H), 7.49 – 7.39 (m, 2H), 7.28 (dd, *J* = 15.3 Hz, 7.9 Hz, 1H), 7.20 (d, *J* = 1.4 Hz, 1H), 7.02 (dt, *J* = 16.2 Hz, 8.1 Hz, 1H). ^{13}C NMR (DMSO-d$_6$,101 MHz) δ (*ppm*) = 186.6, 134.7, 134.1, 130.7, 130.1, 129.0, 127.9, 127.1, 126.1, 126.0, 116.1, 112.2, 100.3. HRMS (ESI): *m/z* [M + H]$^+$ calcd for C$_{15}$H$_{11}$NO + H$^+$ 222.0841, found 222.0822.

2-(4-methoxyphenyl)indolizine-5-carbaldehyde 8b
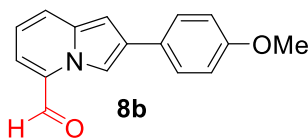
From 2-phenylindolizine **7b** (0.5 mmol, 96.5 mg). Silica gel (hexane/ethyl acetate 8:2); yellow solid: 102.9 mg (82%), mp: 158-160.7°C.

^{1}H NMR (DMSO-d$_6$, 400 MHz) δ (*ppm*) = 9.90 (s, 1H), 9.13 (s, 1H), 7.92 (d, *J* = 8.7 Hz, 1H), 7.70 (d, *J* = 8.6 Hz, 2H), 7.63 (d, *J* = 6.9 Hz, 1H), 7.12 (s, 1H), 7.01 (t, *J* = 7.8 Hz, 3H), 3.79 (s, 3H). ^{13}C NMR (DMSO-d$_6$, 101 MHz) δ (*ppm*) = 186.6, 158.6, 134.7, 130.7, 130.0, 127.7, 127.2, 126.6, 125.8, 115.9, 114.5, 111.7, 99.9, 55.1. HRMS (ESI): *m/z* [M + H]$^+$ calcd for C$_{16}$H$_{13}$NO$_2$ + H$^+$ 252.0946, found 252.1015.

2-(3,4-dimethoxyphenyl)indolizine-5-carbaldehyde 8c
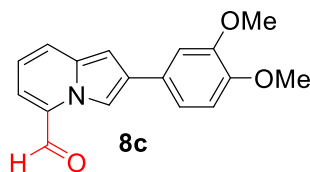
From 2-phenylindolizine **7c** (0.5 mmol, 96.5 mg). Silica gel (hexane/ethyl acetate 7:3); dark brown solid: 112.4 mg (80%), mp: 115-118°C. ^{1}H NMR (DMSO-d$_6$, 400 MHz) δ (*ppm*) = 9.89 (s, 1H), 9.14 (s, 1H), 7.91 (d, *J* = 8.6 Hz, 1H), 7.62 (d, *J* = 6.9 Hz, 1H), 7.36 – 7.27 (m, 2H), 7.17 (t, *J* = 5.0 Hz, 1H), 7.05 – 6.96 (m, 2H), 3.86 (s, 3H), 3.78 (s, 3H). ^{1}H NMR (DMSO-d$_6$, 101 MHz) δ (*ppm*) = 186.5, 149.2, 148.3, 134.6, 131.0, 130.0, 127.7, 127.0, 125.8, 118.3, 115.9, 112.4, 111.9, 109.9, 100.2, 55.6, 55.6. HRMS (ESI): *m/z* [M + H]$^+$ calcd for $C_{17}H_{15}NO_3$ + H$^+$ 282.1052, found 282.1120.

2-(4-fluorophenyl)indolizine-5-carbaldehyde 8d
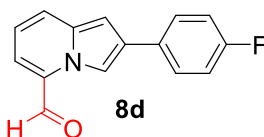
From 2-phenylindolizine **7d** (0.5 mmol, 96.5 mg). Silica gel (hexane/ethyl acetate 6:4).

Brown solid: (58%), mp: 87.8-91.7°C. ^{1}H NMR (Pyridine-d$_5$, 400 MHz) δ (*ppm*) = 9.89 (s, 1H), 9.46 (d, *J* = 1,4 Hz, 1H), 7.81-7.76 (m, 3H), 7.31 (dd, *J* = 6.9, 1.3 Hz, 1H), 7.24 (d, *J* = 8.8 Hz, 2H), 7.10 (d, *J* = 1,5 Hz, 1H), 6.83 (dd, *J* = 8.8, 6.9 Hz, 1H). ^{13}C NMR (Pyridine-d$_5$, 101 MHz) δ (*ppm*) = 186.2, 162.8 (d, $J_{F,C}$ = 244.9 Hz), 132.0 (d, $J_{F,C}$ = 3.1 Hz), 131.2 (d, $J_{F,C}$ = 6.1 Hz), 128.8 (d, $J_{F,C}$ = 7.9 Hz), 128.0, 126.5, 116.6, 116.4 (d, $J_{F,C}$ = 2.0 Hz), 113,9, 101.1. HRMS (ESI): *m/z* [M + H]$^+$ calcd for $C_{15}H_{10}FNO$ + H$^+$ 240.0746, found 240.0814.

2-(4-chlorophenyl)indolizine-5-carbaldehyde 8e
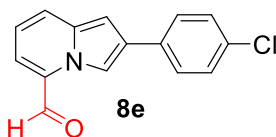
From 2-phenylindolizine **7e** (0.5 mmol, 96.5 mg). Silica gel (hexane/ethyl acetate 7:3).

Orange solid: 104.6 mg (82%). ^{1}H NMR (400 MHz, C$_5$D$_5$N, *ppm*) δ 9.88 (s, 1H), 9.46 (sl, 1H), 7.77-7.74 (m, 3H), 7.47 (d, 2H, *J* = 8.4 Hz), 7.31 (d, 1H, *J* = 6.9 Hz), 7.10 (s, 1H), 6.83 (dd, 1H, = 8.6, 7.0 Hz). ^{13}C NMR (100 MHz, C$_5$D$_5$N, *ppm*) δ 186.3, 134.4,

133.2, 132.3, 131.3, 140.0, 129.8, 128.5, 128.3, 126.6, 119.3, 116.6, 115.1, 114.1, 101.2. HRMS (ESI): m/z [M + H]$^+$ calcd for $C_{15}H_{10}ClNO$ + H$^+$ 256.0451, found 256.0521.

General Procedure I: Preparation of indolizines 9a-e.

In a dry nitrogen-flushed round-bottom flask, the respective 2-aryl-indolizine **7a-e** (0.5 mmol) was dissolved in THF (5.0-20.0 mL) and n-butyllithium (2.48 M in hexanes, 2.0 equiv.) was added dropwise at -70 °C. After 15 minutes, the mixture was warmed to -20 °C and stirred for 5 hours. Then, dry CO_2 was bubbled into the reactional mixture for 15 minutes and the reaction was stirred at room temperature for 24 hours. The reaction mixture was quenched with 1 mL of H_2O and acidified to pH 3 using a solution of HCl 1 M. Then, products were extracted with ethyl acetate (3 x 15 mL). The organic layer was basified to pH 8.0-9.0 and extracted with ethyl acetate (5 x 30 mL). The aqueous layer was acidified to pH 3.0 and extracted with ethyl acetate (3 x 30 mL). After, organic layer was combined and concentrated under reduced pressure. It was not necessary a purification by chromatography column.

2-phenylindolizine-5-carboxylic acid 9a
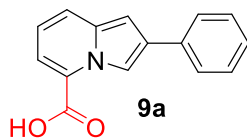
From 2-phenylindolizine **7a** (0.5 mmol, 96.5 mg). Only acid/basic extraction. Orange solid: 111.4 mg (94%), mp: 102 °C. ^{1}H NMR (DMSO-d$_6$, 300 MHz) δ (ppm) = 8.80 (d, J = 1.4 Hz, 1H), 7.60 (dd, J = 12.7, 7.7 Hz, 3H), 7.43 (dd, J = 6.8 Hz, 1.1 Hz, 1H), 7.27 (t, J = 7.4 Hz, 2H), 7.12 (t, J = 7.1 Hz, 1H), 6.93 (d, J = 1.4 Hz, 1H), 6.70 (dd, J = 8.4 Hz, 6.9 Hz, 1H). ^{13}C NMR (DMSO-d$_6$, 75 MHz) δ (ppm) = 164.0, 134.9, 134.5, 129.2, 128.9, 126.8, 125.8, 125.6, 124.1, 118.7, 115.7, 112.3, 112.3, 99.0. HRMS (ESI): m/z [M + H]$^+$ calcd for $C_{15}H_{11}NO_2$ + H$^+$ 238.0790, found 238.0868.

2-(4-methoxyphenyl)indolizine-5-carboxylic acid 9b
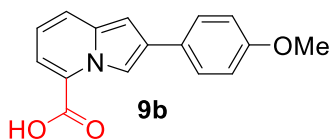
From 2-phenylindolizine **7b** (0.5 mmol, 96.5 mg). Only acid/basic extraction. Green solid. Yield: 125.5 mg (94%), mp: 142 °C. ^{1}H NMR (DMSO-d_6, 400 MHz) δ (*ppm*) = 9.17 (d, *J* = 1.8 Hz, 1H), 7.64 – 7.59 (m, 2H), 7.43 (dd, *J* = 8.8, 1.3 Hz, 1H), 7.29 (dd, *J* = 6.8, 1.4 Hz, 1H), 6.96 – 6.90 (m, 2H), 6.75 (d, *J* = 1.7 Hz, 1H), 6.68 (dd, *J* = 8.7, 6.8 Hz, 1H), 3.76 (s, 3H). ^{13}C NMR (101 MHz, DMSO-d_6) δ (*ppm*) = 174.0, 166.4, 158.0, 134.9, 132.6, 128.1, 127.5, 126.8, 119.9, 116.3, 114.3, 114.2, 112.2, 96.3, 55.1. HRMS (ESI): *m/z* [M + H]$^+$ calcd for $C_{16}H_{13}NO_3$ + H$^+$ 268.0895, found 268.0969.

2-(3,4-dimethoxyphenyl)indolizine-5-carboxylic acid 7c
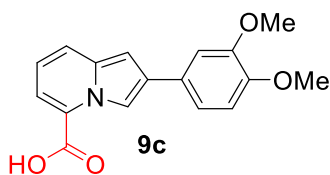
From 2-phenylindolizine **7c** (0.5 mmol, 96.5 mg). Only acid/basic extraction. Brown solid: 130.7 mg (88%). Mp: 122 °C. ^{1}H NMR (DMSO-d_6, 400 MHz) δ (*ppm*) = 8.94 (s, 1H), 7.73 (dd, *J* = 8.7, 1.3 Hz, 1H), 7.56 (dd, *J* = 7.0, 1.4 Hz, 1H), 7.29 – 7.22 (m, 2H), 7.02 (d, *J* = 1.6 Hz, 1H), 6.97 (d, *J* = 8.3 Hz, 1H), 6.80 (dd, *J* = 8.7, 7.0 Hz, 1H), 3.85 (s, 3H), 3.77 (s, 3H). ^{13}C NMR (101 MHz, DMSO-d_6) δ 172.1, 164.1, 149.2, 148.1, 134.9, 129.6, 127.5, 124.0, 118.5, 118.3, 115.5, 112.4, 112.1, 109.9, 99.1, 59.8, 55.6. HRMS (ESI): *m/z* [M + H]$^+$ calcd for $C_{17}H_{15}NO_4$ + H$^+$ 298.1001, found 298.1075.

2-(4-fluorophenyl)indolizine-5-carboxylic acid 9d
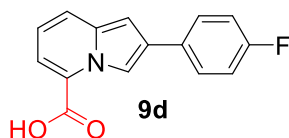
From 2-phenylindolizine **7d** (0.5 mmol, 96.5 mg). Only acid/basic extraction. Black solid: 61.2 mg (48%), mp: 96 °C. ^{1}H NMR (DMSO-d_6, 400 MHz) δ (*ppm*) = 9.22 (d, *J* = 1.8 Hz, 1H), 7.72 – 7.66 (m, 2H), 7.40 (d, *J* = 8.6 Hz, 1H), 7.19 (ddd, *J* = 11.1, 6.3, 3.1 Hz, 3H), 6.76 (d, *J* = 1.9 Hz, 1H), 6.68 (dd, *J* = 8.8, 6.7 Hz, 1H). ^{13}C NMR (101 MHz,

DMSO) δ (*ppm*) = 165.7, 160.9 (d, $J_{F,C}$ = 242.3 Hz), 134.9, 133.9, 132.2, 127.3 (d, $J_{F,C}$ = 7.8 Hz), 126.2, 119.3, 116.8, 115.7, 115.5, 113.5, 112.5, 96.2. HRMS (ESI): *m/z* [M + H]⁺ calcd for $C_{15}H_{10}NO_2$ + H⁺ 256.0696, found 256.0764.

2-(4-chlorophenyl)indolizine-5-carboxylic acid 9e
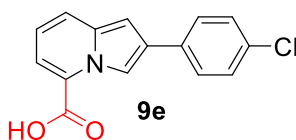
From 2-phenylindolizine **7e** (0.5 mmol, 96.5 mg). Only acid/basic extraction.

Brown solid: 128.7 mg (95%), mp: 132 °C. ¹H NMR (DMSO-*d₆,* 400 MHz) δ (*ppm*) = 9.28 (d, *J* = 1.6 Hz, 1H), 7.72 – 7.66 (m, 2H), 7.46 – 7.36 (m, 3H), 7.16 (dd, *J* = 6.7, 1.3 Hz, 1H), 6.77 (d, *J* = 1.8 Hz, 1H), 6.68 (dd, *J* = 8.8, 6.8 Hz, 1H). ¹³C NMR (DMSO-*d*6, 101 MHz) δ (*ppm*) = 164.0, 135.0, 133.5, 131.2, 128.9, 127.9, 127.5, 124.3, 124.1, 118.8, 116.0, 112.5, 99.0. HRMS (ESI): *m/z* [M + H]⁺ calcd for $C_{15}H_{10}ClNO_2$ + H⁺ 272.0400, found 272.0474.

General Procedure J: In a dry nitrogen-flushed round-bottom flask, the respective 2-aryl-indolizine-5-carboxilic acid (0.3 mmol) was dissolved in DMF (1.0 mL). Then, K_2CO_3 (1.5 equiv., 62.2 mg) and MeI (1.5 equiv.) were added. After 12 h at room temperature, the reaction mixture was quenched with H_2O and products were extracted with HCl (10% 3x15 mL) and ethyl acetate (3 x 15 mL). The organic layers were neutralized with saturated aqueous $NaHCO_3$ and washed with brine, dried over $MgSO_4$, and concentrated under reduced pressure. The crude product was purified by column chromatography (ethyl acetate/hexane).

methyl 2-phenylindolizine-5-carboxylate 10a
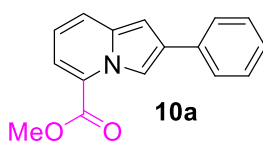
From 2-phenylindolizine-5-carboxylic acid **9a** (0.5 mmol, 125.5 mg). Silica gel (hexane/ethyl acetate 95:5). Green solid: 114.2 mg (91%), mp:112.6-155.7°C. ¹H NMR (DMSO-*d₆,*400 MHz) δ (*ppm*) = 8.94 (d, *J* = 1.6 Hz, 1H), 7.75 (dd, *J* = 8.2, 1.3 Hz, 2H),

7.59 (dd, *J* = 7.1, 1.3 Hz, 1H), 7.46 – 7.38 (m, 2H), 7.31 – 7.24 (m, 1H), 7.09 (d, *J* = 1.7 Hz, 1H), 6.83 (dd, *J* = 8.8, 7.1 Hz, 1H), 3.94 (s, 3H). ^{13}C NMR (DMSO-d_6,101 MHz) δ (*ppm*) = 162.7, 134.9, 134.3, 128.9, 126.9, 125.9, 124.6, 123.2, 118.9, 115.6, 112.3, 99.4, 52.5. HRMS (ESI): *m/z* [M + H]$^+$ calcd for $C_{16}H_{13}NO_2$ + H$^+$ 252.0946, found 252.1020.

methyl 2-(4-methoxyphenyl)indolizine-5-carboxylate 10b
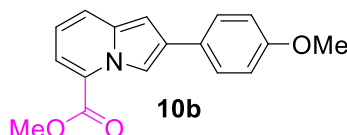
From 2-(4-methoxyphenyl)indolizine-5-carboxylic acid **9b** (0.5 mmol, 133.5 mg). Silica gel (hexane/ethyl acetate 95:5). Yellow solid: 68.1 mg (51%), mp: 138.6-139.8°C. ^{1}H NMR (DMSO-d_6 ,400 MHz) δ (*ppm*) = 8.87 (d, *J* = 1.3 Hz, 1H), 7.77 (d, *J* = 8.7 Hz, 1H), 7.67 (d, *J* = 8.7 Hz, 2H), 7.60 – 7.54 (m, 1H), 7.03 – 6.95 (m, 3H), 6.85 – 6.77 (m, 1H), 3.94 (s, 3H), 3.78 (s, 3H). ^{13}C NMR (DMSO-d_6, 101 MHz) (*ppm*) = 162.8, 158.4, 134.9, 129.5, 127.0, 126.8, 124.2, 123.0, 118.6, 115.3, 114.4, 111.7, 100.0, 55.1, 52.5. HRMS (ESI): *m/z* [M + H]$^+$ calcd for $C_{17}H_{15}NO_3$ + H$^+$ 282.10852, found 282.1124.

methyl 2-(3,4-dimethoxyphenyl)indolizine-5-carboxylate 10c
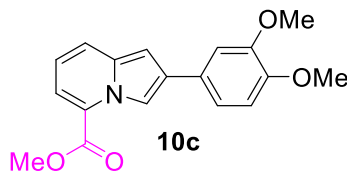
From 2-(3,4-dimethoxyphenyl)indolizine-5-carboxylic acid **9c** (0.5 mmol, 148.5 mg). Silica gel (hexane/ethyl acetate 8:2). Yellow solid: 145.6 mg (98%), mp: 113.2-114.6°C. ^{1}H NMR (DMSO-d_6,400 MHz) (*ppm*) = 8.89 (s, 1H), 7.78 (d, *J* = 8.6 Hz, 1H), 7.60 – 7.55 (m, 1H), 7.31 – 7.25 (m, 2H), 7.06 (d, *J* = 1.3 Hz, 1H), 6.99 (d, *J* = 8,1 Hz, 1H), 6.82 (dd, *J* = 8.6 Hz, 7.2 Hz, 1H), 3.94 (s, 3H), 3.85 (s, 3H), 3.78 (s, 3H). ^{13}C NMR (DMSO-d_6,101 MHz) δ (*ppm*) = 162.8, 149.2, 148.2, 134.8, 129.8, 127.3, 124.3 123.0, 118.7, 118.2, 115.4, 112.4, 111.9, 109.8, 99.3, 55.6, 55.6, 52.5. HRMS (ESI): *m/z* [M + H]$^+$ calcd for $C_{18}H_{17}NO_4$ + H$^+$ 312.1158, found 312.1229.

methyl 2-(4-fluorophenyl)indolizine-5-carboxylate 10d

10d
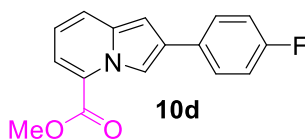
From 2-(4-fluorophenyl)indolizine-5-carboxylic acid **9d** (0.5 mmol, 127.5 mg). Silica gel (hexane/ethyl acetate 95:5). Green solid: 102.0 mg (80%), mp: 88 °C. ^{1}H NMR (DMSO-d_6,400 MHz) (*ppm*) = 8.89 (d, *J* = 1.6 Hz, 1H), 7.82 – 7.73 (m, 3H), 7.58 (dd, *J* = 7.1, 1.3 Hz, 1H), 7.27 – 7.20 (m, 2H), 7.05 (d, *J* = 1.7 Hz, 1H), 6.83 (dd, *J* = 8.8, 7.1 Hz, 1H), 3.93 (s, 3H). ^{13}C NMR (DMSO-d_6,101 MHz) δ (ppm) = 162.8, 161.4 (d, $J_{F,C}$ = 243.5 Hz), 135.0, 131.0, 128.6, 127.8 (d, $J_{F,C}$ = 8.0 Hz), 124.6, 123.3, 119.0, 115.9, 115.7 (d, $J_{F,C}$ = 4.7 Hz), 112.3, 99.4, 52.6. HRMS (ESI): *m/z* [M + H]$^+$ calcd for $C_{16}H_{12}FNO_2$ + H$^+$ 270.0852, found 270.0925.

methyl 2-(4-chlorophenyl)indolizine-5-carboxylate 10e

10e
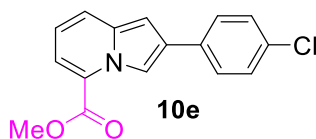
From 2-(4-chlorophenyl)indolizine-5-carboxylic acid **9e** (0.5 mmol, 142.5 mg). Silica gel (hexane/ethyl acetate 95:5). Yellow solid: 125.4 mg (88%), mp: 107.7-110.9°C. ^{1}H NMR (DMSO-d_6,400 MHz) δ (*ppm*) = 8.92 (d, *J* = 1.5 Hz, 1H), 7.82 – 7.73 (m, 3H), 7.58 (dd, *J* = 7.1 Hz, 1.2 Hz, 1H), 7.48 – 7.42 (m, 2H), 7.08 (d, *J* = 1.5 Hz, 1H), 6.83 (dd, *J* = 8.7 Hz, 7.1 Hz, 1H), 3.93 (s, 3H). ^{13}C NMR (DMSO-d_6,101 MHz) δ (ppm): 162.7, 134.9, 133.3, 131.3, 128.8, 128.1, 127.5, 124.6, 123.3, 119.0, 115.8, 112.4, 99.4, 52.5. HRMS (ESI): *m/z* [M + H]$^+$ calcd for $C_{16}H_{12}ClNO_2$ + H$^+$ 286.0557, found 286.0629.

General Procedure K: In a dry nitrogen-flushed round-bottom flask, the respective 2-aryl-indolizine-5-carboxilic acid (0.3 mmol) was dissolved in DMF (1.0 mL). Then, HBTU (1.2 equiv., 136.5 mg), HBOt (1.2 equiv., 48.6 mg) and Et$_3$N (0,1 mL) were added. After 10 minutes at room temperature diethylamine (2.0 equiv, 0.06 mL) was added and the reaction mixture was stirred for 12 hours at room temperature. Products were extracted with saturated aqueous NaHCO$_3$ and EtOAc (3x15 mL). The Oganic layers were washed with brine, dried over MgSO$_4$, and concentrated under reduced

pressure. The crude product was purified by flash column chromatography (ethyl acetate/hexane).

N,N-diethyl-2-phenylindolizine-5-carboxamide 11a
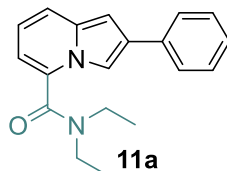
From 2-phenylindolizine-5-carboxylic acid **9a** (0.5 mmol, 125.5 mg). Silica gel (hexane/ethyl acetate 7:3). Dark Green oil: 109.5 mg (75%). ^{1}H NMR (DMSO-d_6,400 MHz) δ (*ppm*) = 7.75 – 7.70 (m, 2H), 7.62 (d, *J* = 1.6 Hz, 1H), 7.51 – 7.45 (m, 1H), 7.39 (t, *J* = 7.8 Hz, 2H), 7.28 – 7.22 (m, 1H), 6.91 (d, *J* = 1.7 Hz, 1H), 6.77 (dd, *J* = 9.0, 6.7 Hz, 1H), 6.61 (dd, *J* = 6.7, 1.2 Hz, 1H), 3.60 – 3.15 (m, 4H), 1.34 – 0.88 (m, 6H). ^{13}C NMR (DMSO-d_6,101 MHz) δ (*ppm*) = 163.6, 134.3, 133.5, 130.7, 129.0, 128.8, 126.7, 125.7, 119.2, 116.9, 108.7, 107.8, 97.4, 42.5, 41.7, 14.0, 12.5. HRMS (ESI): *m/z* [M + H]$^+$ calcd for $C_{19}H_{20}N_2O$ + H$^+$ 293.1576, found 293.1648.

N,N-diethyl-2-(4-methoxyphenyl)indolizine-5-carboxamide 11b
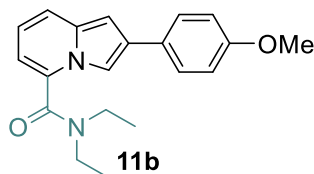
From **2-(4-methoxyphenyl)indolizine-5-carboxylic acid 9b** (0.5 mmol, 133.5 mg). Silica gel (hexane/ethyl acetate 6:4). Green solid: 80.5 mg (50%), mp: 96-100°C. ^{1}H NMR (DMSO-d_6, 400 MHz) δ (*ppm*) = 7.66 – 7.61 (m, 2H), 7.51 (d, *J* = 1.6 Hz, 1H), 7.48 – 7.43 (m, 1H), 6.98 – 6.93 (m, 2H), 6.83 (d, *J* = 1.6 Hz, 1H), 6.75 (dd, *J* = 9.0, 6.7 Hz, 1H), 6.59 (dd, *J* = 6.6, 1.2 Hz, 1H), 3.77 (s, 3H), 3.54 (q, *J* = 12.5 Hz, 2H), 3.33 – 3.13 (m, 2H), 1.29 – 1.01 (m, 6H). ^{13}C NMR (DMSO-d_6, 101 MHz) δ (*ppm*) = 163.7, 158.3, 133.5, 130.6, 129.0, 126.9, 119.0, 116.8, 114.3, 108.5, 107.1, 97.1, 55.1, 42.4, 14.3, 12.5. HRMS (ESI): *m/z* [M + H]$^+$ calcd for $C_{20}H_{22}N_2O_2$ + H$^+$ 323.1681, found 323.1750.

2-(3,4-dimethoxyphenyl)-N,N-diethylindolizine-5-carboxamide 11c
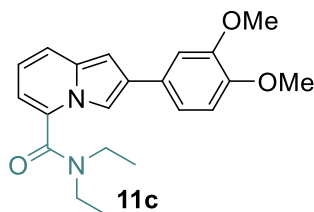
From 2-(3,4-dimethoxyphenyl)indolizine-5-carboxylic acid x (0.5 mmol, 148.5 mg). Silica gel (hexane/ethyl acetate 6:4). Dark green oil: 105.6 mg (60%). ^{1}H NMR (DMSO-d_6,400 MHz) δ (*ppm*) = 7.54 (d, *J* = 1.6 Hz, 1H), 7.49 – 7.44 (m, 1H), 7.28 – 7.21 (m, 2H), 6.96 (d, *J* = 8.1 Hz, 1H), 6.88 (d, *J* = 1.6 Hz, 1H), 6.76 (dd, *J* = 9.0, 6.6 Hz, 1H), 6.60 (dd, *J* = 6.6, 1.2 Hz, 1H), 3.83 (s, 3H), 3.77 (s,3H), 3.55 (m, 2H), 3.29 – 3.12 (m, 2H), 1.15 (m, 6H). ^{13}C NMR (DMSO-d_6,101 MHz) δ (*ppm*) = 163.7, 149.1, 148.0, 133.4, 130.6, 129.3, 127.3, 119.0, 118.2, 116.7, 112.3, 109.9, 108.5, 107.4, 97.4, 59.7, 55.6, 42.5, 14.1. HRMS (ESI): *m/z* [M + H]$^+$ calcd for $C_{21}H_{24}N_2O_3$ + H$^+$ 353.1787, found 353.1859.

N,N-diethyl-2-(4-fluorophenyl)indolizine-5-carboxamide 11d
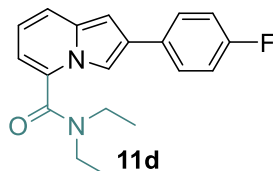
From 2-(4-fluorophenyl)indolizine-5-carboxylic acid x (0.5 mmol, 127.5 mg). Silica gel (hexane/ethyl acetate 6:4). Green solid: 93.0 mg (60%), mp: 85.9-88.2°C. ^{1}H NMR (DMSO-d_6,500 MHz) δ (*ppm*) = 7.75 – 7.70 (m, 2H), 7.64 – 7.61 (m, 1H), 7.48 (d, *J* = 8.9 Hz, 1H), 7.39 (t, *J* = 7.7 Hz, 2H), 7.29 – 7.21 (m, 1H), 6.91 (d, *J* = 1.5 Hz, 1H), 6.77 (dd, *J* = 9.0, 6.7 Hz, 1H), 6.61 (dd, *J* = 6.7, 1.1 Hz, 1H), 3.60 – 3.17 (m, 4H), 1.40 – 0.95 (m, 6H). ^{13}C NMR (DMSO-d_6,126 MHz) δ (*ppm*) = 163.6, 161.3 (d, $J_{F,C}$ = 243.4 Hz), 133.6, 130.9 (d, $J_{F,C}$ = 3.1 Hz), 130.8, 128.1, 127.7 (d, $J_{F,C}$ = 7.9 Hz), 119.2, 117.0, 115.5, 108.8, 107.8, 97.4, 42.6, 12.7. HRMS (ESI): *m/z* [M + H]$^+$ calcd for $C_{19}H_{19}FN_2O$ + H$^+$ 311.1481, found 311.1555.

2-(4-chlorophenyl)-*N,N*-diethylindolizine-5-carboxamide 11e
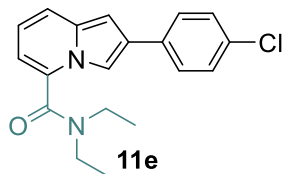
From 2-(4-chlorophenyl)indolizine-5-carboxylic acid x (0.5 mmol, 142.5 mg). Silica gel (hexane/ethyl acetate 7:3). Dark brown solid: 117.4 mg (72%), mp: 118-121°C. ^{1}H NMR (DMSO-d_6,400 MHz) δ (*ppm*) = 7.79 – 7.73 (m, 2H), 7.64 (d, *J* = 1.2 Hz, 1H), 7.49 (d, *J* = 8.9 Hz, 1H), 7.46 – 7.40 (m, 2H), 6.91 (d, *J* = 1.5 Hz, 1H), 6.78 (dd, *J* = 9.0 Hz, 6.7 Hz, 1H), 6.63 (dd, *J* = 6.7 Hz, 1.1 Hz, 1H), 3.55 (s, 2H), 3.22 (d, *J* = 6,4 Hz, 2H), 1.32 – 0.97 (m, 6H). ^{13}C NMR (DMSO-d_6,101 MHz) δ (*ppm*) = 163.5, 133.6, 133.3, 131.1, 130.8, 128.7, 127.7, 127.5, 119.3, 117.1, 108.9, 108.1, 97.5, 42.6, 14.2, 12.9. HRMS (ESI): *m/z* [M + H]$^+$ calcd for $C_{19}H_{19}ClN_2O$ + H$^+$ 327.1186, found 327.1258.

General Procedure L: Preparation of [Ir(cod)(OMe)]$_2$

Step 1: A 1 L 2-necked round bottom flask was charged with IrCl$_3$ (5.0 g, 17 mmol), water (150 mL), and propan-2-ol (250 mL). To the dark purple/black solution, excess of 1,5 cyclooctadiene (25 mL) was added. The flask was fitted with a reflux condenser and heated to reflux under vigorous shaking for 4 hours. Upon completion the solution was bright clear red orange colour. The reaction was cooled and fitted with distillation apparatus (150 mL distilled). The reaction mixture was left to cool to room temperature for 2 hours allowing a red crystalline solid to form. The solid as filtered and washed with cold methanol and dried under reduced pressure to afford [Ir(Cl)cod)]$_2$ (71%).

Step 2: A 500 mL 1-necked round bottom flask was charged with [Ir(Cl)cod)]$_2$ (5.0 g, 7.5 mmol), KOH (1.0 g, 18 mmol). The flask was purged with nitrogen and degassed MeOH (150 mL) was added. The reaction was stirred at room temperature for 3 hours under nitrogen, with a continuous flown of nitrogen bubbling through the reaction solvent. Upon completion no orange/red solid remained, and a pale-yellow precipitate had formed. Degassed water (200 mL) was added to the reaction and the vessel was cooled to 0 °C for 1 hour. The solid was filtered and washed with water and cold MeOH. The solid, was transferred to a round bottom flask and placed under reduced pressure for 12 hours affording [Ir(cod)(OMe)]$_2$ as fine free flowing yellow powder (63%).

General Procedure M: One-pot C-H borylation/Suzuki–Miyaura cross-coupling of substituted indolizines.

An oven-dried thick-walled microwave synthesis vial was charged with the corresponding indolizine (0.5 mmol, 1.0 equiv.) and degassed MTBE (1 mL) (vial A). A separate vial was charged with [Ir(cod)(OMe)]$_2$ (5 mol %), dtbpy (10 mol %), B$_2$pin$_2$ (1.0 equiv.) and it was evacuated and placed under N$_2$ with three evacuation/refill cycles, before degassed MTBE was added. The vial was sealed with a crimp top septum cap and shaken to develop a deep red colour. Once it was homogeneous, the solution of vial A was added to vial B. The vial was heated for 1 hour or 4 hours. Upon completion (determined by GC–MS) the volatiles were removed in vacuum to afford the crude boronate product. Pd(dppf)Cl$_2$ (10 mol%), K$_2$PO$_3$ (1.0 equiv.) and aryl halide (1.3 equiv.) were added, and the vial was sealed and purged with three evacuation/refill (Ar) cycles. Degassed DMAc/H$_2$O (2 mL/1 mL) was added, and the mixture was heated to 80 °C for 12 hours in an oil bath. The reaction mixture was diluted with water (10 mL) and extracted with AcOEt (3 × 10 mL). The combined organic layers were washed with brine (10 mL), dried with anhydrous MgSO$_4$, filtered through Celite, and concentrated in vacuo to afford the crude product. The residue was purified by pre-packed silica Redisep® *R*f cartridges with the stated solvent gradient and at a constant flow rate of 35 mL/min using an automated Teledyne Isco CombiFlash *R*f machine.

3-Phenylindolizine-1-carbonitrile 13a
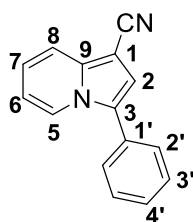
From indolizine-1-carbonitrile (71 mg, 0.5 mmol) and iodobenzene (0.07 mL, 0.65 mmol), pre-packed silica Redisep® *R*f cartridges (ethyl acetate/hexane, 2:8), yield: 33 mg (30%), brown oil. ^{1}H NMR (600 MHz, CDCl$_3$, 25 °C) δ = 8.28 (d, *J* = 7.2 Hz, H-5), 7.70 (d, *J* = 9.0 Hz, H-8), 7.55–7.50 (m, 4H-2'-3'), 7.46–7.42 (m, H-4'), 7.09 (ddd, *J* = 9.0, 6.6, 1.0 Hz, H-7), 7.05 (s, H-2), 6.74 (td, *J* = 6.8, 1.3 Hz, H-6). ^{13}C NMR (151 MHz, CDCl$_3$) δ = 138.6 (C-9), 130.4 (C-1'), 129.4, 128.9, 128.8, 127.1, 123.9 (C-5), 122.5

(C-7), 118.4 (C-8), 117.1 (CN), 116.4 (C-2), 113.2 (C-6), 82.4 (C-1). Accurate mass (EI): calcd. for $C_{15}H_{10}N_2$ 218.0844, found 218.0927.

3-(4-methoxyphenyl)indolizine-1-carbonitrile 13b
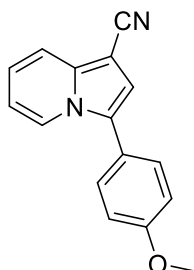
From indolizine-1-carbonitrile (71 mg, 0.5 mmol) and iodobenzene (152 mg, 0.65 mmol), pre-packed silica Redisep® Rf cartridges (ethyl acetate/hexane, 2:8), yield: 24.8 mg (20%), mp: 105 °C, brown solid.^{1}H NMR (400 MHz, Chloroform-d) δ 8.20 (dt, J = 7.2, 1.1 Hz, 1H), 7.68 (dt, J = 8.9, 1.2 Hz, 1H), 7.46 – 7.39 (m, 2H), 7.09 – 7.01 (m, 3H), 6.99 (s, 1H), 6.72 (td, J = 6.9, 1.3 Hz, 1H), 3.88 (s, 3H). ^{13}C NMR (101 MHz, CDCl$_3$) δ 160.0, 138.3, 130.4, 130.0, 126.9, 123.9, 122.6, 118.3, 117.2, 116.0, 114.8, 113.1, 82.1, 55.6. Accurate mass (EI): calcd. for $C_{16}H_{12}N_2O$ 248.0950, found 248.1028.

6-Phenylindolizine-1-carbonitrile 14a
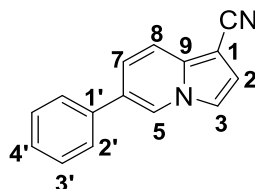
From indolizine-1-carbonitrile (71 mg, 0.5 mmol) and iodobenzene (0.07 mL, 0.65 mmol), pre-packed silica Redisep® Rf cartridges (ethyl acetate/hexane, 1:9), yield: 11 mg (10%), brown oil. ^{1}H NMR (600 MHz, CDCl$_3$, 25 °C) δ = 8.20 (t, J = 1.3 Hz, H-5), 7.71 (d, J = 9.2 Hz, H-8), 7.58–7.54 (m, 2H-2'), 7.48 (dd, J = 8.4, 7.0 Hz, 2H-3'), 7.44–7.39 (m, H-4'), 7.34 (dd, J = 9.3, 1.6 Hz, H-7), 7.31 (d, J = 3.0 Hz, H-3), 7.06 (d, J = 2.9 Hz, H-2). ^{13}C NMR (151 MHz, CDCl$_3$) δ = 129.3 (C-3'), 128.3 (C-4'), 127.6, 127.0, 126.5 (C-2'), 123.4 (C-7), 123.8 (C-5), 120.4, 118.0, 117.6 (C-8), 117.0 (C-2), 114.5 (C-3). Accurate mass (EI): calcd. for $C_{15}H_{10}N_2$ 218.0844, found 218.0952.

3-[4-(Trifluoromethyl)phenyl]indolizine-1-carbonitrile 13c
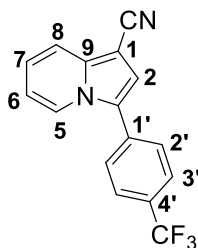
From indolizine-1-carbonitrile (71 mg, 0.5 mmol) and 1-bromo-4-(trifluoromethyl)benzene (0.09 mL, 0.65 mmol), pre-packed silica Redisep® Rf cartridges (ethyl acetate/hexane, 2:8), yield: 42 mg (33%), pale yellow solid, mp: 157–158 °C. ^{1}H NMR (700 MHz, CDCl$_3$, 25 °C) δ = 8.29 (dt, J = 7.1, 1.1 Hz, 1H, H-5), 7.80–7.76 (m, 2H, H-3'), 7.72 (dt, J = 9.0, 1.2 Hz, 1H, H-8), 7.68–7.64 (m, 2H, H-2'), 7.14 (ddd, J = 9.0, 6.6, 1.0 Hz, 1H, H-7), 7.12 (s, 1H, H-3), 6.81 (td, J = 6.9, 1.3 Hz, 1H, H-6). ^{13}C NMR (176 MHz, CDCl$_3$) δ = 139.0 (C-9), 133.9 (C-1'), 130.5 (q, $J_{F,C}$ = 32.7 Hz, C-4') 128.80 (2C-2'), 126.4 (q, $J_{F,C}$ = 3.7 Hz, 2C, C-3'), 125.5 (C-3), 124.8 (q, $J_{F,C}$ = 272 Hz, CF$_3$), 123.6 (C-5), 123.1 (C-7), 118.6 (C-8), 117.3 (C-2), 116.5 (CN), 113.8 (C-6), 83.1 (C-1). Accurate mass (EI): calcd. for C$_{16}$H$_9$F$_3$N$_2$ 286.0718, found 286.0820.

6-[4-(Trifluoromethyl)phenyl]indolizine-1-carbonitrile 14b
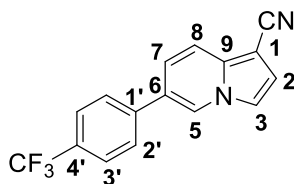
From indolizine-1-carbonitrile (71 mg, 0.5 mmol) and 1-bromo-4-(trifluoromethyl)benzene (0.09 mL, 0.65 mmol), pre-packed silica Redisep® Rf cartridges (ethyl acetate/hexane, 2:8), yield: 17 mg (12%), brown oil. ^{1}H NMR (600 MHz, CDCl$_3$, 25 °C) δ = 8.11 (dd, J = 7.1, 0.9 Hz, 1H, H-5), 7.87 (dd, J = 1.8, 0.9 Hz, 1H. H-8), 7.77–7.72 (m, 4H-ArCF$_3$), 7.30 (d, J = 3.1 Hz, 1H, H-3), 7.08 (d, J = 2.9 Hz, 1H, H-2), 7.04 (dd, J = 7.2, 1.9 Hz, 1H, H-7). ^{13}C NMR (151 MHz, CDCl3) δ = 141.7, 137.9 (C-9), 133.8, 130.5 (q, $J_{F,C}$ = 32.6 Hz, C-4'), 127.1, 126.9, 126.1 (q, $J_{F,C}$ = 3.7 Hz, 2C-3'), 124.2 (q, $J_{F,C}$ = 272 Hz, CF$_3$), 118.0 (C-2), 116.8 (CN), 115.6 (C-8), 114.2 (C-3), 112.6 (C-7), 83.3 (C-1'). Accurate mass (EI): calcd. for C$_{16}$H$_9$F$_3$N$_2$ 286.0718, found 286.0805.

Dimethyl-5-[4-(Trifluoromethyl)phenyl]indolizine-1,2-dicarboxylate 15
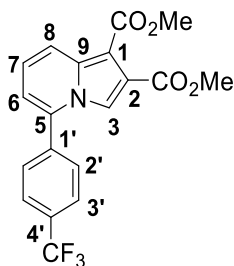
From dimethyl indolizine-1,2-dicarboxylate (116.5 mg, 0.5 mmol) and 1-bromo-4-(trifluoromethyl)benzene (0.09 mL, 0.65 mmol), pre packed silica Redisep® Rf cartridges (ethyl acetate/ hexane, 1:9), yield: 90 mg (48%), pale yellow solid, mp: 147 °C. ^{1}H NMR (600 MHz, CDCl$_3$, 25 °C) δ = 8.21 (ddd, J = 9.2, 1.2, 0.6 Hz, 1H, H-8), 7.83 (dt, J = 8.1, 0.8 Hz, 2H, H-3'), 7.73–7.70 (m, 2H, H-2'), 7.57 (d, J = 0.7 Hz, 1H, H-3), 7.17 (dd, J = 9.3, 6.8 Hz, 1H, H- 7), 6.72 (dd, J = 6.8, 1.2 Hz, 1H, H-6), 3.93 (s, 3H), 3.87 (s, 3H). ^{13}C NMR (151 MHz, CDCl$_3$) δ = 165.2 (CO$_2$Me), 164.4 (CO$_2$Me), 137.3, 137.1, 136.6, 132.2 (q, $J_{F,C}$ = 32.8 Hz, C-4'), 130.4, 129.4 (C-3), 126.6 (q, $J_{F,C}$ = 3.7 Hz),123.83 (q, $J_{F,C}$ = 272 Hz, CF$_3$), 123.3 (C-7), 122.9, 121.9, 120.3 (C-8), 115.2, 114.9 (C-6), 103.8 (C-1), 52.3 (CH$_3$), 51.6 (CH$_3$). Accurate mass (EI): calcd. for C$_{19}$H$_{14}$F$_3$NO$_4$ 377.0875, found 377.0965.

Dimethyl-6-[4-(Trifluoromethyl)phenyl]indolizine-1,2-dicarboxylate 16
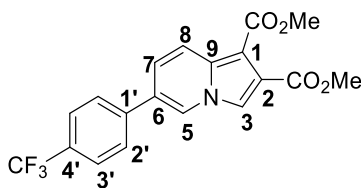
From dimethyl indolizine-1,2-dicarboxylate (116.5 mg, 0.5 mmol) and 1-bromo-4-(trifluoromethyl)benzene (0.09 mL, 0.65 mmol), pre-packed silica Redisep® Rf cartridges (ethyl acetate/ hexane, 1:9), yield: 33 mg (12%), pale yellow solid, mp: 172–173 °C. ^{1}H NMR (600 MHz, CDCl$_3$, 25 °C) δ = 8.23 (dt, J = 9.5, 0.8 Hz, 1H, H-8), 8.16 (dd, J = 1.6, 1.0 Hz, 1H, H-5), 7.77–7.72 (m, 2H, H-3'), 7.72 (s, 1H, H-3), 7.67 (dt, J = 8.0, 0.8 Hz, 2H, H-2'), 7.33 (dd, J = 9.5, 1.6 Hz, 1H, H-7), 3.93 (d, J = 1.0 Hz, 6H). ^{13}C NMR (151 MHz, CDCl$_3$) δ = 164.8 (CO$_2$Me), 164.1 (CO$_2$Me), 140.4 (C-1'), 135.2 (C-9), 130.3 (q, $J_{F,C}$ = 32.6 Hz, C-4'), 127.1, 126.6 (C-6), 126.1 (q, $J_{F,C}$ = 3.9 Hz, 2C, C-3'), 124.0 (q, $J_{F,C}$ = 272 Hz, CF$_3$), 123.5 (C-5), 123.3 (C-7), 123.1, 122.3, 121.0 (C-8), 117.5

(C-3), 103.3 (C-1), 52.2 (CH$_3$), 51.4 (CH$_3$). Accurate mass (EI): calcd. for C$_{19}$H$_{14}$F$_3$NO$_4$ 377.0875, found 377. 0965.

Dimethyl-5,6-Bis[4-(trifluoromethyl)phenyl]indolizine-1,2-dicarboxylate 17
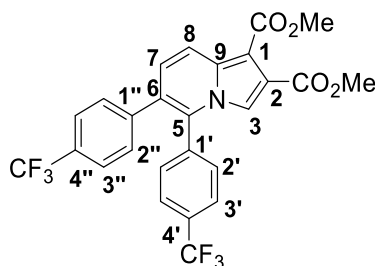
From dimethyl indolizine-1,2-dicarboxylate (116.5 mg, 0.5 mmol) and 1-bromo-4-(trifluoromethyl)benzene (0.09 mL, 0.65 mmol), pre-packed silica Redisep® *R*f cartridges (ethyl acetate/hexane, 1:9), yield: 31 mg (12%), yellow solid, mp: 203–204 °C. ^{1}H NMR (600 MHz, CDCl$_3$, 25 °C) δ = 8.50 (d, *J* = 1.6 Hz, 1H, H-8), 7.90–7.85 (m, 2H), 7.83–7.77 (m, 4H), 7.73 (d, *J* = 8.3 Hz, 2H), 7.59 (d, *J* = 0.6 Hz, 1H, H-3), 7.02 (d, *J* = 1.9 Hz, 1H, H-7), 3.95 (s, 3H), 3.89 (s, 3H). ^{13}C NMR (151 MHz, CDCl$_3$) 165.4 (CO$_2$Me), 164.8 (CO$_2$Me), 142.2, 137.5, 137.4, 135.2, 132.4, 132.2, 130.5, 130.3, 130.2, 129.3, 127.6, 127.0, 126.5 (q, $J_{F,C}$ = 3.6 Hz, 2C), 126.0 (q, $J_{F,C}$ = 3.7 Hz, 2C), 125.4, 124.0 (q, $J_{F,C}$ = 272 Hz, CF3), 123.5 (q, $J_{F,C}$ = 298 Hz, CF3), 118.1 (C-8), 115.7 (C-3), 114.7 (C-7), 105.2 (C-1), 52.8 (CH$_3$), 52.1 (CH$_3$). Accurate mass (EI): calcd. for C$_{26}$H$_{17}$F$_6$NO$_4$ 521.1062, found 521.1141.

7. Appendix

7.1 NMR Spectra

^{1}H NMR spectrum **36** DMSO-*d$_6$* (300 MHz).
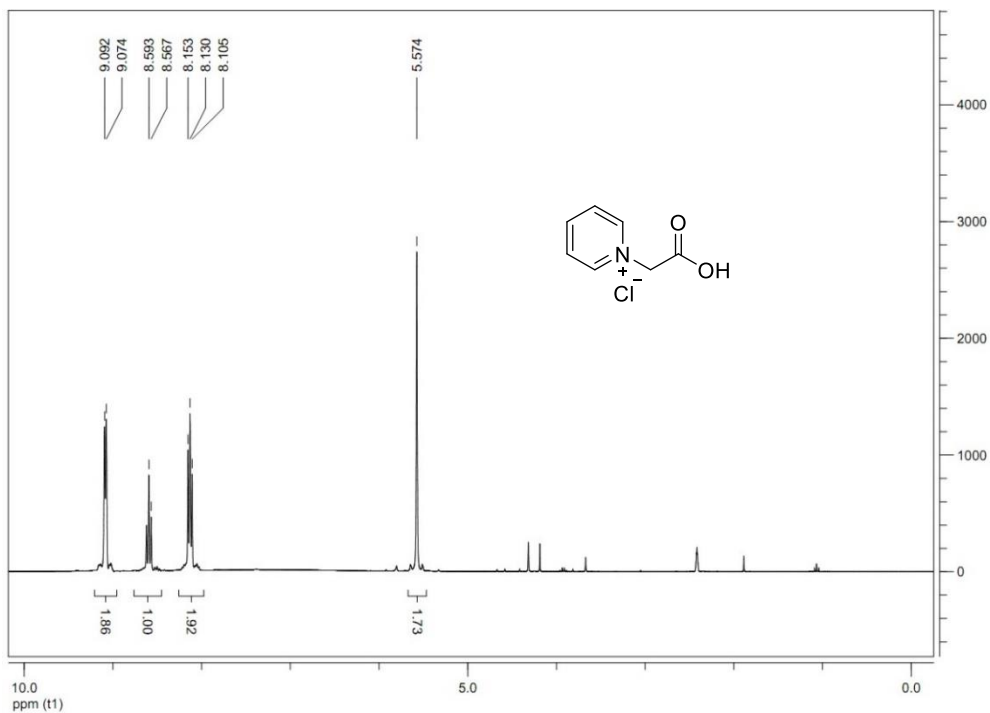
¹³C NMR spectrum **36** (DMSO-*d₆* (75 MHz).
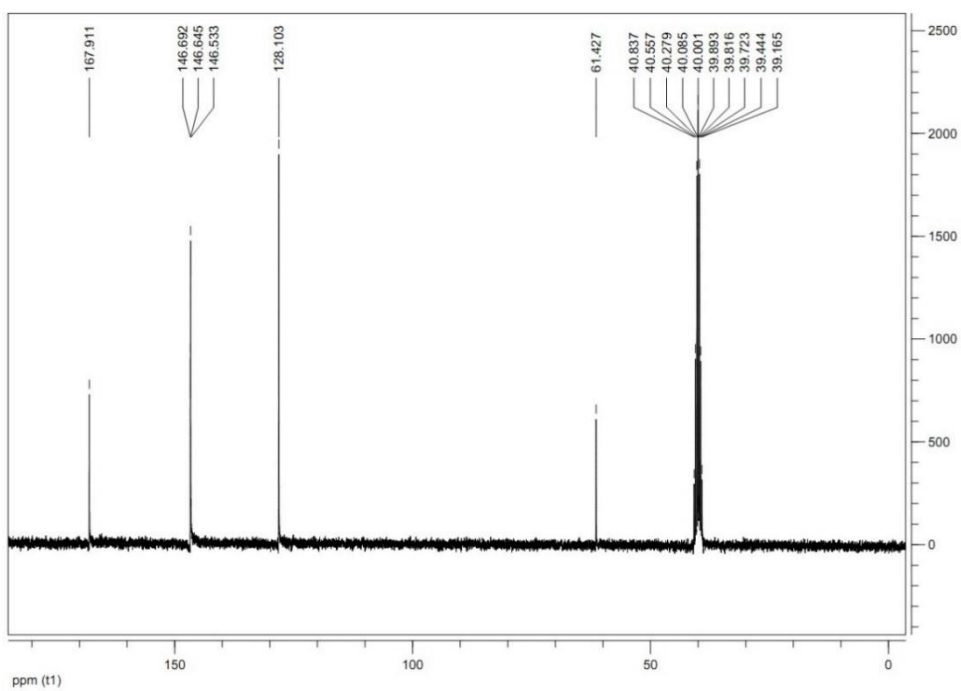
Compound **4:** ^{1}H NMR (600 MHz, CDCl$_3$).
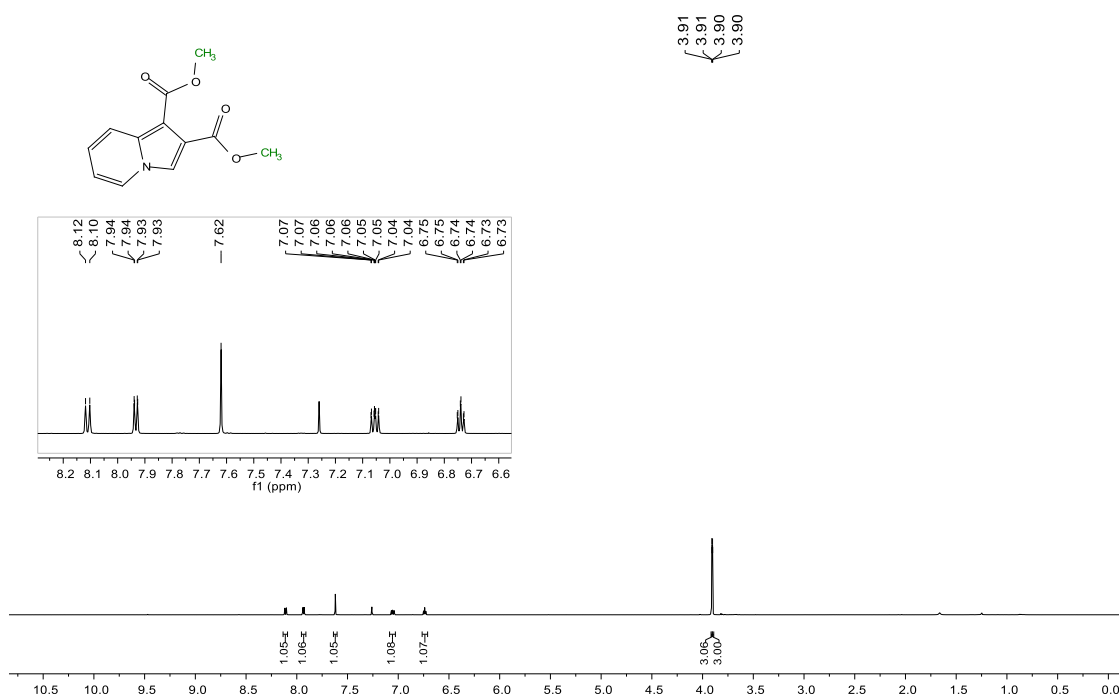
Compound **4:** ^{13}C NMR (151 MHz, CDCl$_3$).
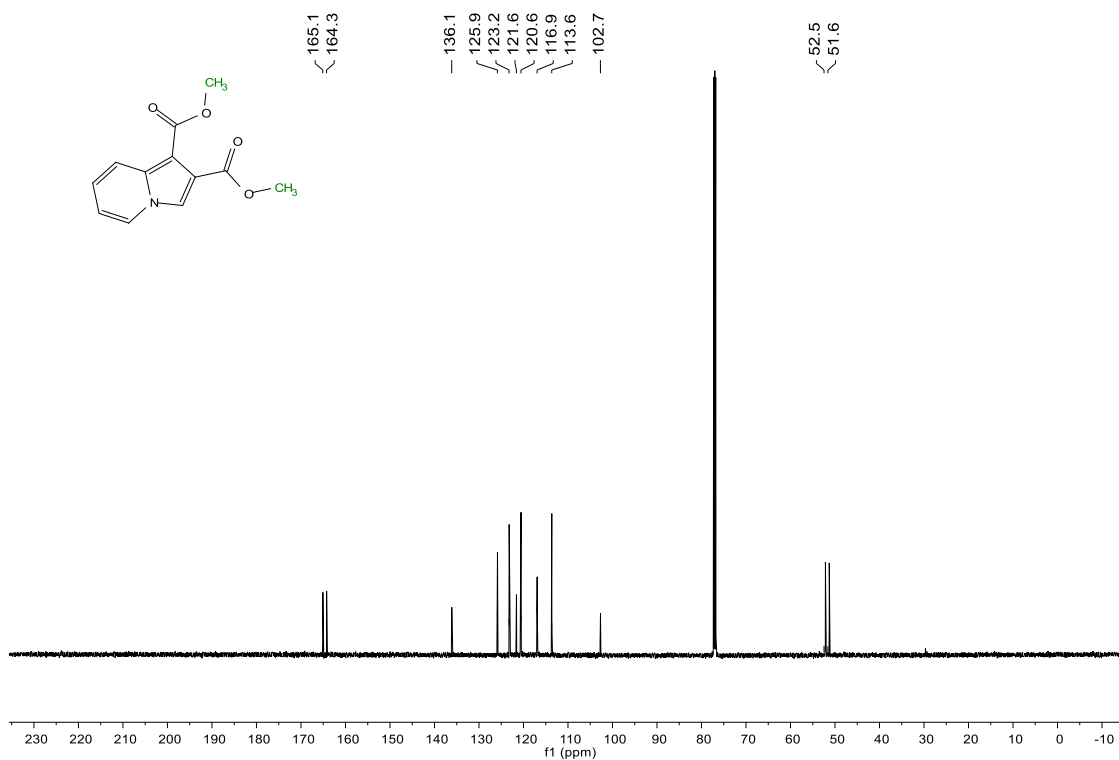
Compound **4**: NOESY (^{1}H NMR 600 MHz, CDCl$_3$; ^{13}C NMR 151 MHz, CDCl$_3$).
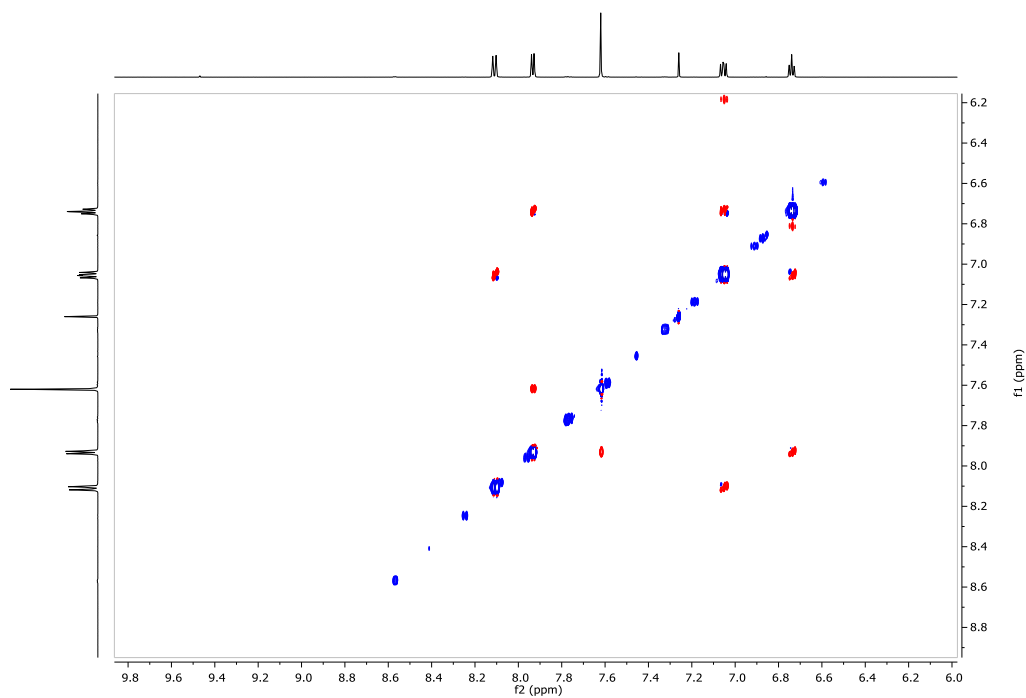
Compound **4**: HSQC (^{1}H NMR 600 MHz, CDCl$_3$; ^{13}C NMR 151 MHz, CDCl$_3$).
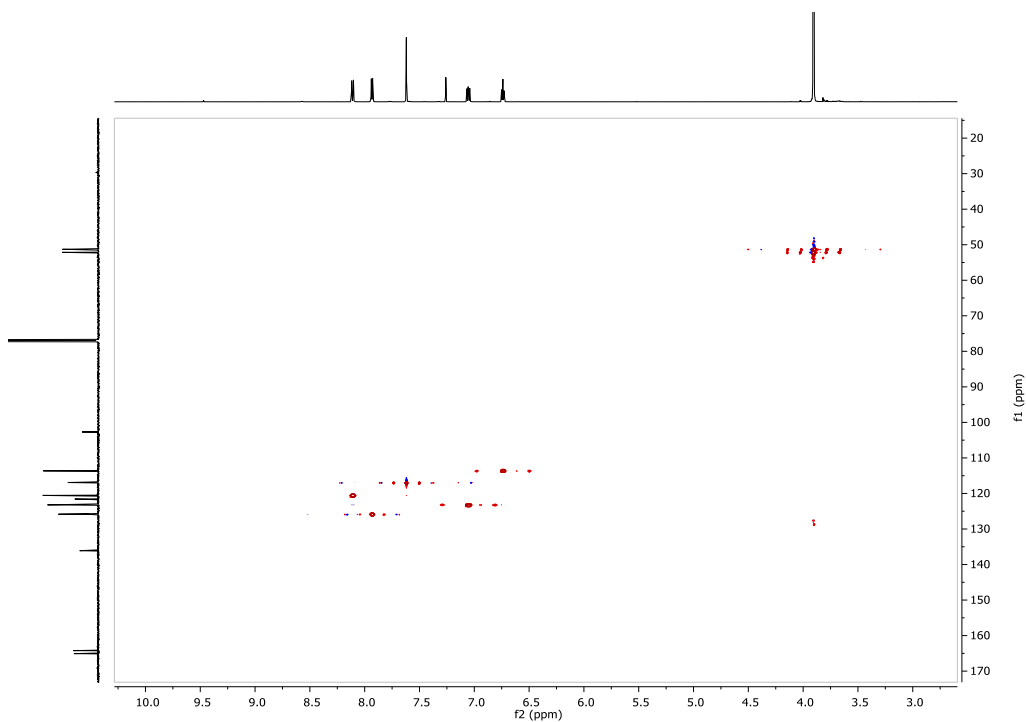
Compound **4**: HMBC (^{1}H NMR 600 MHz, CDCl$_3$; ^{13}C NMR 151 MHz, CDCl$_3$).
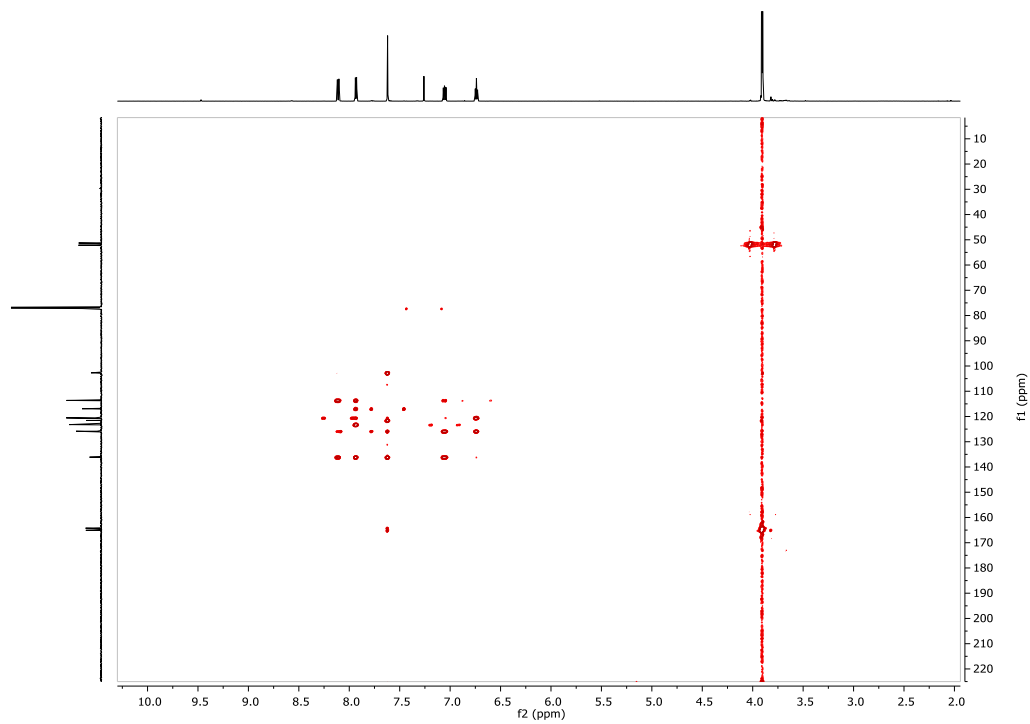
^{1}H NMR spectrum **12** CDCl$_3$ (500 MHz).
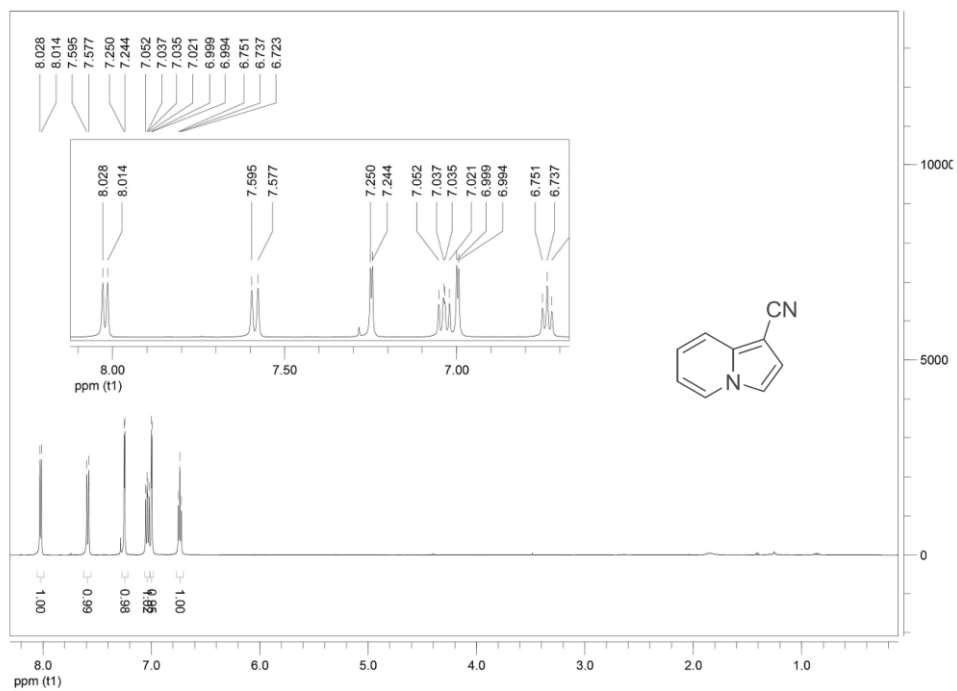
^{13}C NMR spectrum **12** (125 MHz, CDCl$_3$)
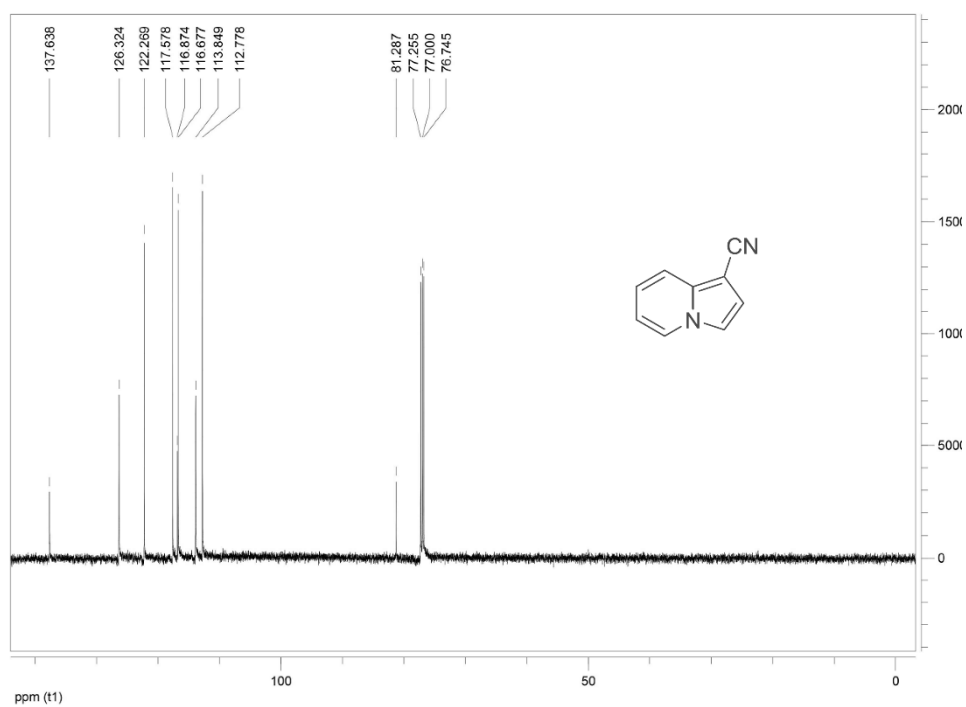
^{1}H NMR spectrum **4** (CDCl$_3$, 700 MHz).
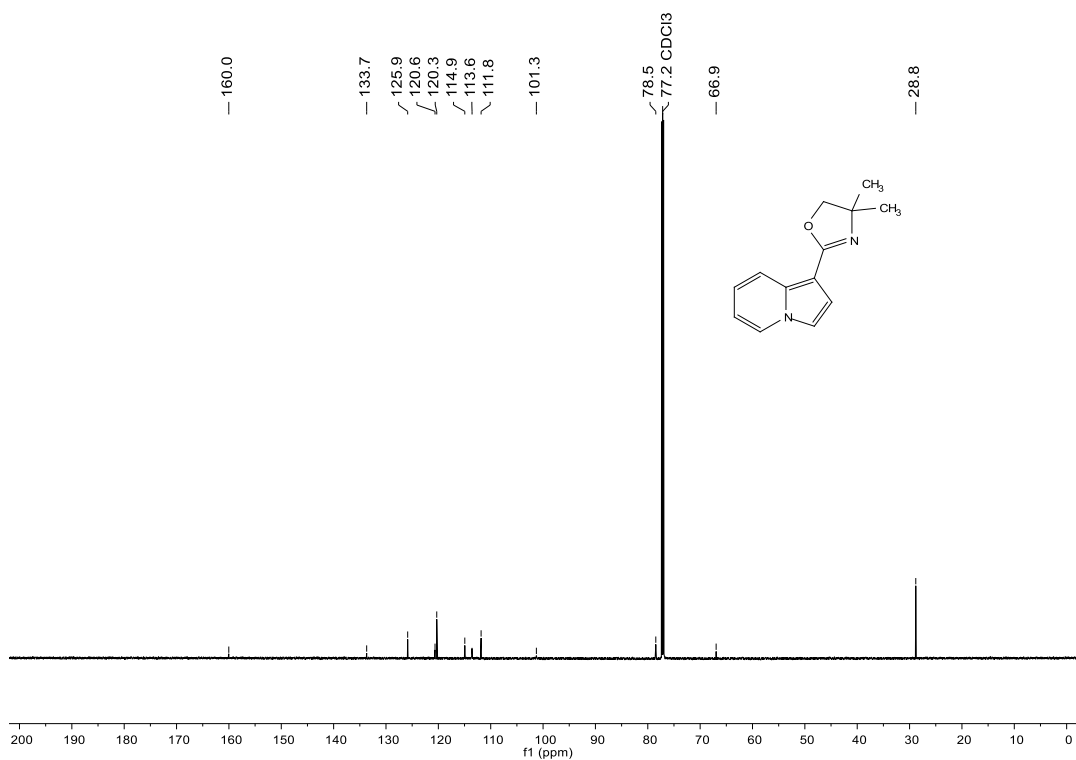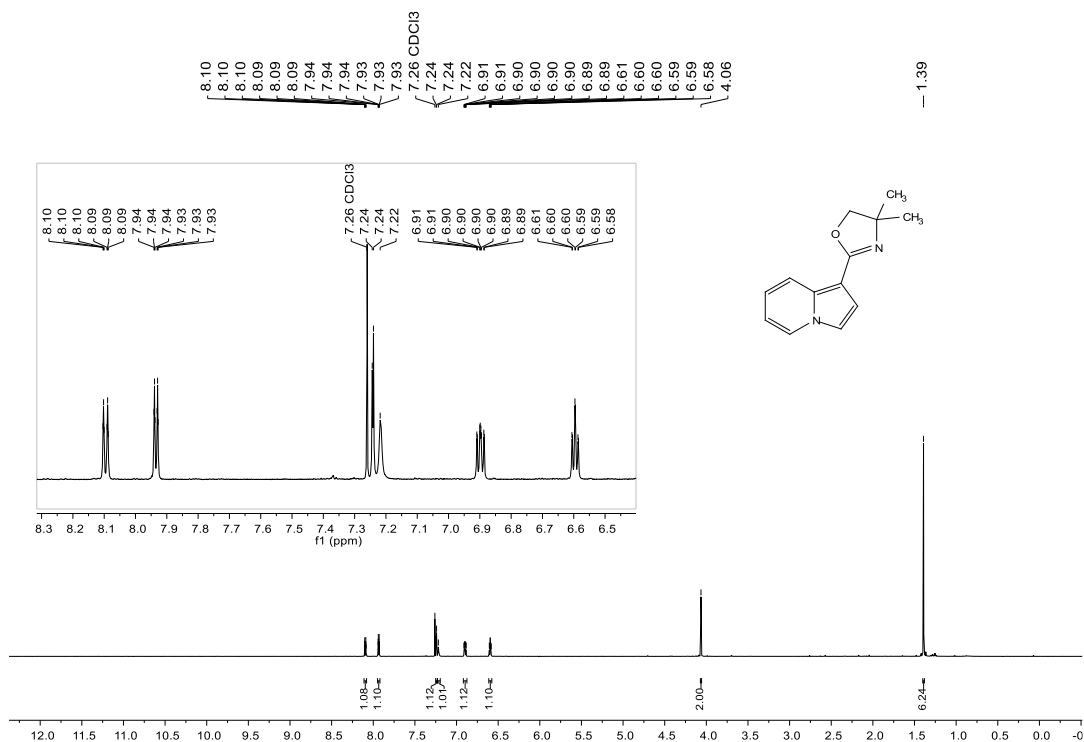
Compound **2b:** ^{1}H NMR (400 MHz, DMSO-d_6)**.**
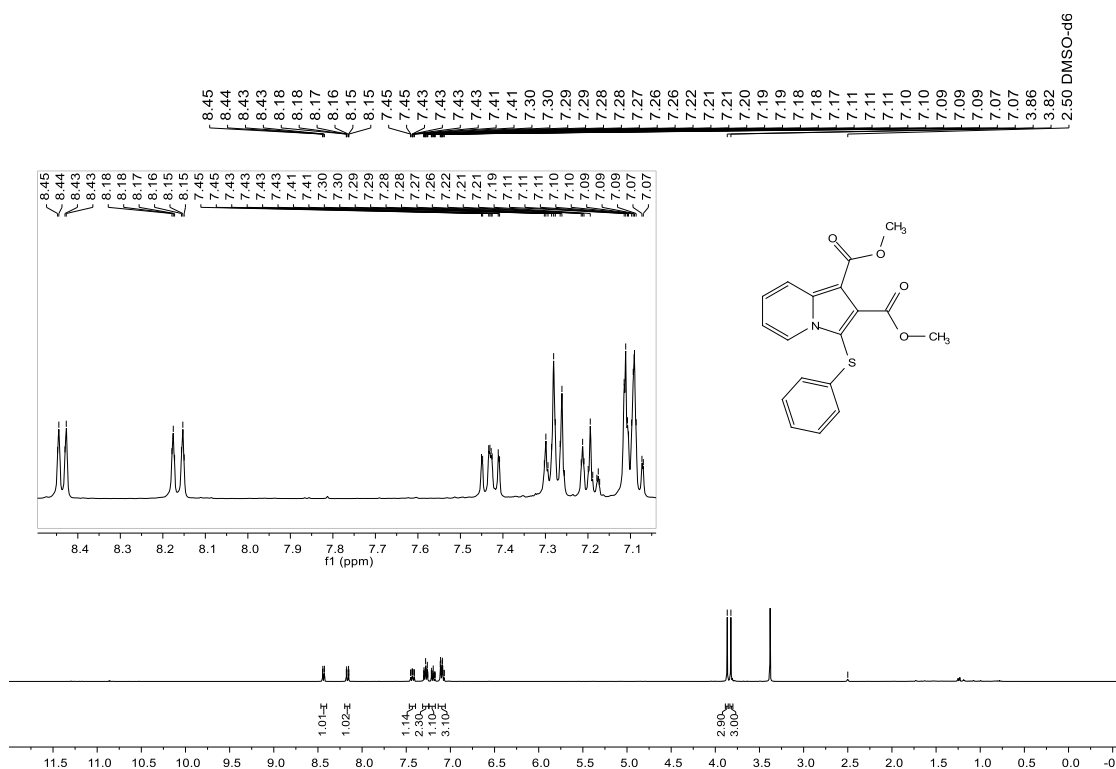
Compound **2b:** ^{13}C NMR (101 MHz, DMSO-d_6)**.**
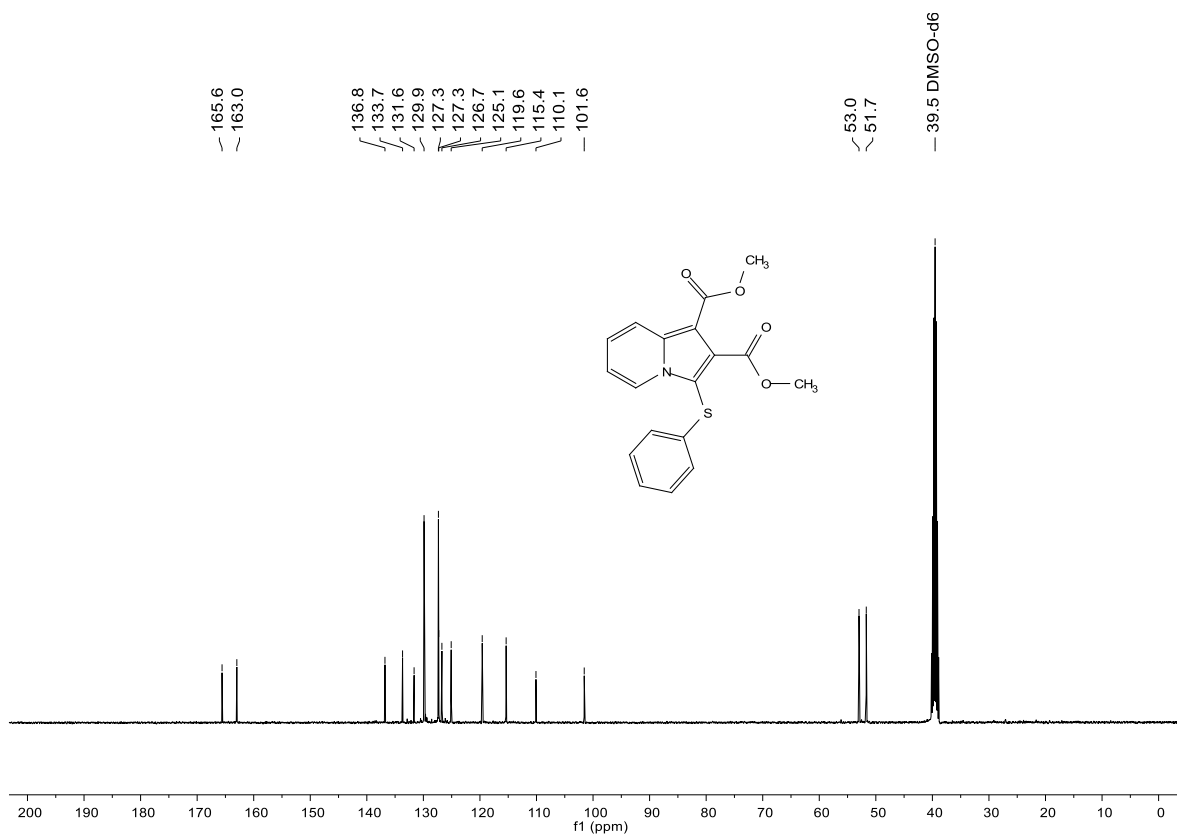
NOESY Compound **2b**
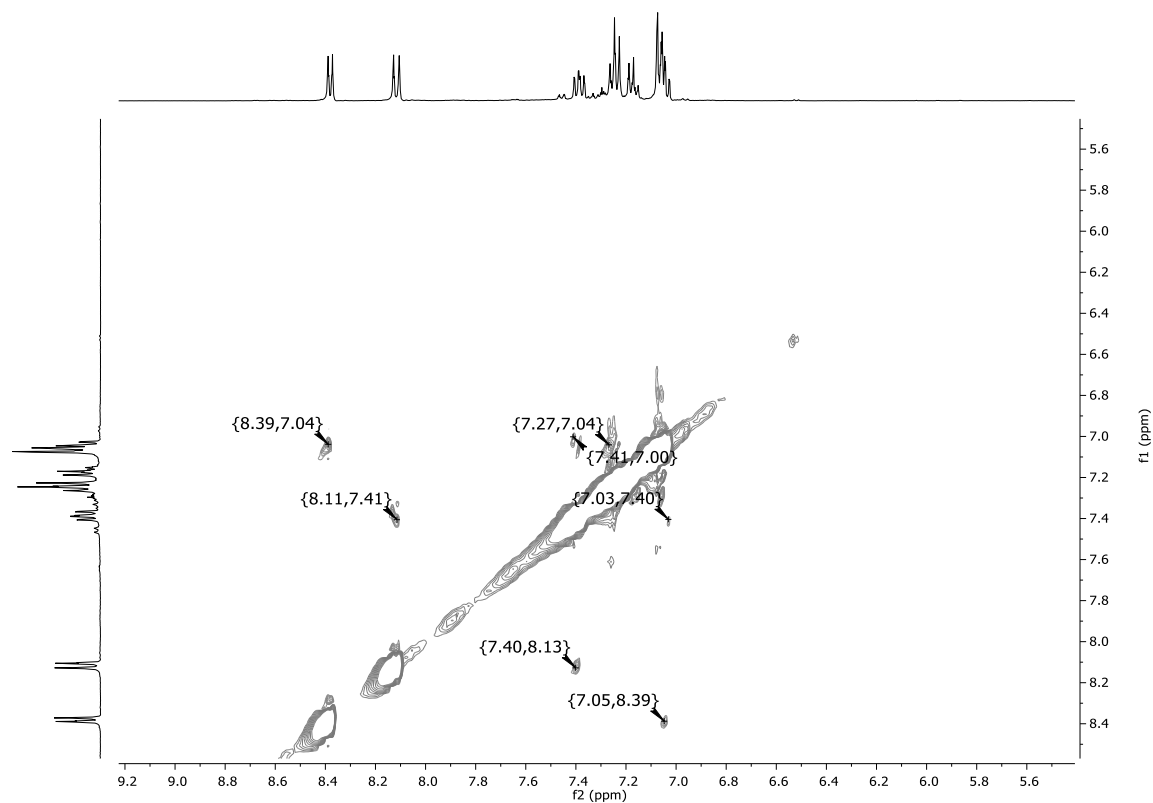
HSQC Compound **2b**
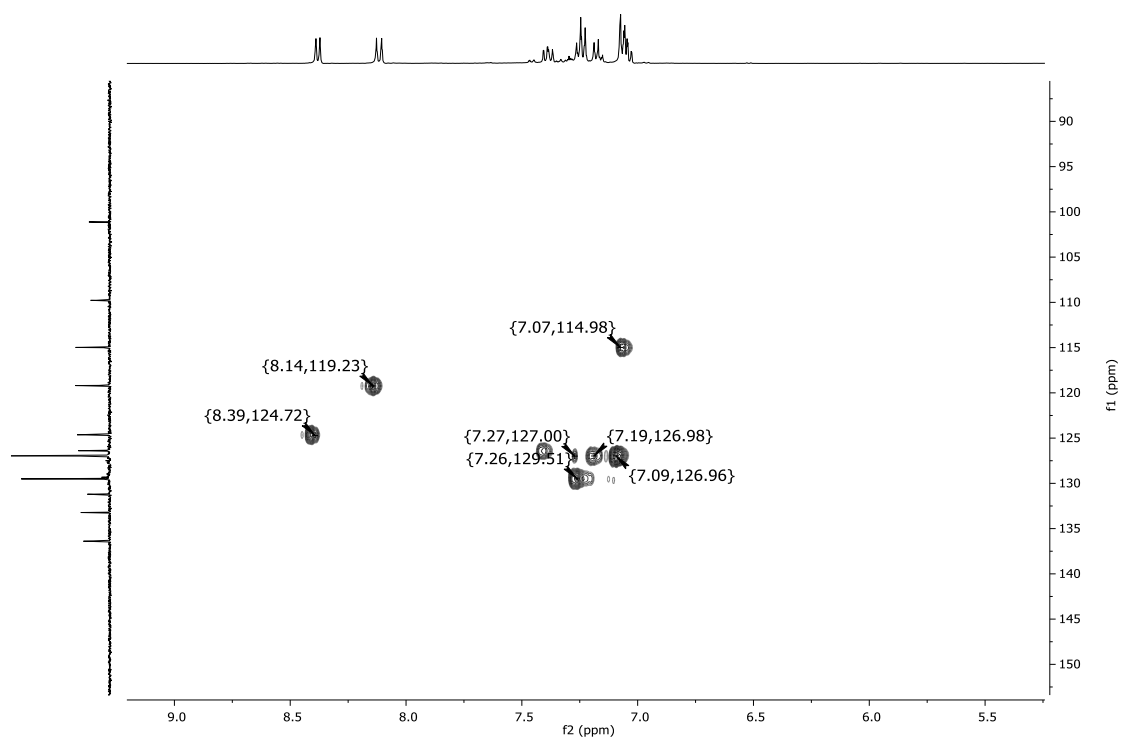
HMBC Compound **2b**
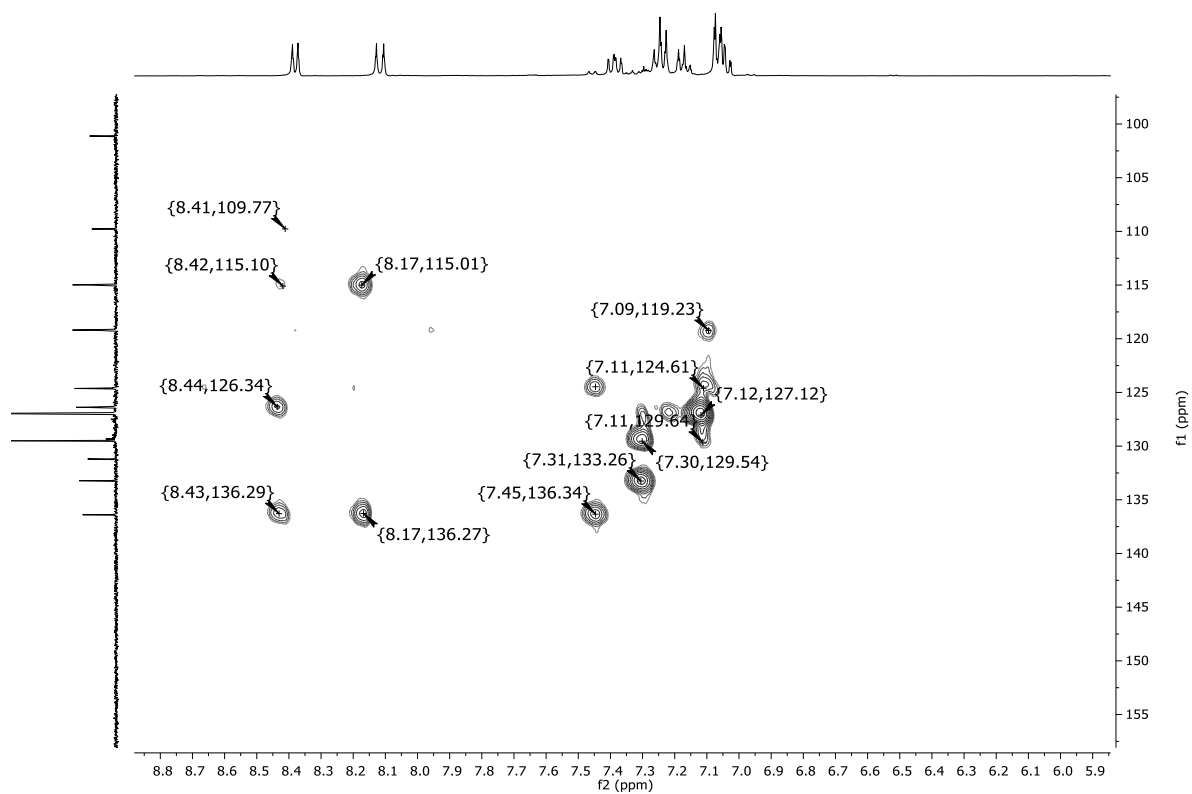
^{1}H NMR (500 MHz, CDCl$_3$) Compound **2c.**
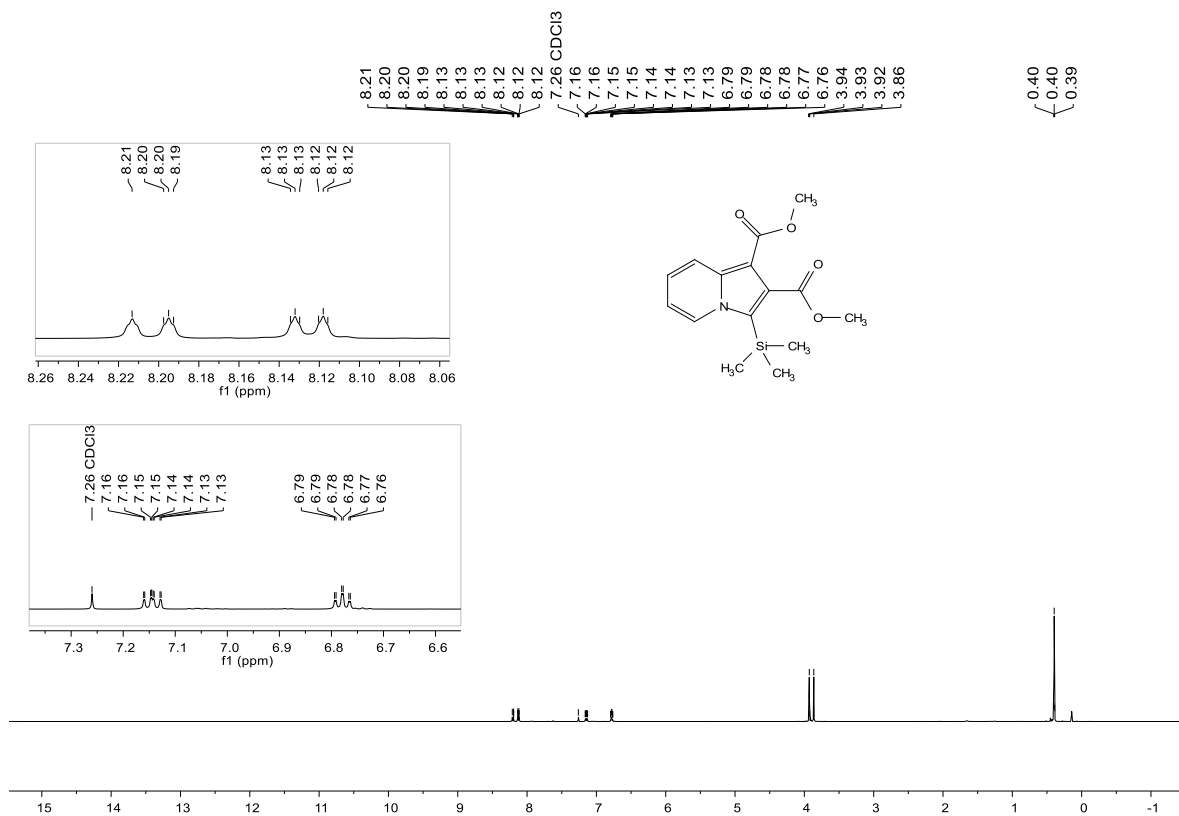
^{13}C NMR (126 MHz, CDCl$_3$) Compound **2c.**

NOESY Compound **2c** (500 mHz, CDCl₃).

{8.11,6.78}
{7.15,6.80}
{8.19,7.15}
{6.77,7.17}
{6.77,8.10}
{7.14,8.20}
{6.77,8.19}

HSQC Compound **2c** (500 mHz, CDCl₃).

{0.40,-2.12}
{3.94,52.13} {3.85,51.42}
{6.77,113.18}
{8.19,120.55}
{8.12,126.85}
{7.13,123.95}
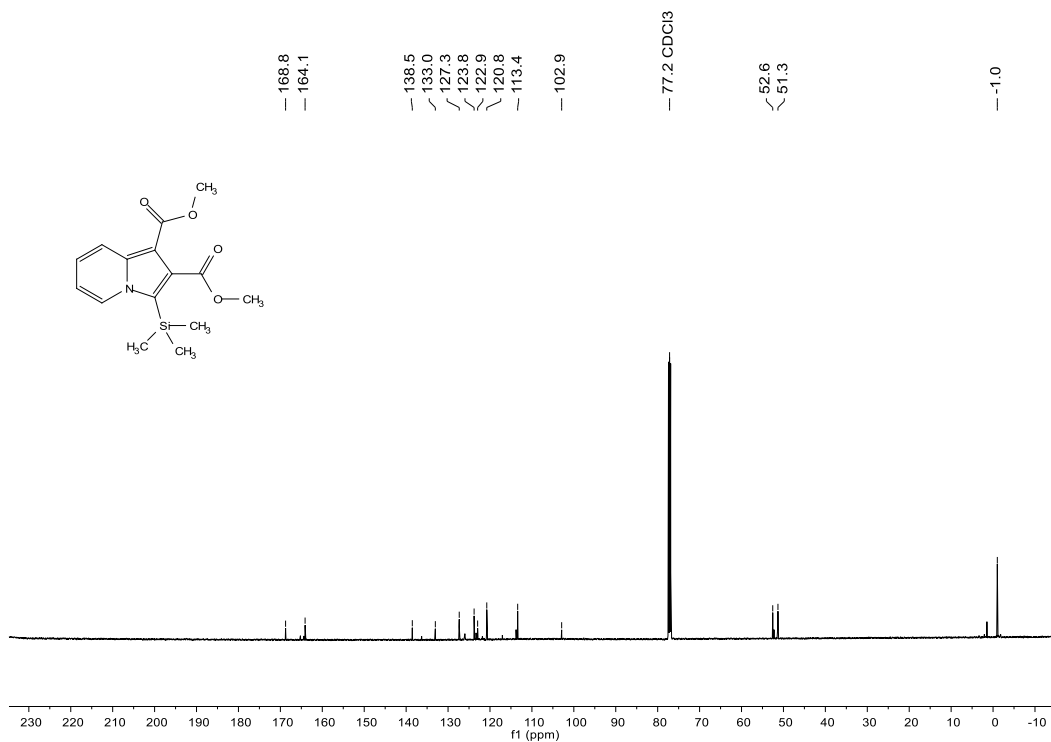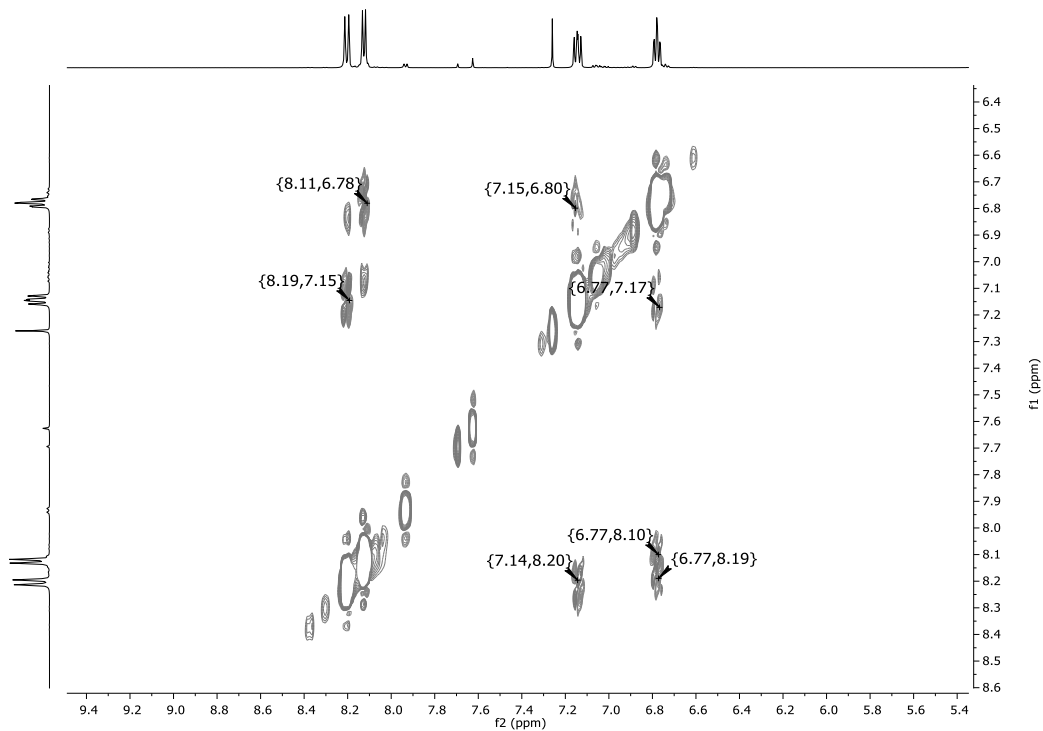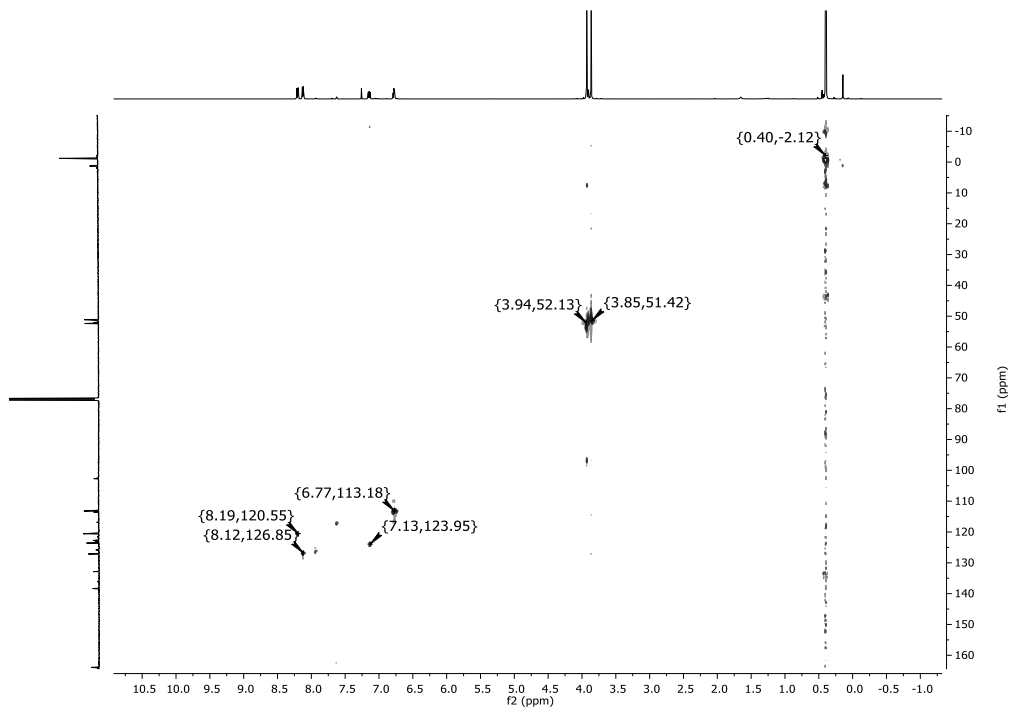
HMBC Compound **2c** (500 mHz, CDCl$_3$).
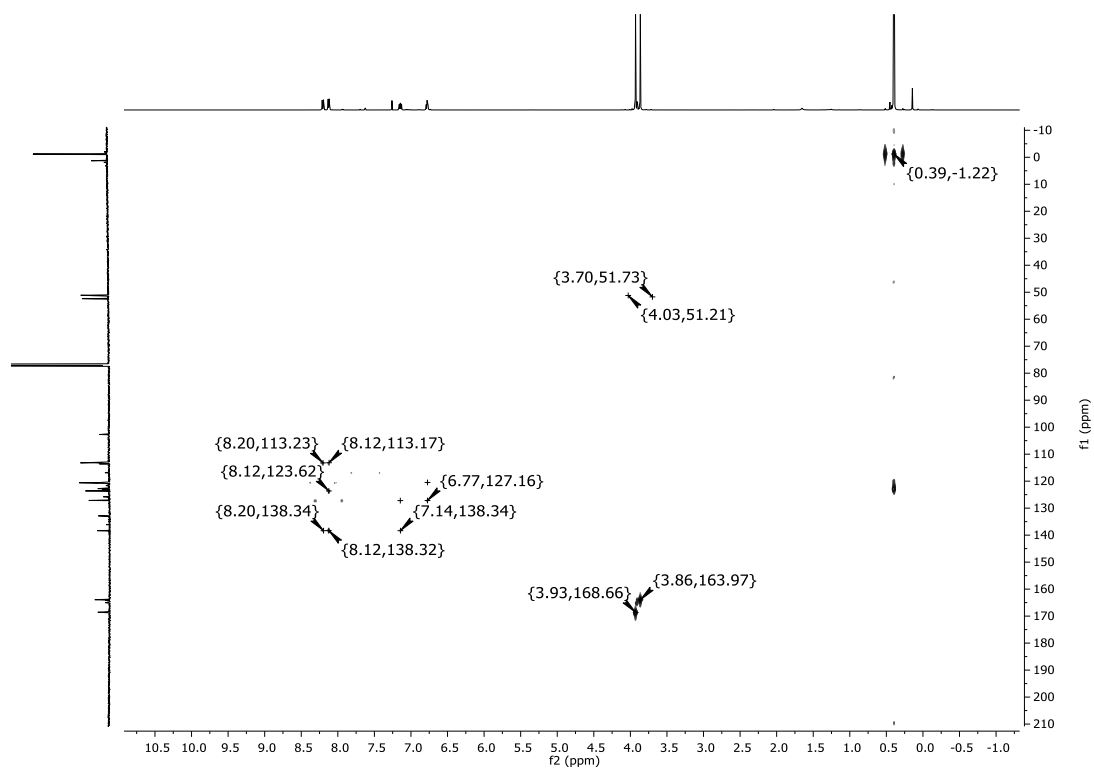
Compound **2d:** ^{1}H NMR (400 MHz, CDCl$_3$).
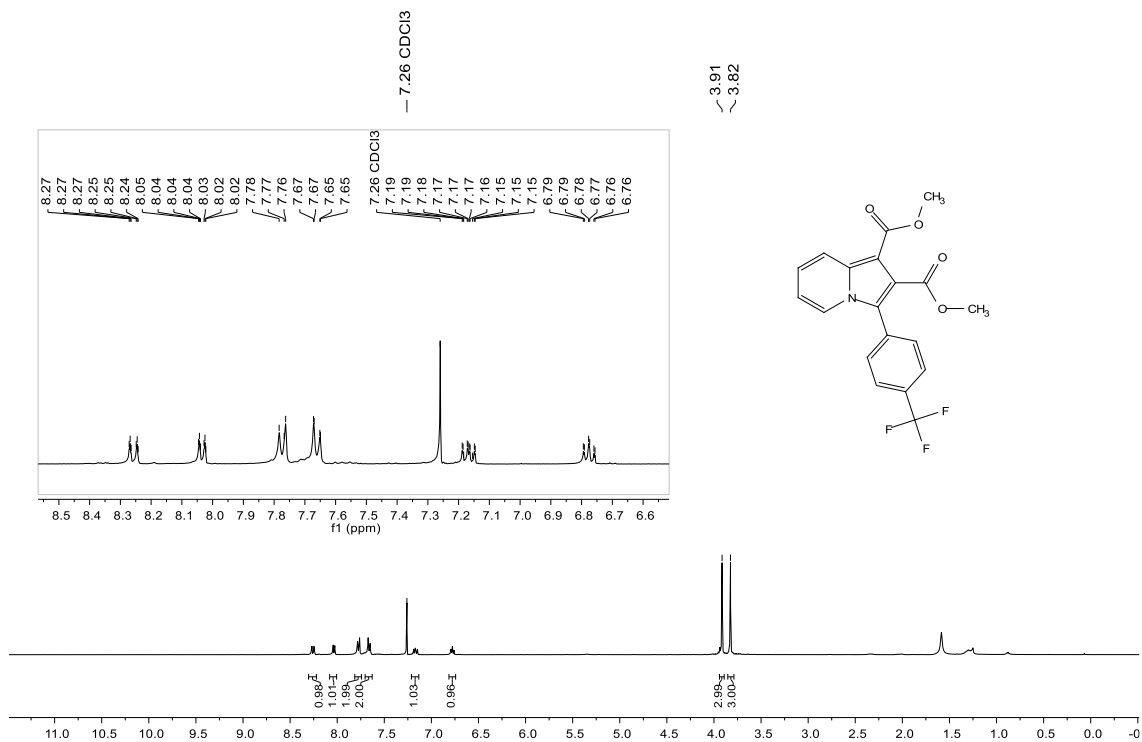
Compound **2d:** ^{13}C NMR (101 MHz, CDCl$_3$).
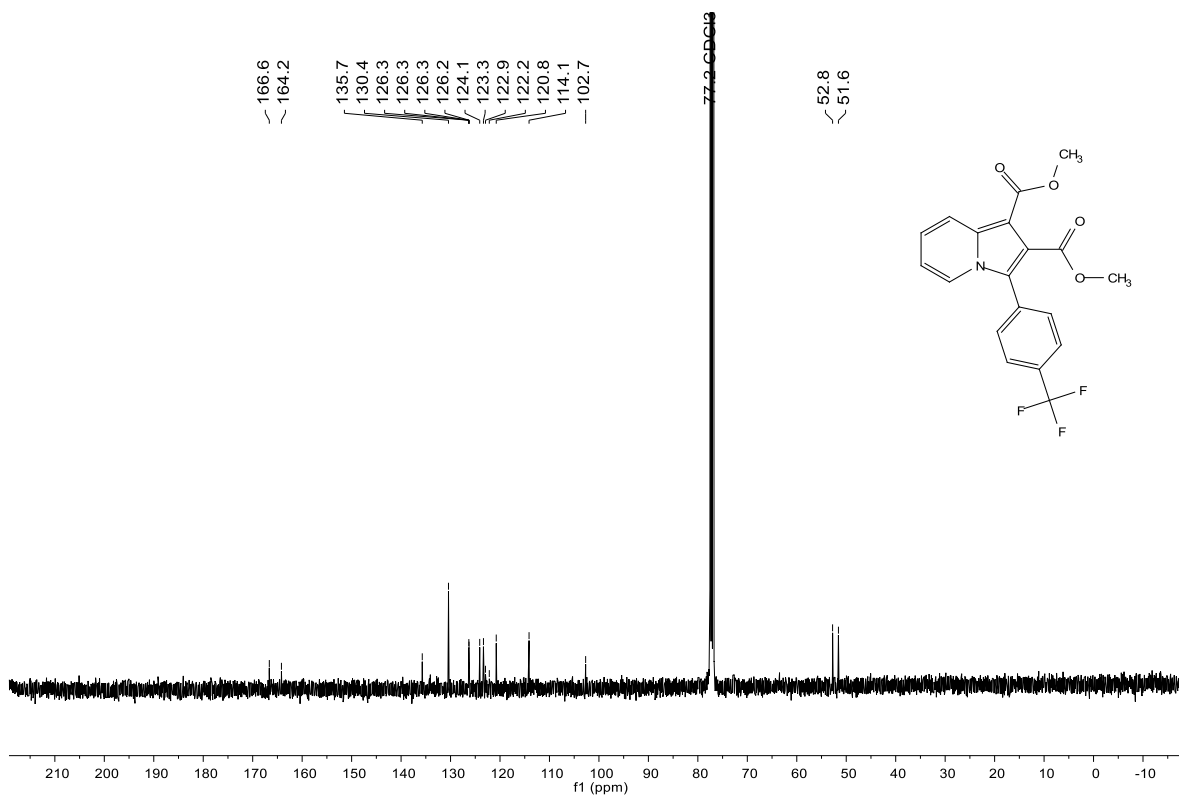
NOESY expansion Compound **2d (**DMSOd$_6$, 400MHz)
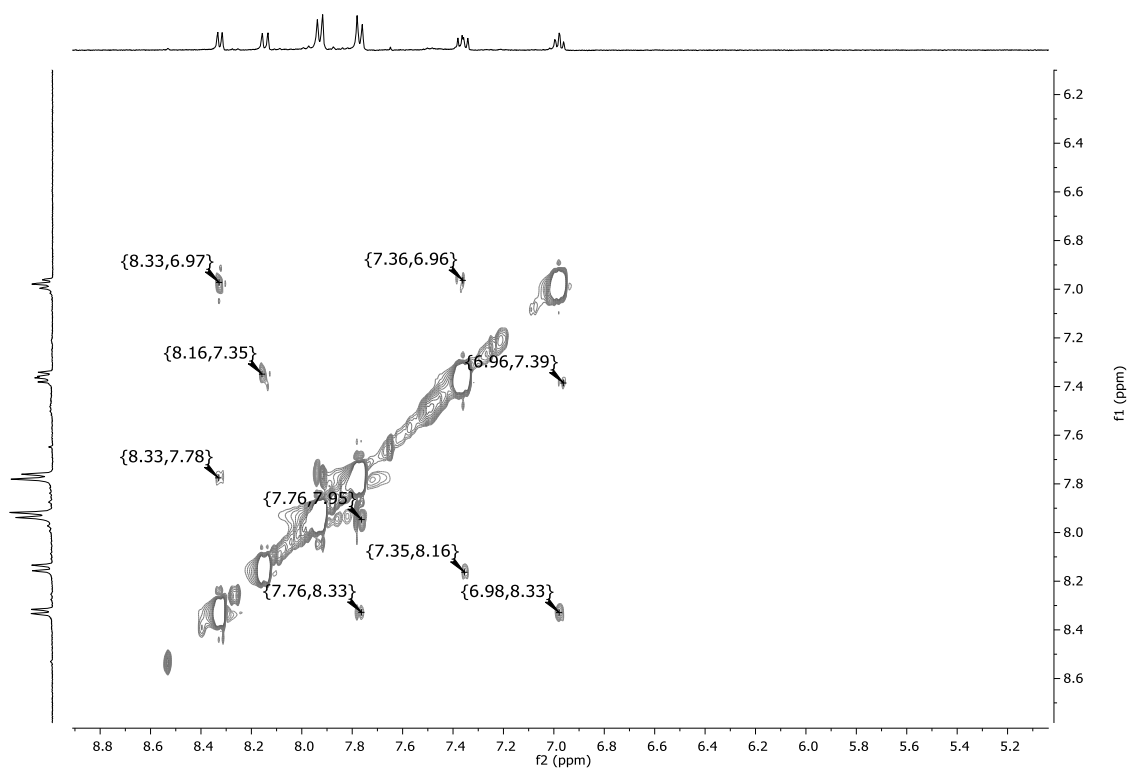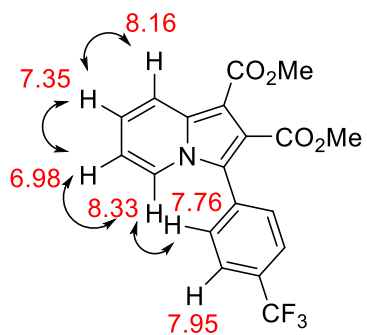
NOESY Compound **2d (**DMSOd$_6$, 400MHz)
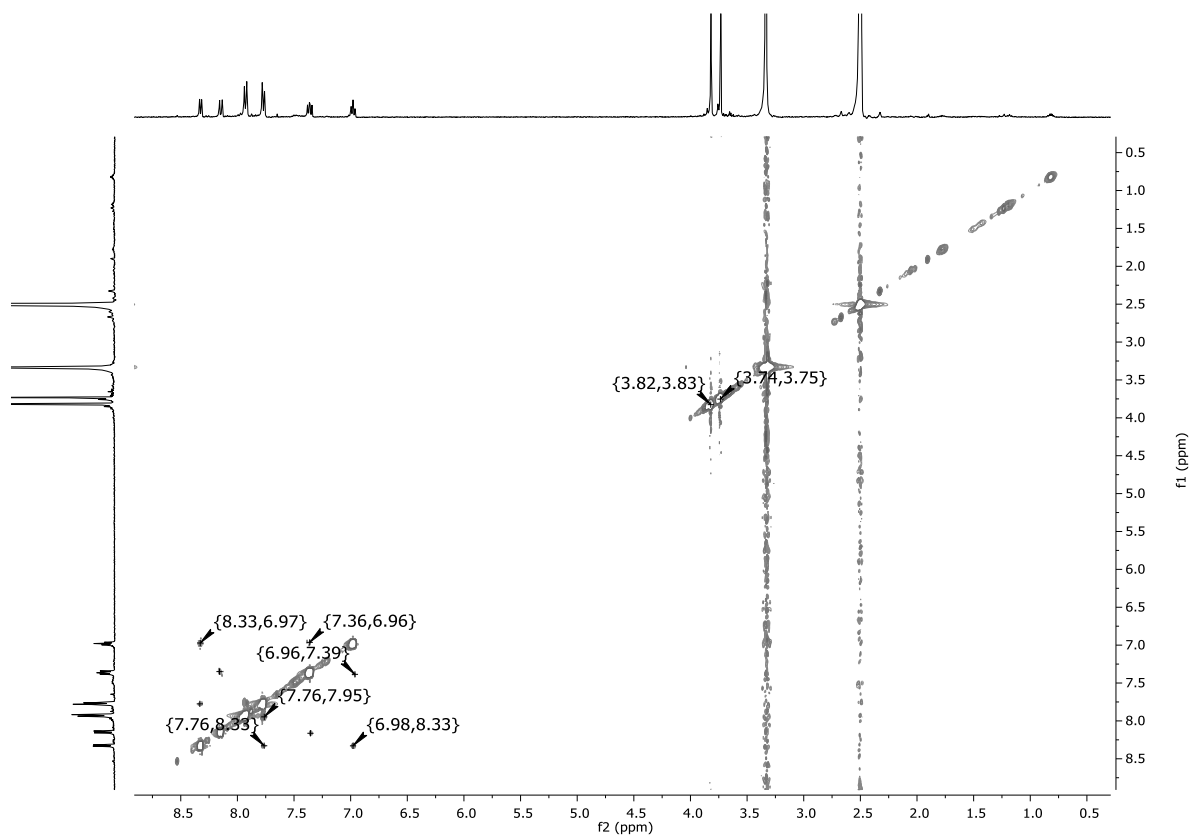
Compound **2e**: ^{1}H NMR (400 MHz, CDCl$_3$).
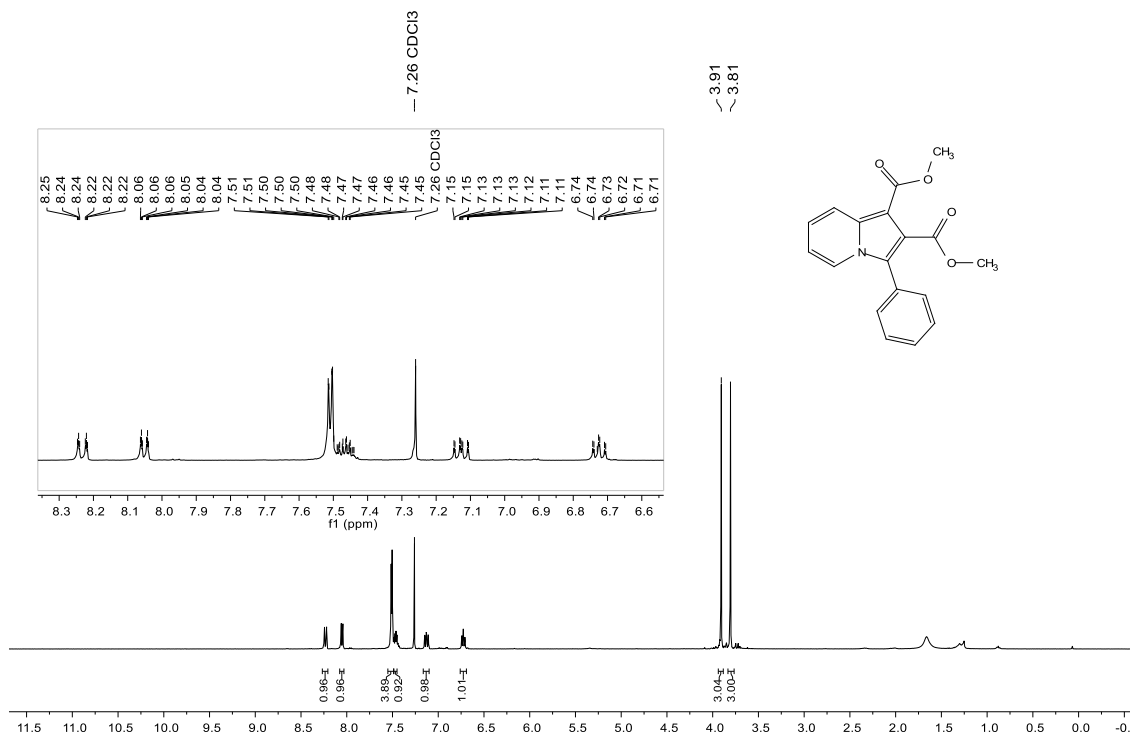
Compound **2e**: ^{13}C NMR (101 MHz, CDCl$_3$).
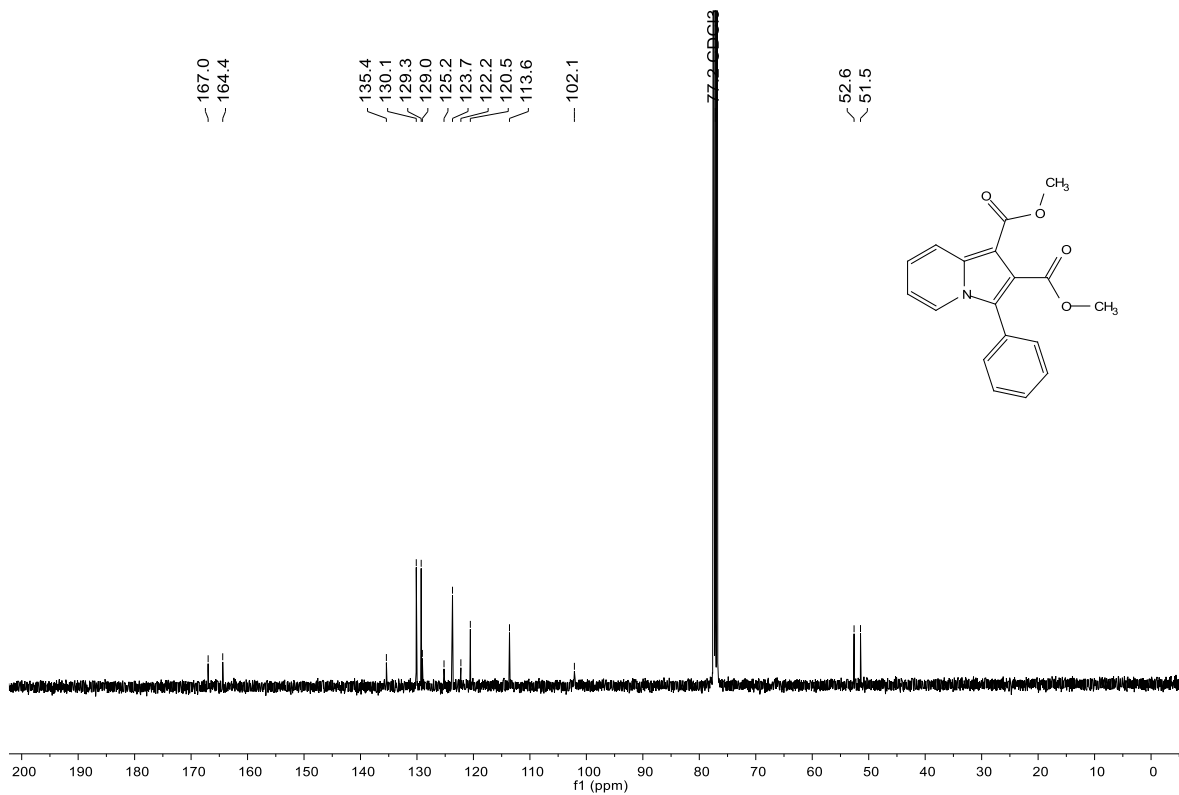
Compound **3a:** ^{1}H NMR (400 MHz, DMSO-*d$_6$*)**.**
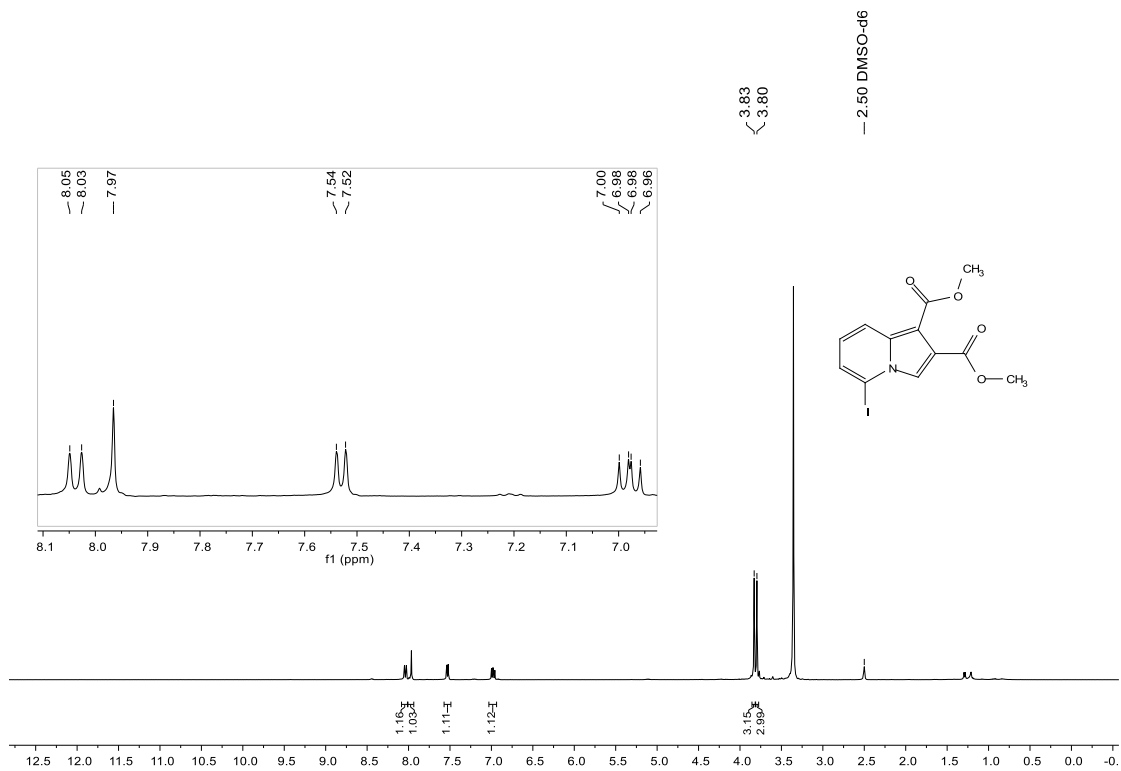
Compound **3a:** ^{13}C NMR (101 MHz, DMSO-*d$_6$*)**.**
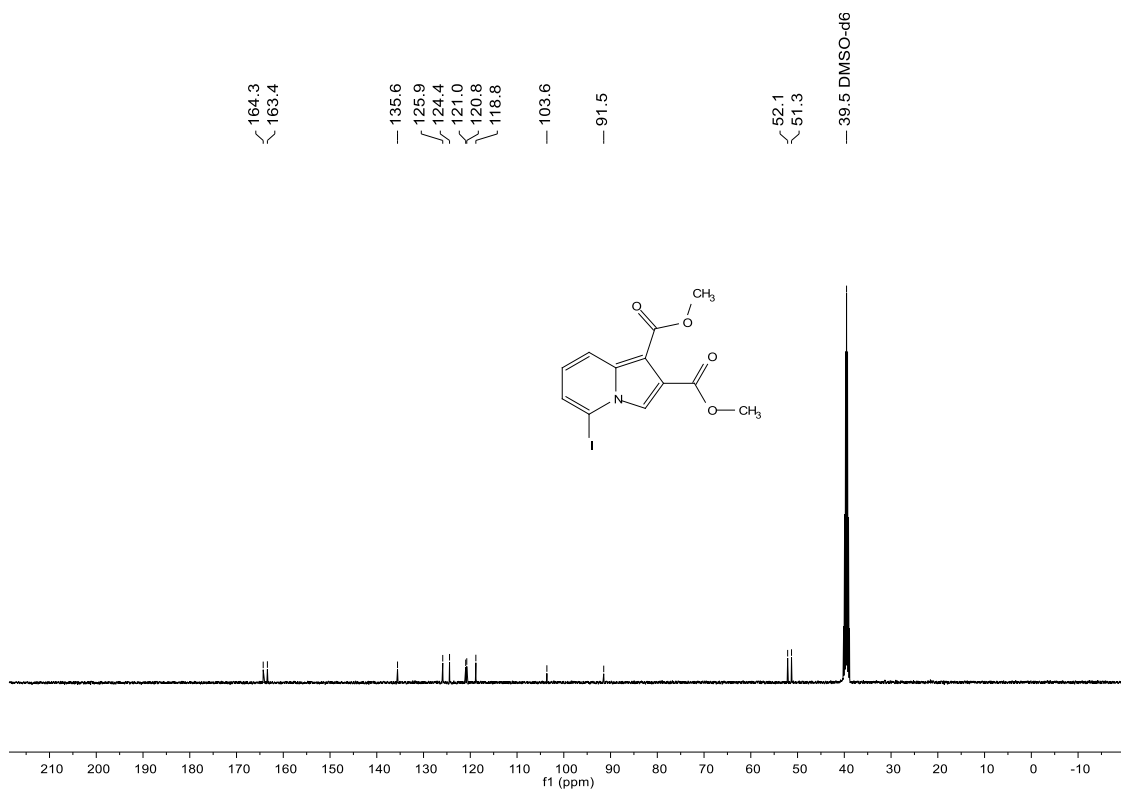
NOESY expansion Compound **3a** (500MHz, CDCl₃).
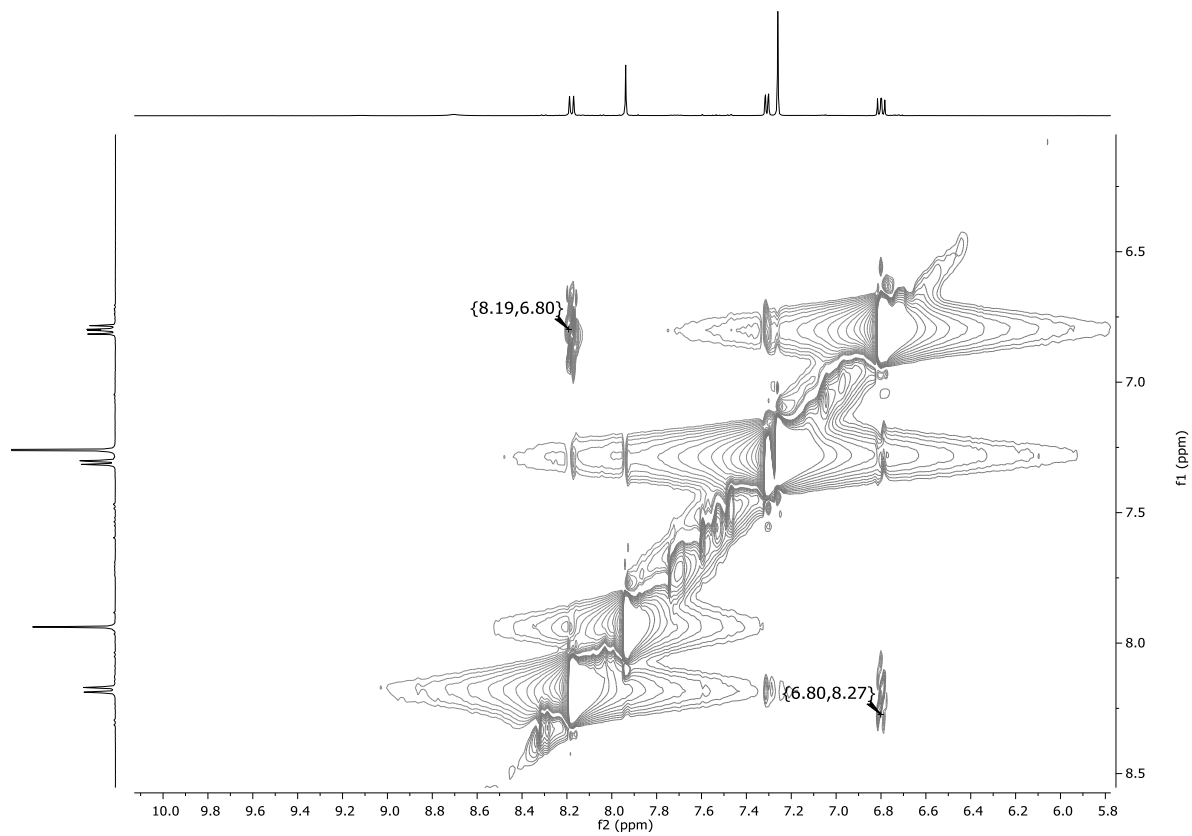
Compound **3b:** ¹H NMR (500 MHz, DMSO-*d₆*)**.**
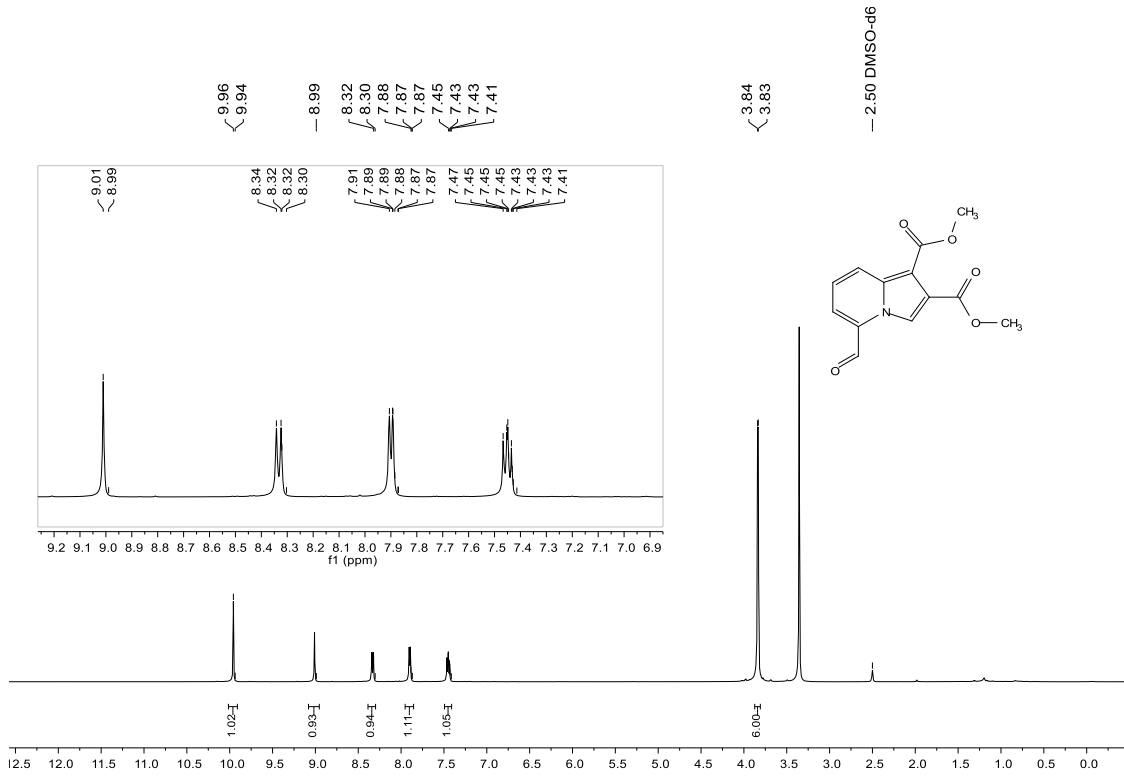
Compound **3b:** ¹³C NMR (126 MHz, DMSO-*d₆*)**.**
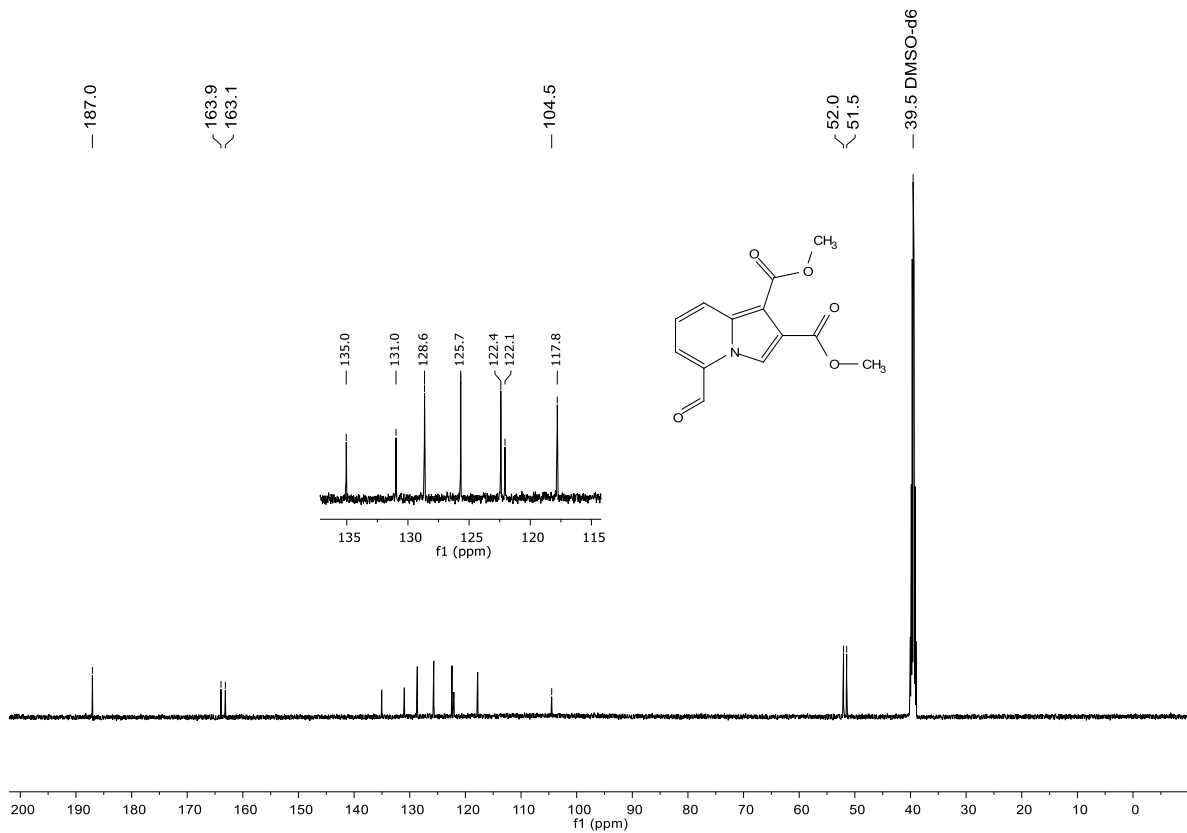
Compound **5a**: ¹H NMR (300 MHz, CDCl₃)**.**
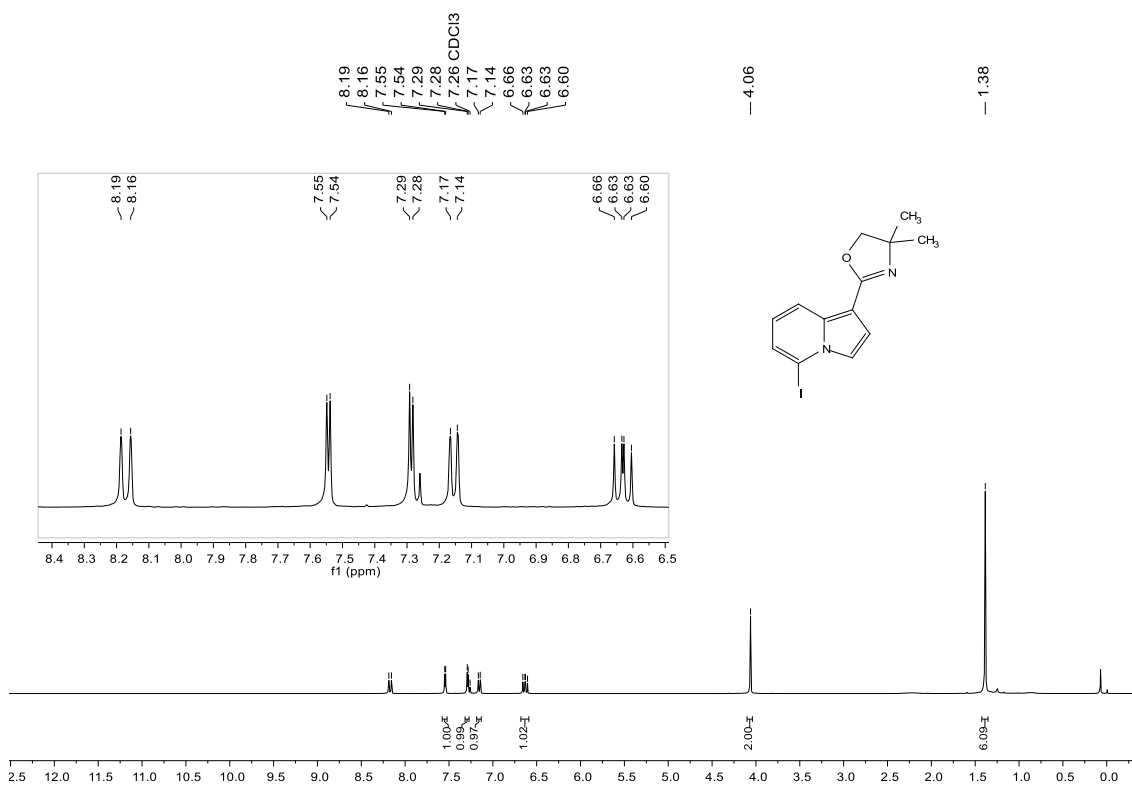
Compound **5a**: ¹³C NMR (75 MHz, DMSO-*d₆*)**.**
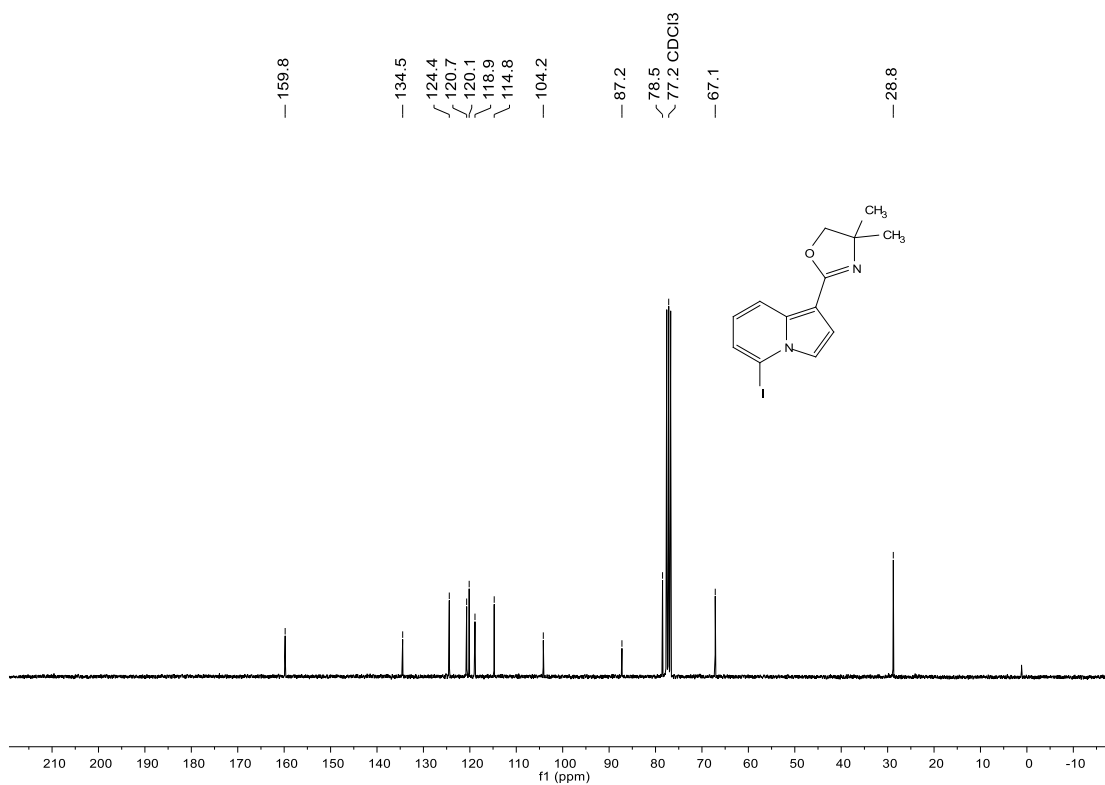
Compound **5b:** ^{1}H NMR (500 MHz, DMSO-d_6)**.**
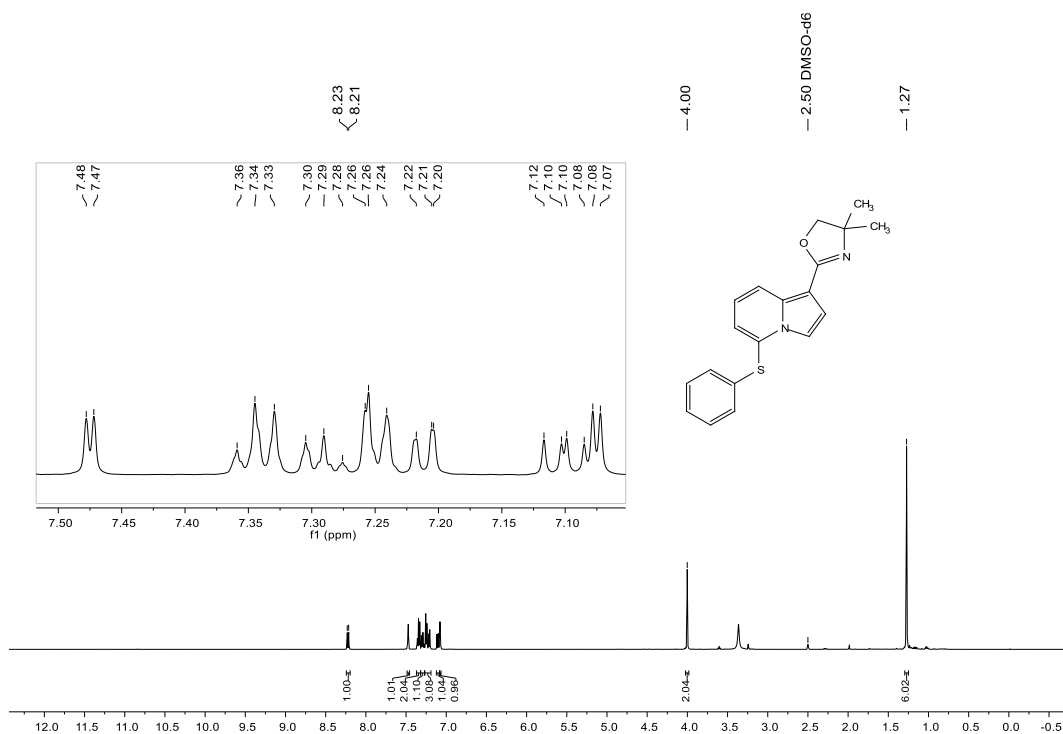
Compound **5b:** ^{13}C NMR (126 MHz, DMSO-d_6)**.**
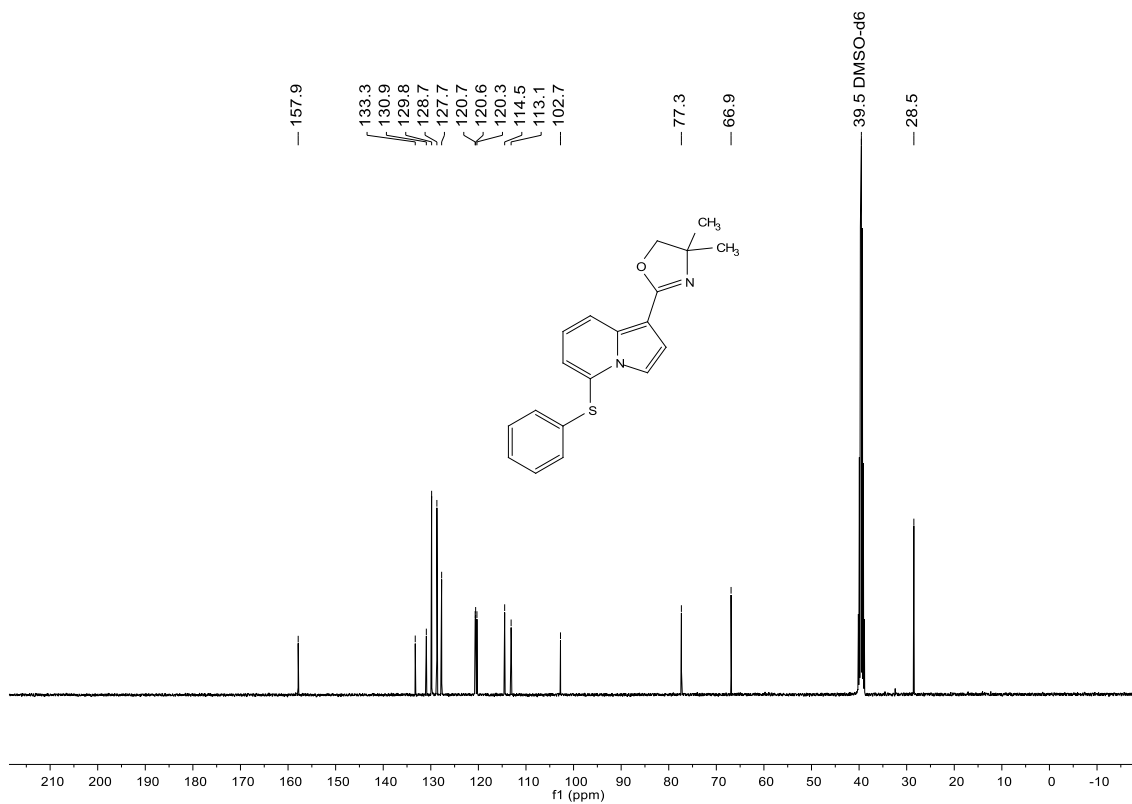
Compound **5c**: ^{1}H NMR (500 MHz, DMSO-d_6)
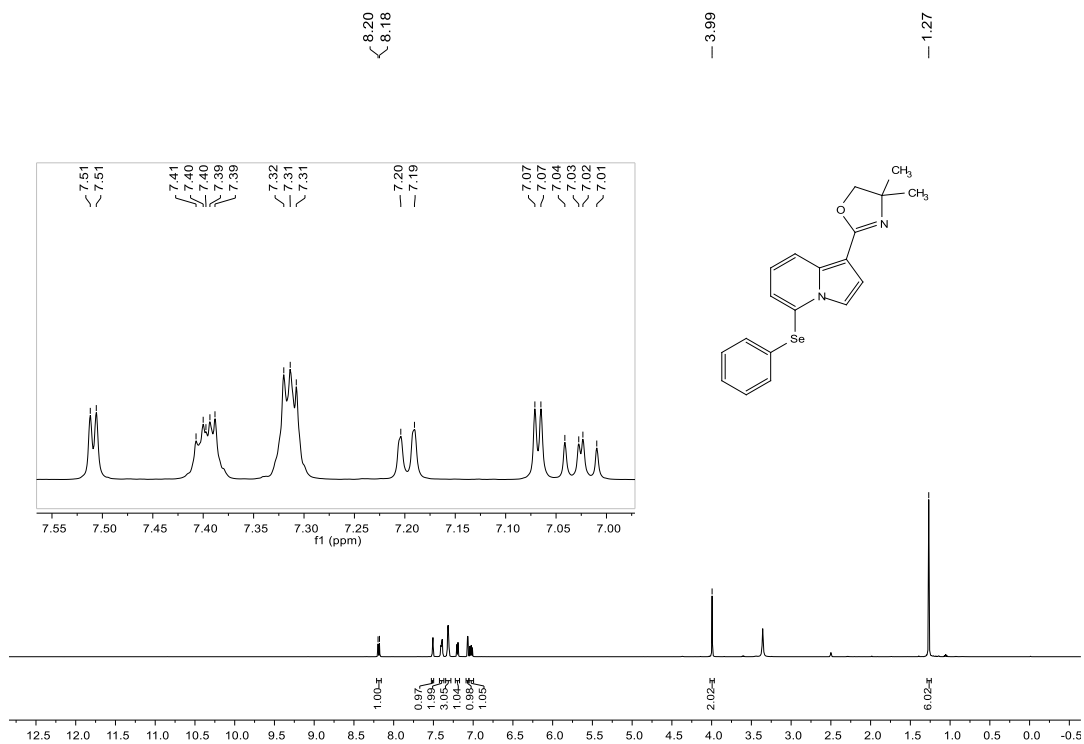
Compound **5c**: ^{13}C NMR (126 MHz, DMSO-d_6).
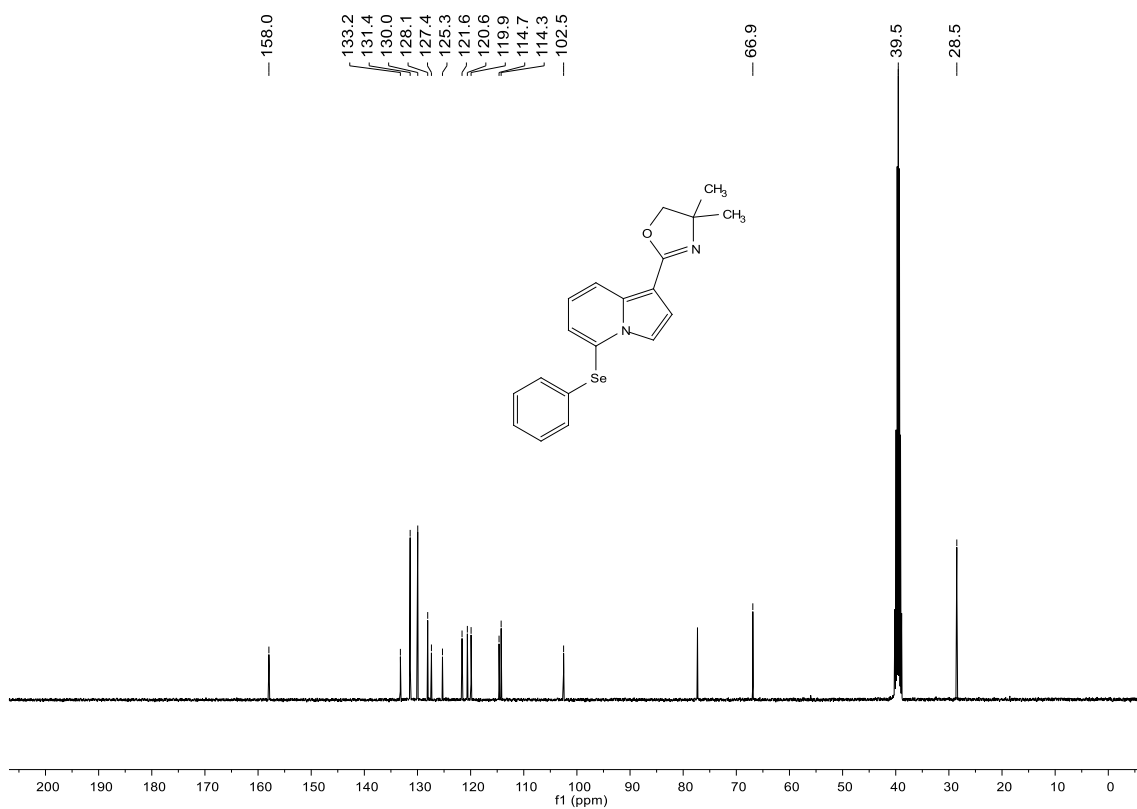
Compound **5d:** ^{1}H NMR (400 MHz, DMSO-d$_6$)**.**
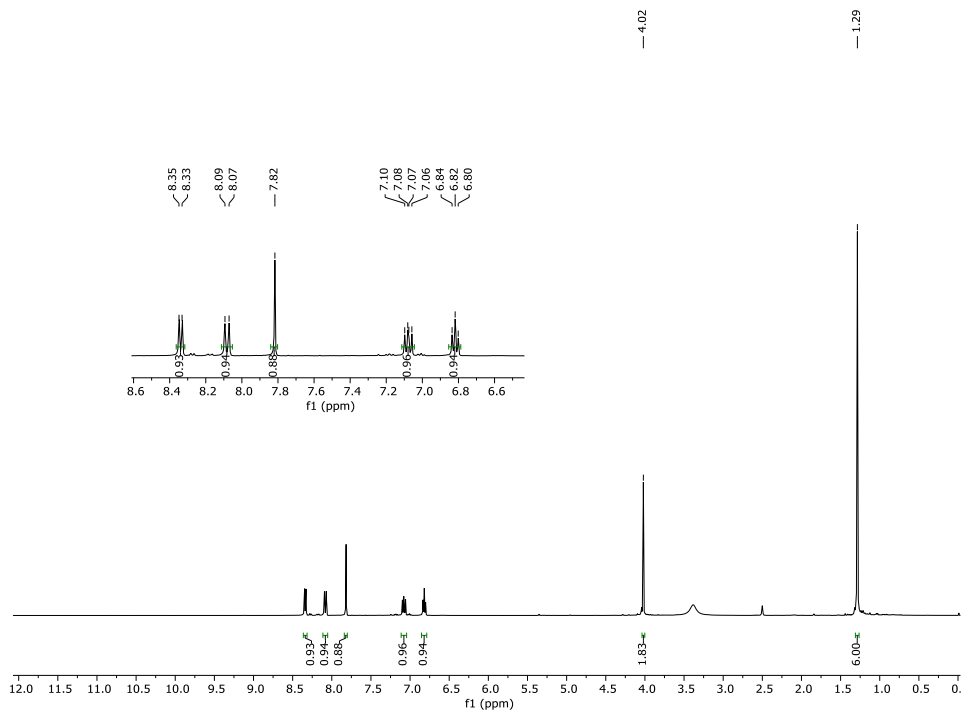
Compound **5d:** ^{1}H NMR (101 MHz, DMSO-d$_6$)**.**
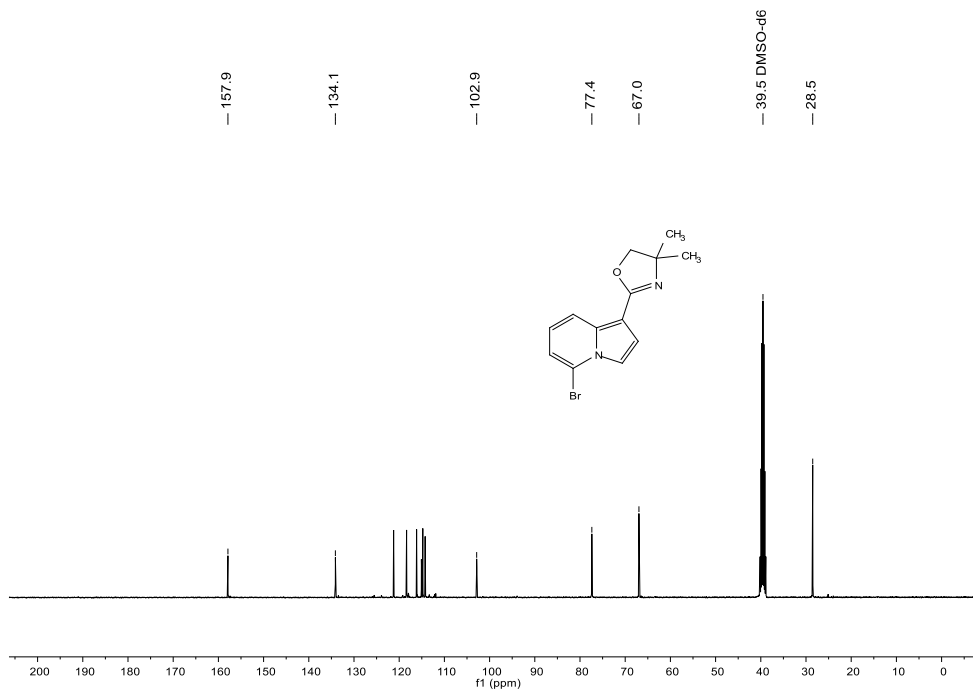
Compound **6a:** ¹H NMR (300 MHz, MeOD)**.**
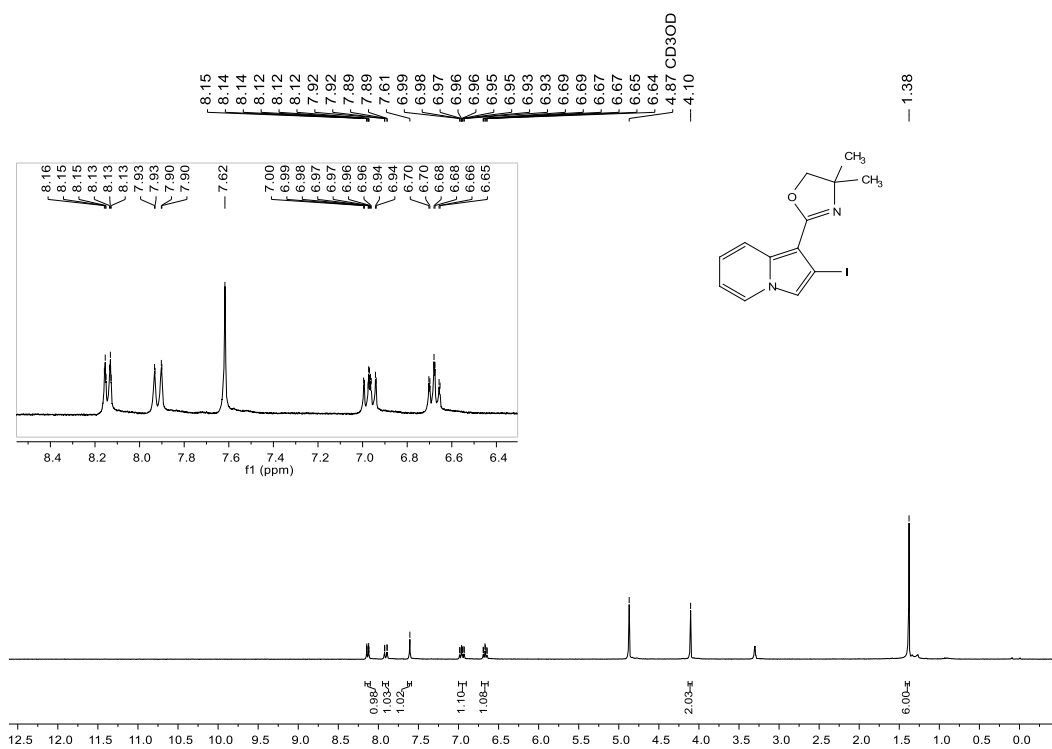
Compound **6a:** ¹³C NMR (75 MHz, MeOD)**.**
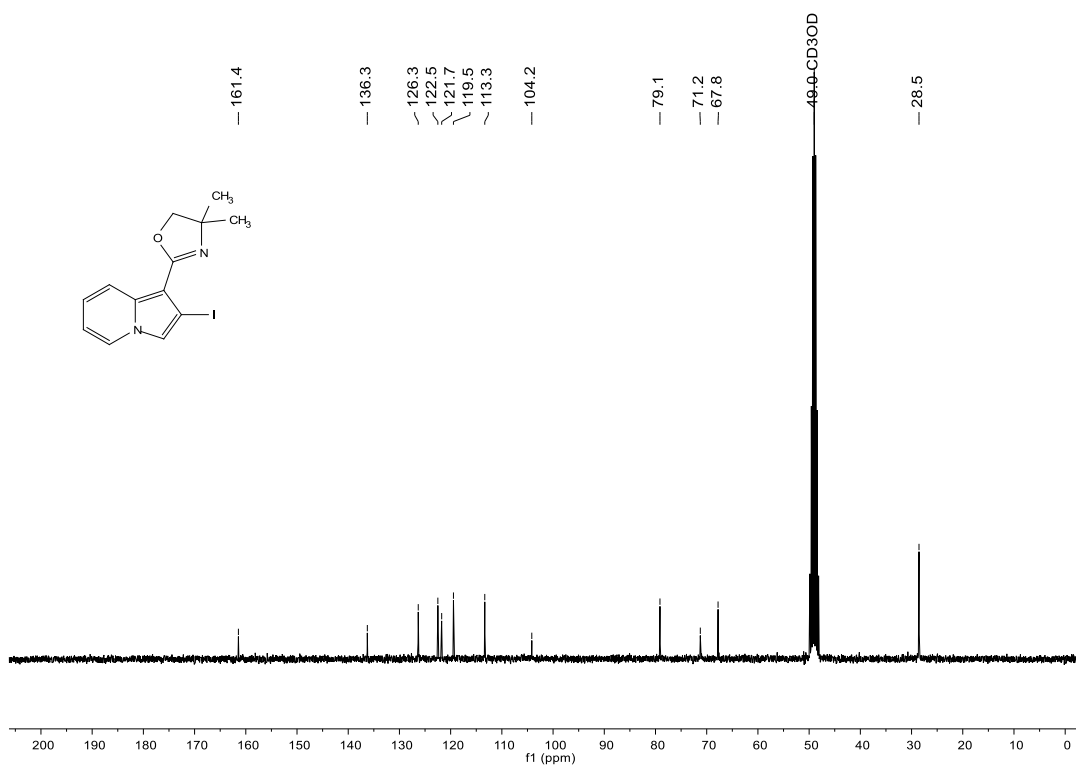
Compound **6b:** ^{1}H NMR (400 MHz, CDCl$_3$)**.**
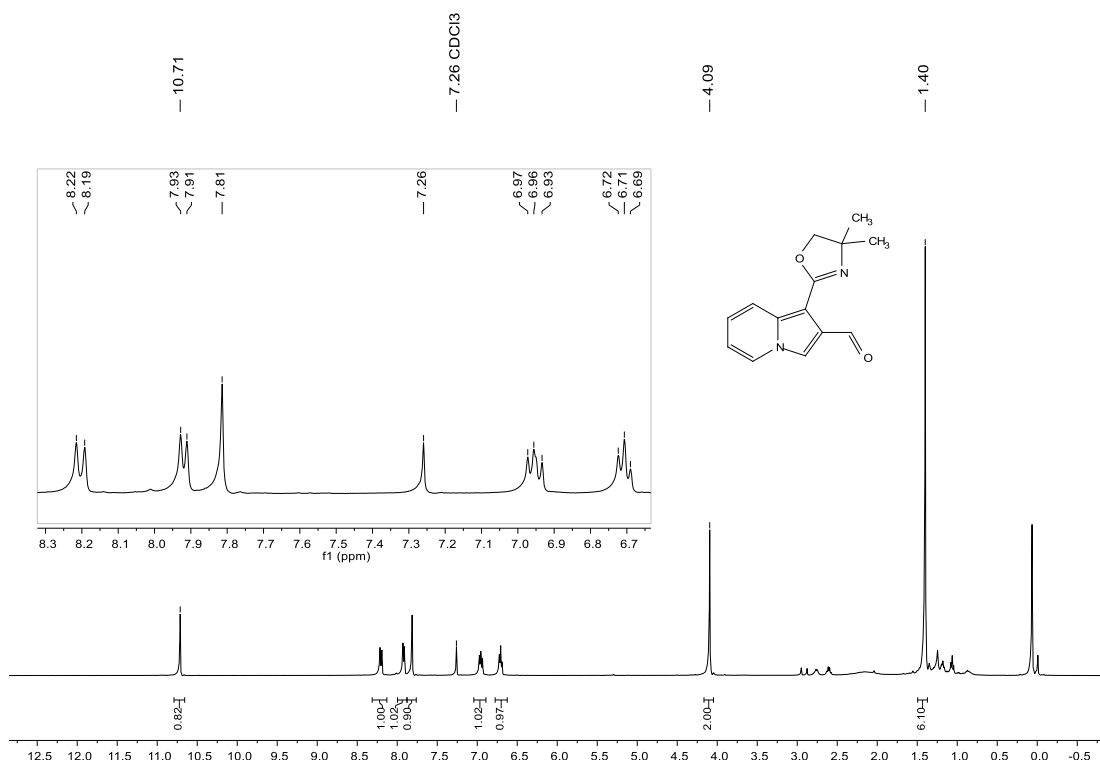
Compound **6b:** ^{13}C NMR (101 MHz, CDCl$_3$)**.**
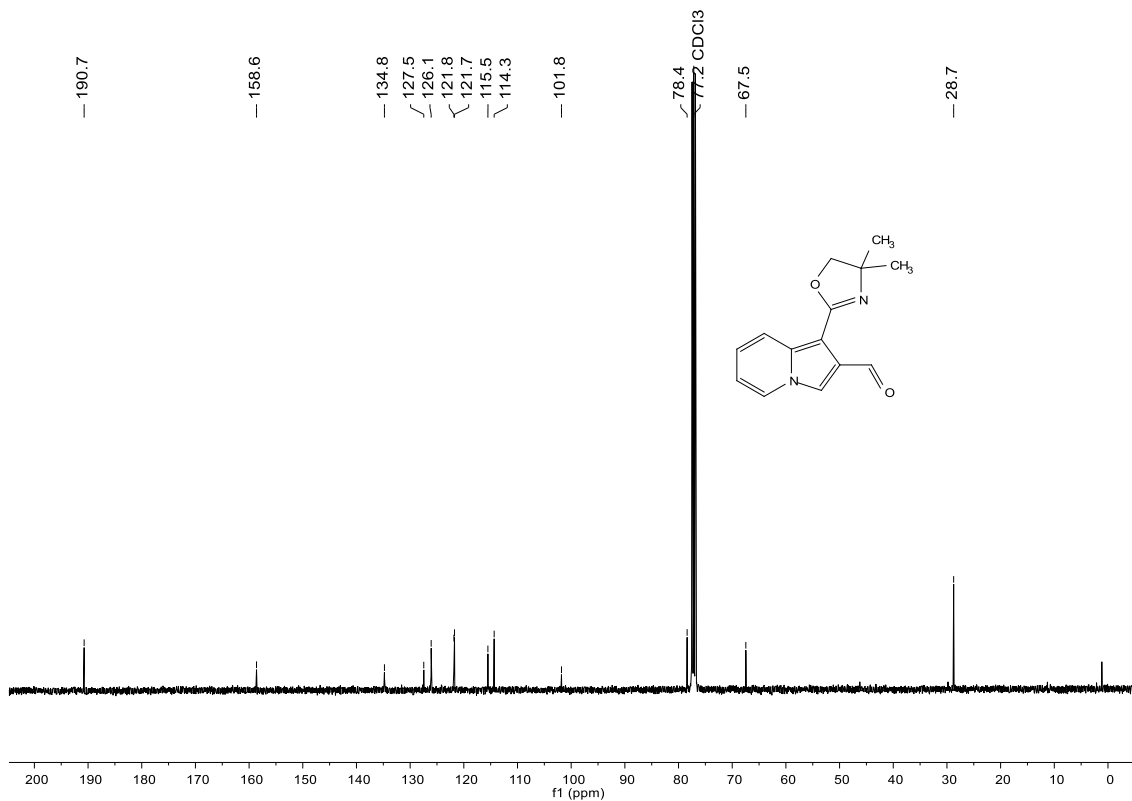
Compound **6c:** ^{1}H NMR (400 MHz, CDCl$_3$)**.**
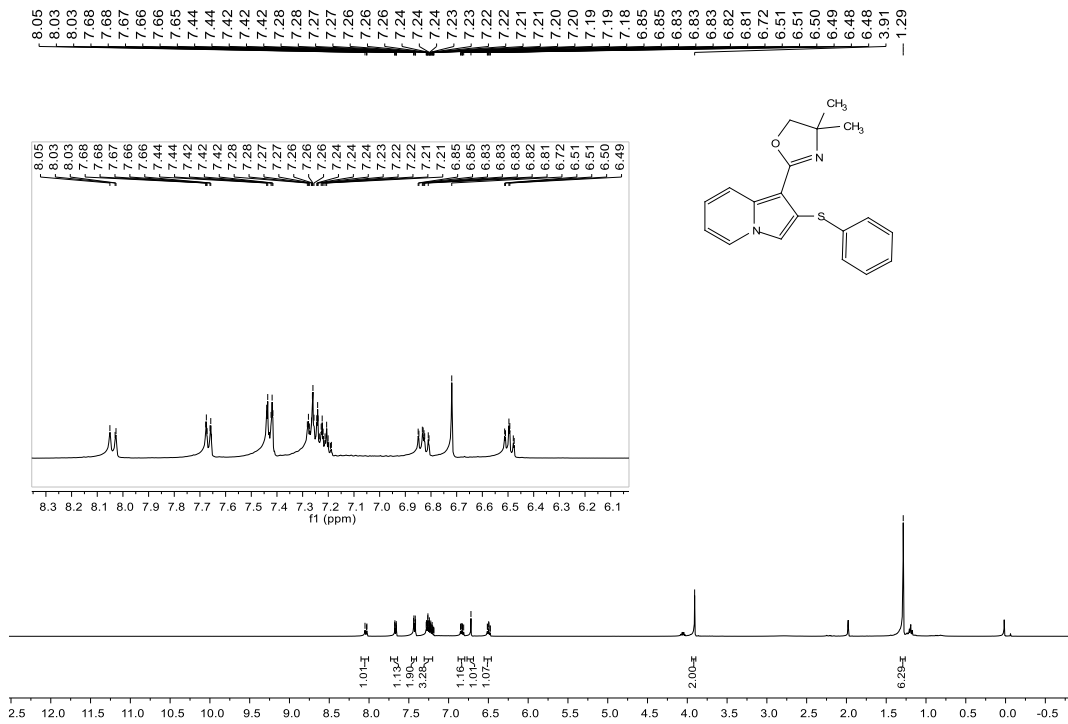
Compound **6c:** ^{13}C NMR (101 MHz, CDCl$_3$)**.**
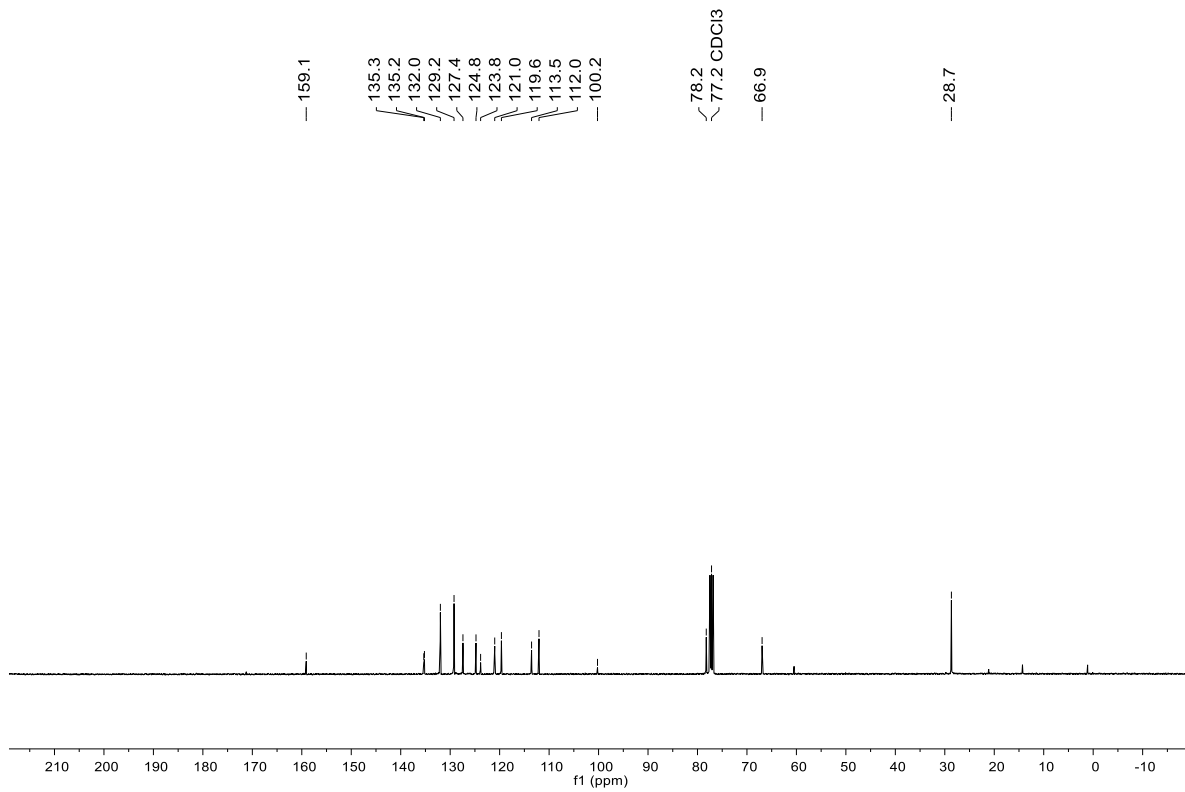
Compound **6d:** ^{1}H NMR (300 MHz, CDCl$_3$)**.**
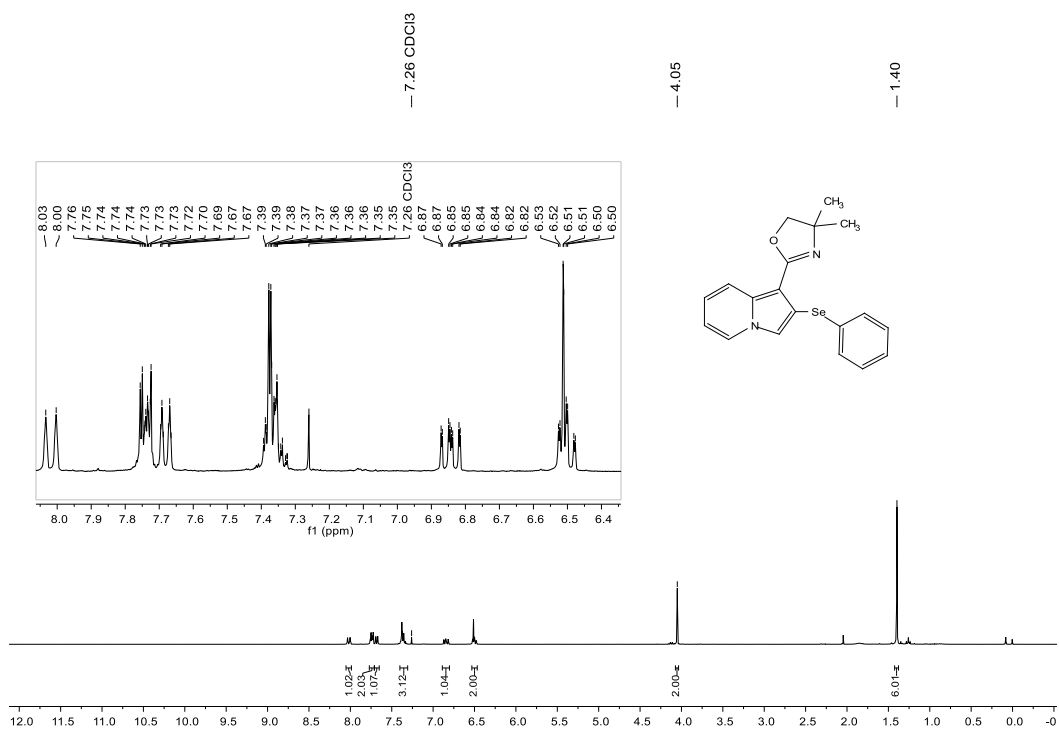
Compound **6d:** ^{13}C NMR (75 MHz, CDCl$_3$)**.**
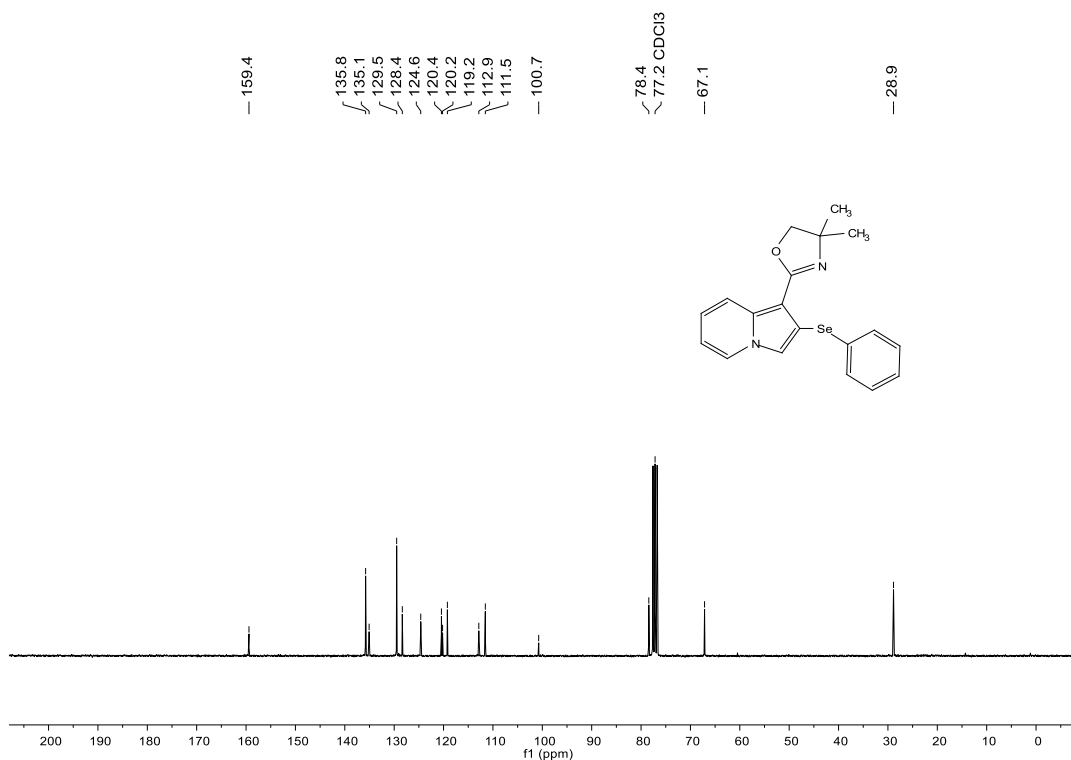
Compound **6e** ^{1}H NMR (400 MHz, DMSO-d_6)
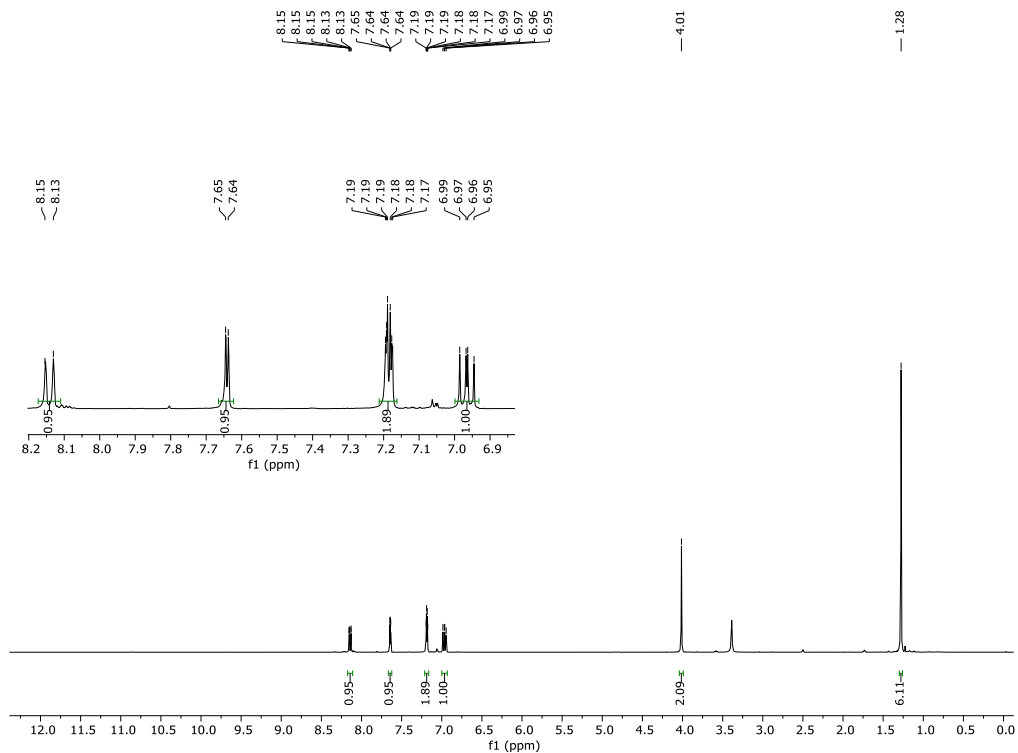
Compound **6e**: ^{13}C NMR (101 MHz, DMSO-d_6).
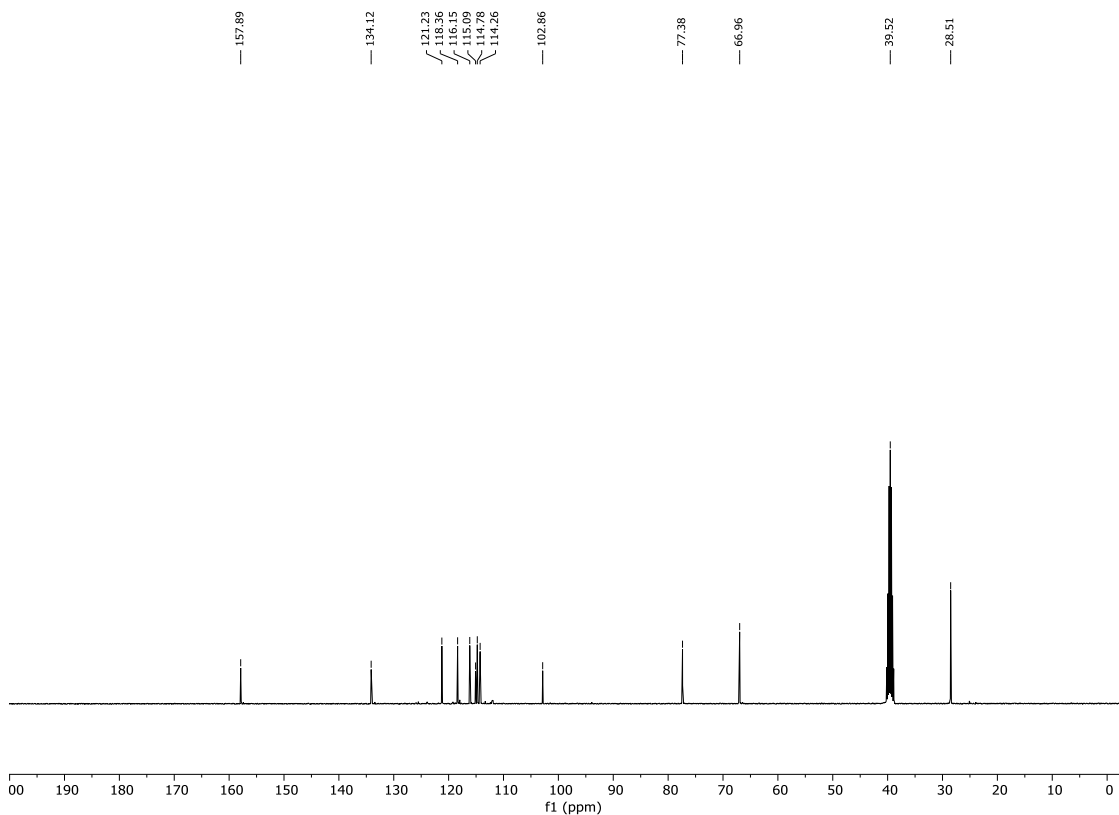
Compound **6f:** ^{1}H NMR (500 MHz, DMSO-d_6)**.**
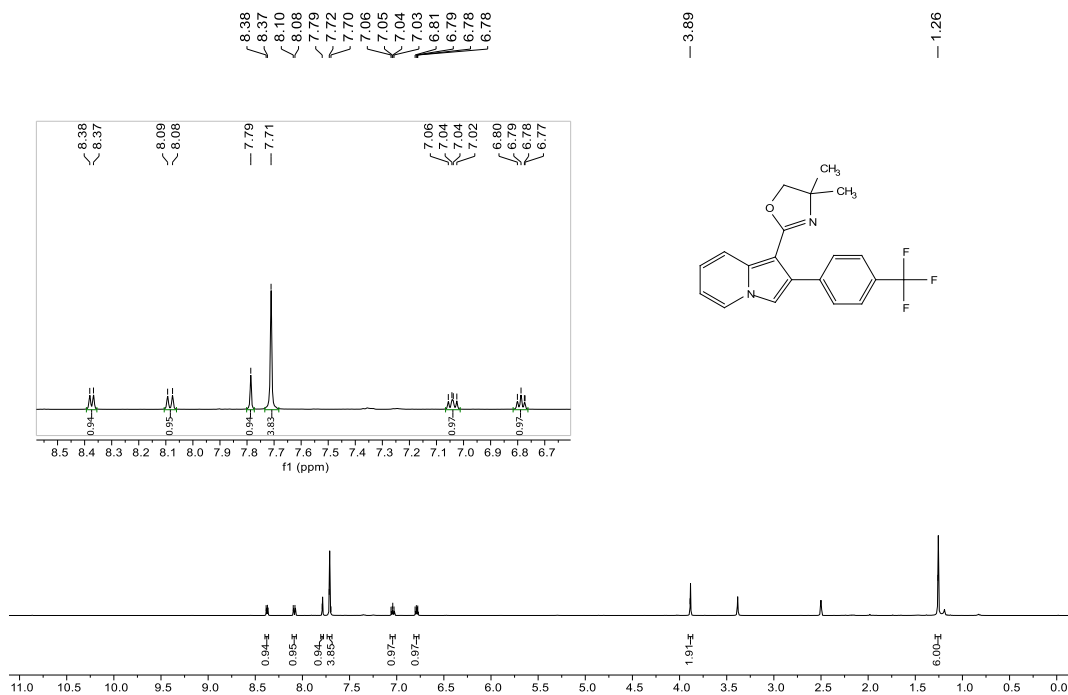
Compound **6f:** ^{13}C NMR (126 MHz, DMSO-d_6)**.**
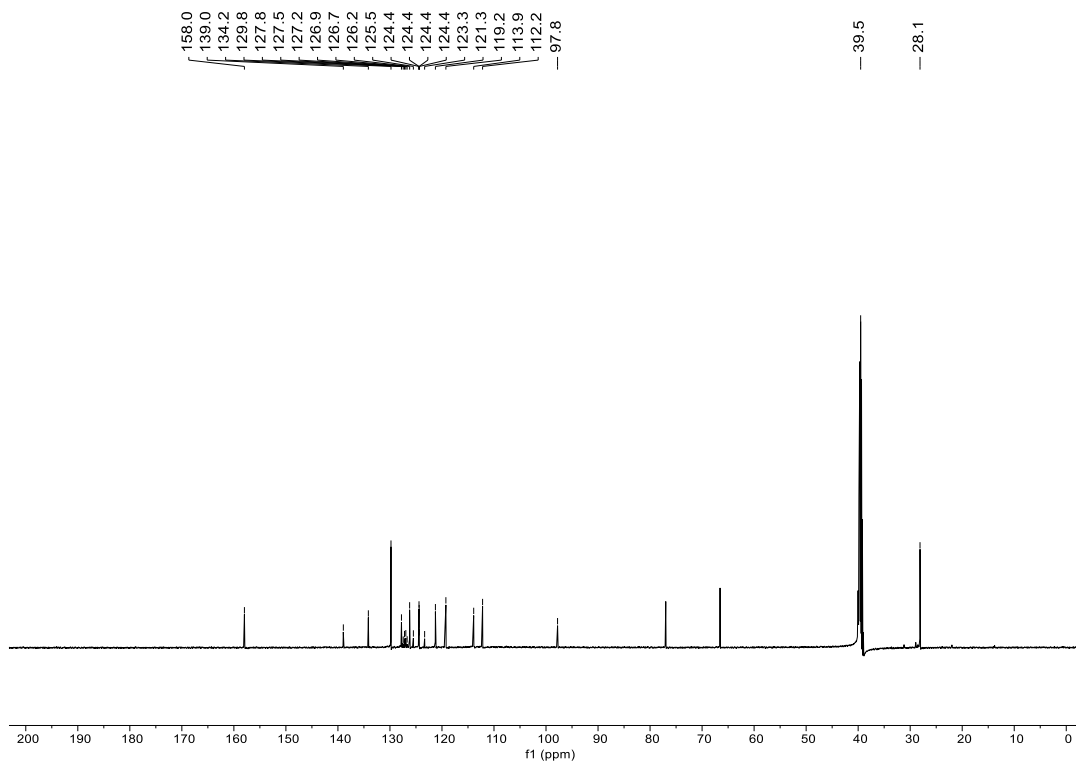
Compound **6f**: HSQC (^{1}H NMR 500 MHz, CDCl$_3$; ^{13}C NMR 101 MHz, DMSO-d$_6$).
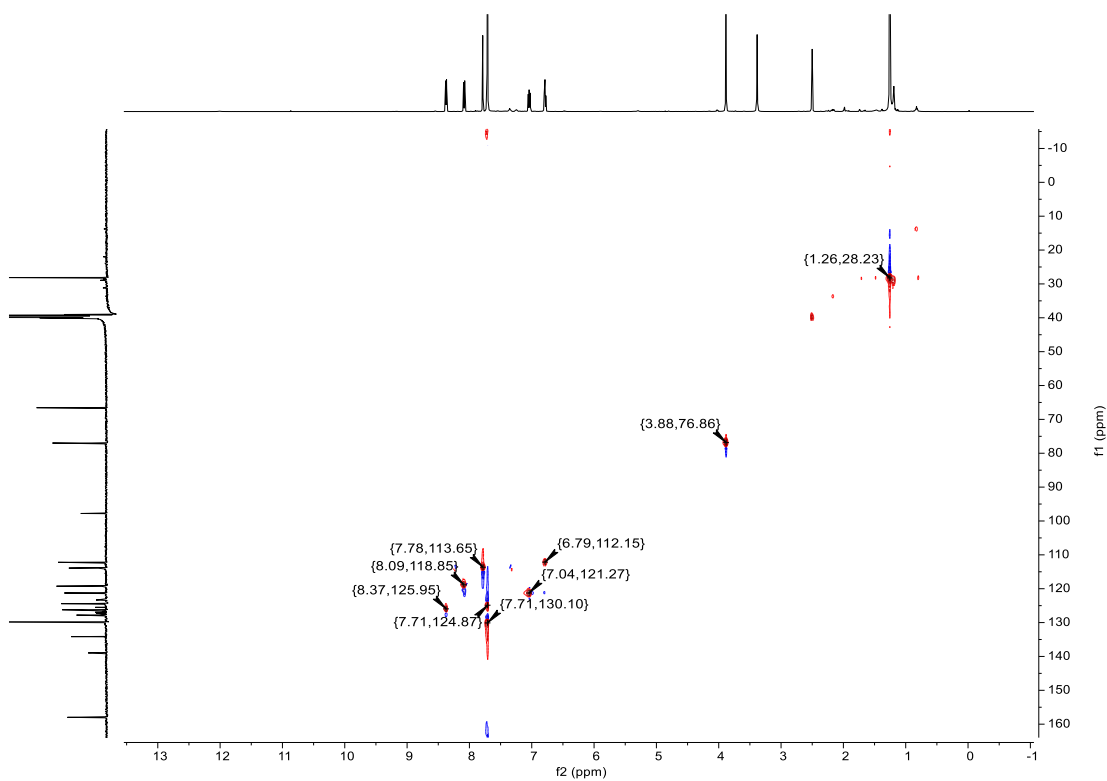
Compound **12: HMBC** (^{1}H NMR 500 MHz, CDCl$_3$; ^{13}C NMR 101 MHz, DMSO-d$_6$).
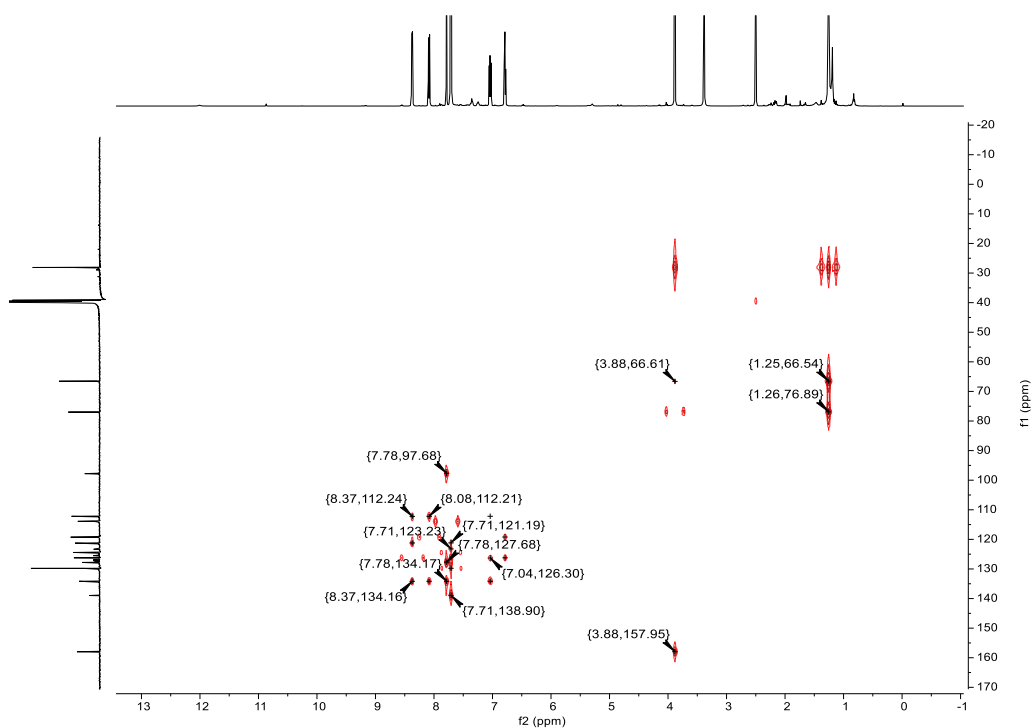
Compound **6f**: NOESY (^{1}H NMR 500 MHz, CDCl$_3$; ^{13}C NMR 101 MHz, DMSO-d$_6$).
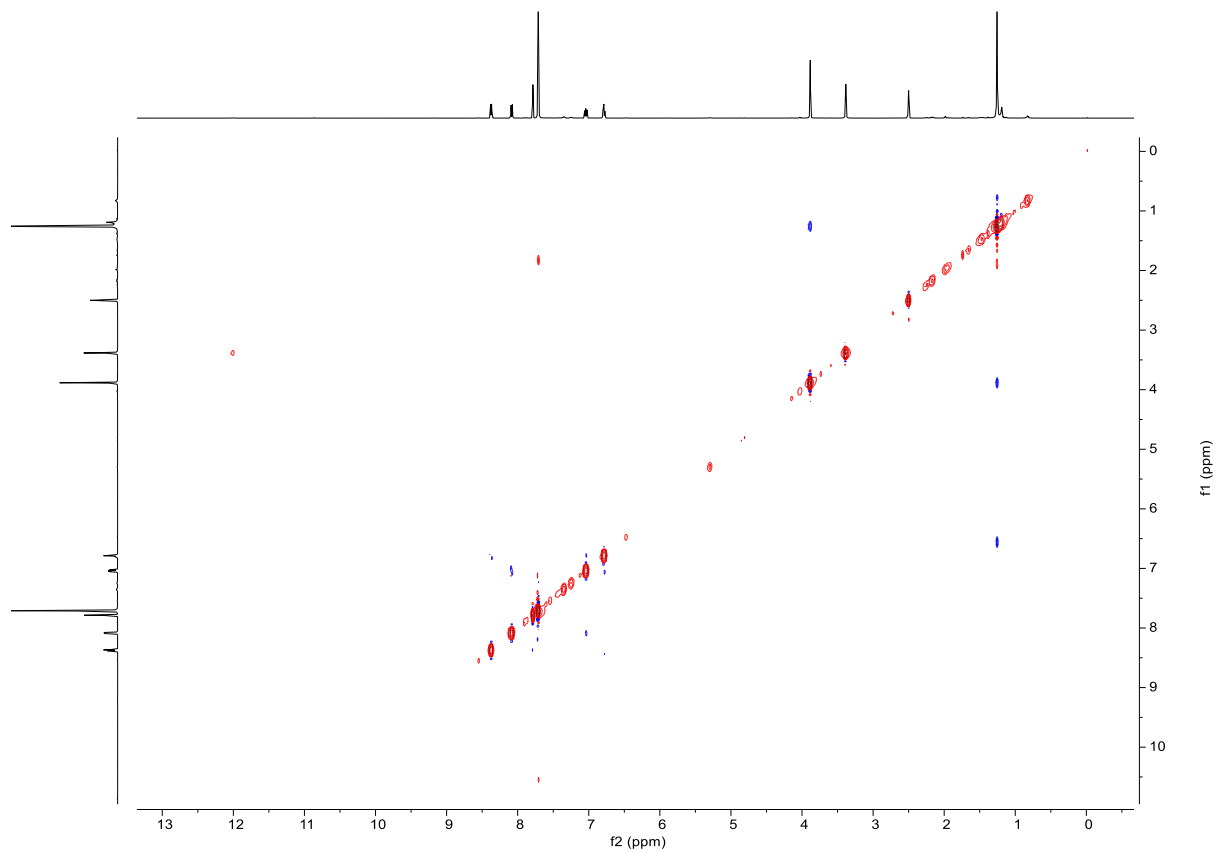
Compound **5e:** ^{1}H NMR (400 MHz, CDCl$_3$)**.**
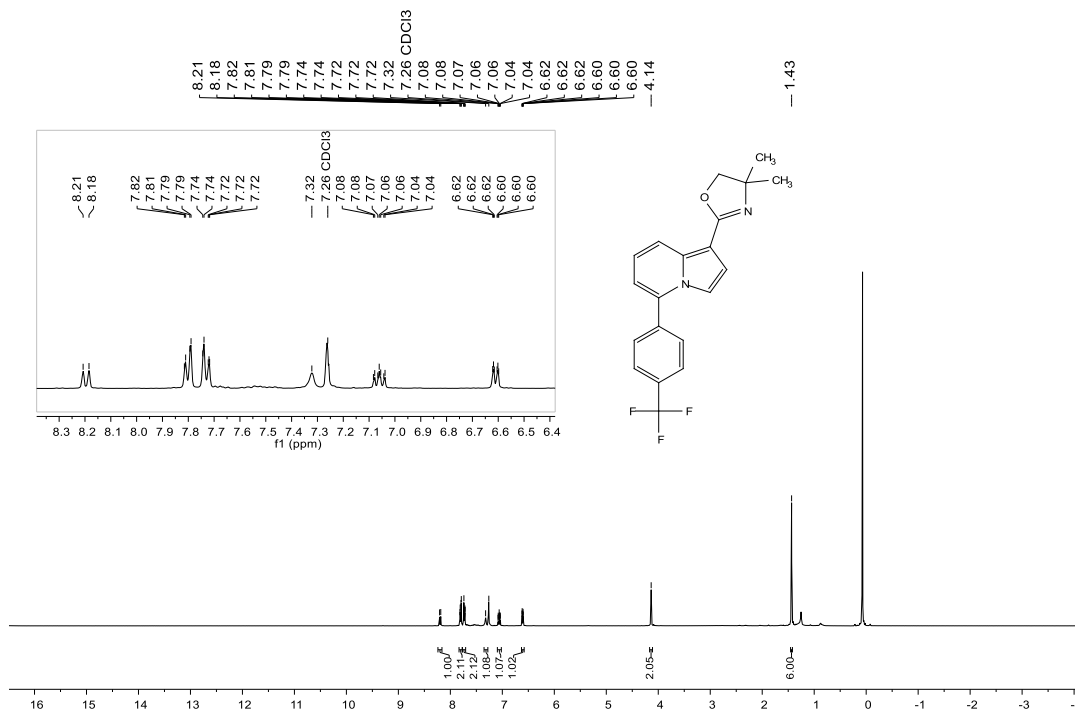
Compound **5e:** ^{13}C NMR (101 MHz, CDCl$_3$)**.**
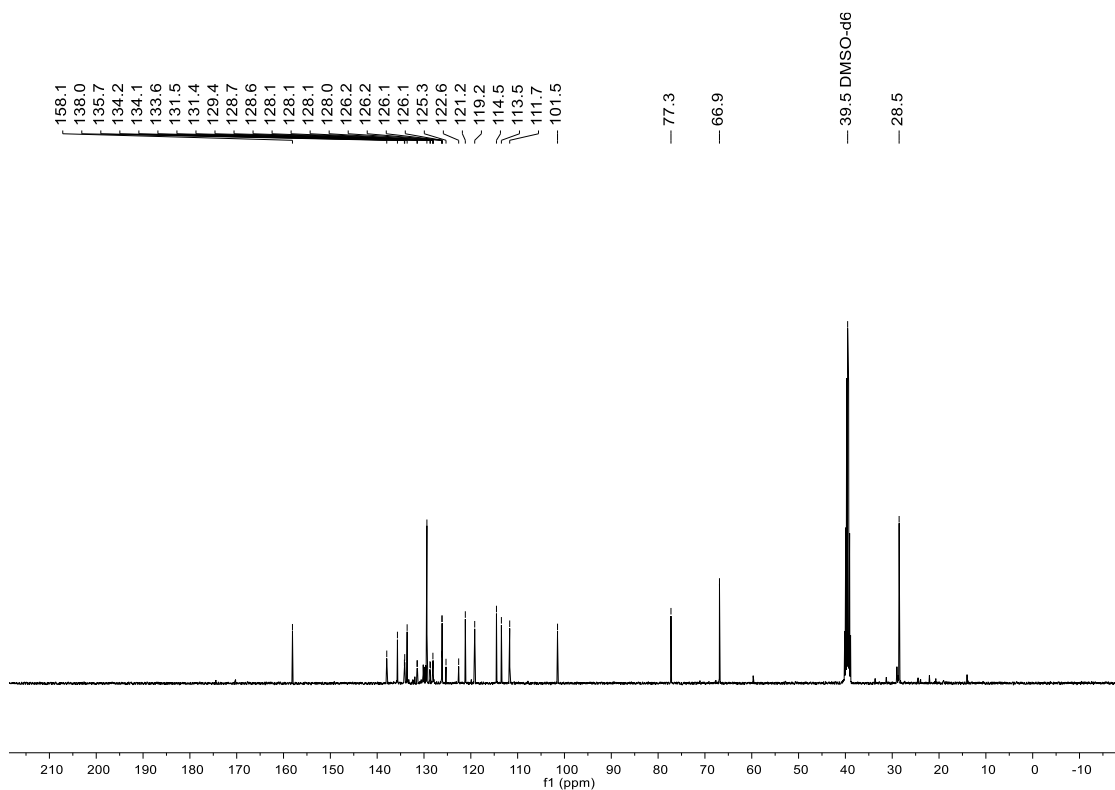
Compound **7a:** ¹H NMR (400 MHz, DMSO-d₆)**.**
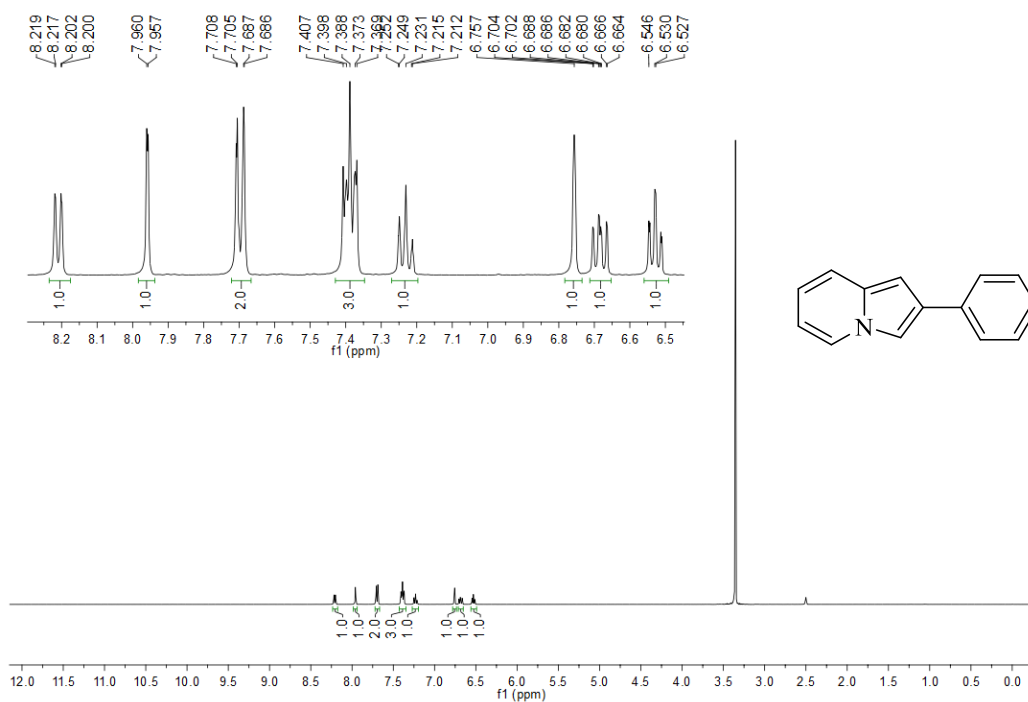
Compound **7a:** ¹³C NMR (101 MHz, DMSO-*d₆*)**.**
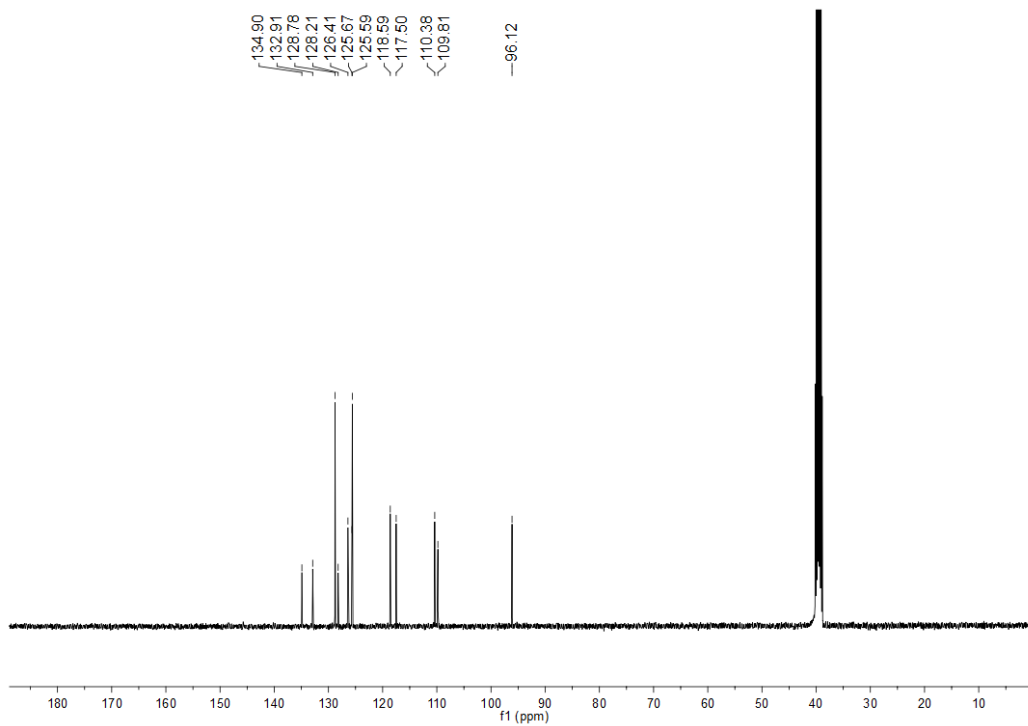
Compound **7b:** ¹H NMR (400 MHz, DMSO-d₆).
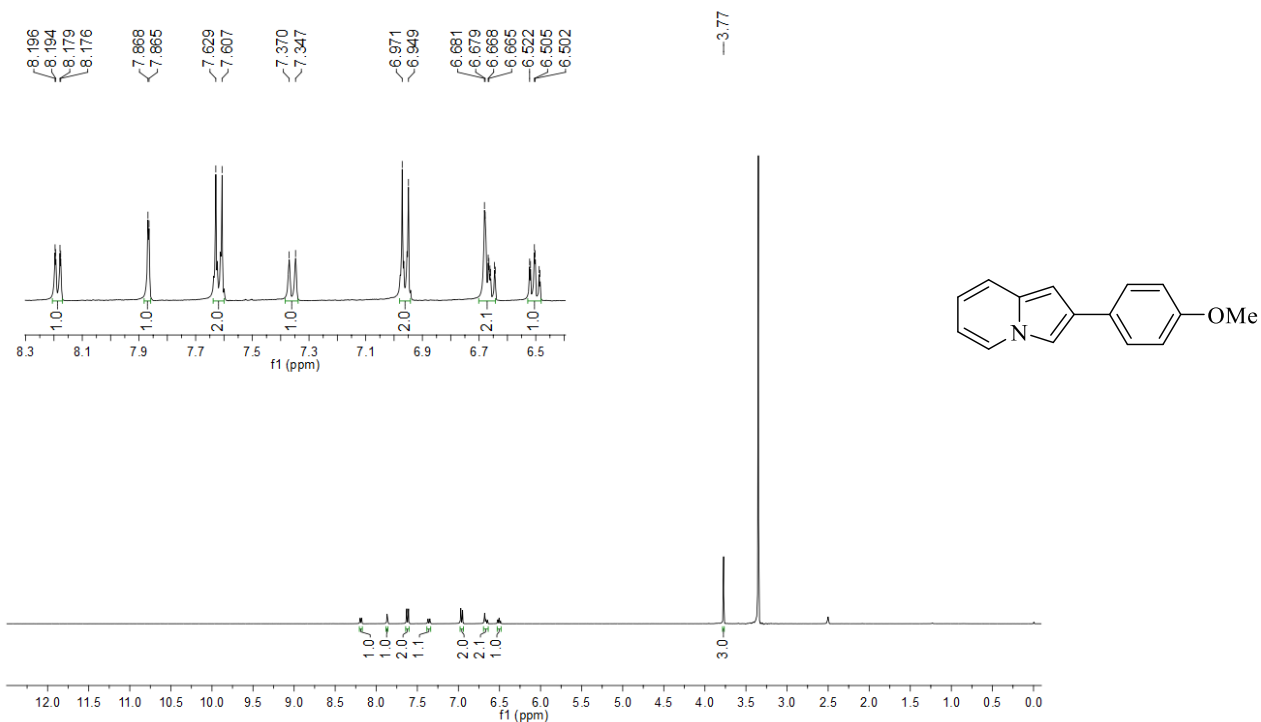
Compound **7b:** ¹³C NMR (101 MHz, DMSO-d₆).
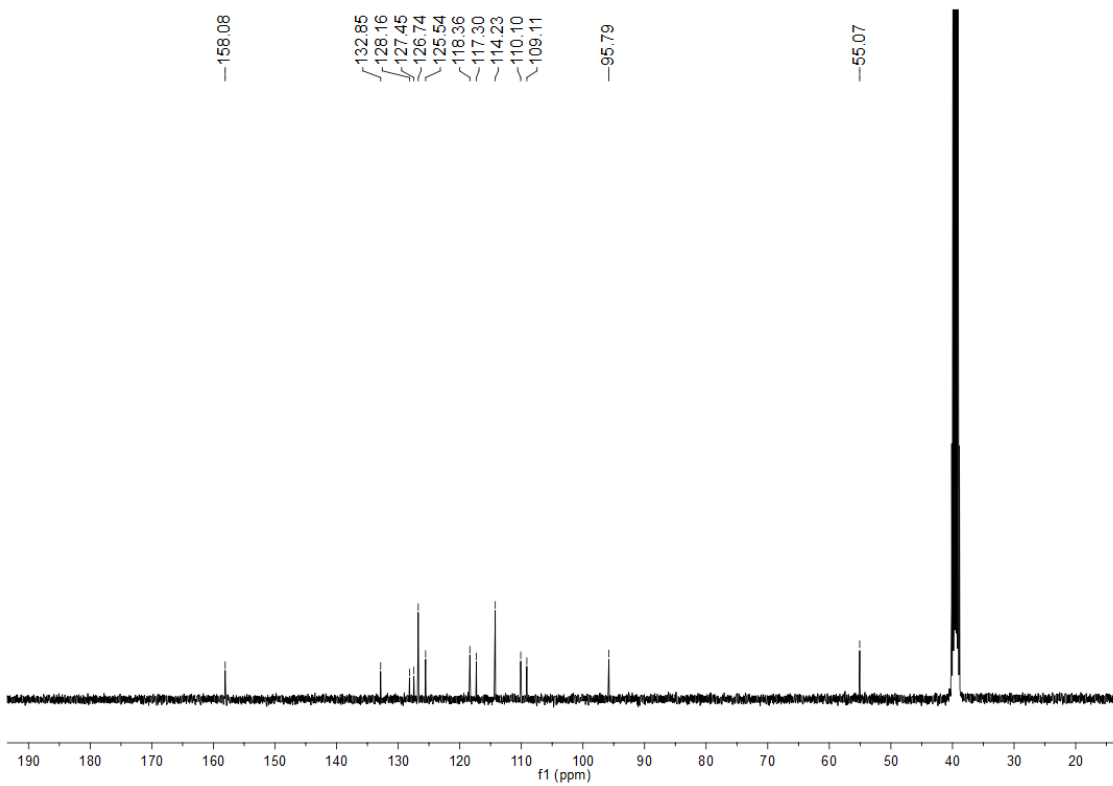
Compound **7c:** ^{1}H NMR (500 MHz, DMSO-d$_6$)**.**
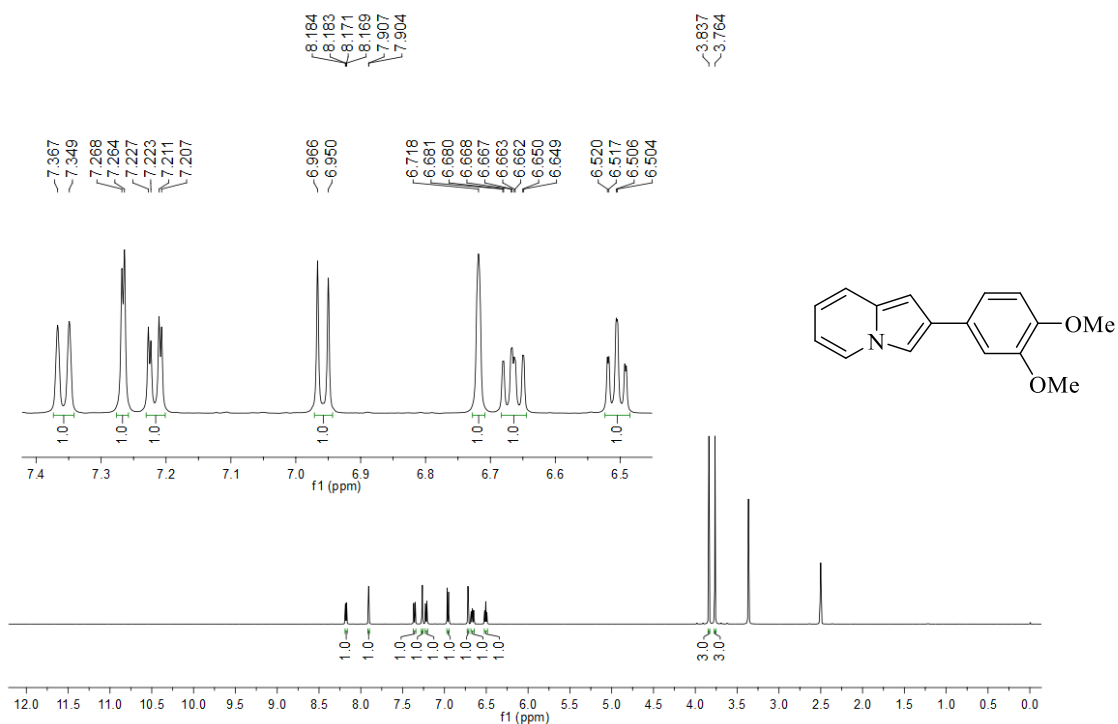
Compound **7c:** ^{13}C NMR (126 MHz, DMSO-d$_6$)**.**
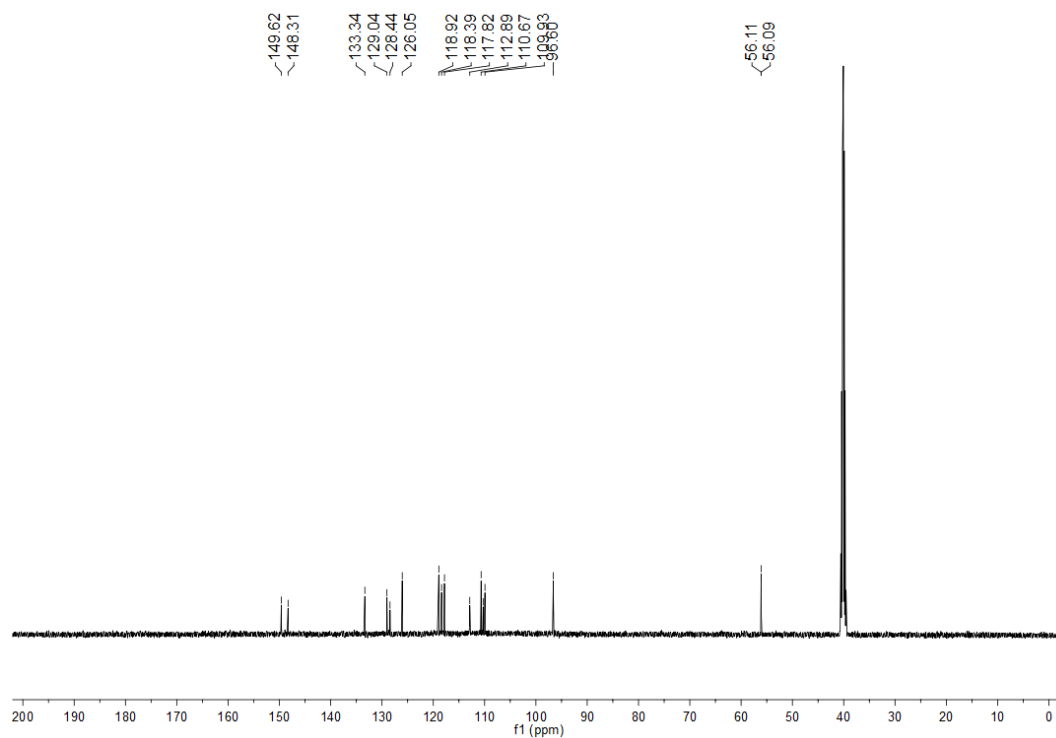
Compound **7d:** ^{1}H NMR (400 MHz, C$_5$D$_5$N)**.**
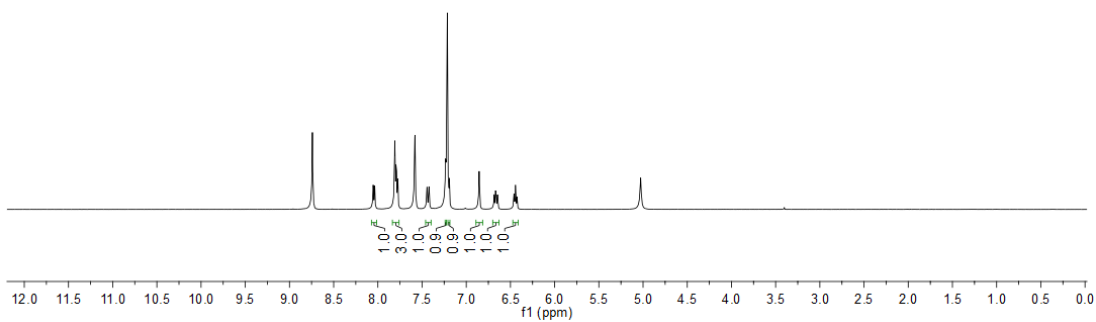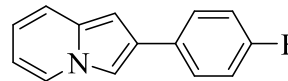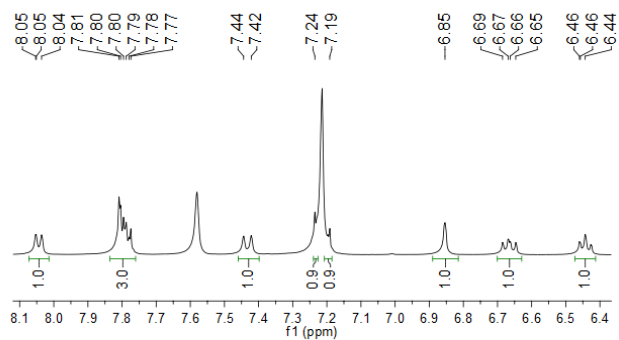
Compound **7d:** ^{13}C NMR (101 MHz, C$_5$D$_5$N).
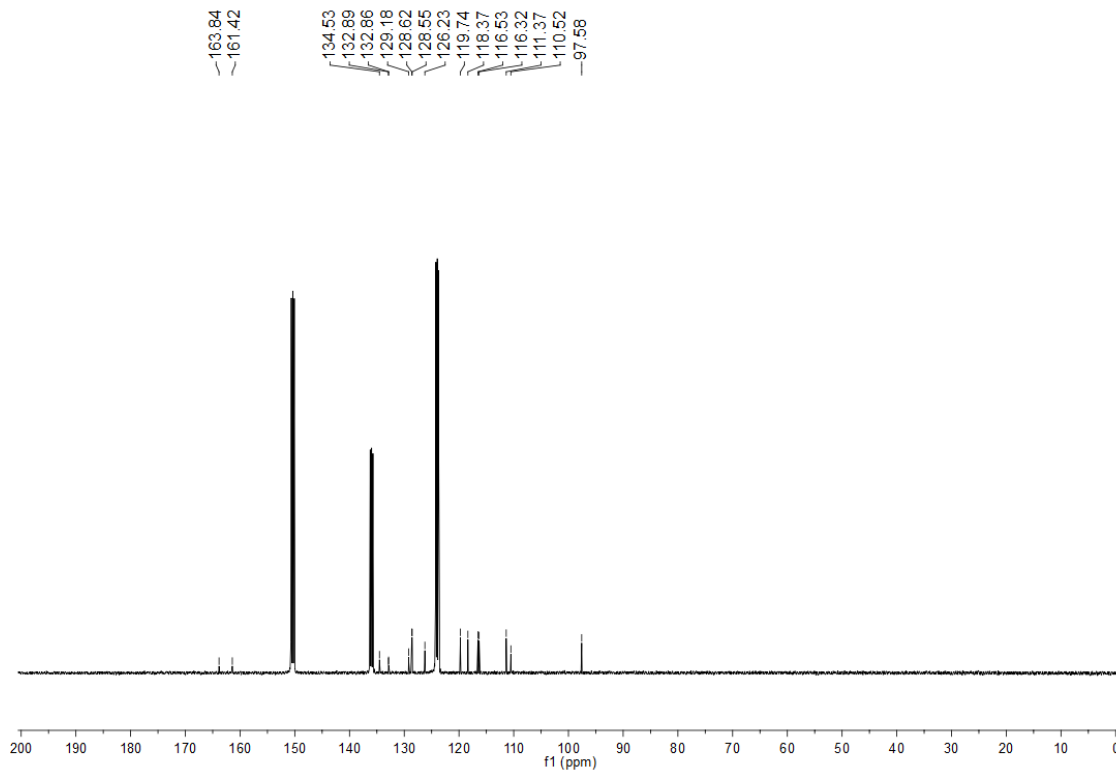
Compound **7e:** ^{1}H NMR (400 MHz, C$_5$D$_5$N)**.**
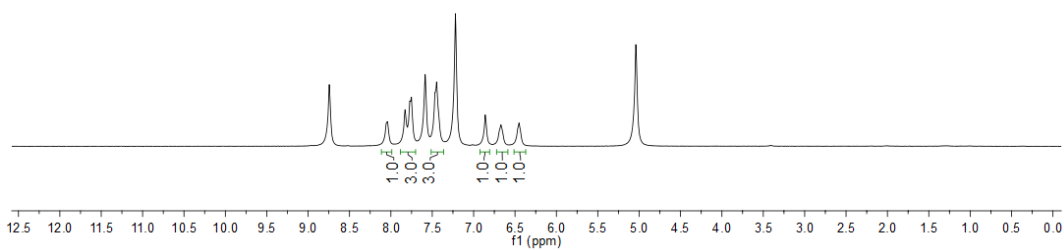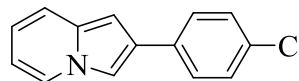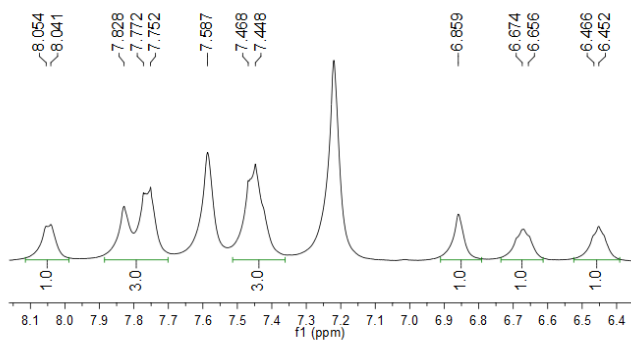
Compound **7d:** ^{13}C NMR (101 MHz, C$_5$D$_5$N)**.**
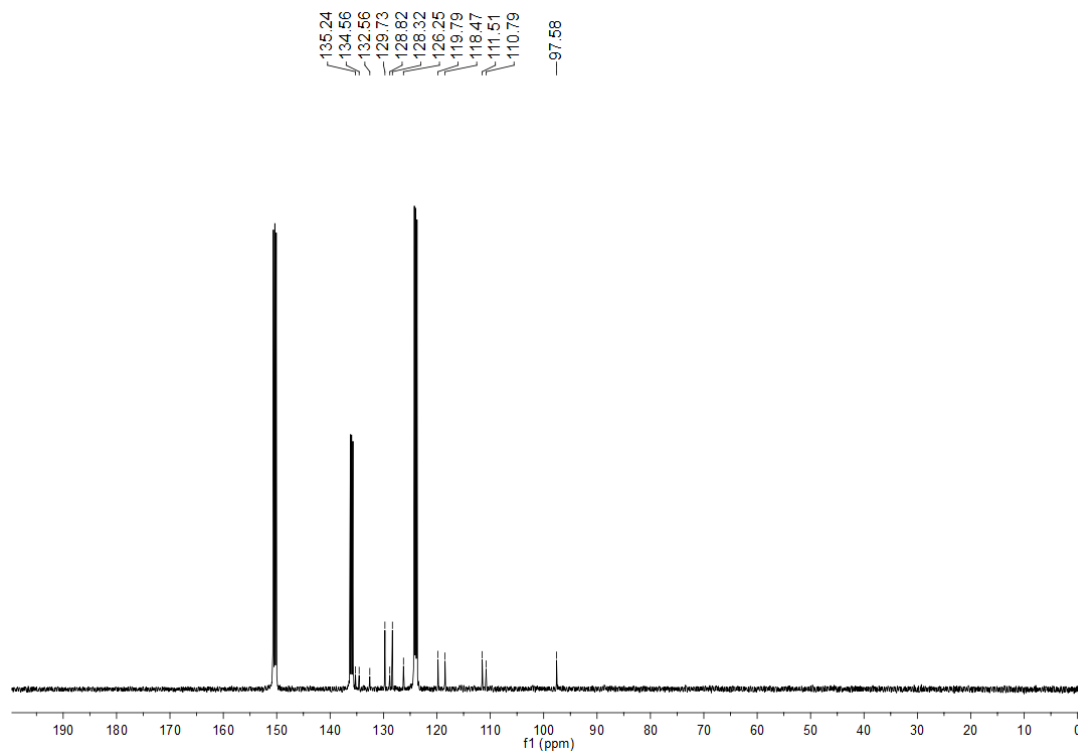
Compound **8a:** ¹H NMR (DMSO-d₆, 400 MHz).
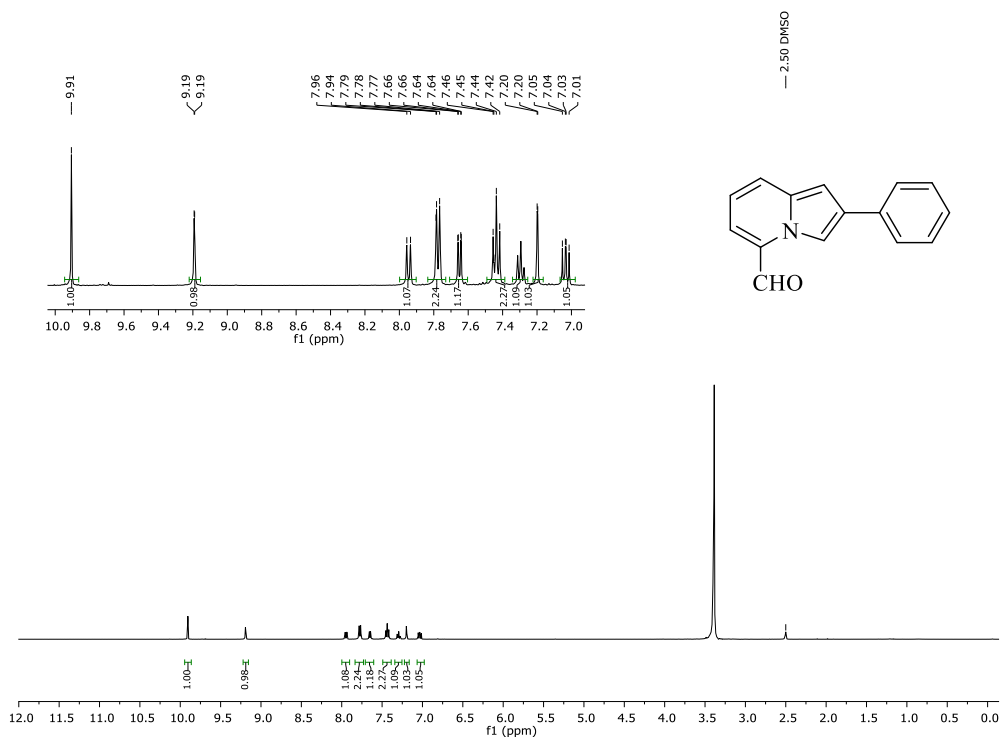
Compound **8a:** ¹³C NMR (DMSO-d₆, 101 MHz).
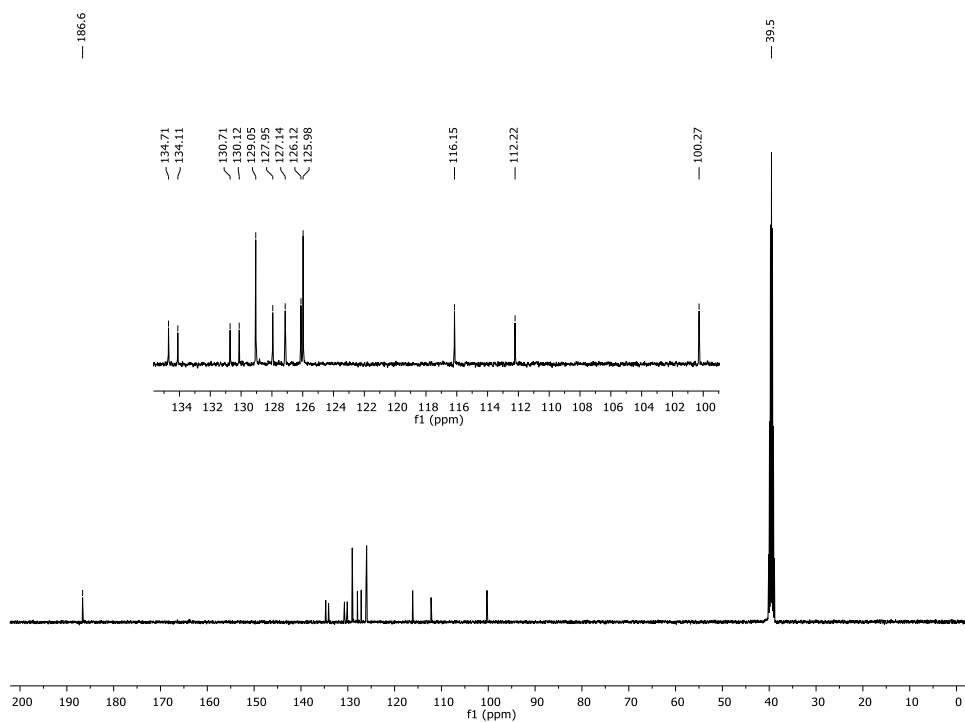
Compound **8b:** ^{1}H NMR (DMSO-d$_6$, 400 MHz).
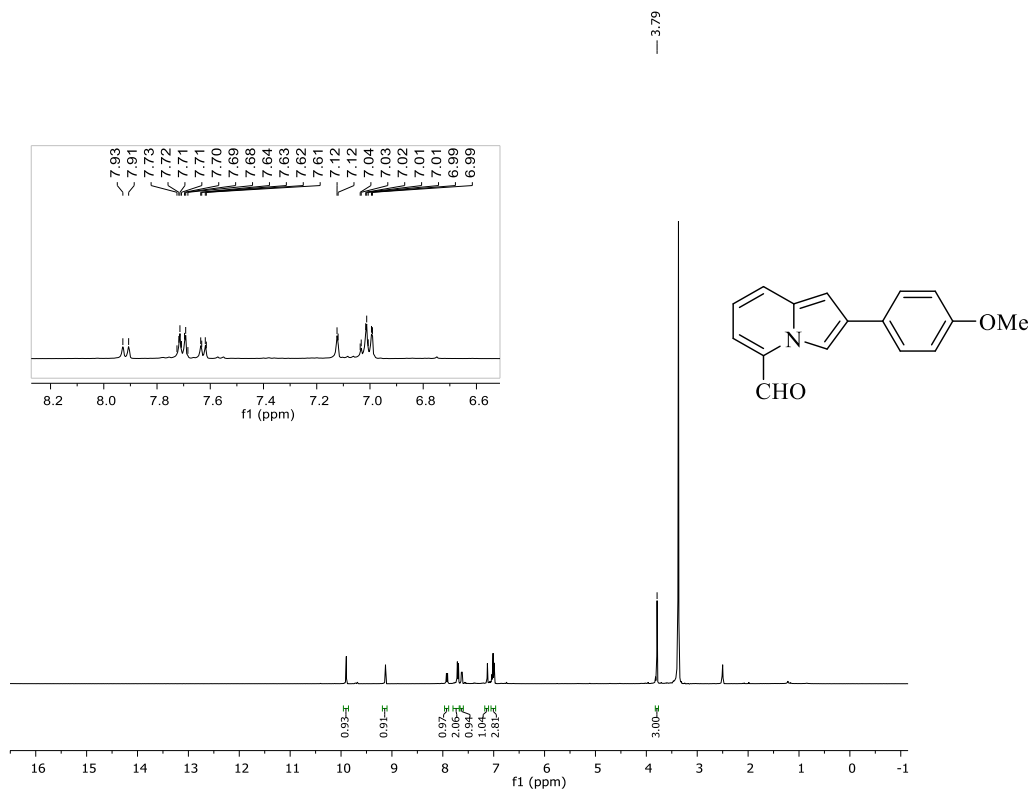
Compound **8b:** ^{13}C NMR (DMSO-d$_6$, 101 MHz).
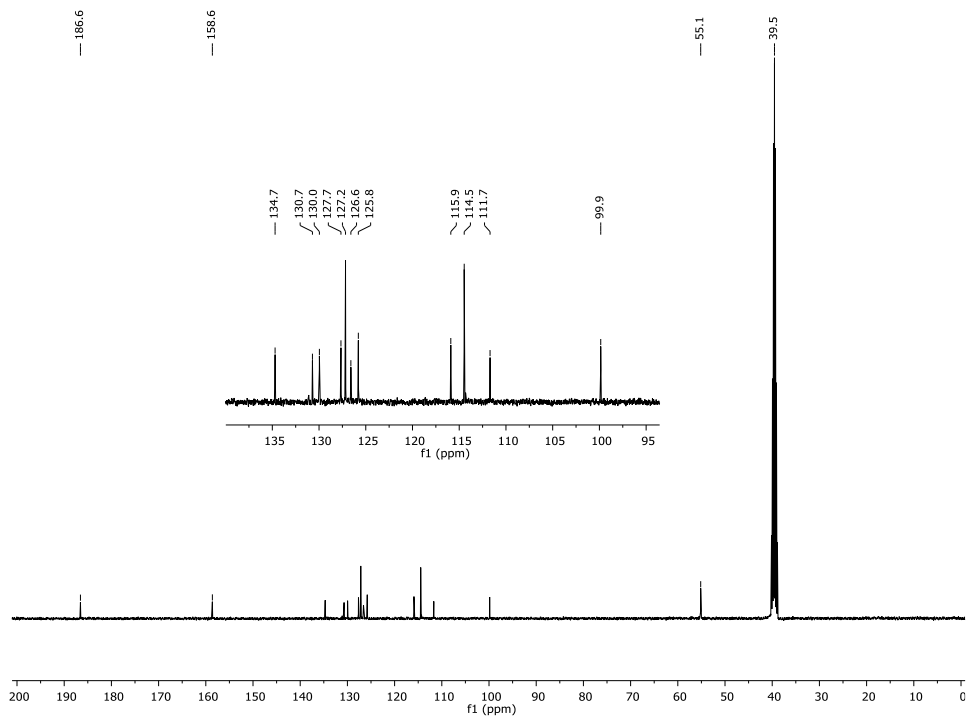
Compound **8c:** ^{1}H NMR (DMSO-d$_6$, 400 MHz).
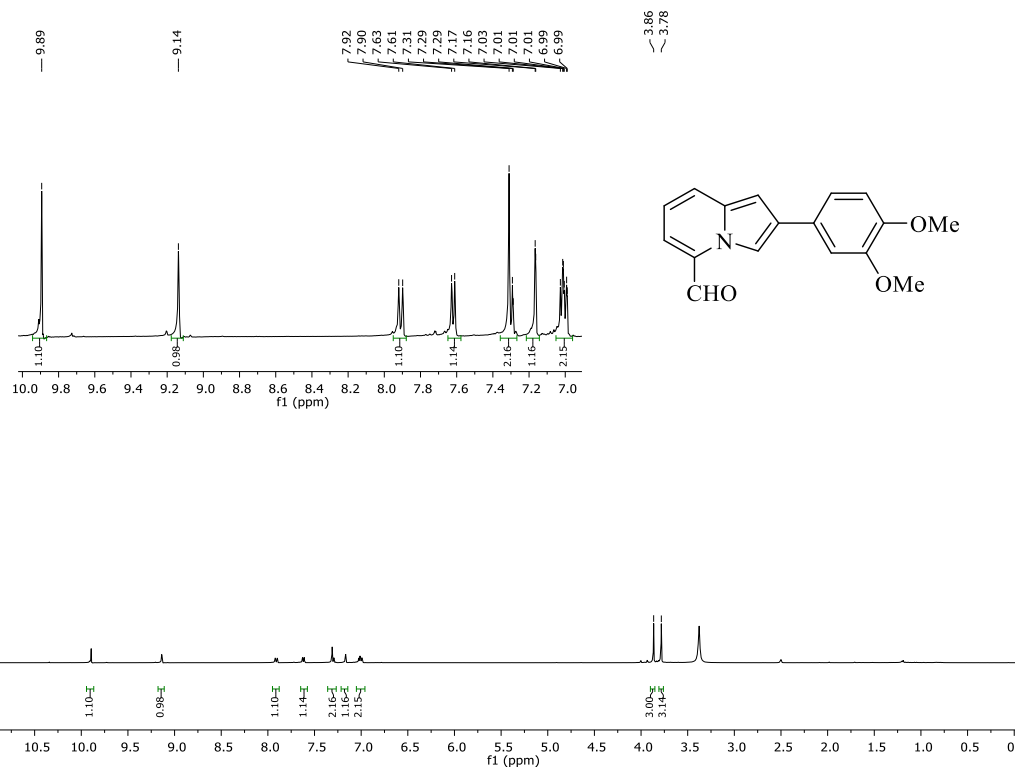
Compound **8c:** ^{13}C NMR (DMSO-d$_6$, 101 MHz).
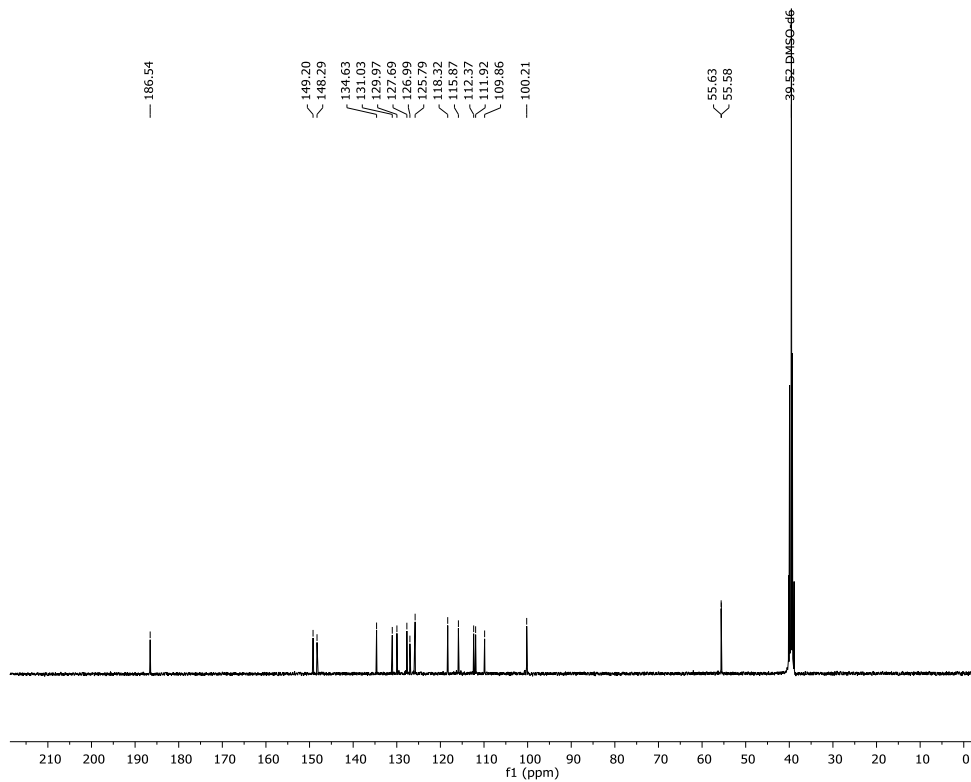
Compound **8d:** ^{1}H NMR (400 MHz, C$_5$D$_5$N)**.**
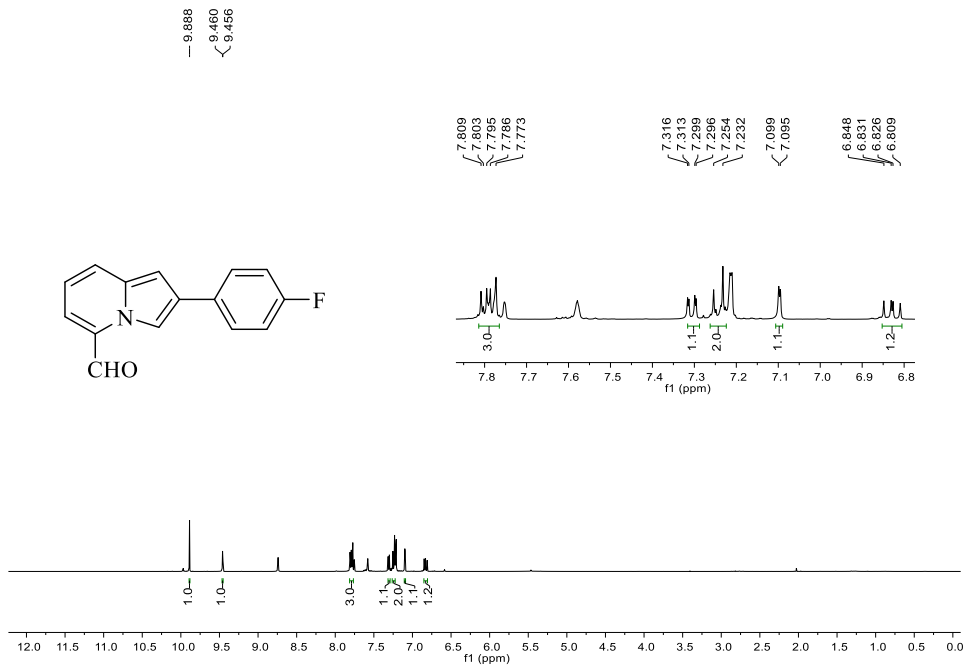
Compound **8d:** ^{13}C NMR (101 MHz, C$_5$D$_5$N)**.**
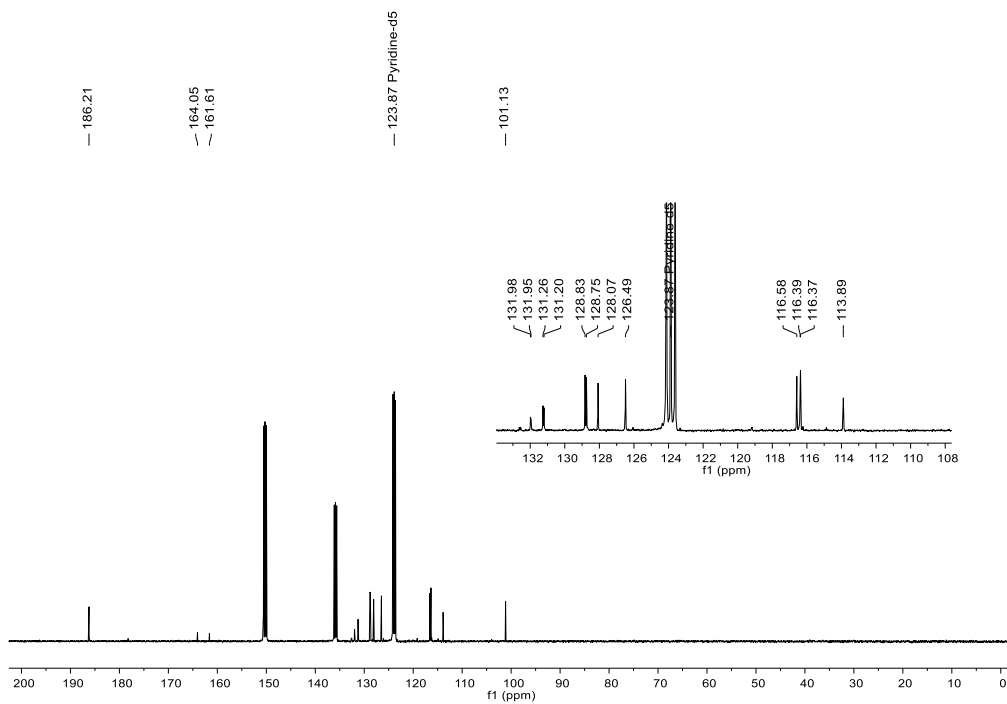
Compound **8e:** ^{1}H NMR (400 MHz, C$_5$D$_5$N).
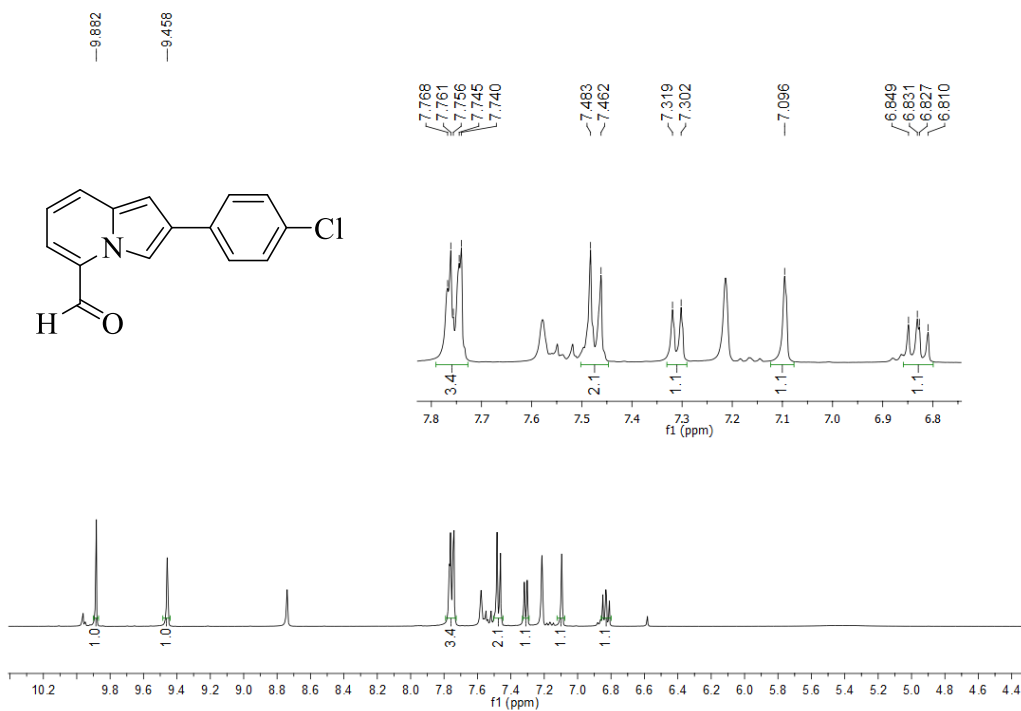
Compound **8e:** ^{13}C NMR (101 MHz, C$_5$D$_5$N).
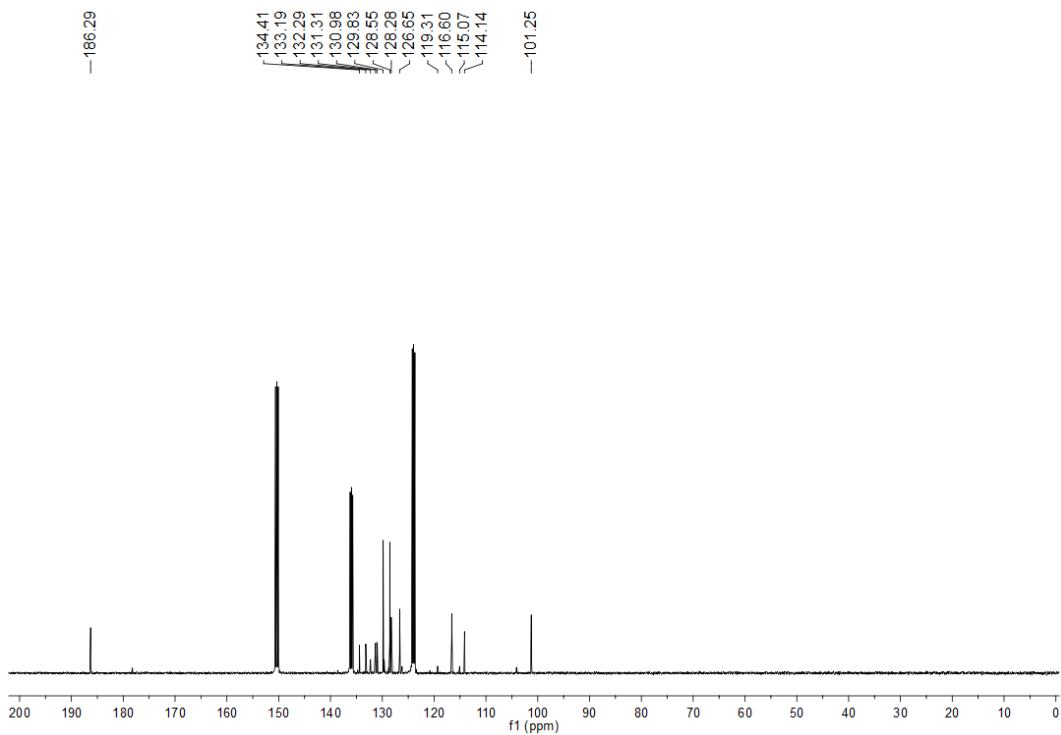
Compound **9a**: ^{1}H NMR (DMSO-d$_6$, 300 MHz).
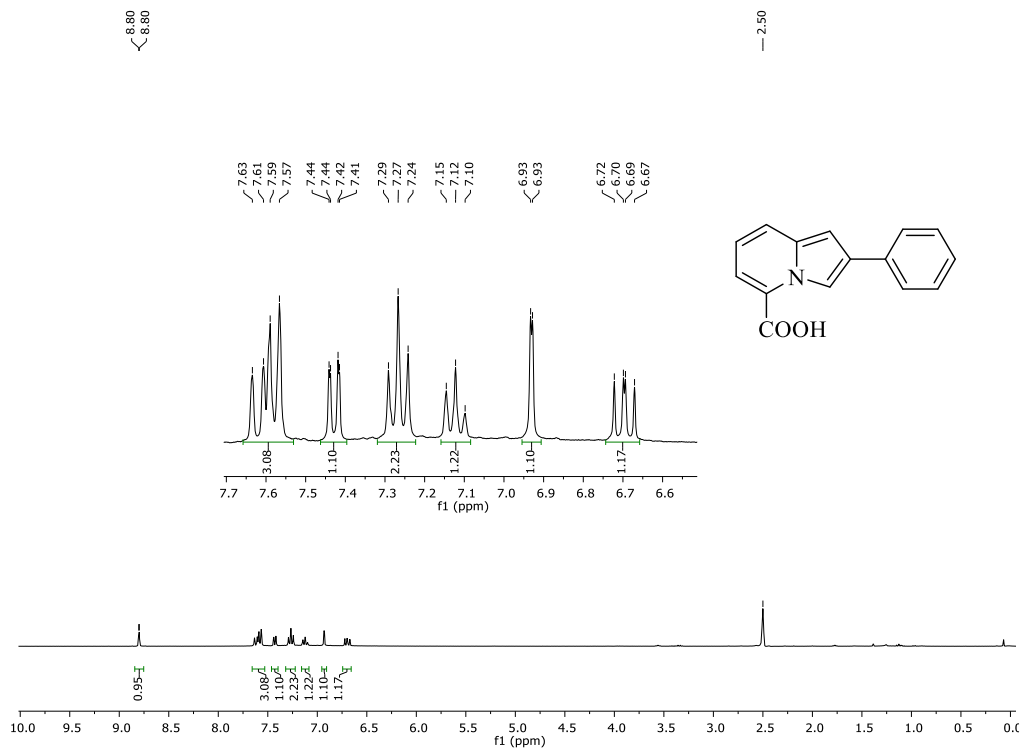
Compound **9a**: ^{13}C NMR (DMSO-d$_6$, 75 MHz).
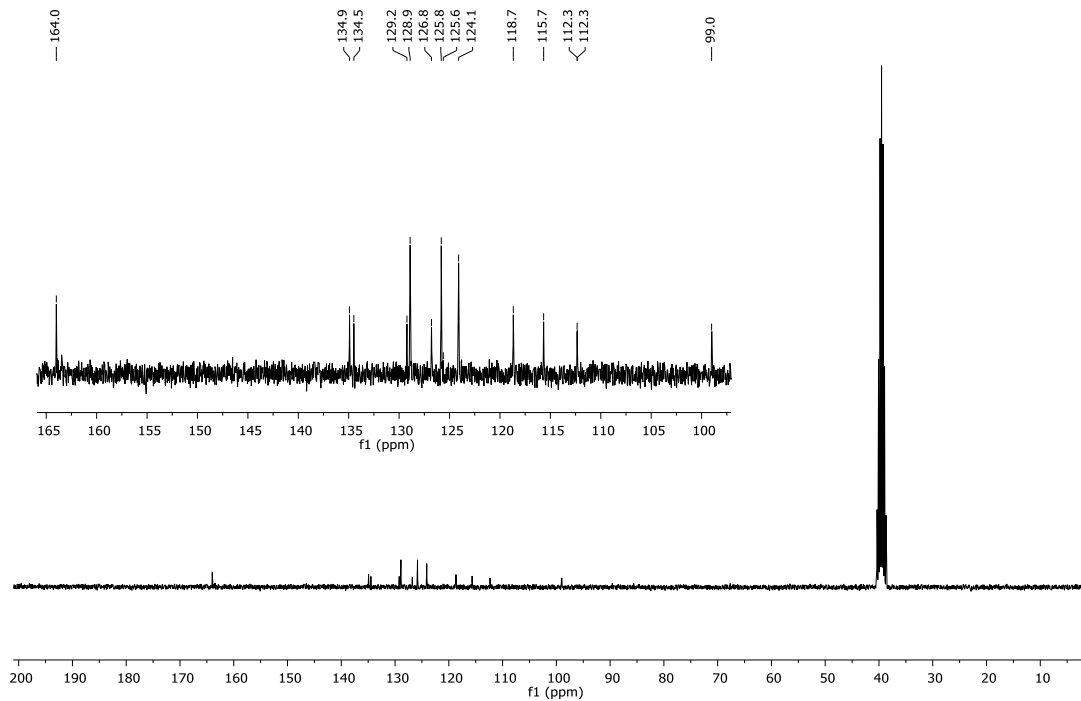
Compound **9b:** ^1H NMR (DMSO-d6, 400 MHz).
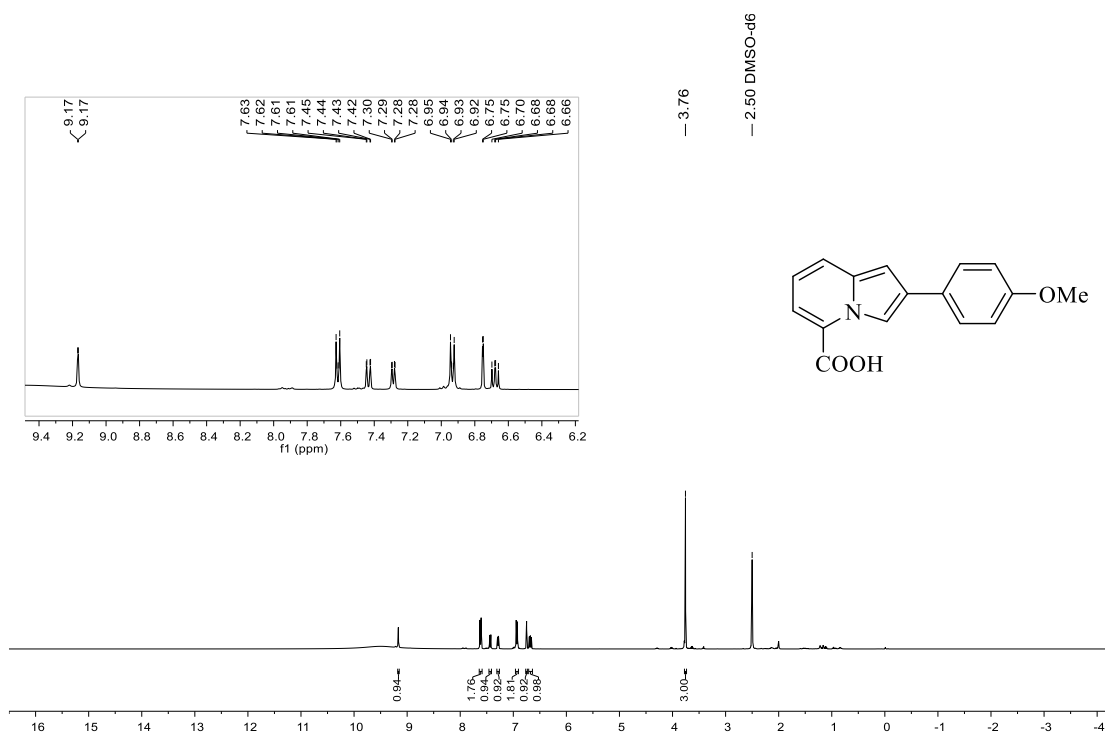
Compound **9b:** ^13C NMR (DMSO-d6, 101 MHz).
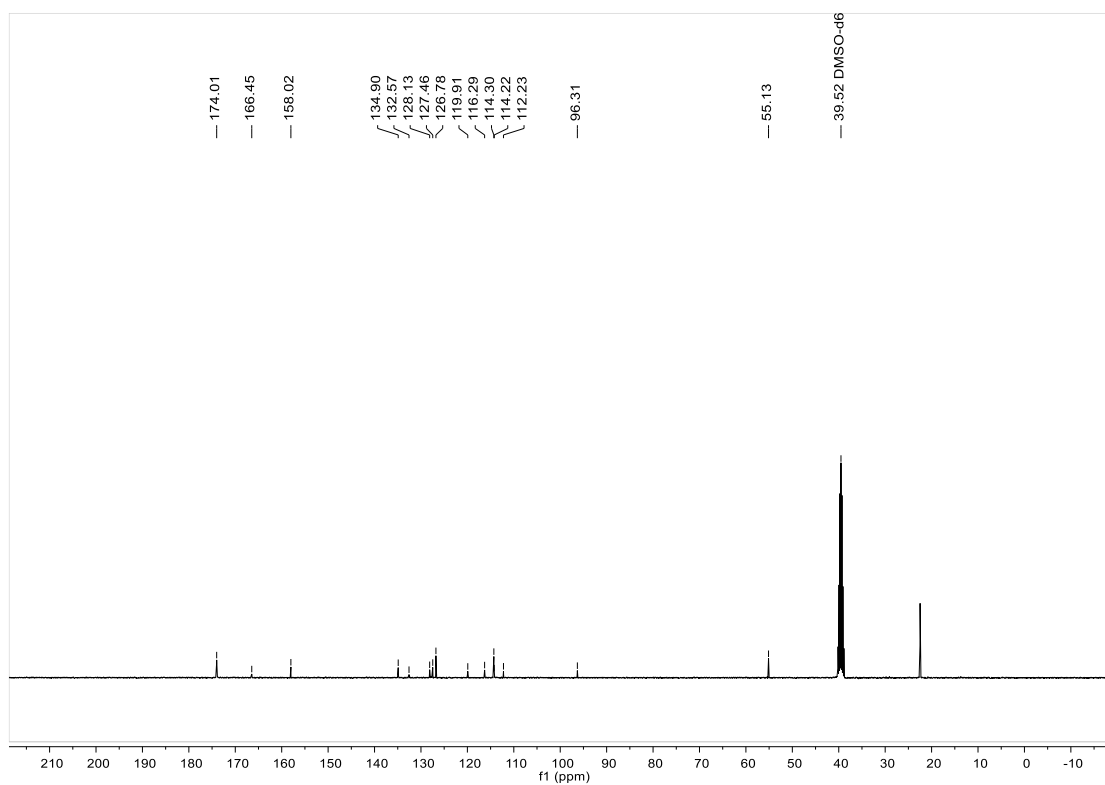
Compound **9c:** ^{1}H NMR (DMSO-d$_6$, 400 MHz).
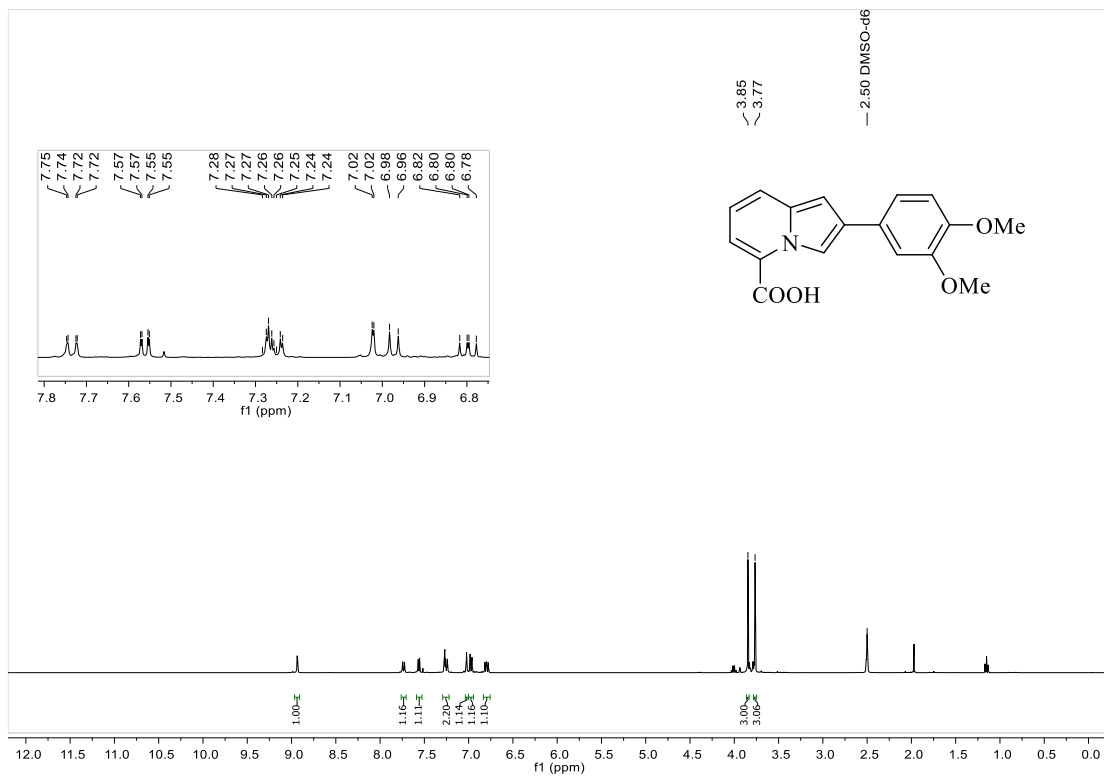
Compound **9c:** ^{13}C NMR (DMSO-d$_6$, 101 MHz).
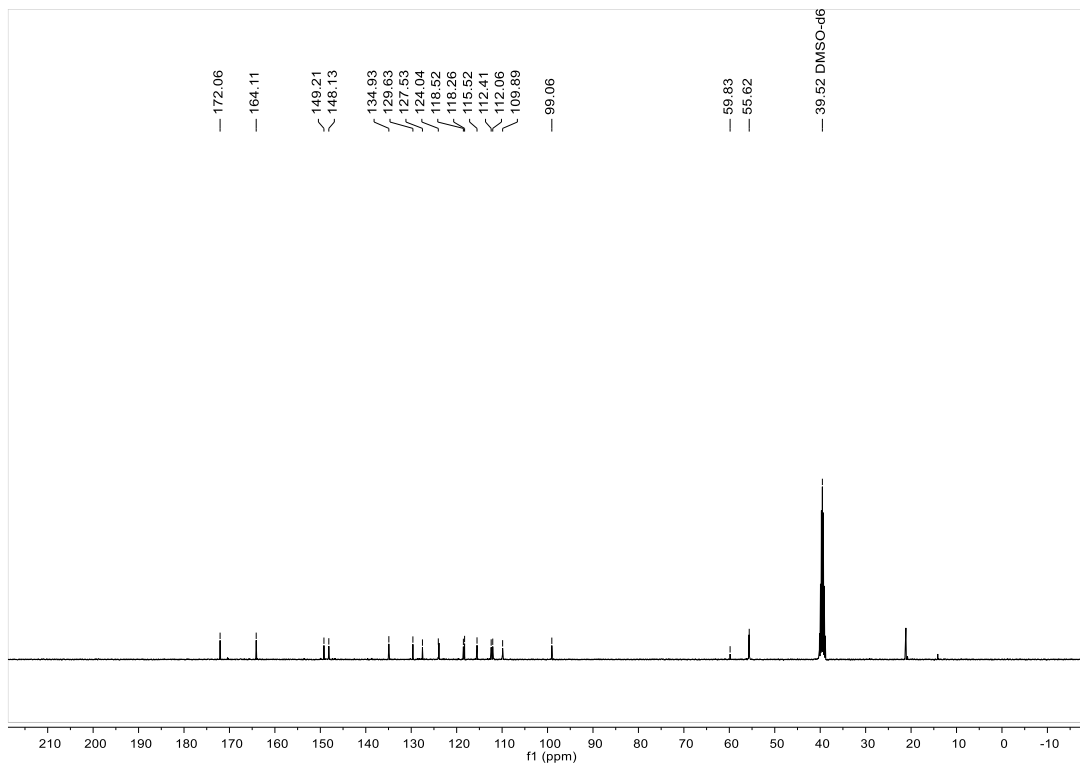
Compound **9d:** ^{1}H NMR (DMSO-d$_6$, 400 MHz).
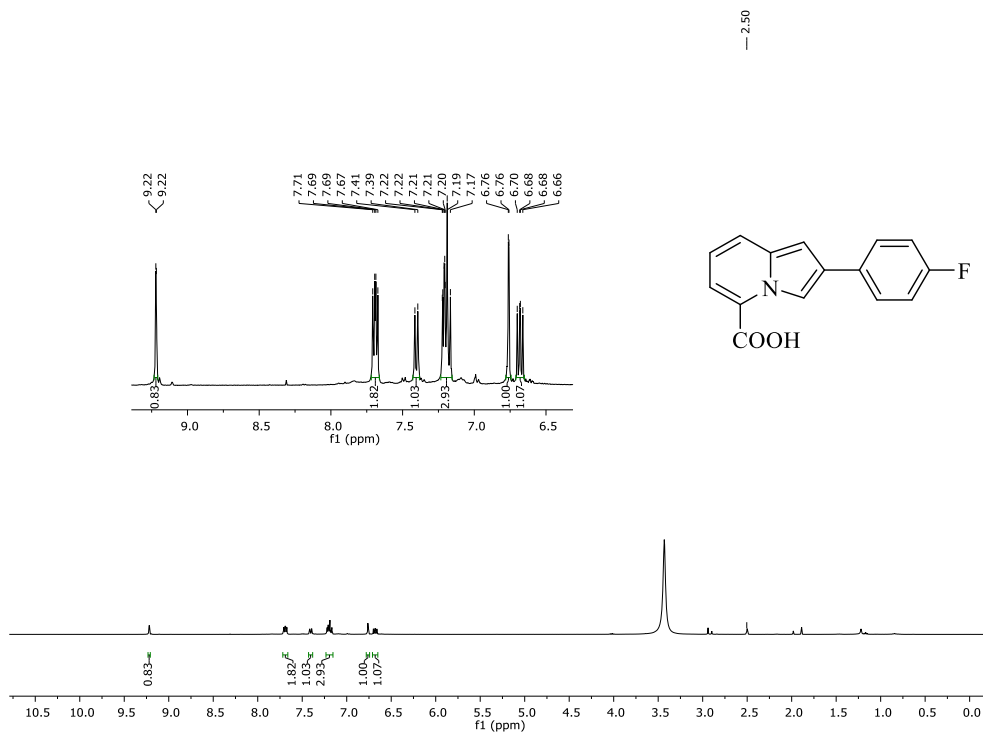
Compound **9d:** ^{13}C NMR (DMSO-d$_6$, 101 MHz).
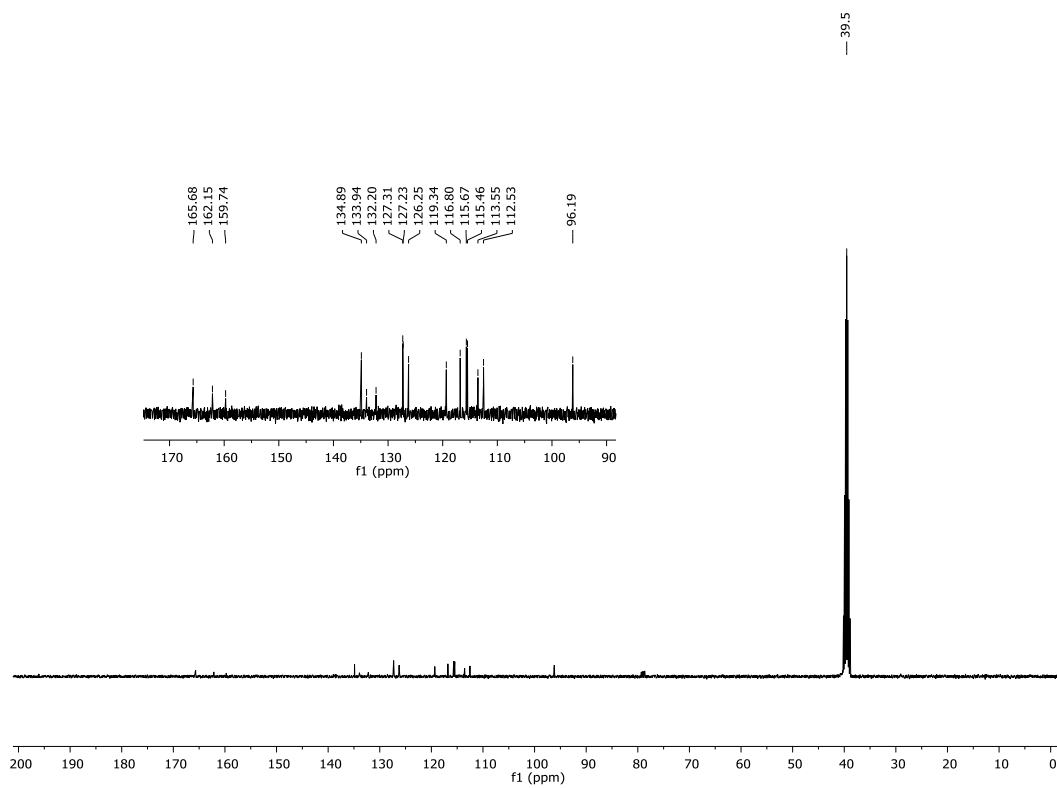
Compound **9e:** ^{1}H NMR (DMSO-d$_6$, 400 MHz).
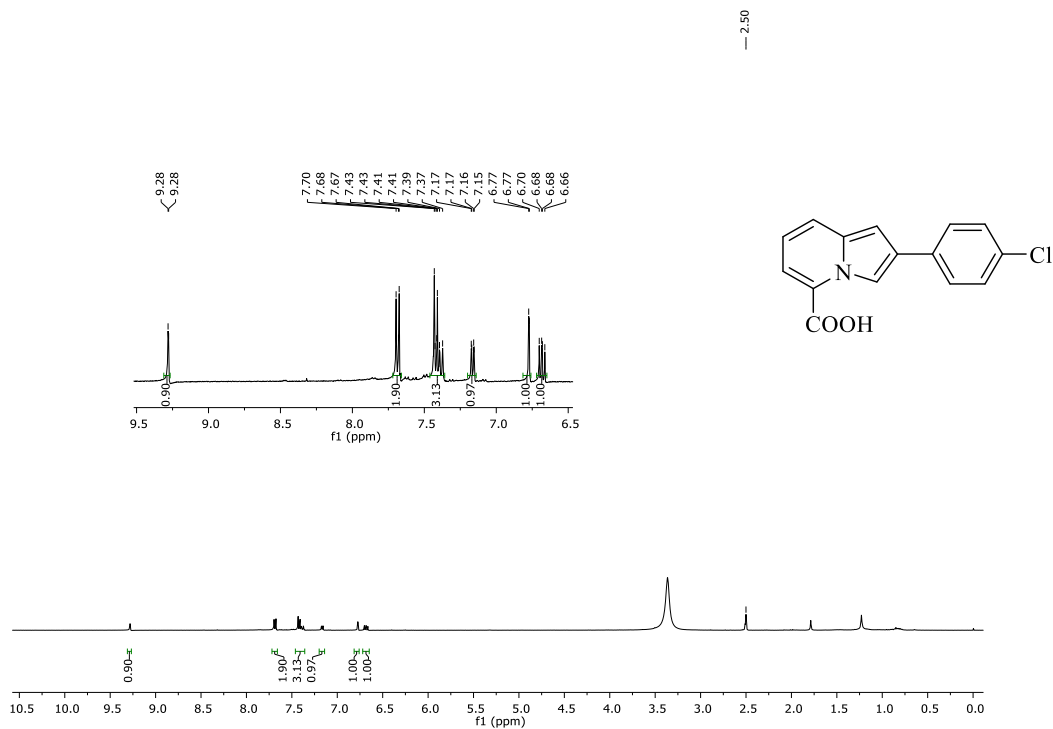
Compound **9e:** ^{13}C NMR (DMSO-d$_6$, 101 MHz).
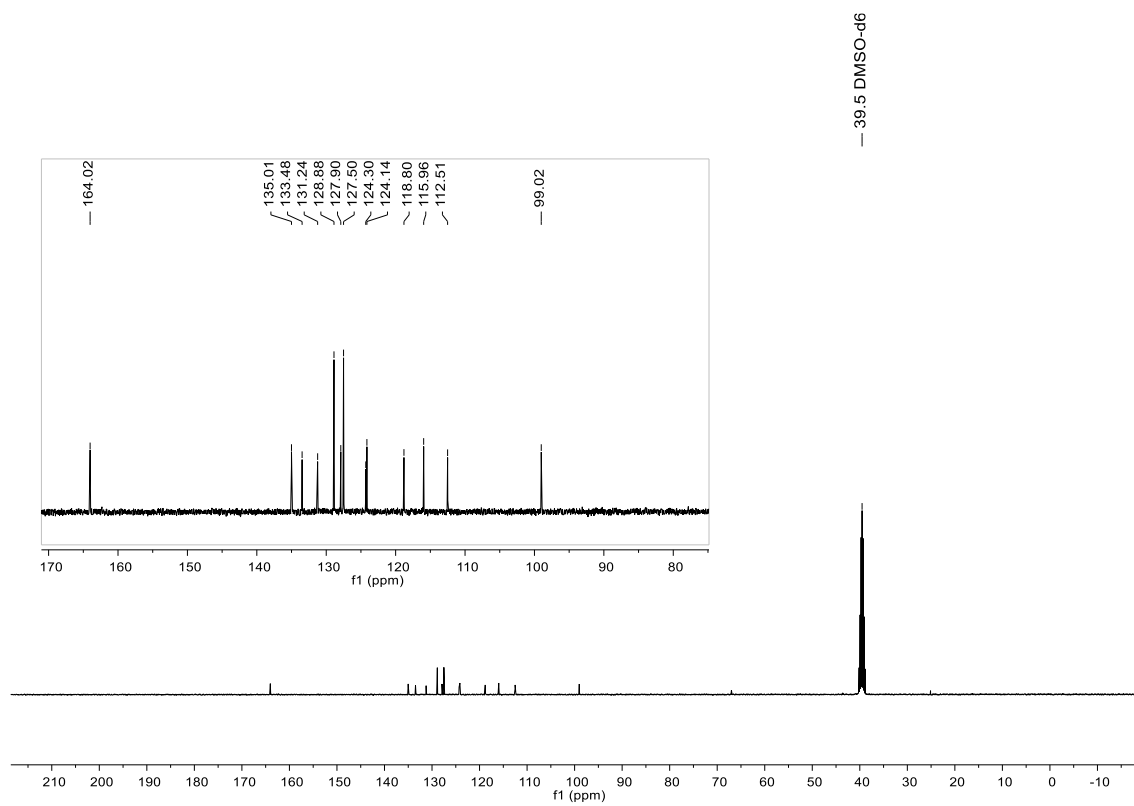
Compound **10a:** ^{1}H NMR (DMSO-d$_6$, 400 MHz).
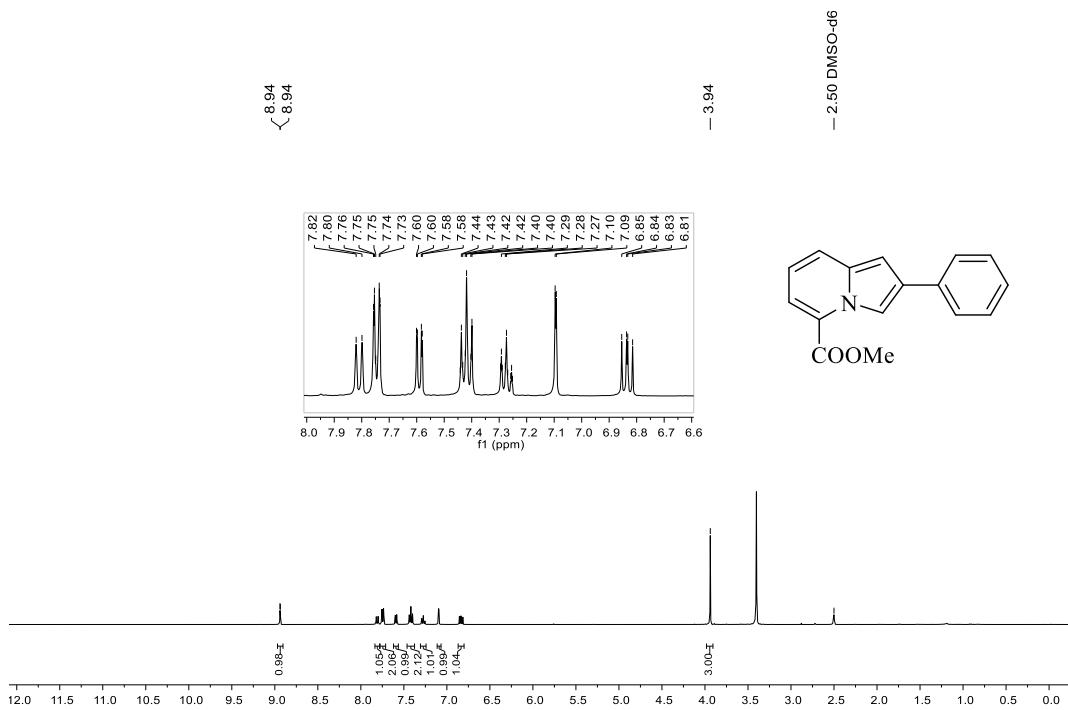
Compound **10a:** ^{13}C NMR (DMSO-d$_6$, 101 MHz).
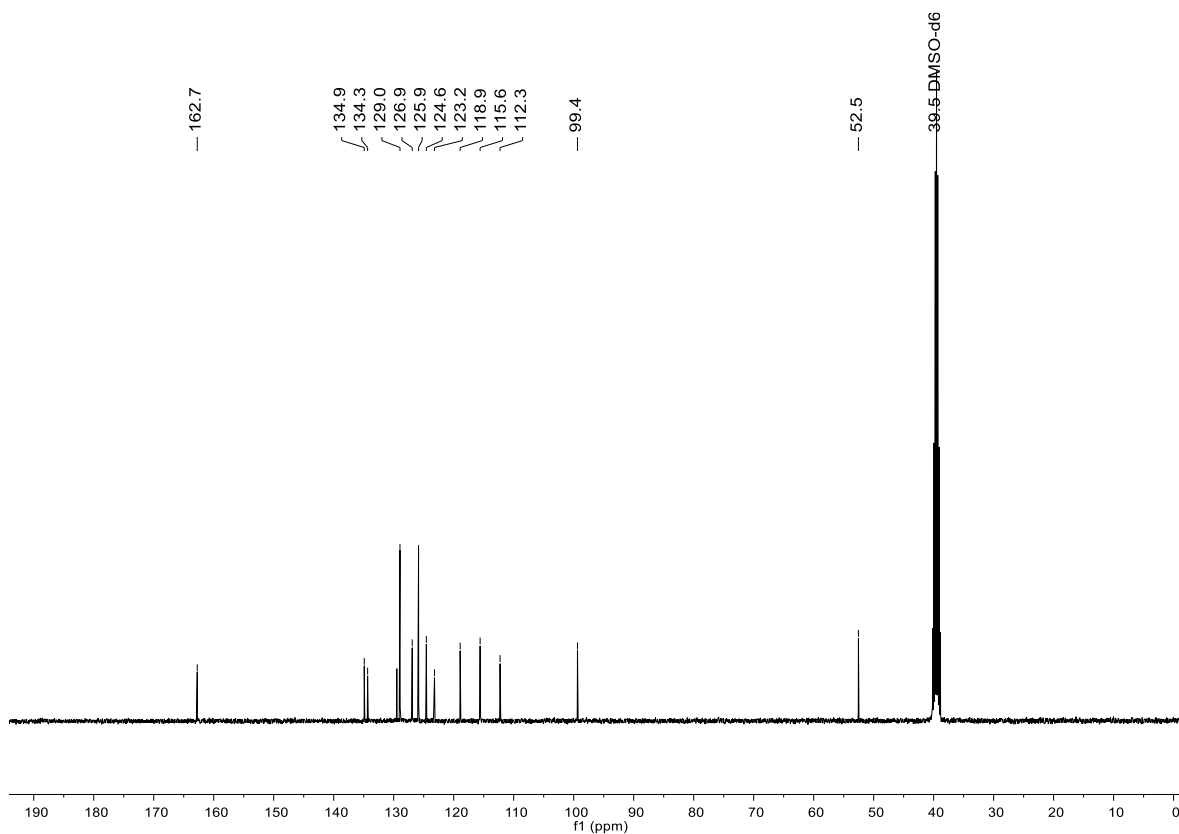
Compound **10b:** ^{1}H NMR (DMSO-d$_6$, 400 MHz).
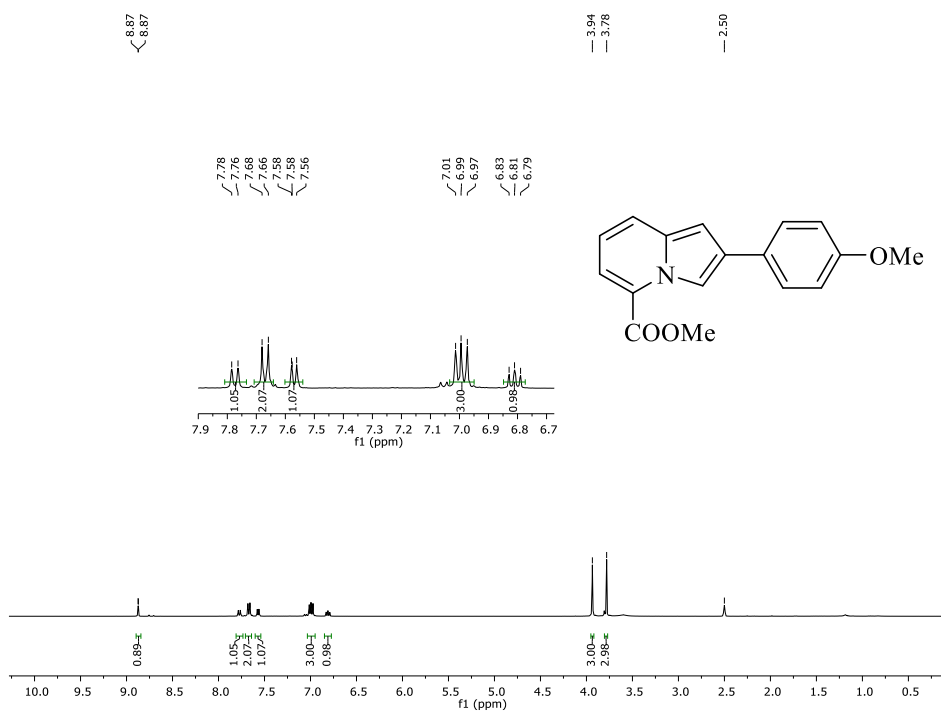
Compound **10b:** ^{13}C NMR (DMSO-d$_6$, 101 MHz).
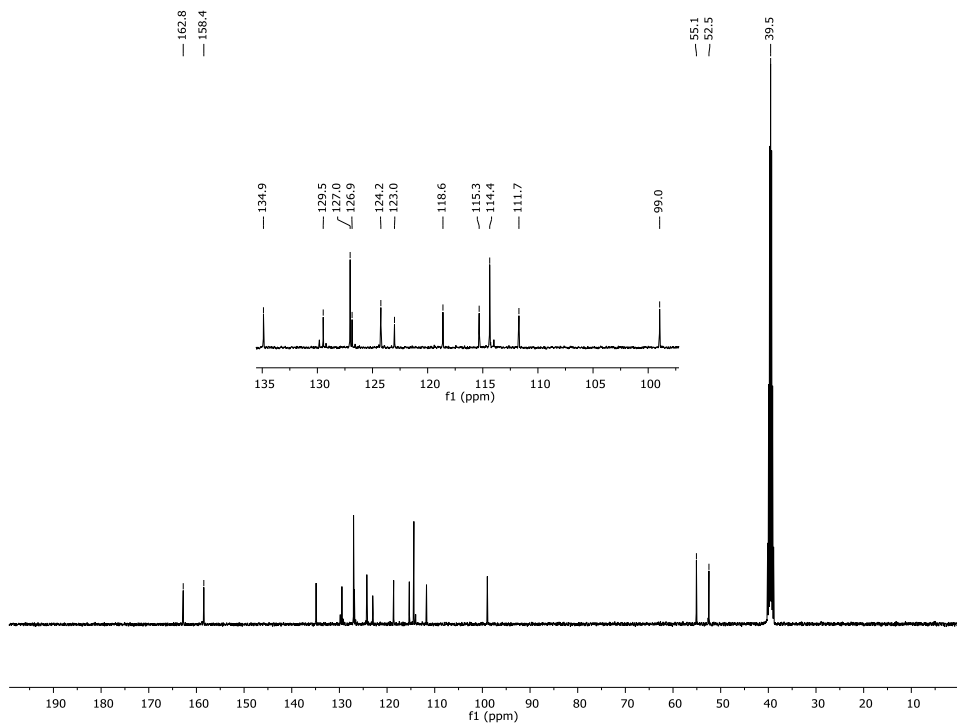
Compound **10c:** ^{1}H NMR (DMSO-d$_6$, 400 MHz).
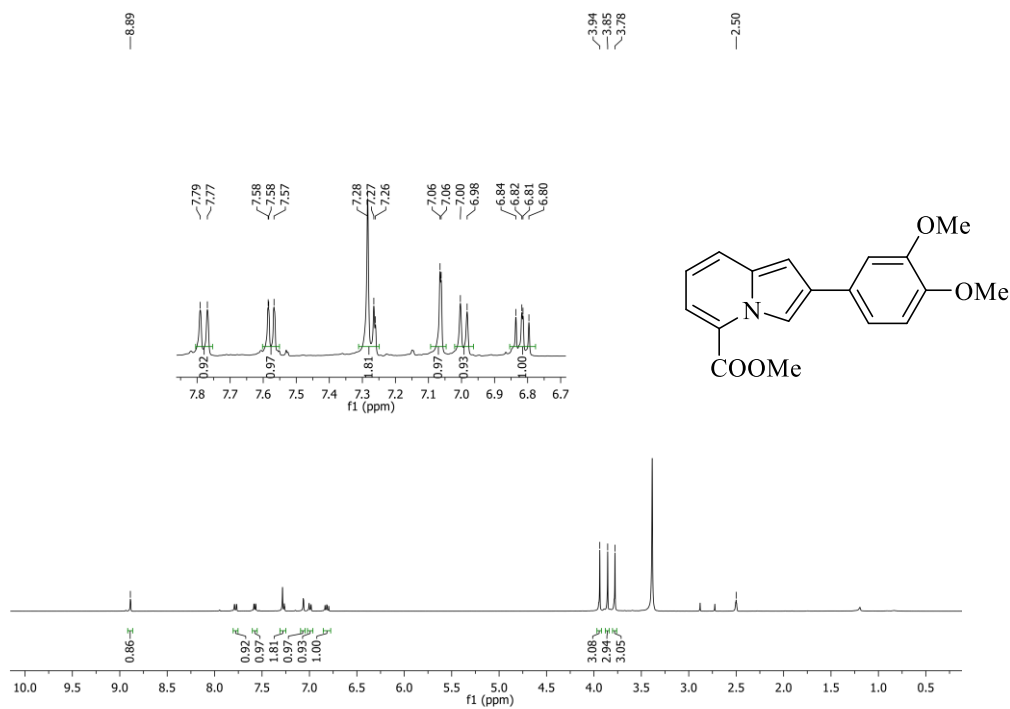
Compound **10a:** ^{13}C NMR (DMSO-d$_6$, 101 MHz).
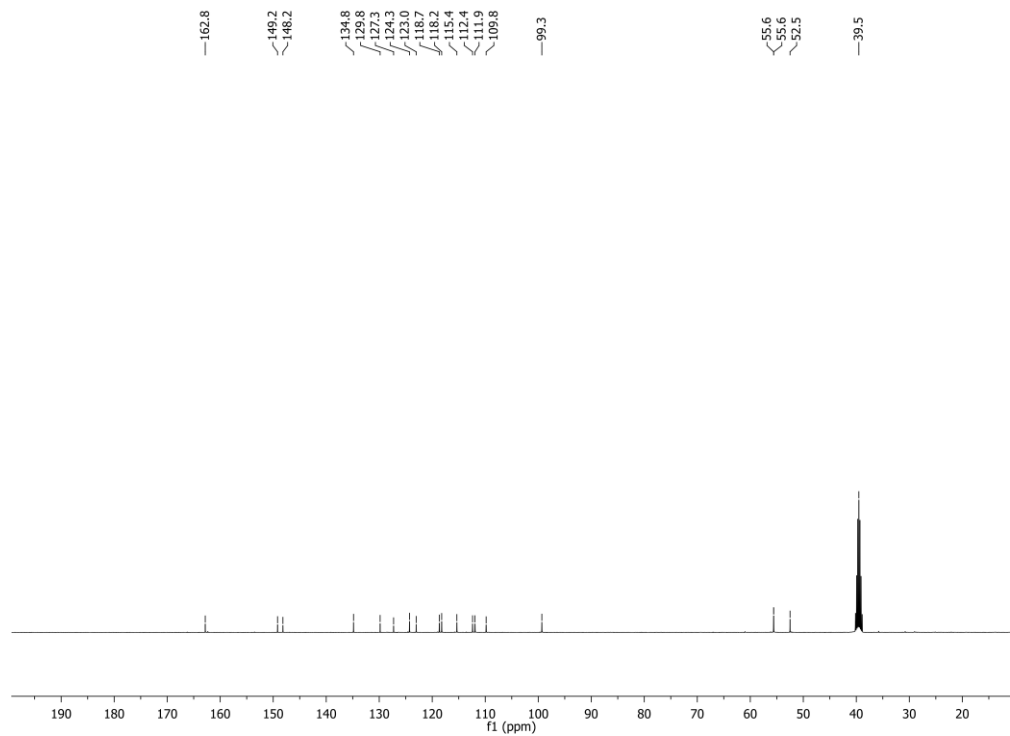
Compound **10d:** ^{1}H NMR (DMSO-d$_6$, 400 MHz).
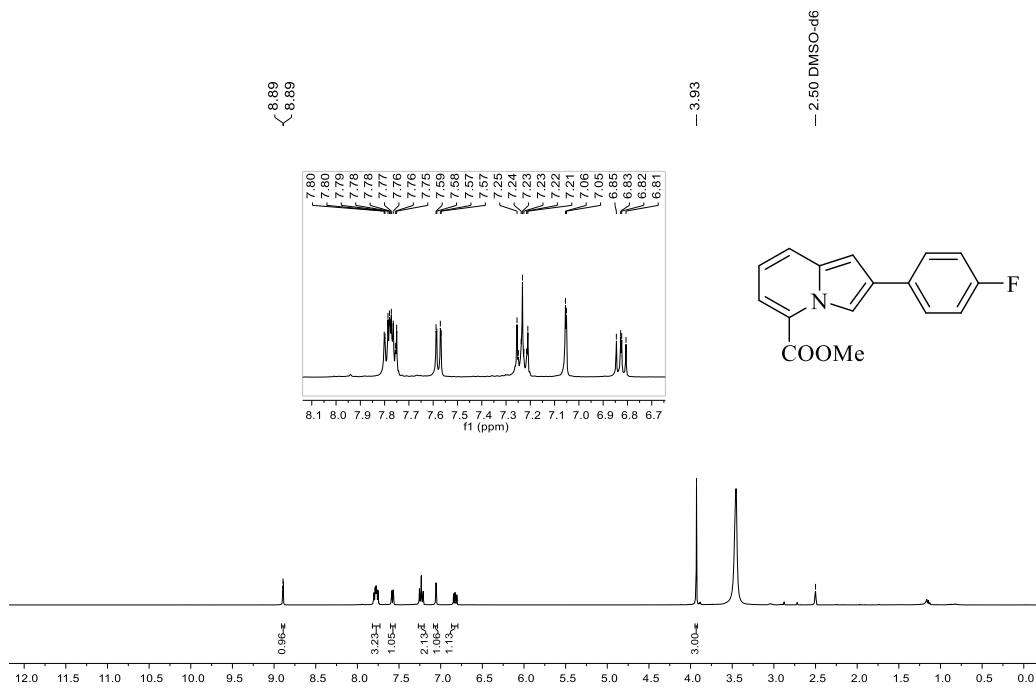
Compound **10c:** ^{13}C NMR (DMSO-d$_6$, 101 MHz).
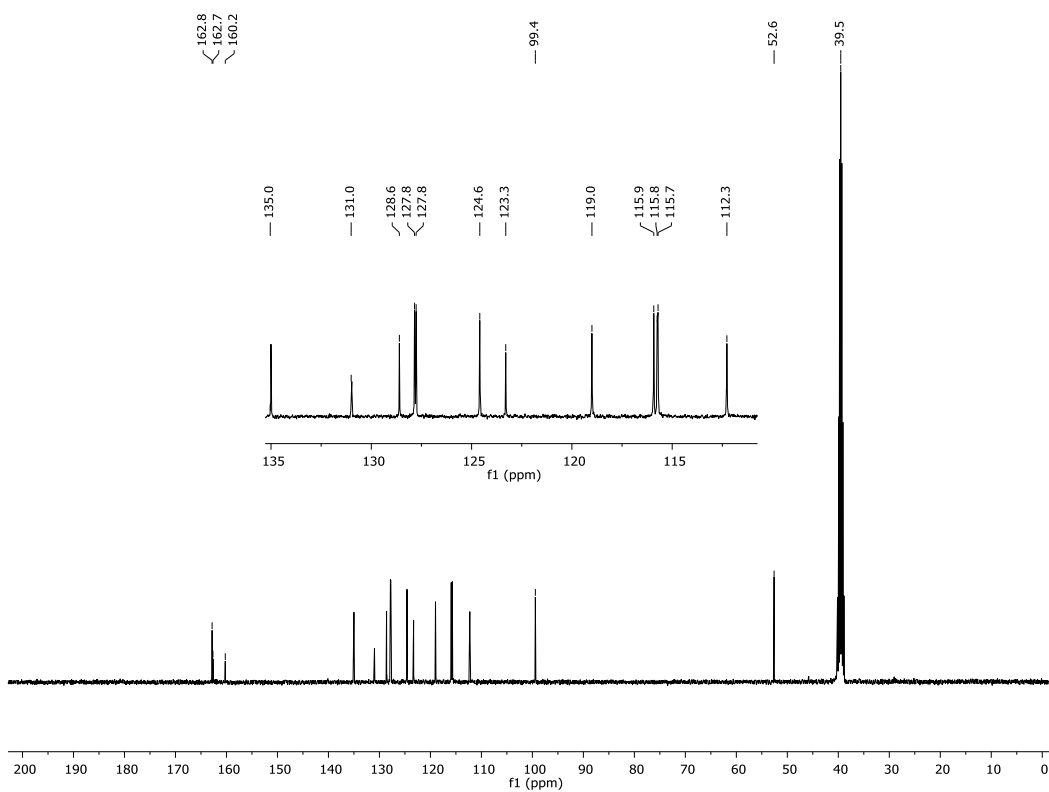
Compound **10e:** ^{1}H NMR (DMSO-d$_6$, 400 MHz).
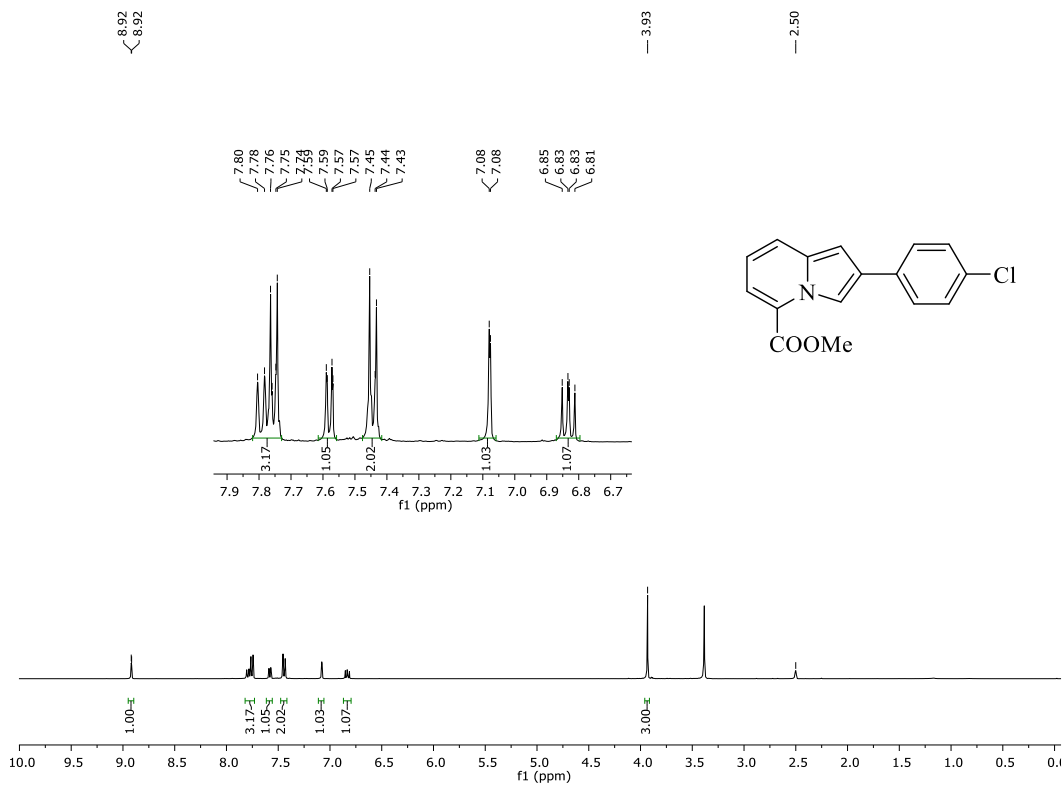
Compound **10e:** ^{13}C NMR (DMSO-d$_6$, 101 MHz).
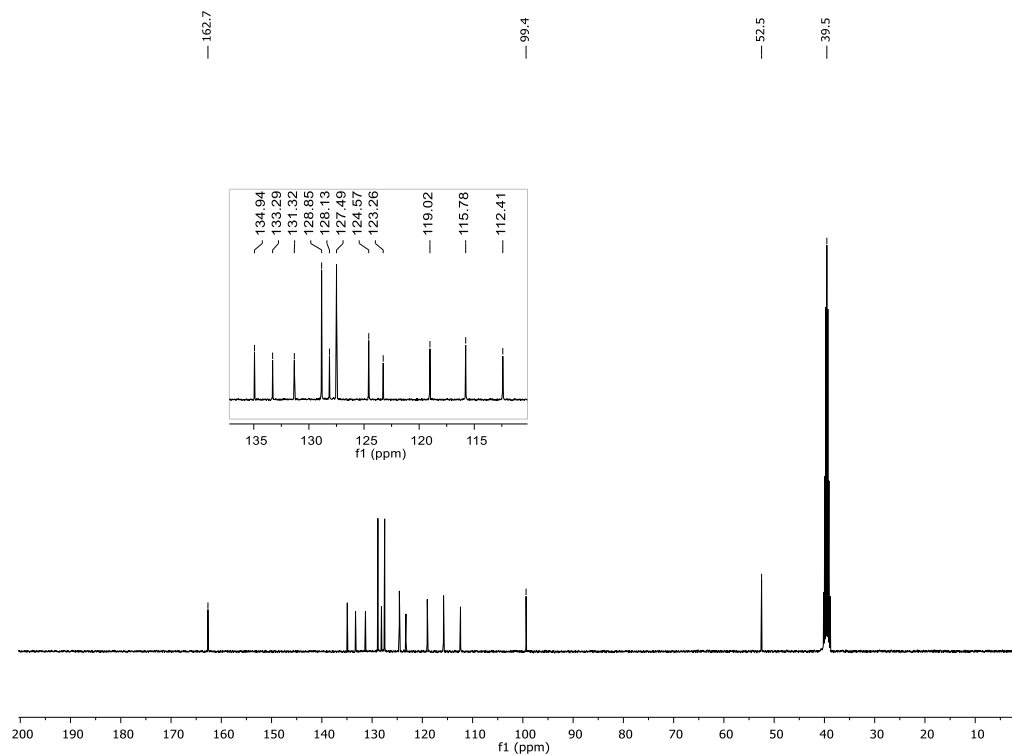
Compound **11a:** ^{1}H NMR (DMSO-d$_6$, 400 MHz).
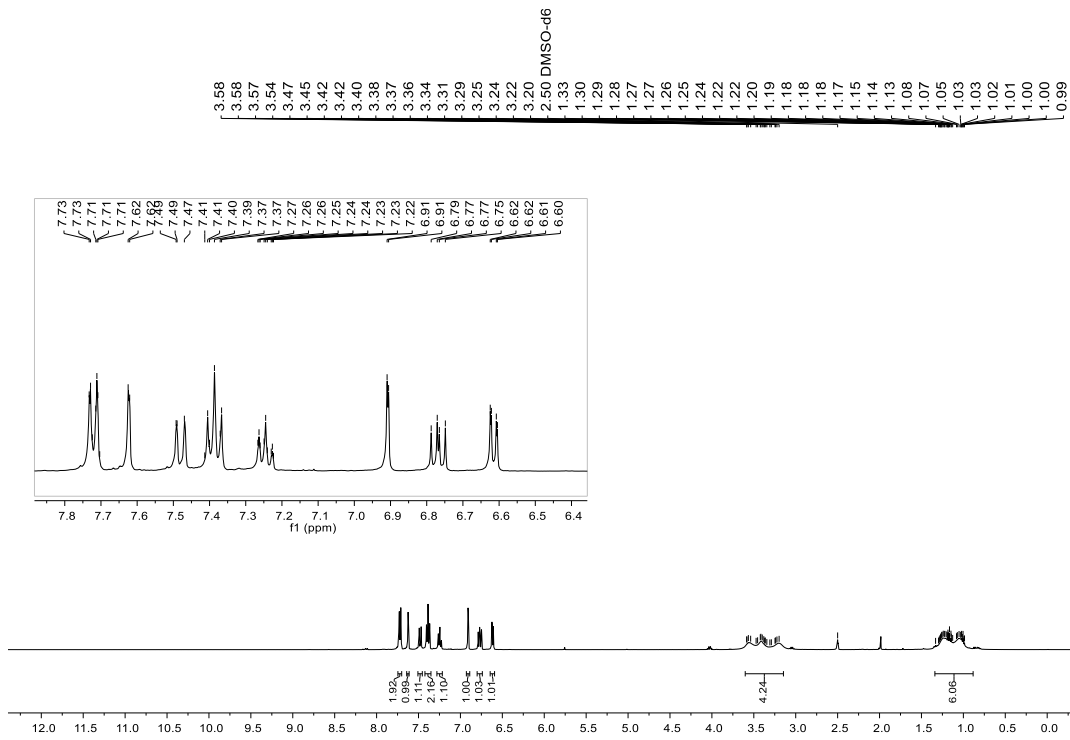
Compound **11a:** ^{13}C NMR (DMSO-d$_6$, 101 MHz).
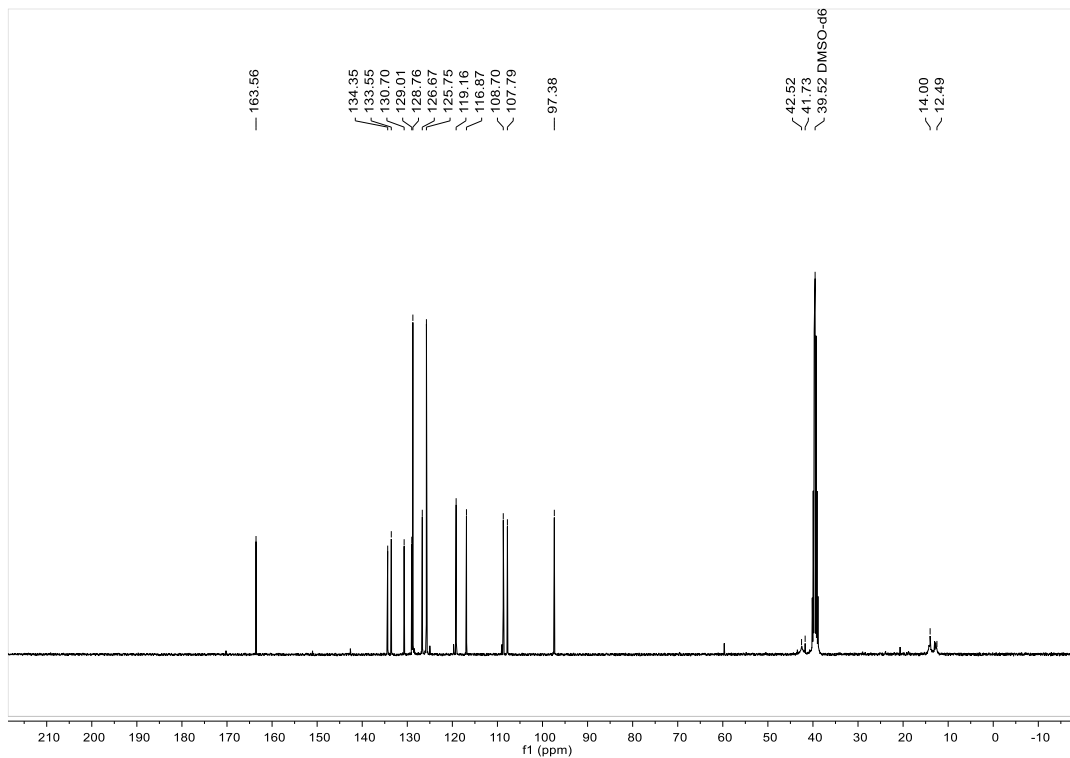
Compound **11b:** ^{1}H NMR (DMSO-d$_6$, 400 MHz).
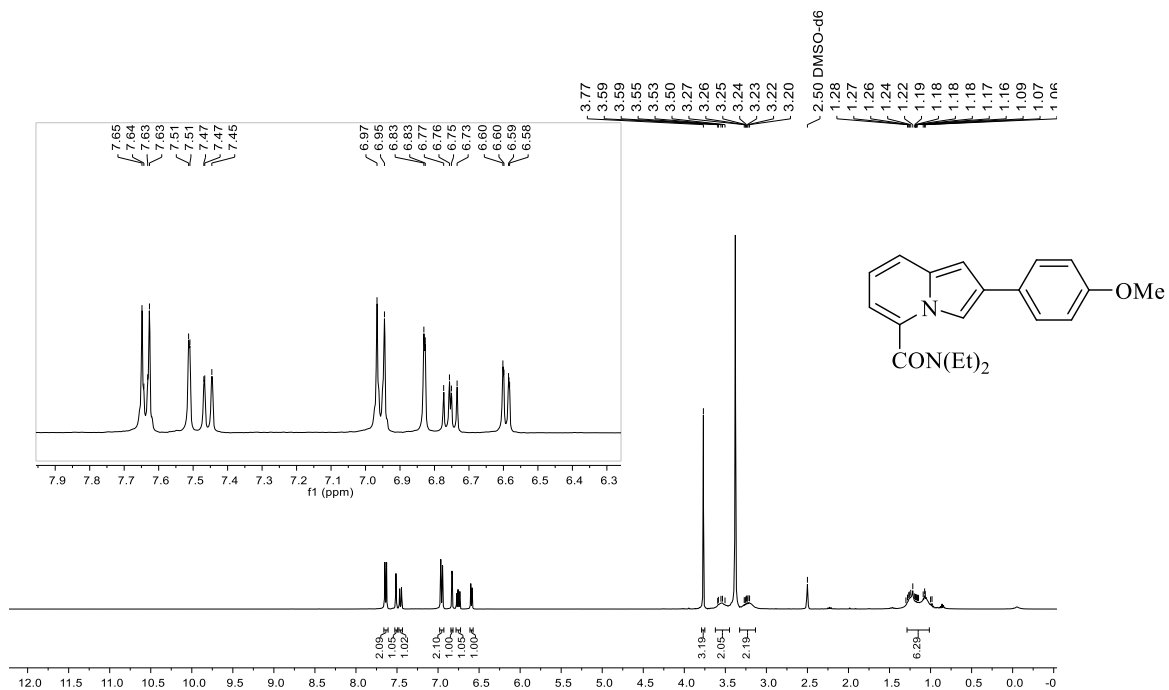
Compound **11b:** ^{13}C NMR (DMSO-d$_6$, 101 MHz).
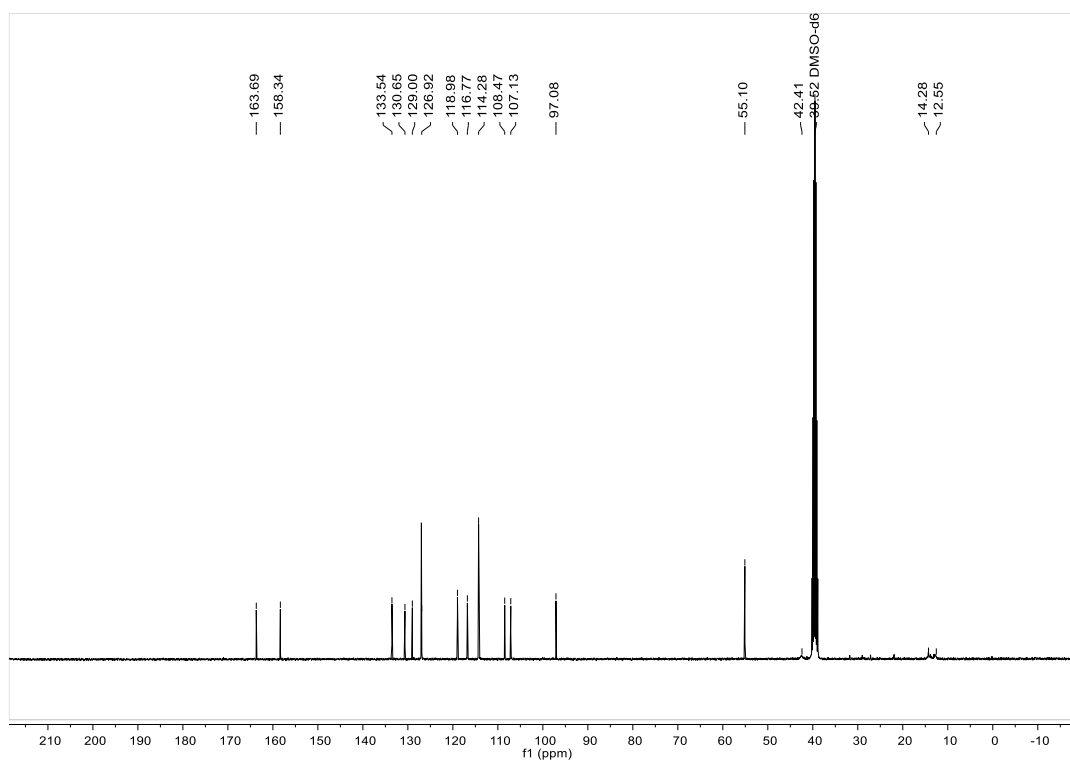
Compound **11c:** ^{1}H NMR (DMSO-d$_6$, 400 MHz).
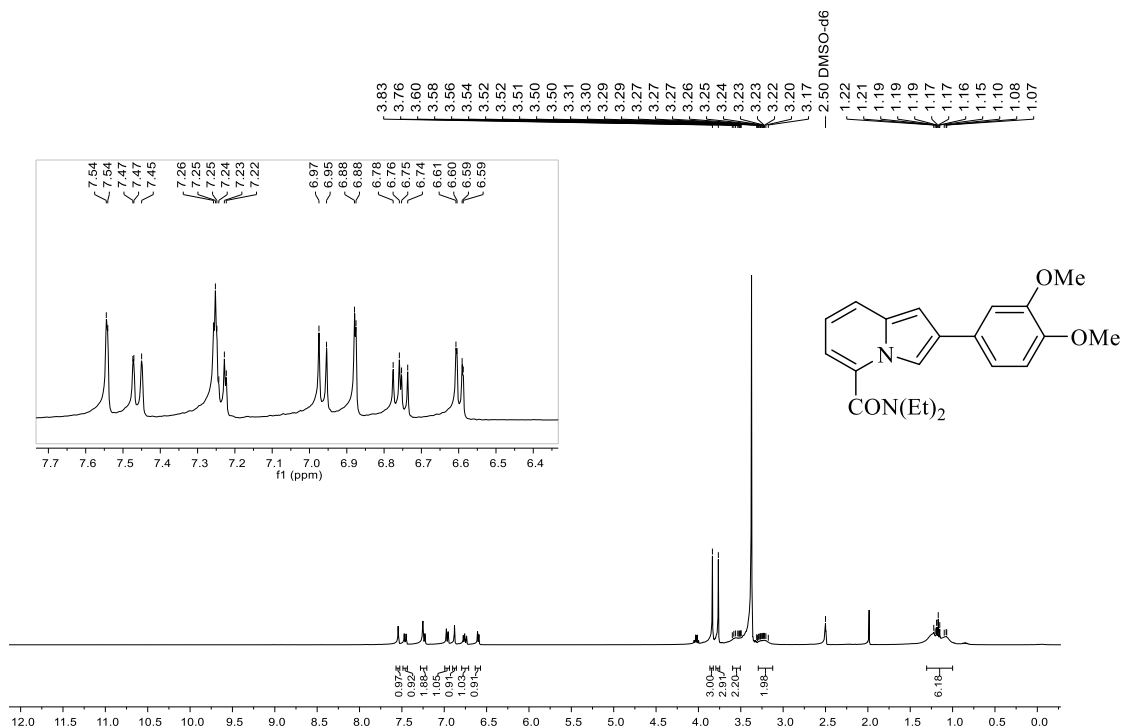
Compound **11c:** ^{13}C NMR (DMSO-d$_6$, 101 MHz).
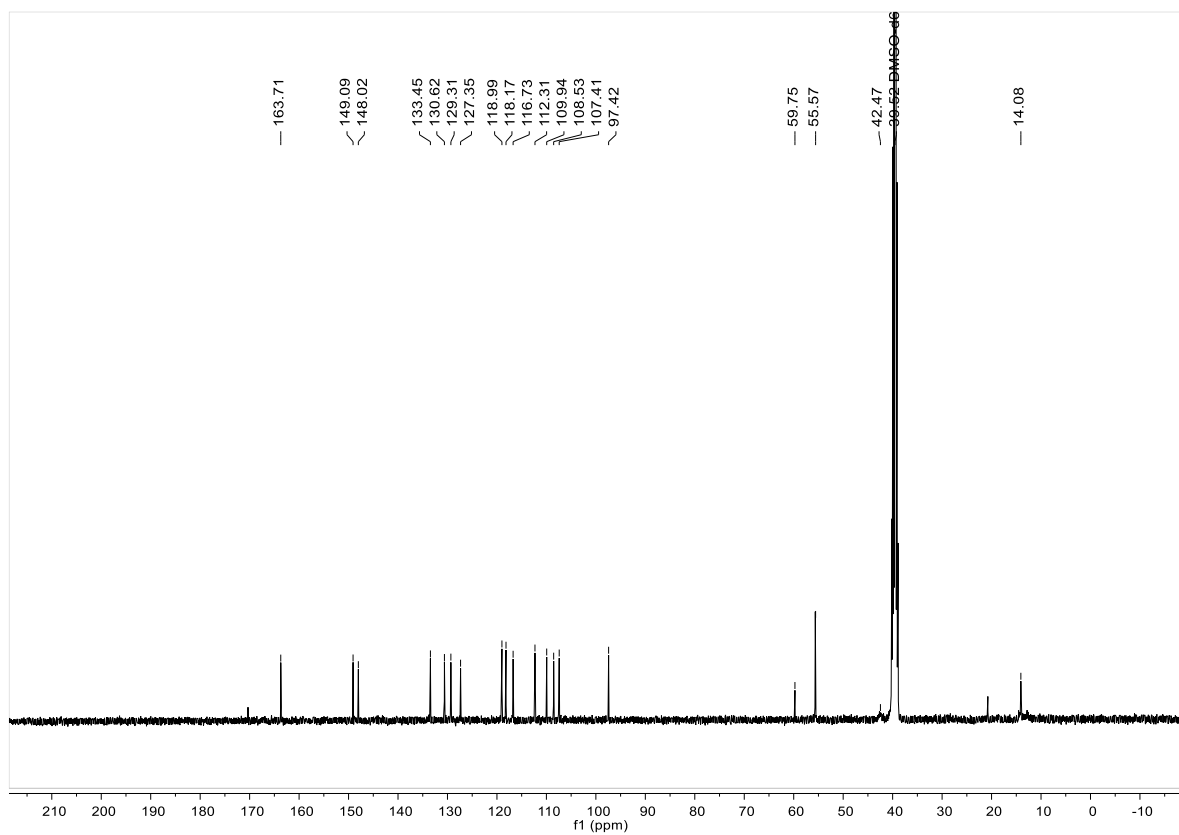
Compound **11d:** ^{1}H NMR (DMSO-d$_6$, 500 MHz).
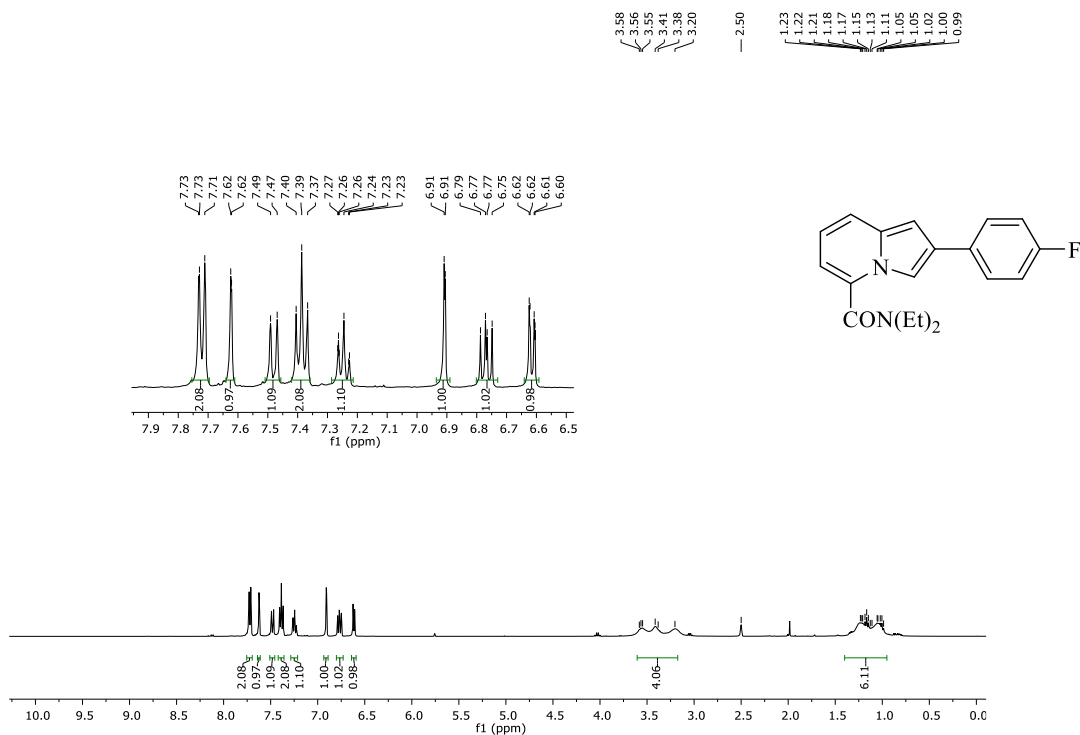
Compound **11d:** ^{13}C NMR (DMSO-d$_6$, 126 MHz).
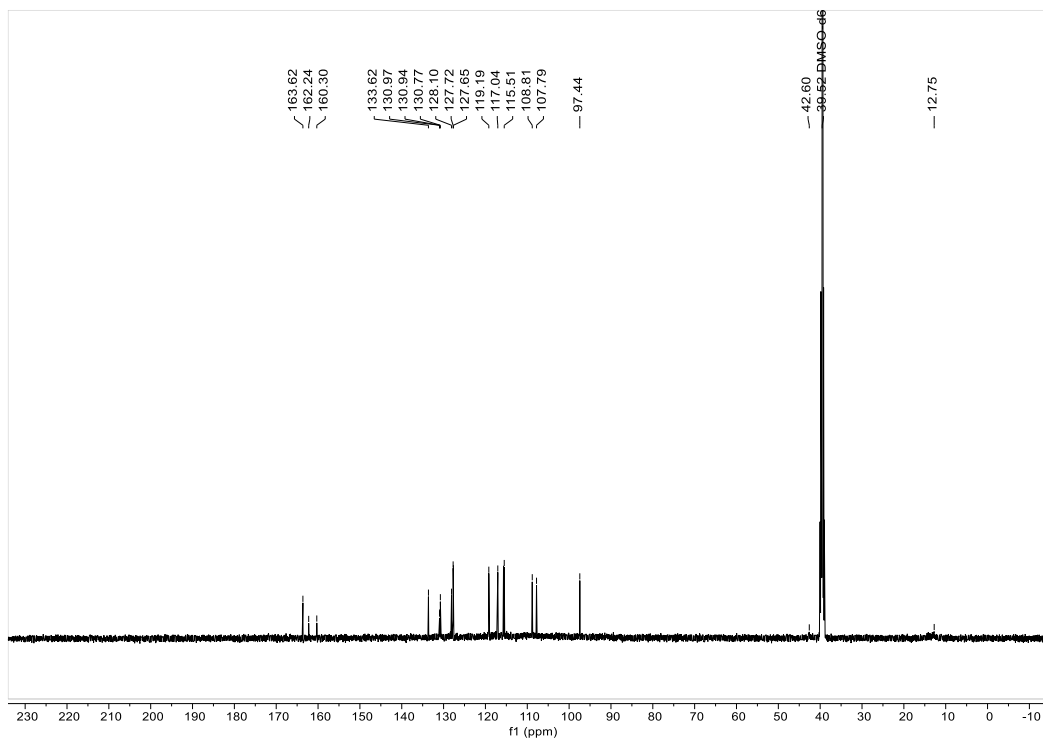
Compound **11e:** ^{1}H NMR (DMSO-d$_6$, 400 MHz).
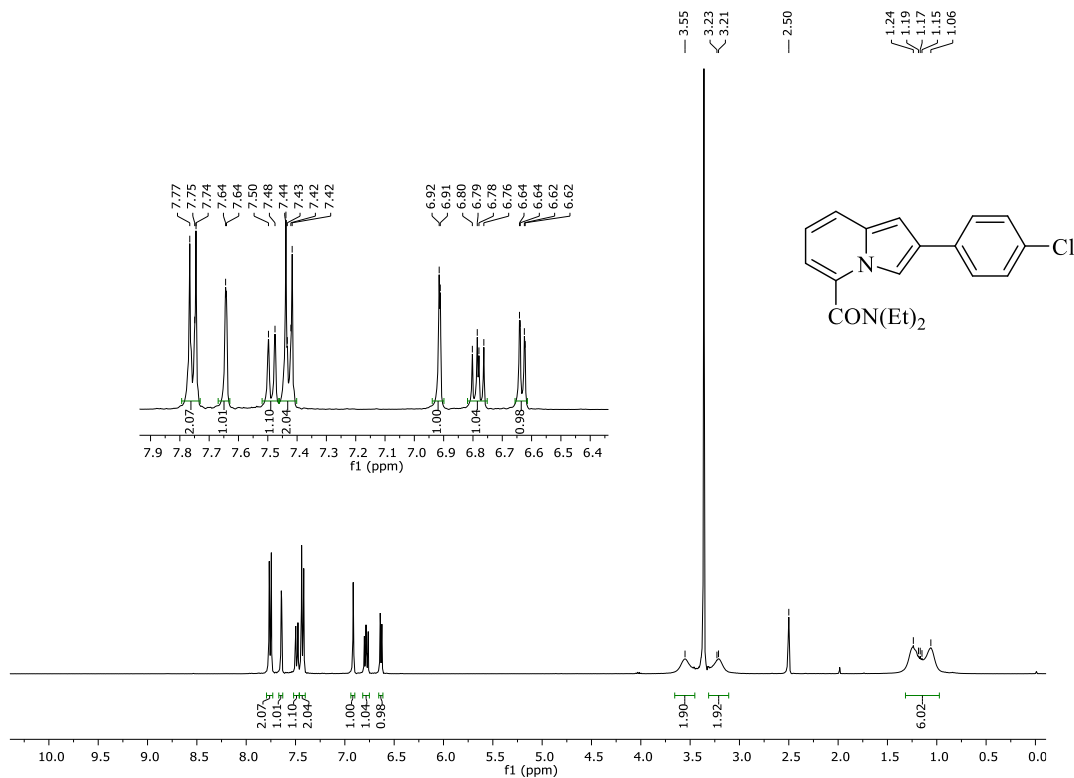
Compound **11e:** ^{13}C NMR (DMSO-d$_6$, 101 MHz).
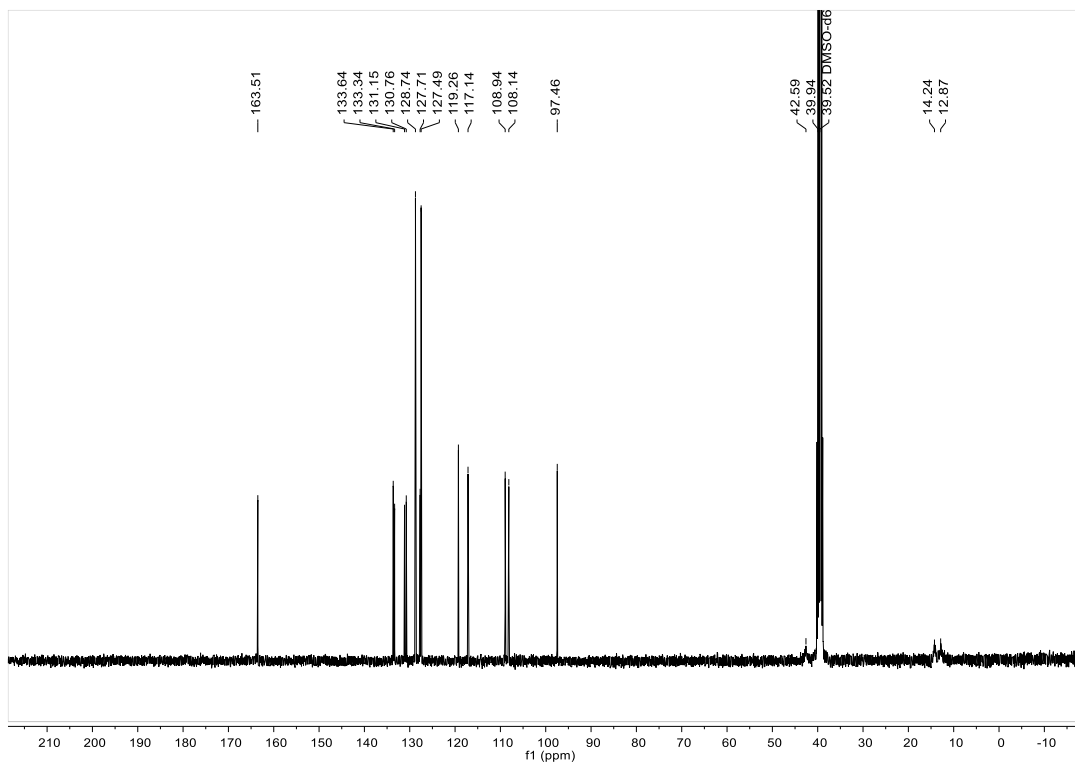
Compound **12**: ¹H NMR (600 MHz, CDCl₃).
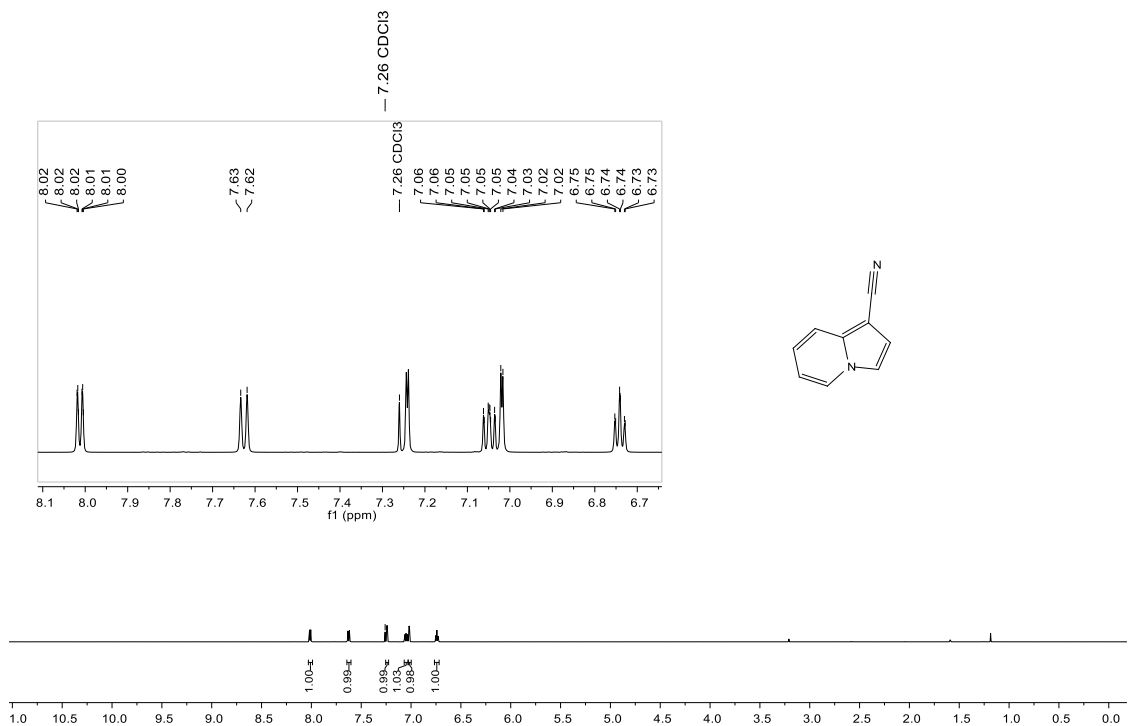
Compound **12**: ¹³C NMR (151 MHz, CDCl₃).
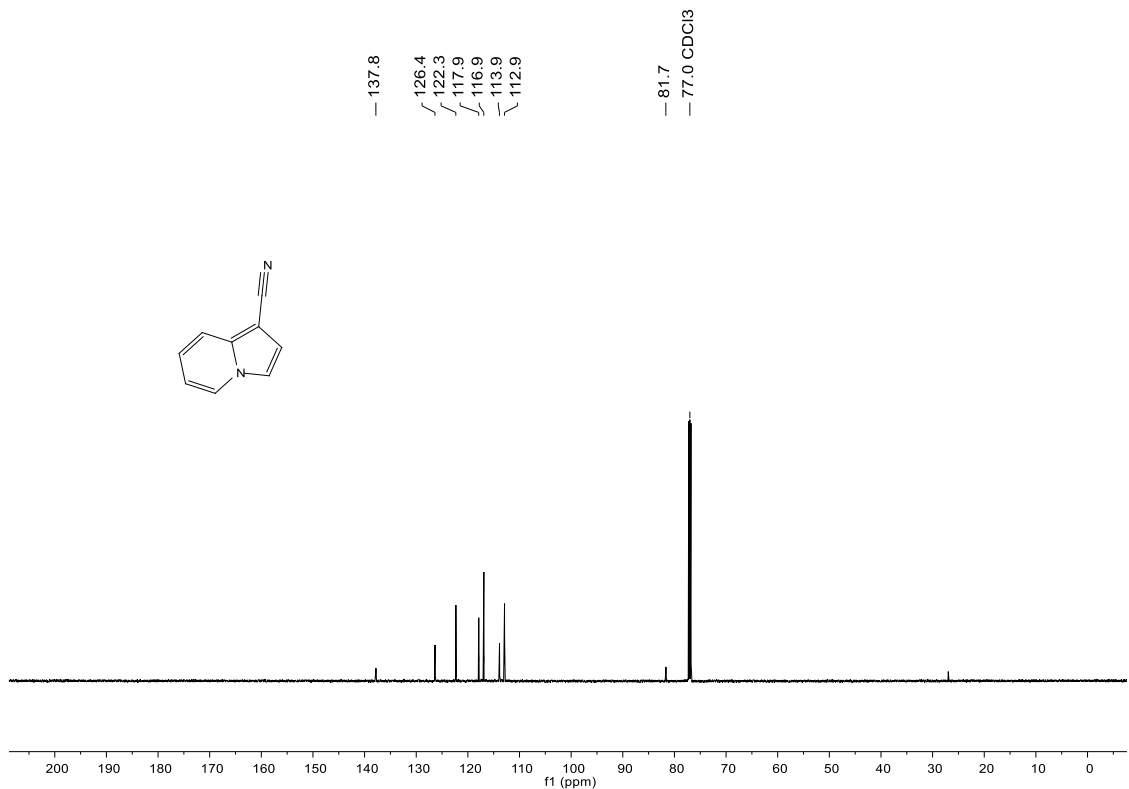
Compound **12**: NOESY (^{1}H NMR 600 MHz, CDCl$_3$; ^{13}C NMR 151 MHz, CDCl$_3$).
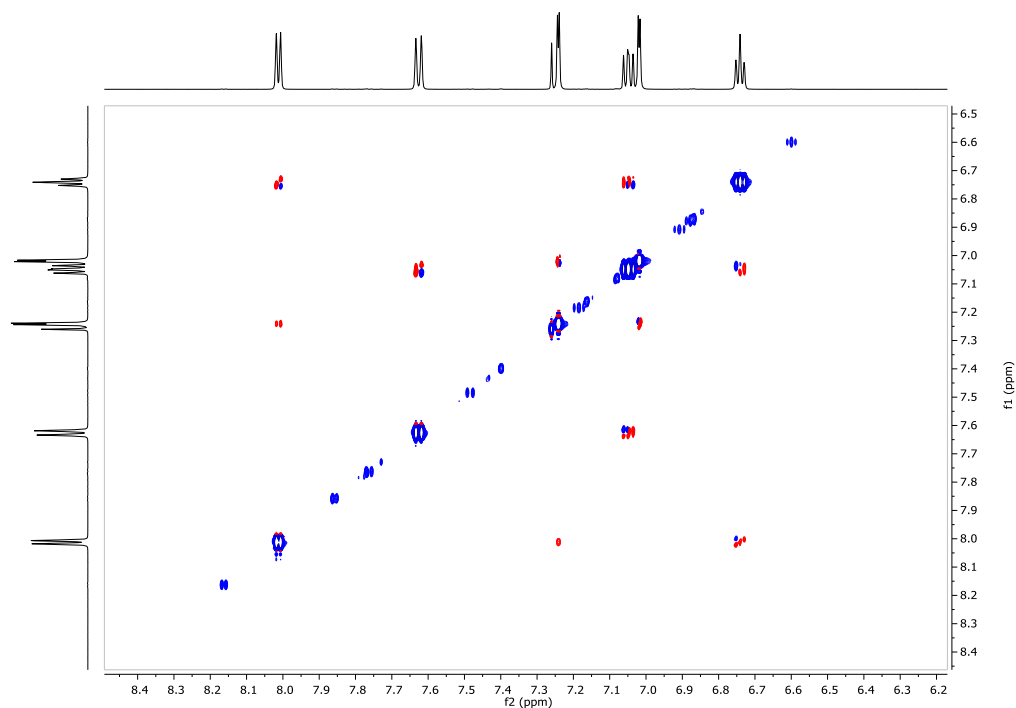
Compound **12**: HSQC (^{1}H NMR 600 MHz, CDCl$_3$; ^{13}C NMR 151 MHz, CDCl$_3$).
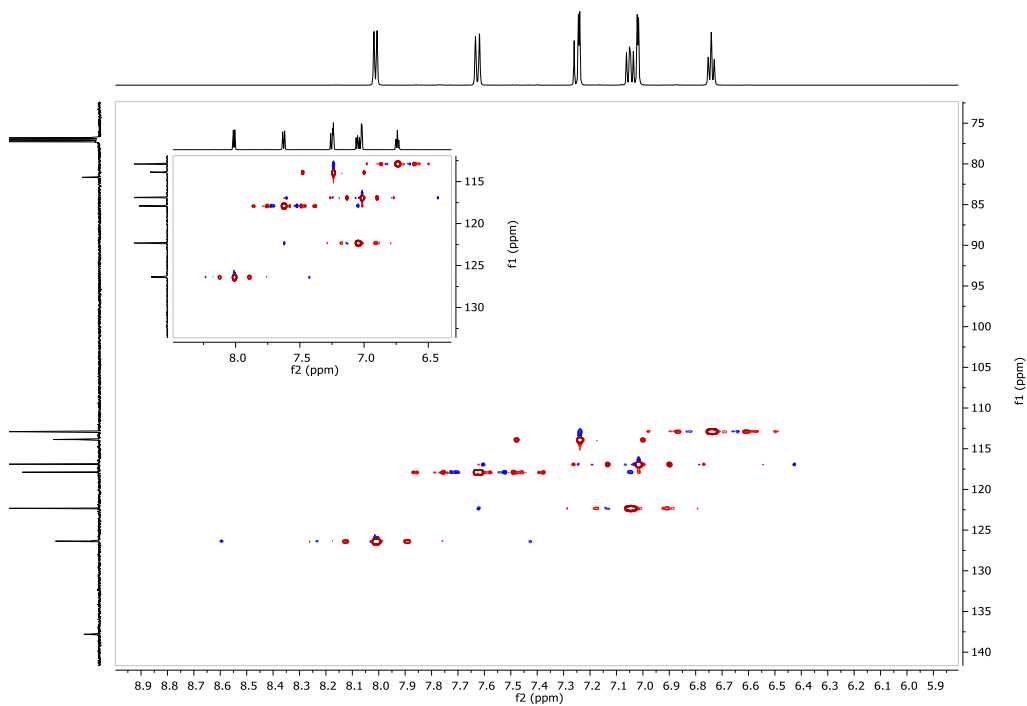
Compound **12: HMBC** (¹H NMR 600 MHz, CDCl₃ ; ¹³C NMR 151 MHz, CDCl₃).
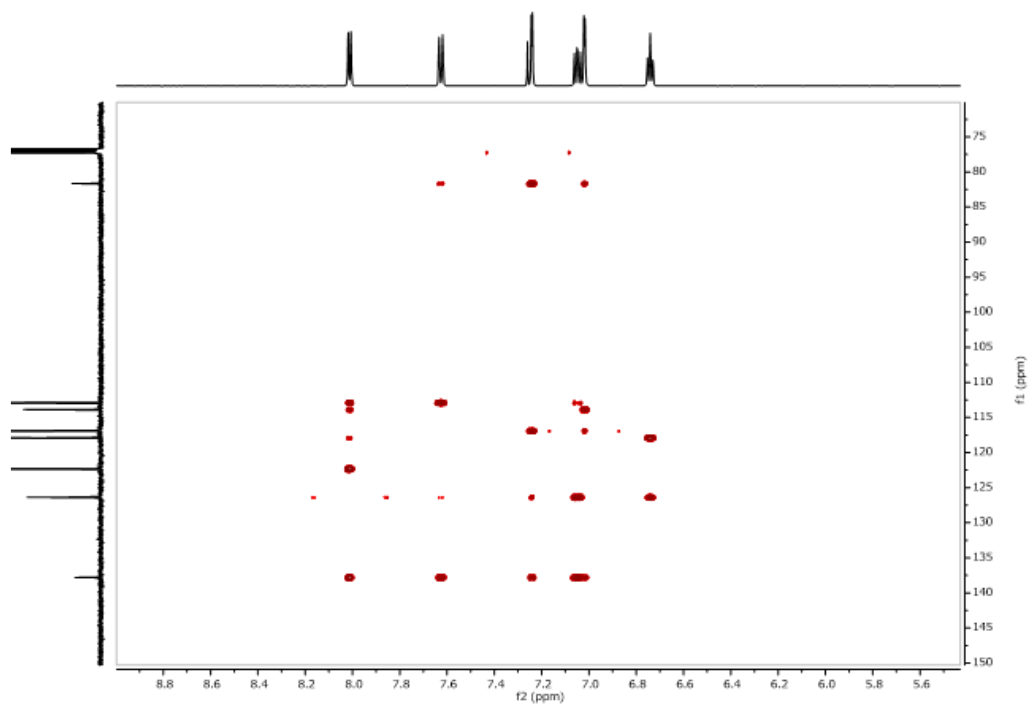
Compound **13a:** ^{1}H NMR (600 MHz, CDCl$_3$).
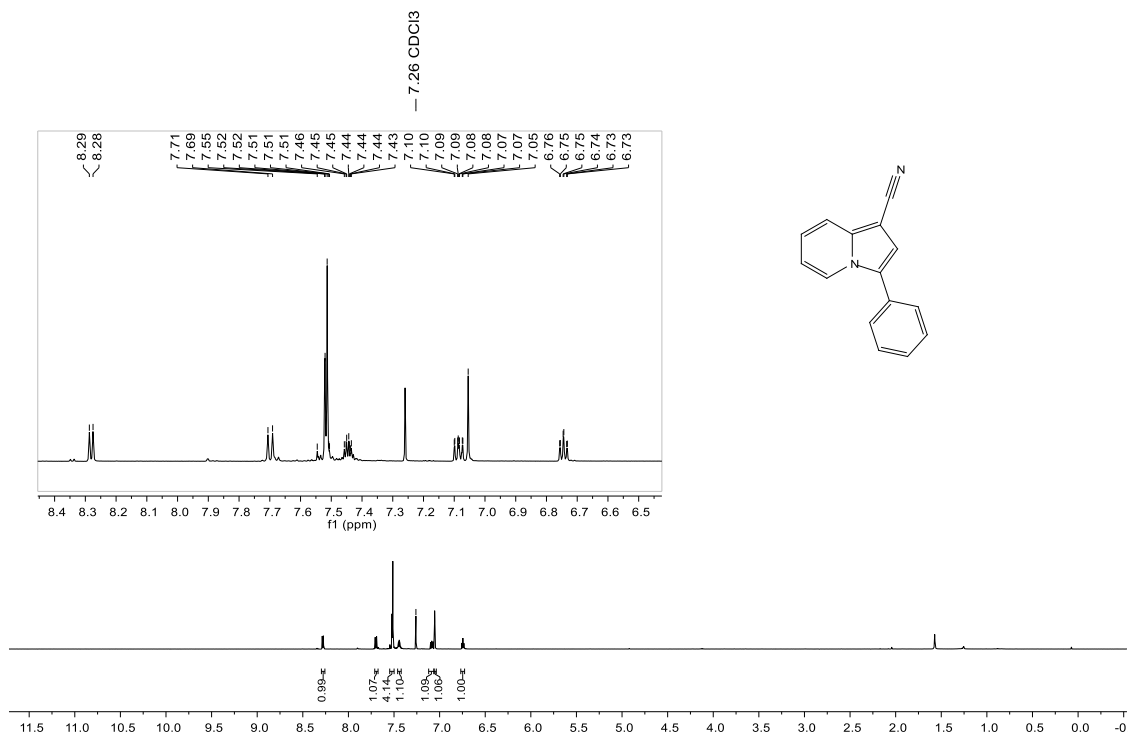
Compound **13a:** ^{13}C NMR (151 MHz, CDCl$_3$).
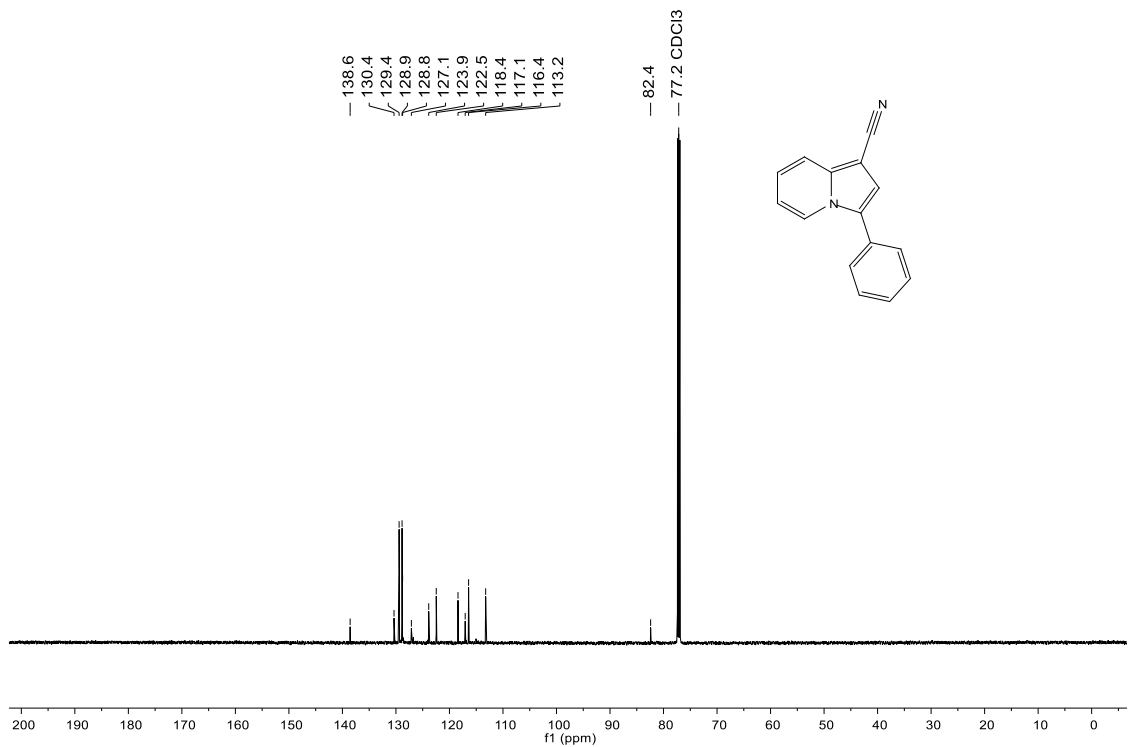
Compound **13a**: NOESY (^{1}H NMR 600 MHz, CDCl$_3$; ^{13}C NMR 151 MHz, CDCl$_3$).
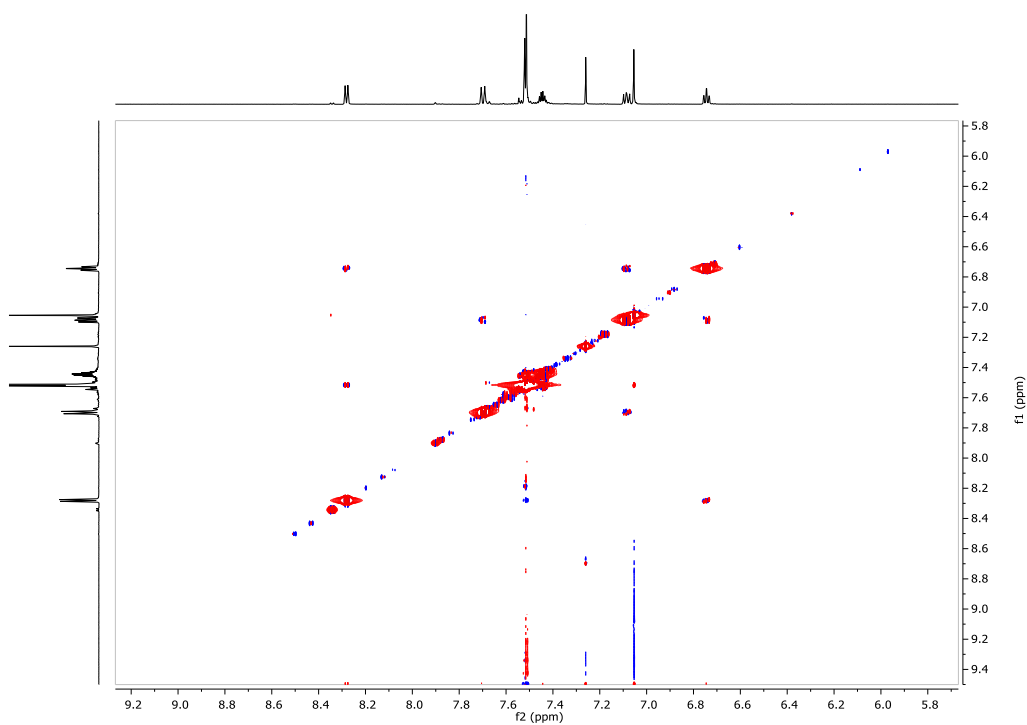
Compound **13a**: HSQC (^{1}H NMR 600 MHz, CDCl$_3$; ^{13}C NMR 151 MHz, CDCl$_3$).
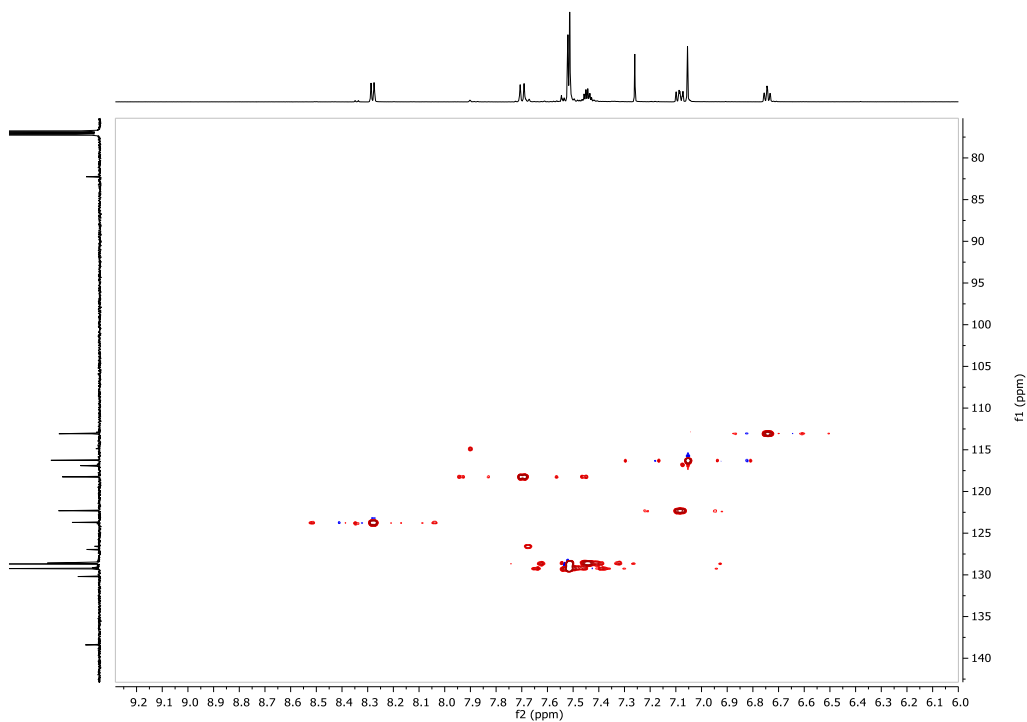
Compound **13a: HMBC** (^{1}H NMR 600 MHz, CDCl$_3$; ^{13}C NMR 151 MHz, CDCl$_3$).
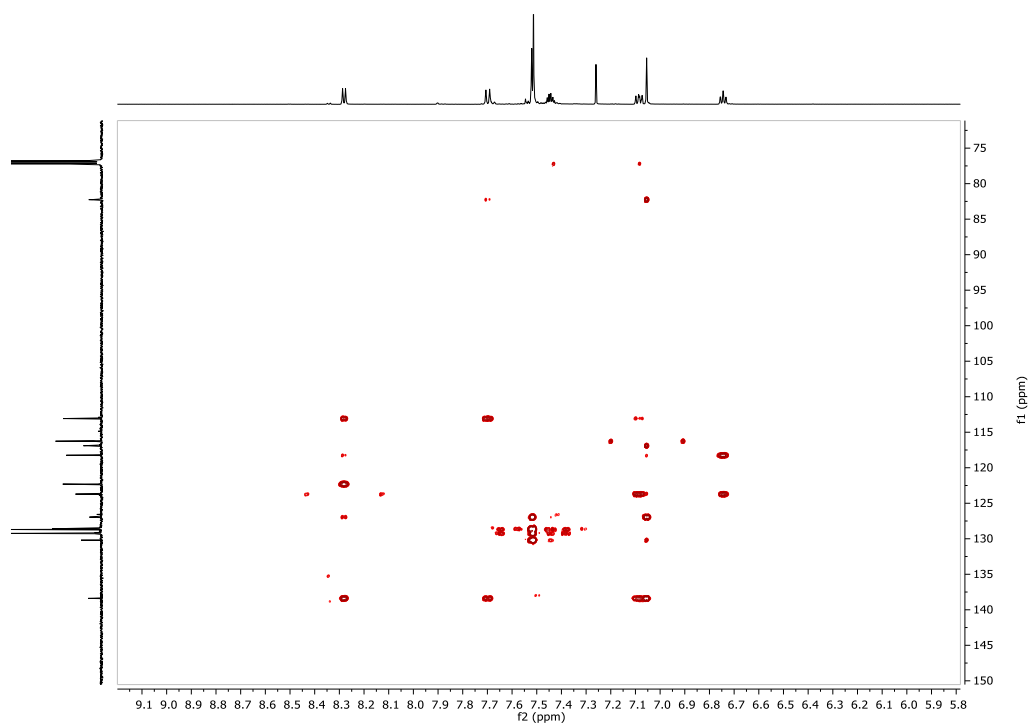
Compound **13b:** ^{1}H NMR (400 MHz, CDCl$_3$).
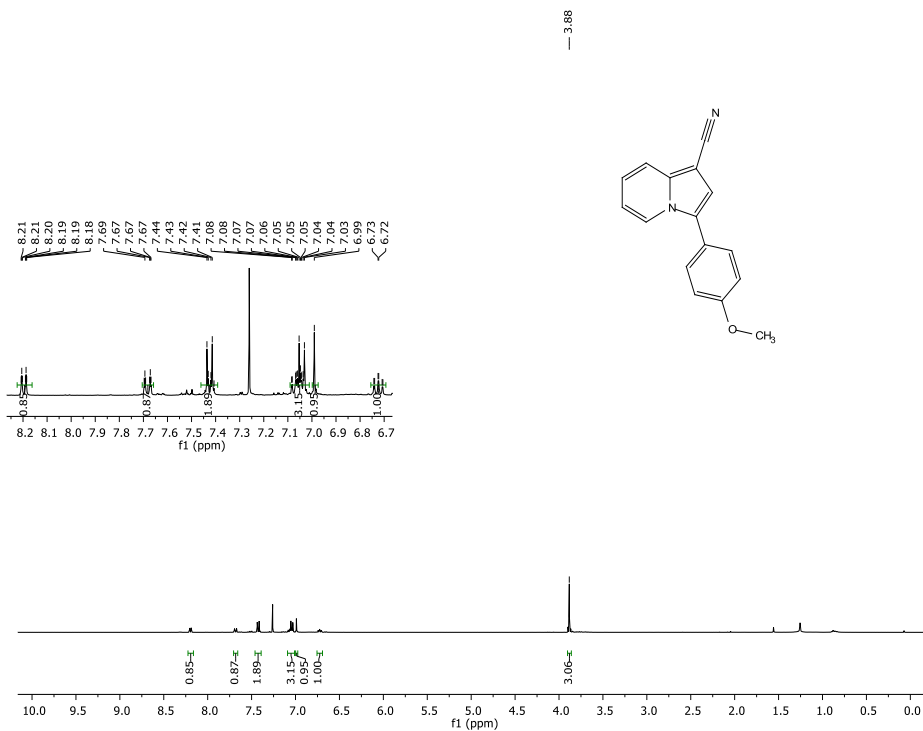
Compound **13b:** ^{13}C NMR (101 MHz, CDCl$_3$).
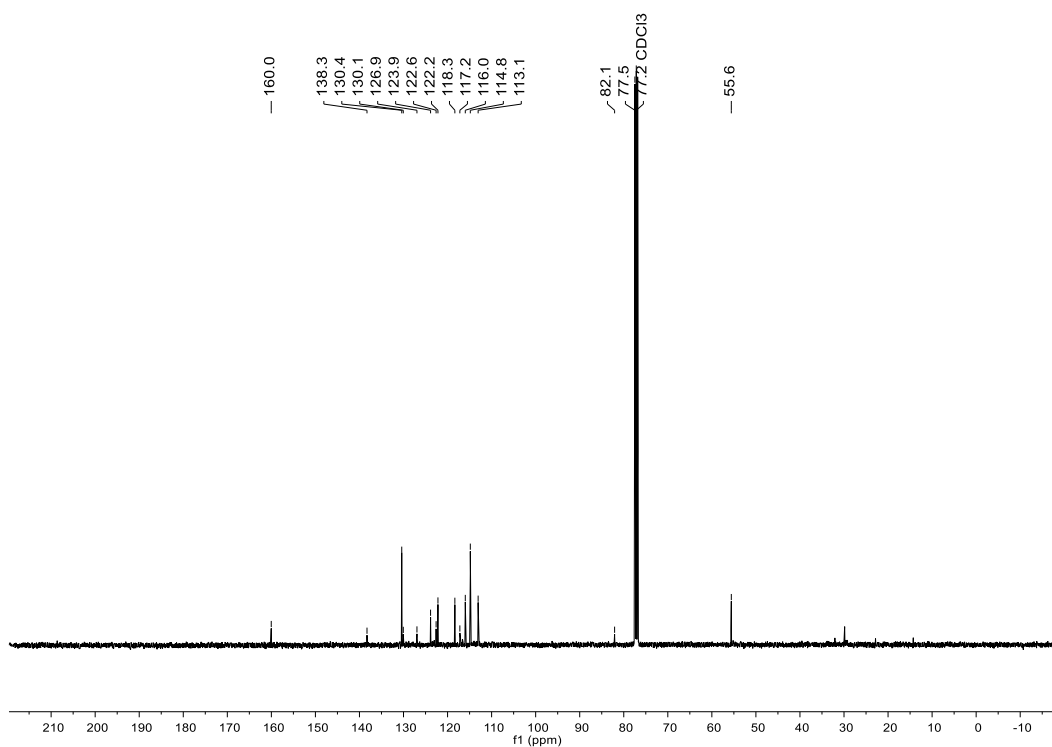
Compound **14a:** ^{1}H NMR (600 MHz, CDCl$_3$).
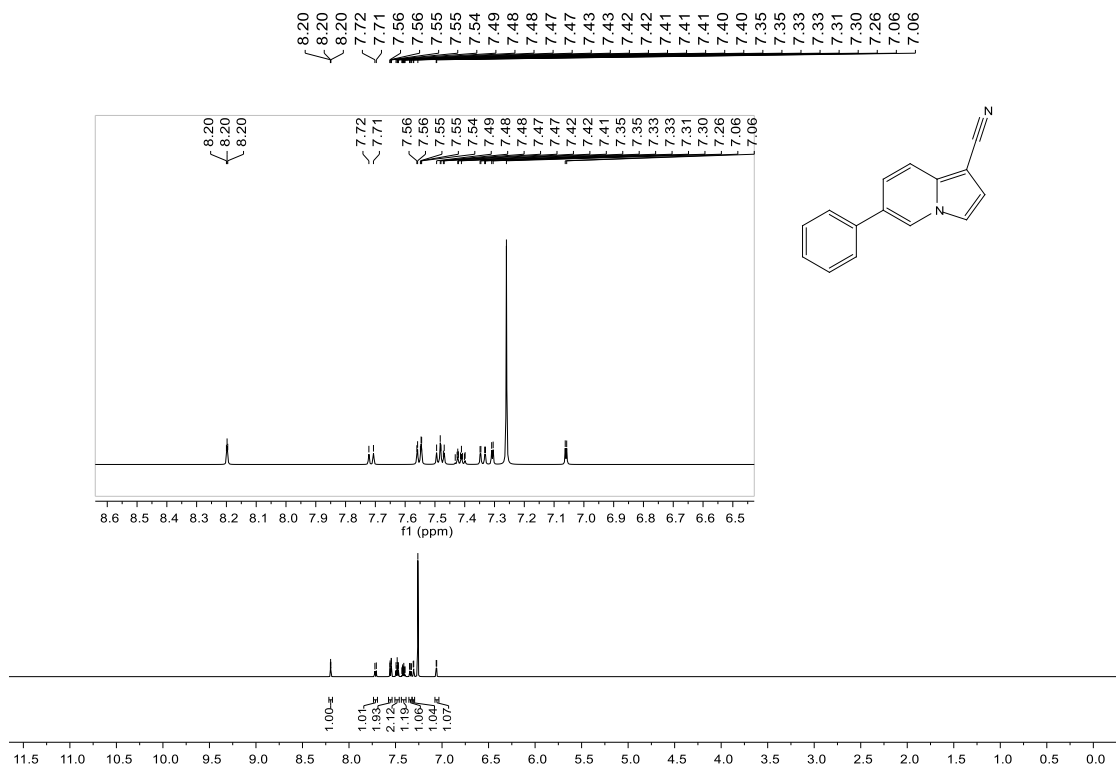
Compound **14a:** ^{13}C NMR (151 MHz, CDCl$_3$).
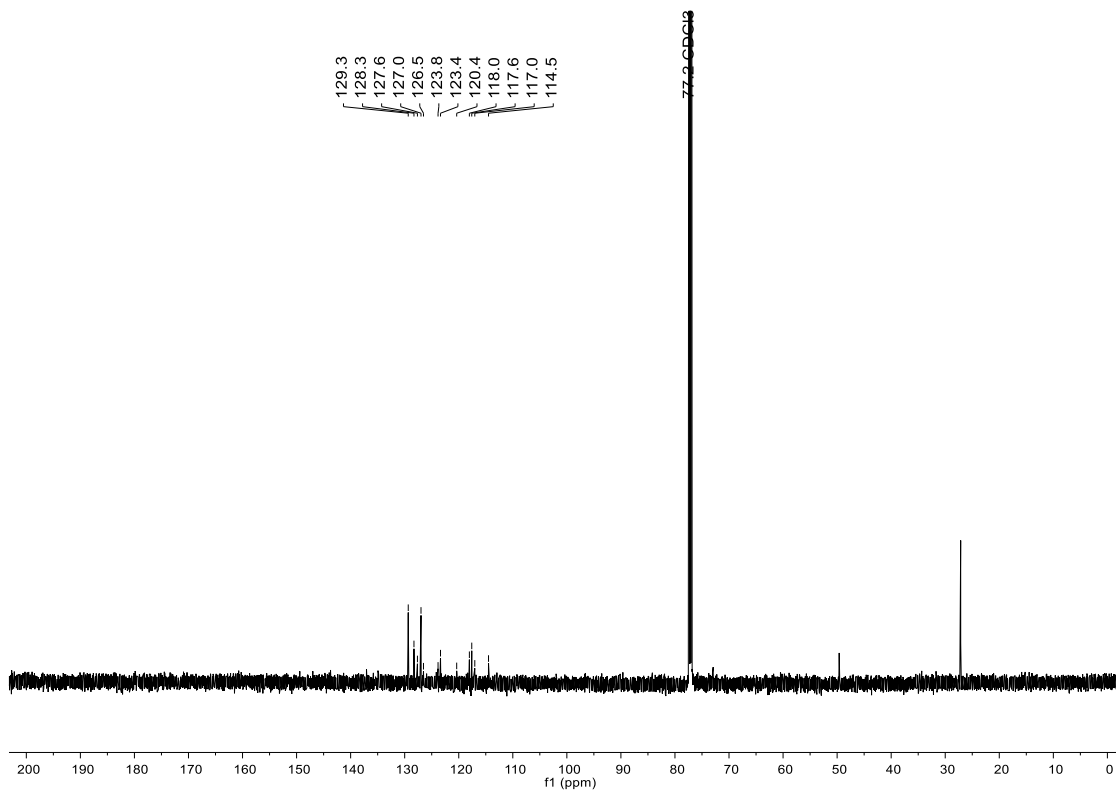
Compound **14a**: NOESY (^{1}H NMR 600 MHz, CDCl$_3$; ^{13}C NMR 151 MHz, CDCl$_3$).
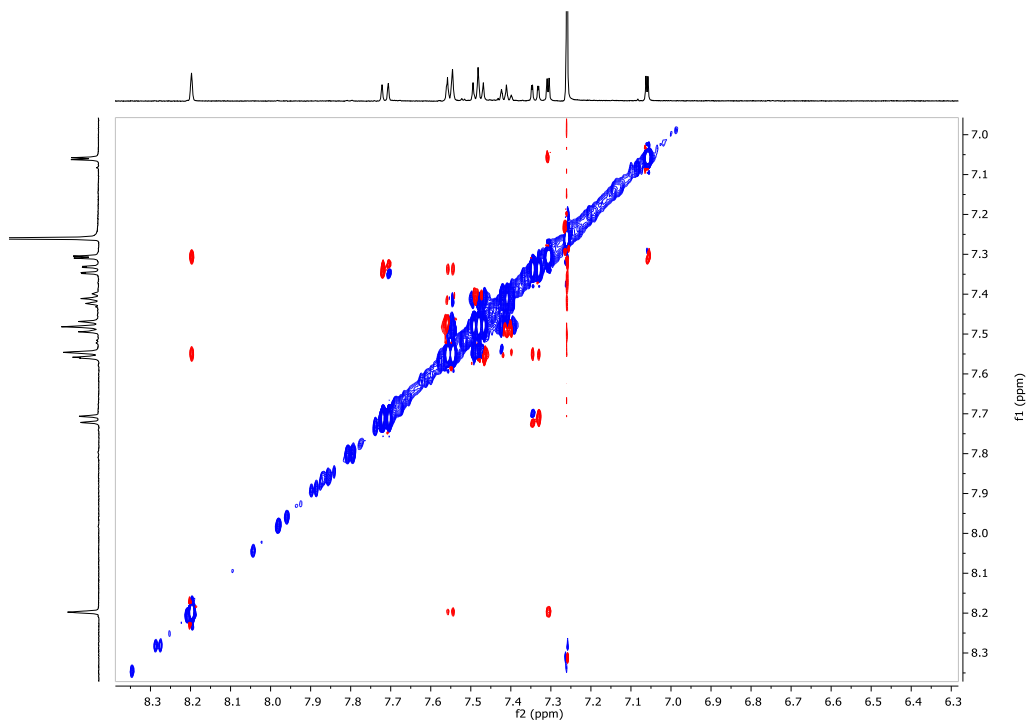
Compound **14a**: HSQC (^{1}H NMR 600 MHz, CDCl$_3$; ^{13}C NMR 151 MHz, CDCl$_3$).
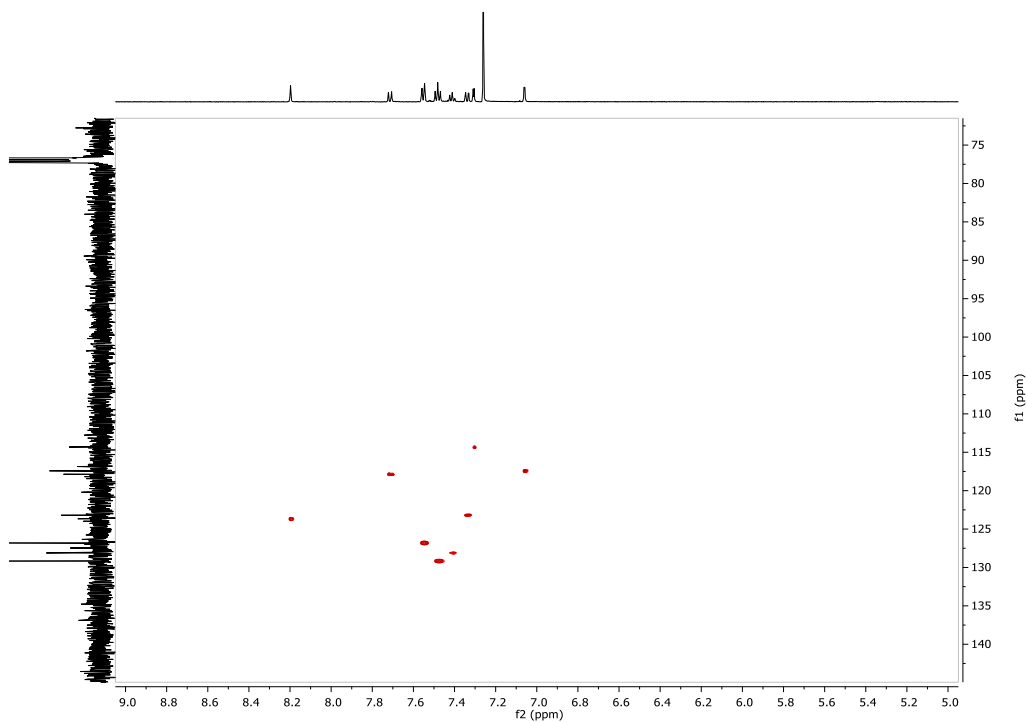
Compound **13c:** ^{1}H NMR (700 MHz, CDCl$_3$).
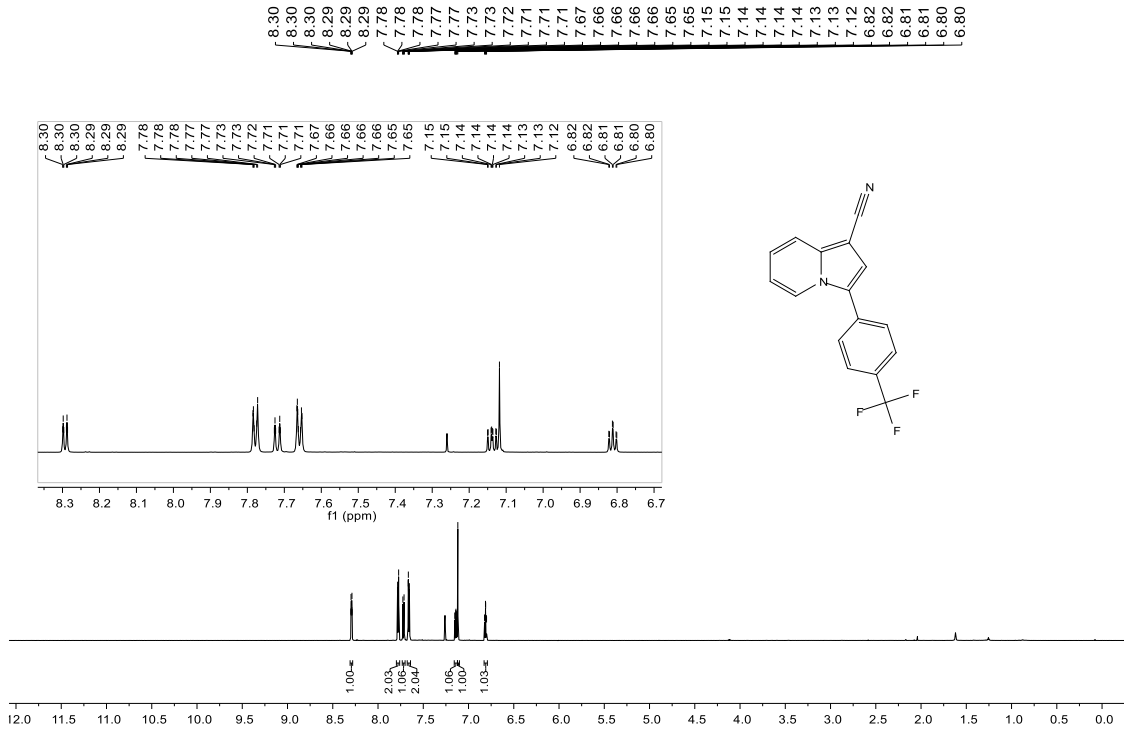
Compound **13c:** ^{13}C NMR (176 MHz, CDCl$_3$).
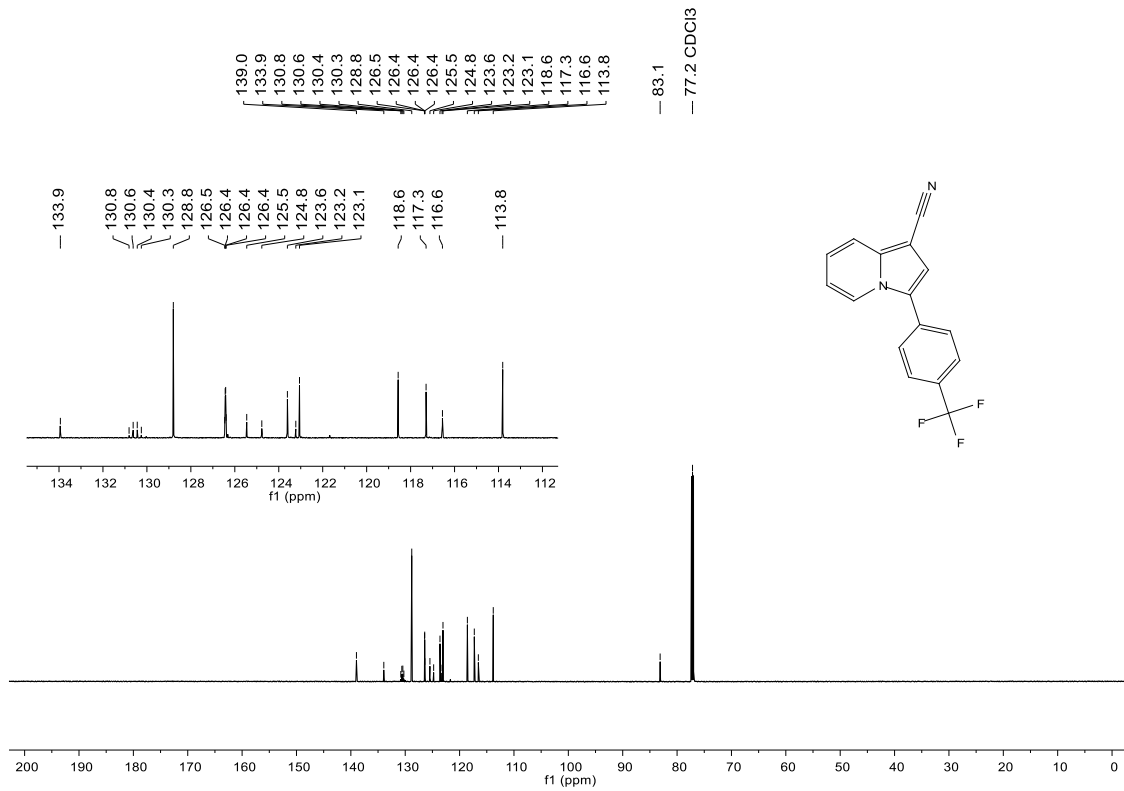
Compound **13c**: NOESY (^{1}H NMR 700 MHz, CDCl$_3$; ^{13}C NMR 176 MHz, CDCl$_3$).
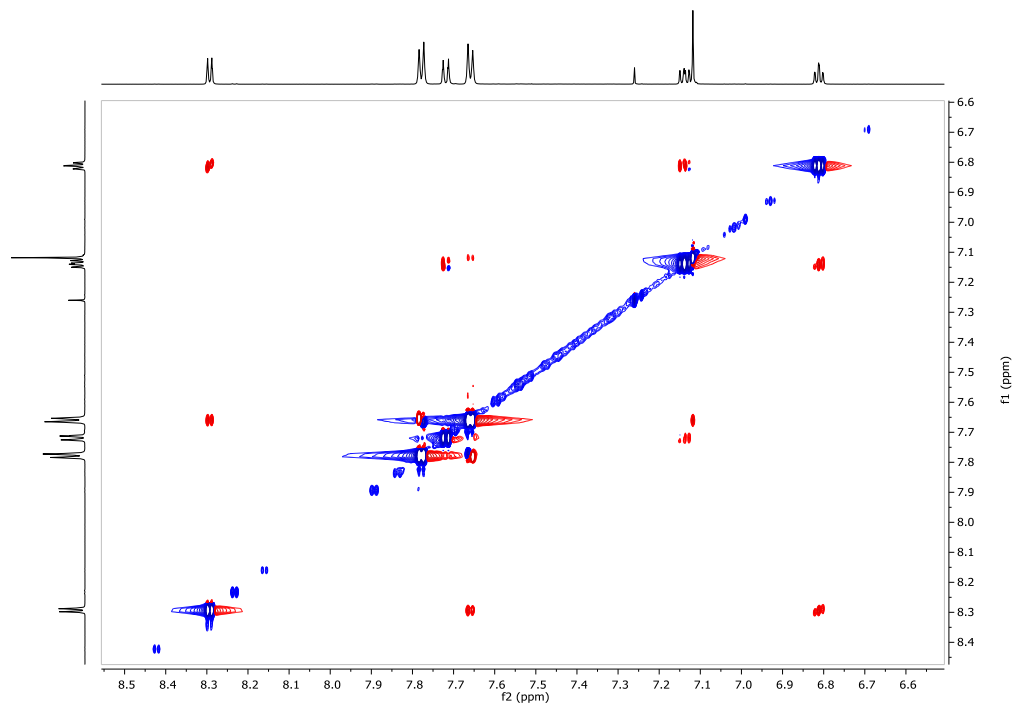
Compound **13c**: HSQC (^{1}H NMR 700 MHz, CDCl$_3$; ^{13}C NMR 176 MHz, CDCl$_3$).
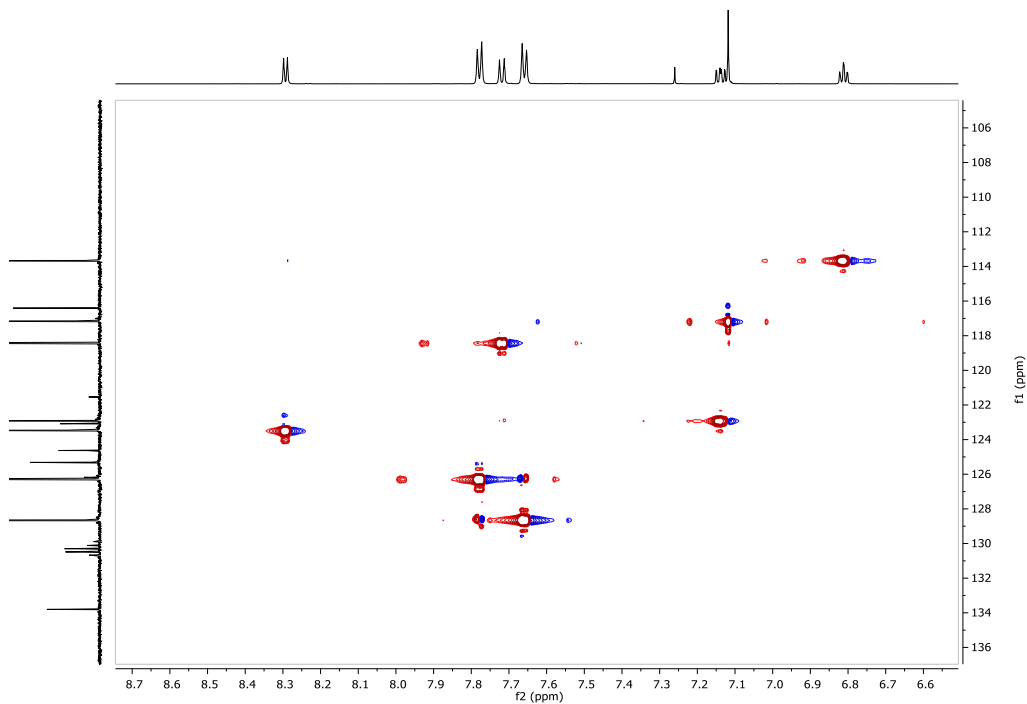
Compound **13c**: HMBC (^{1}H NMR 700 MHz, CDCl$_3$; ^{13}C NMR 176 MHz, CDCl$_3$).
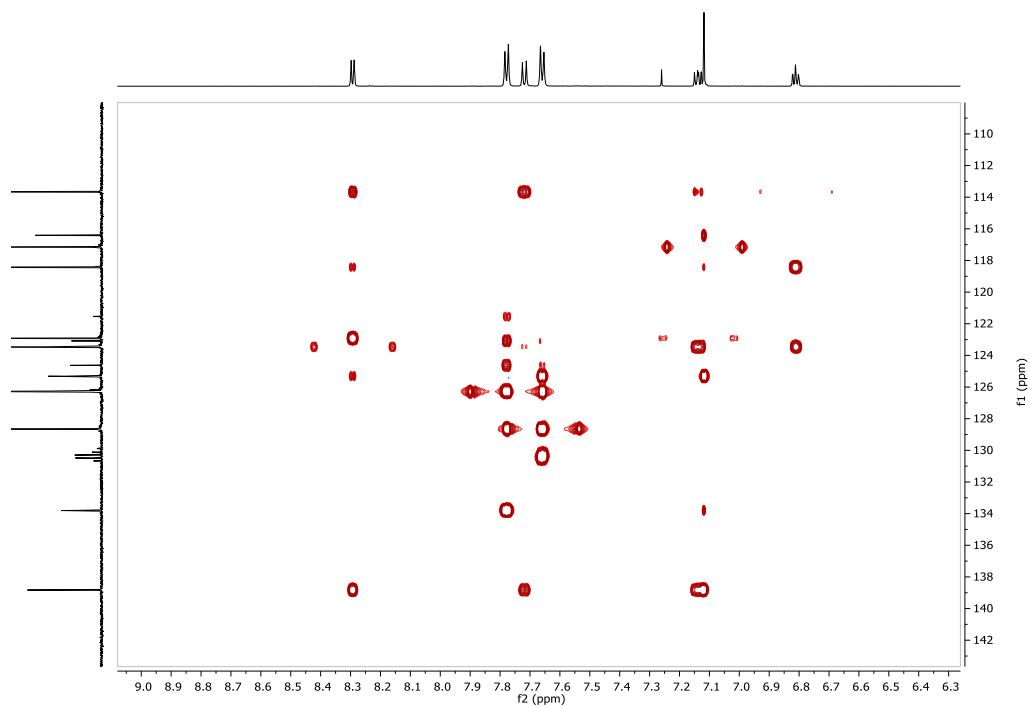
Compound **14b:** ^{1}H NMR (600 MHz, CDCl$_3$).
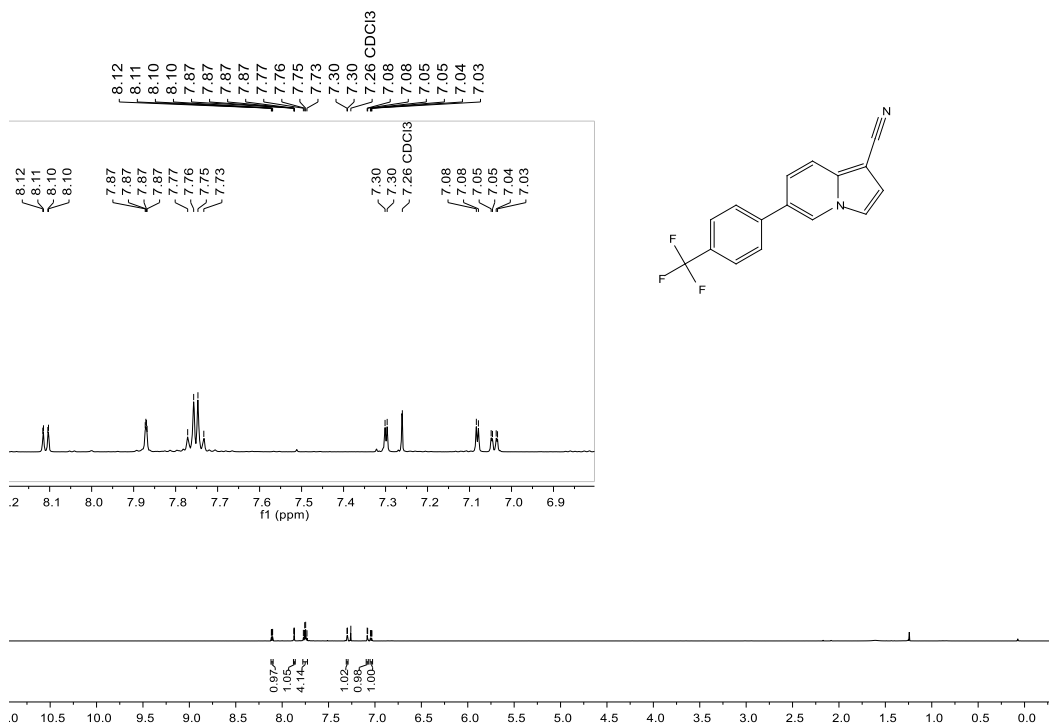
Compound **14b:** ^{13}C NMR (151 MHz, CDCl$_3$).
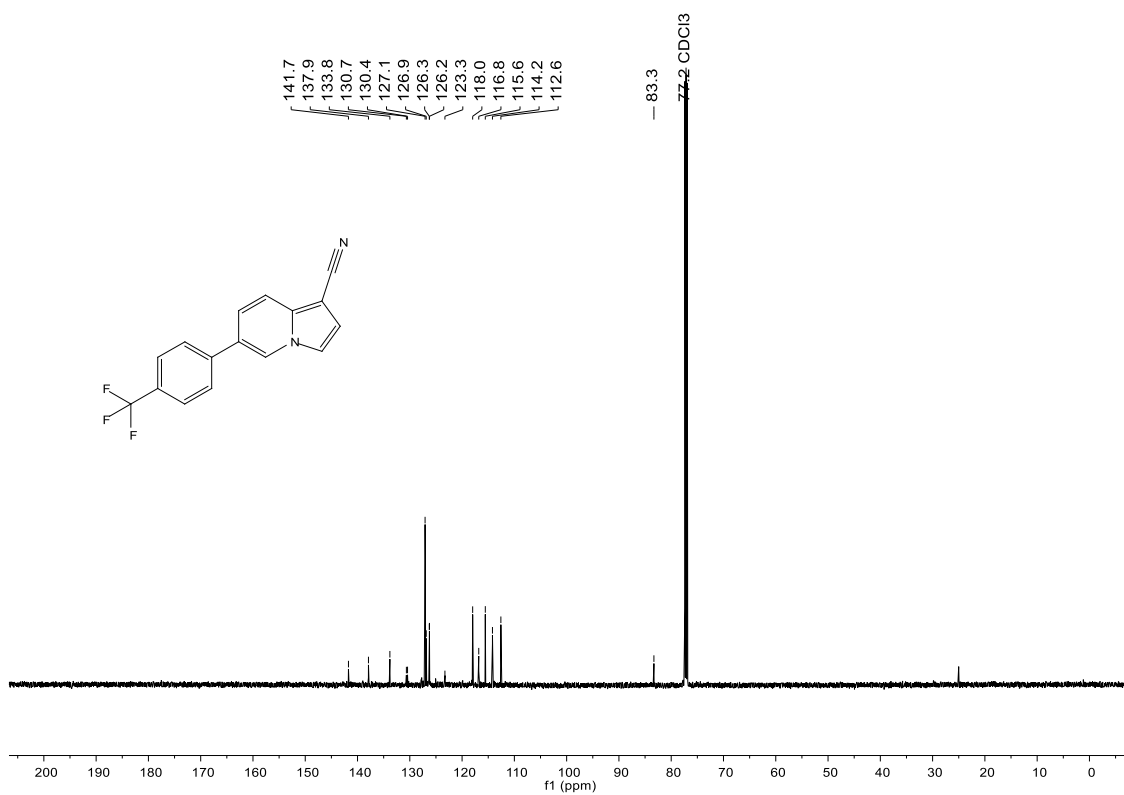
Compound **14b**: NOESY (^{1}H NMR 600 MHz, CDCl$_3$; ^{13}C NMR 151 MHz, CDCl$_3$).
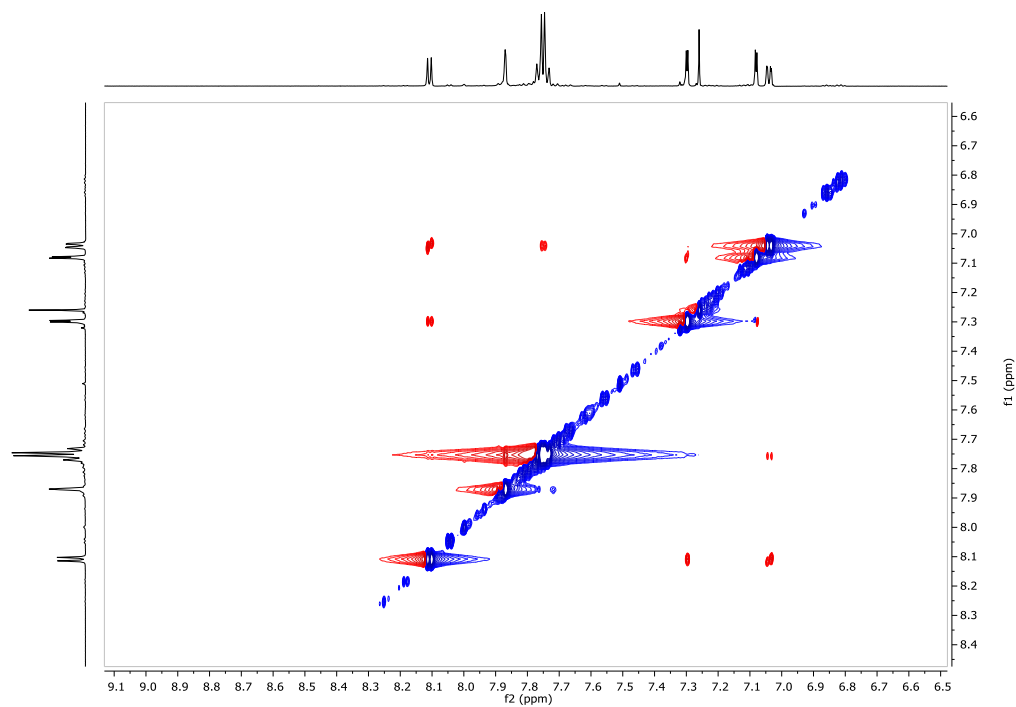
Compound **14b**: HSQC (^{1}H NMR 600 MHz, CDCl$_3$; ^{13}C NMR 151 MHz, CDCl$_3$).
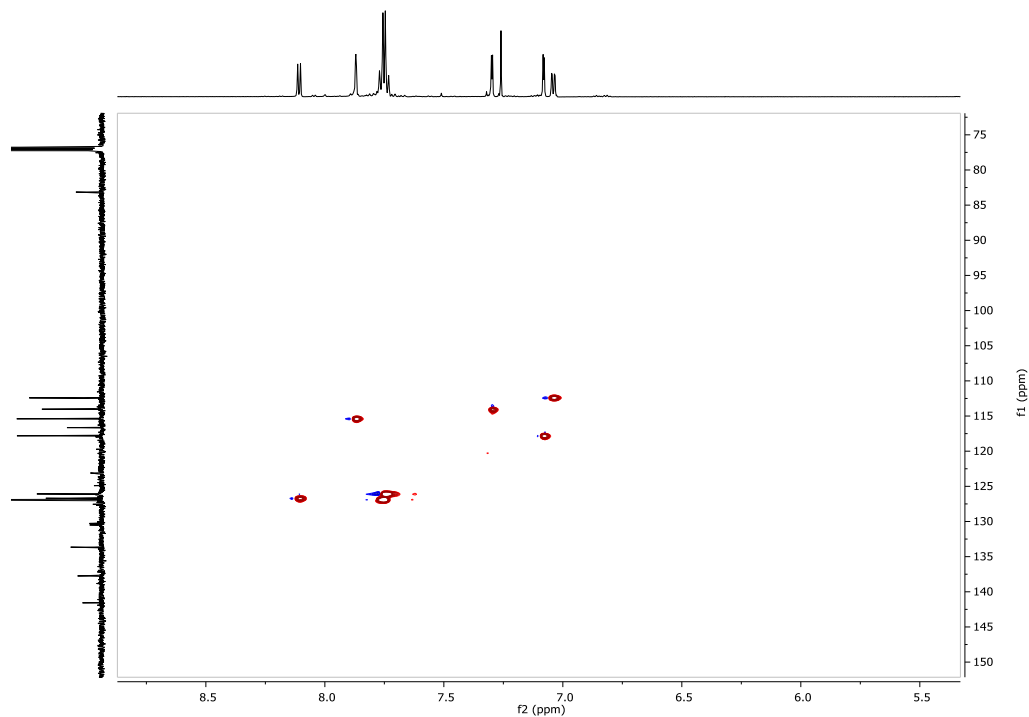
Compound **14b**: HMBC (^{1}H NMR 600 MHz, CDCl$_3$; ^{13}C NMR 151 MHz, CDCl$_3$).
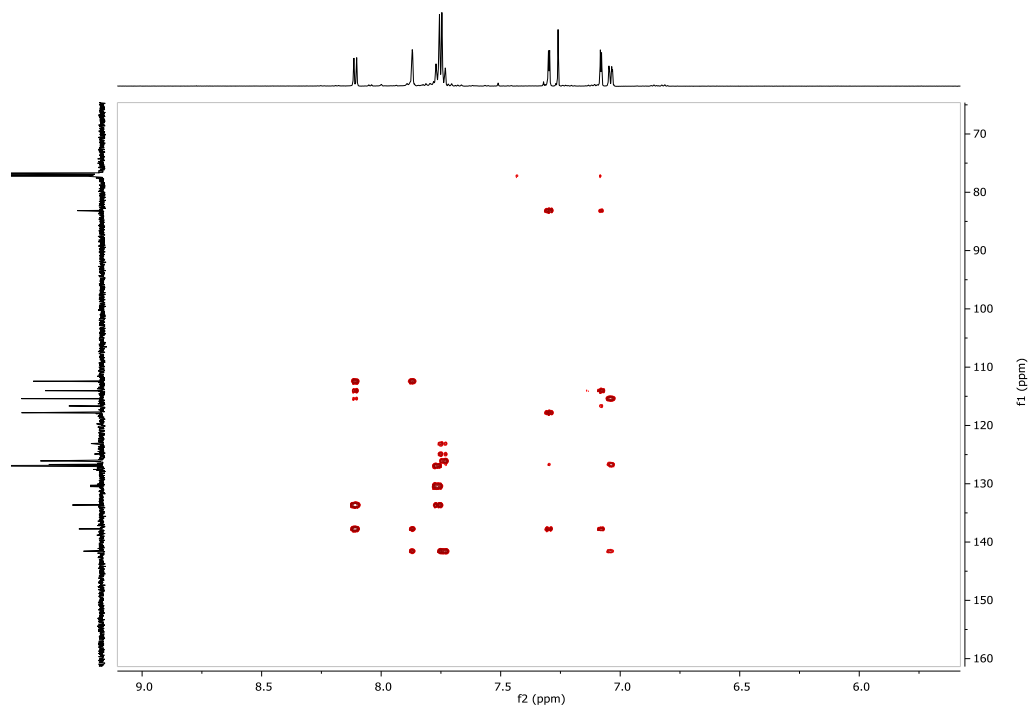
Compound **15**: ^{1}H NMR (600 MHz, CDCl$_3$)**.**
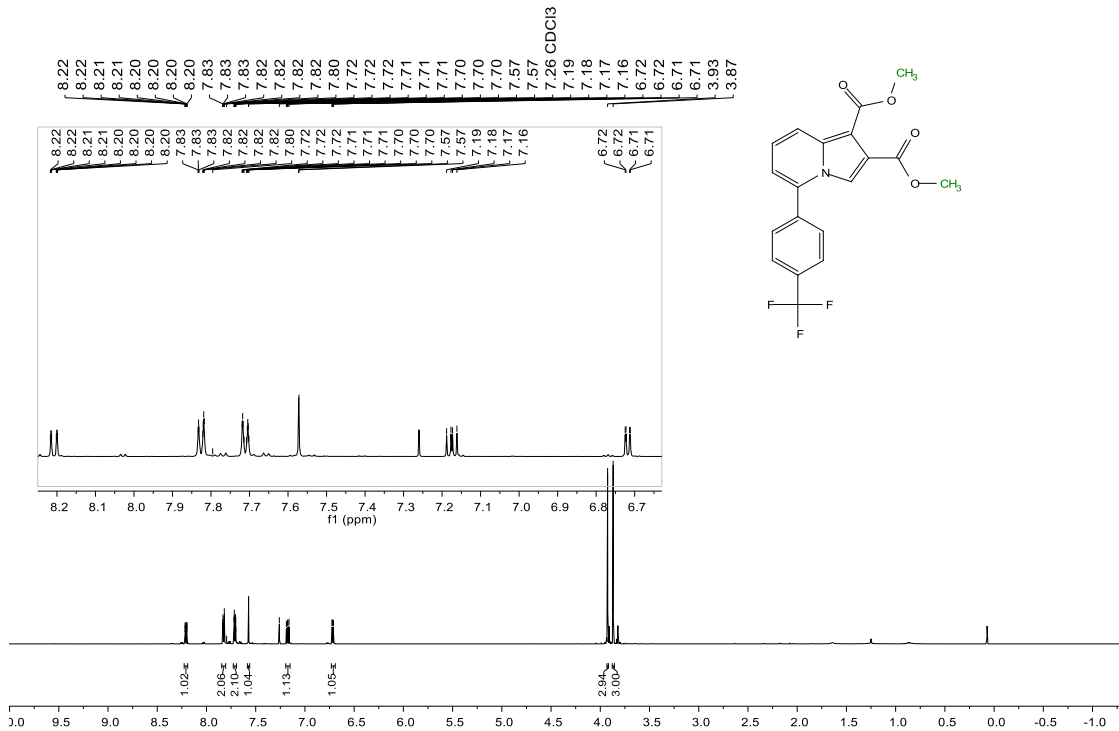
Compound **15**: ^{13}C NMR (151 MHz, CDCl$_3$).
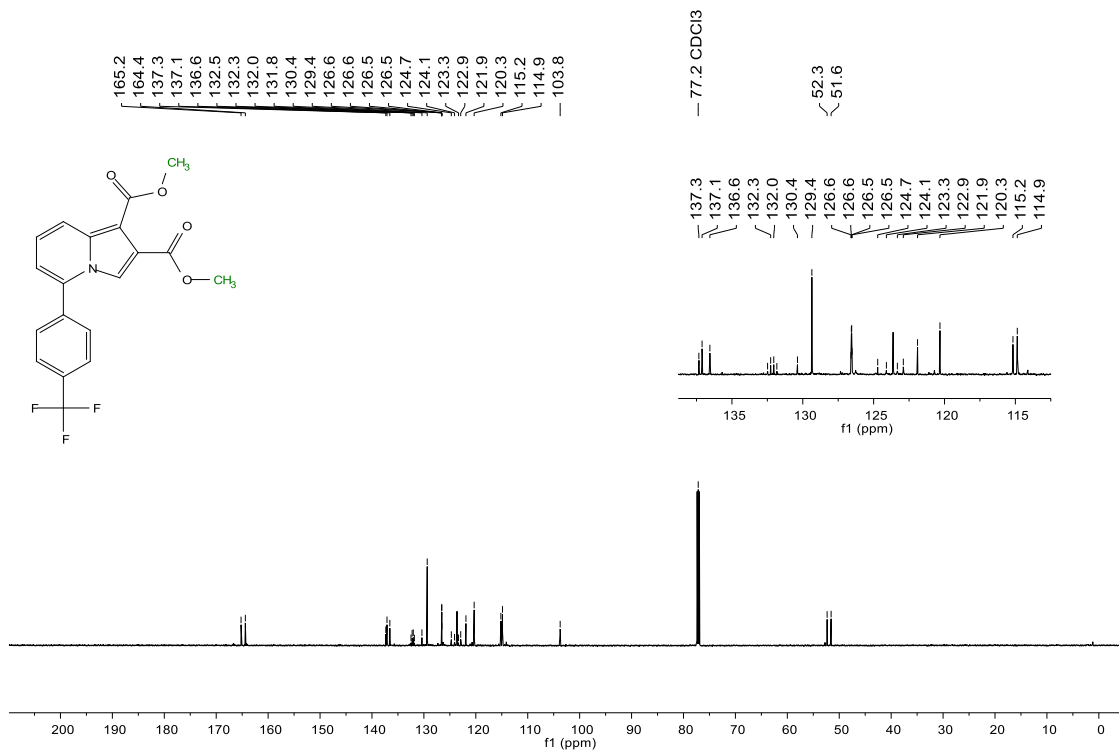
Compound **15**: NOESY (^{1}H NMR 600 MHz, CDCl$_3$; ^{13}C NMR 151 MHz, CDCl$_3$).
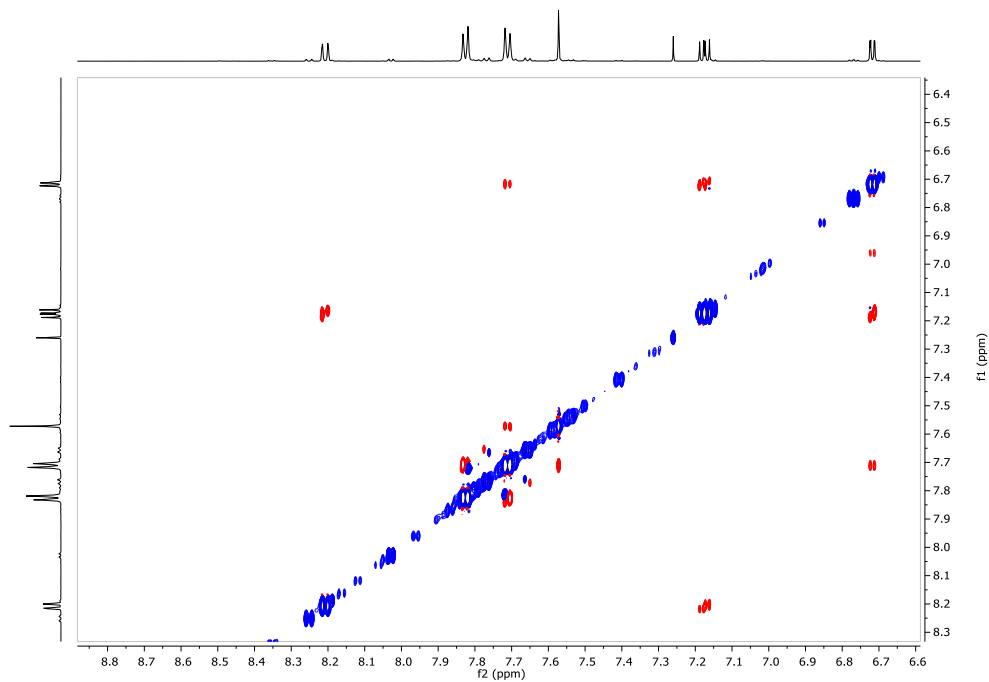
Compound **15**: HSQC (^{1}H NMR 600 MHz, CDCl$_3$; ^{13}C NMR 151 MHz, CDCl$_3$).
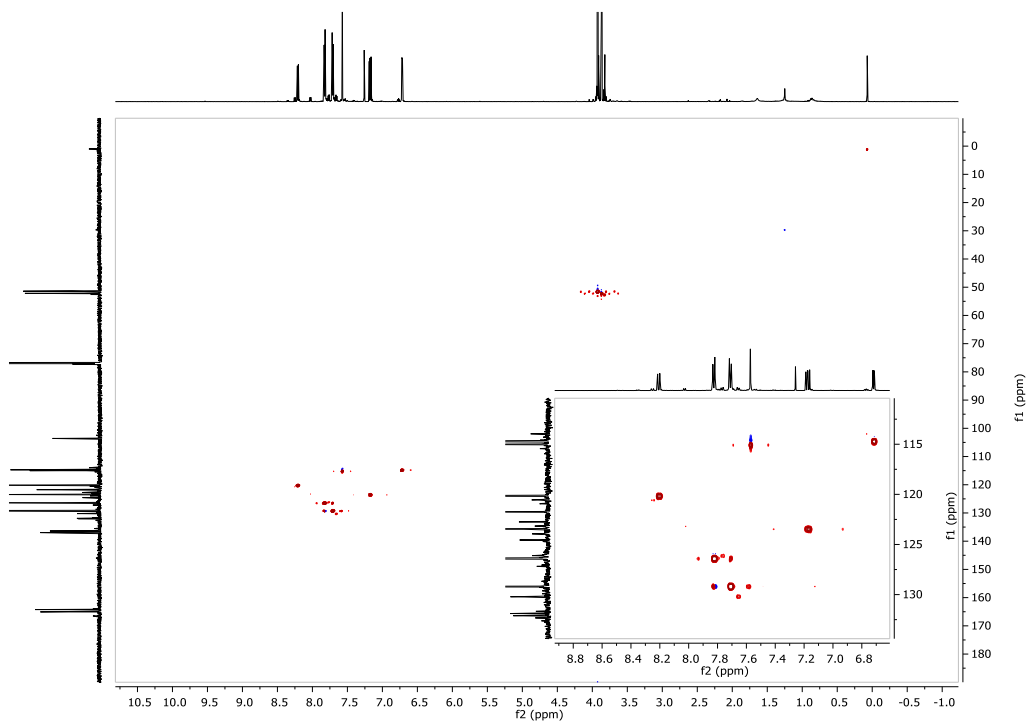
Compound **15**: HMBC (^{1}H NMR 600 MHz, CDCl$_3$; ^{13}C NMR 151 MHz, CDCl$_3$).
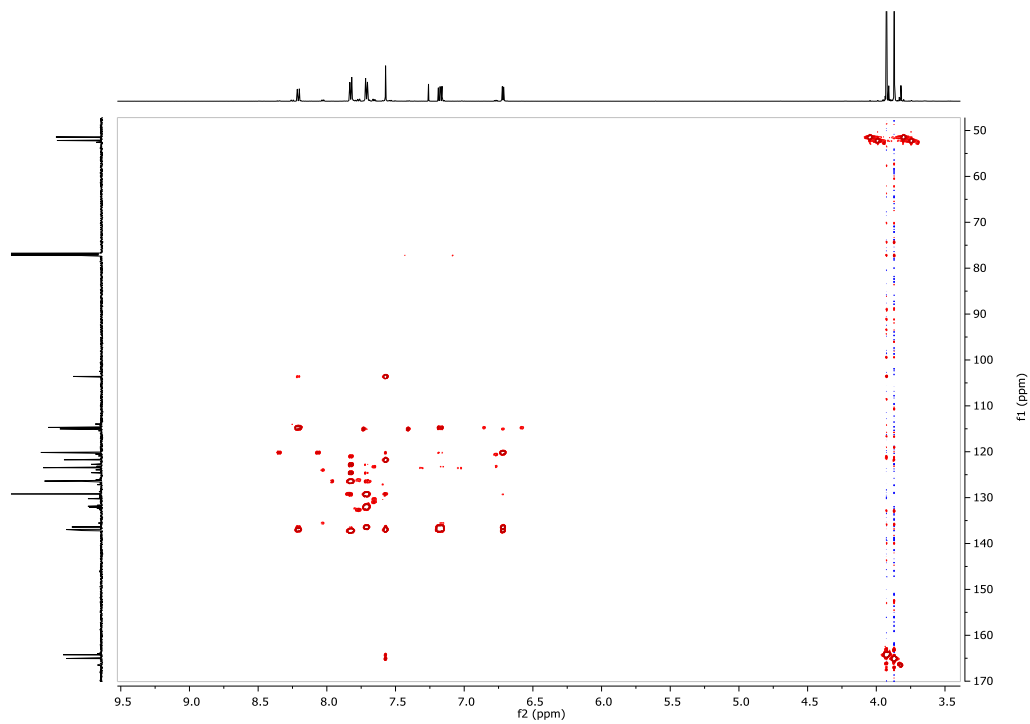
Compound **16:** ^{1}H NMR (600 MHz, CDCl$_3$)**.**
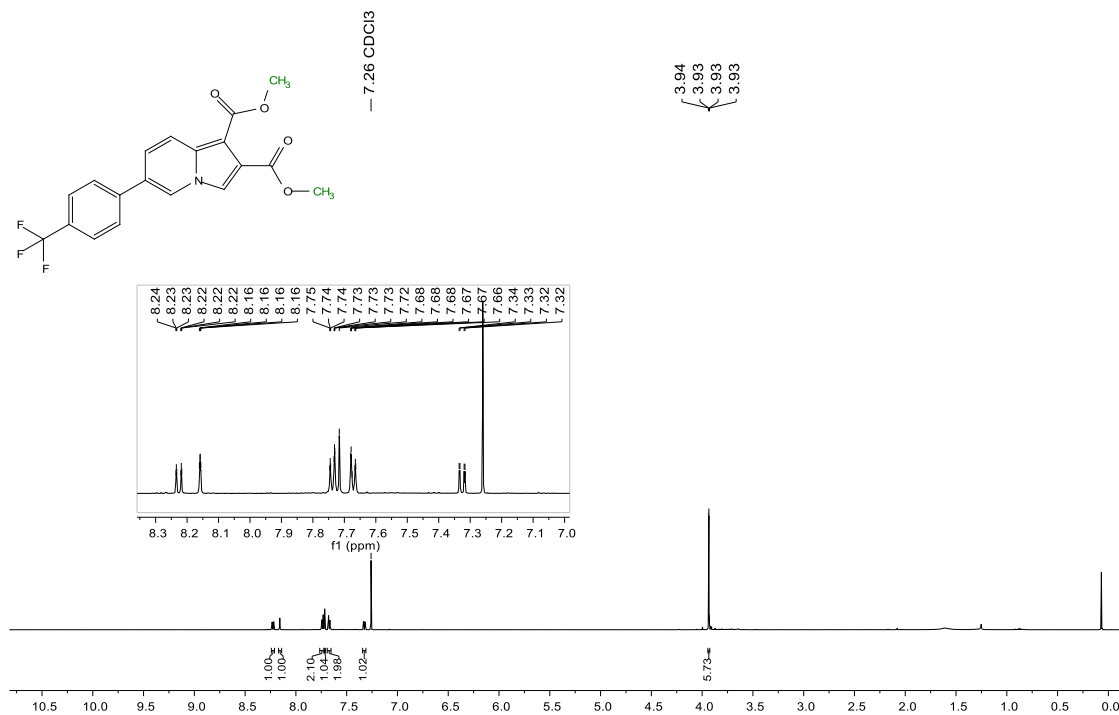
Compound **16:** ^{13}C NMR (151 MHz, CDCl$_3$).
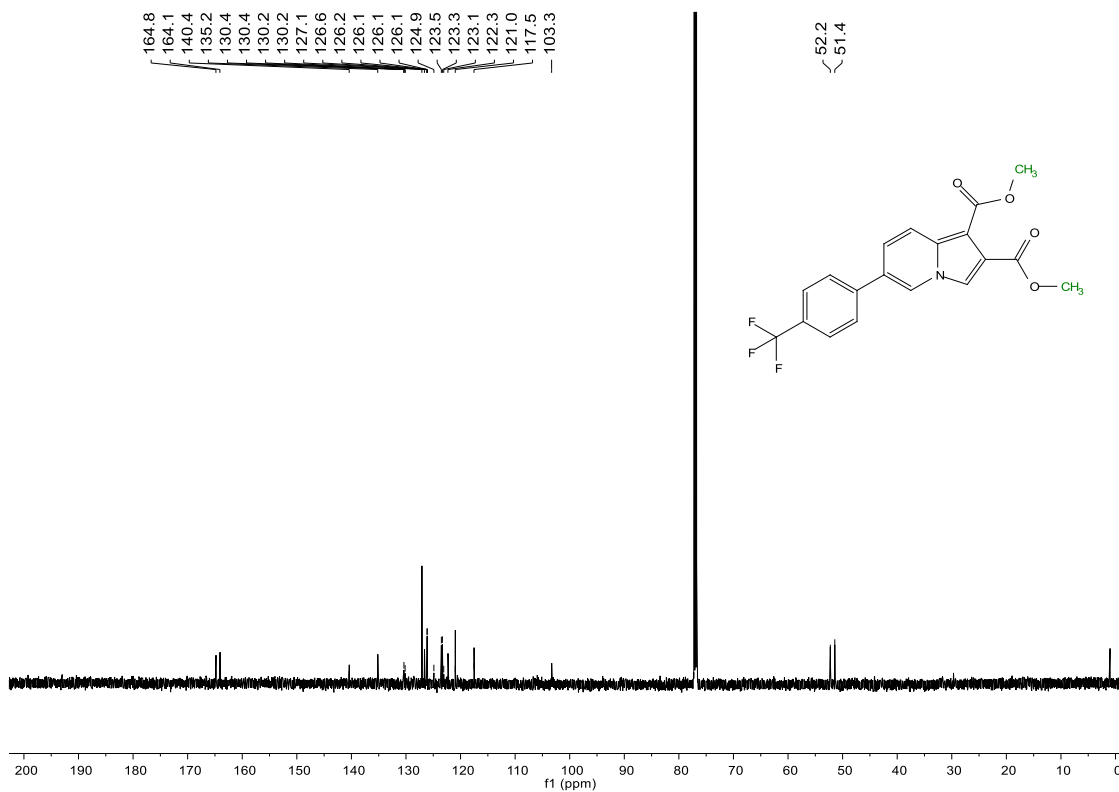
Compound **16**: NOESY (¹H NMR 600 MHz, CDCl₃; ¹³C NMR 151 MHz, CDCl₃).
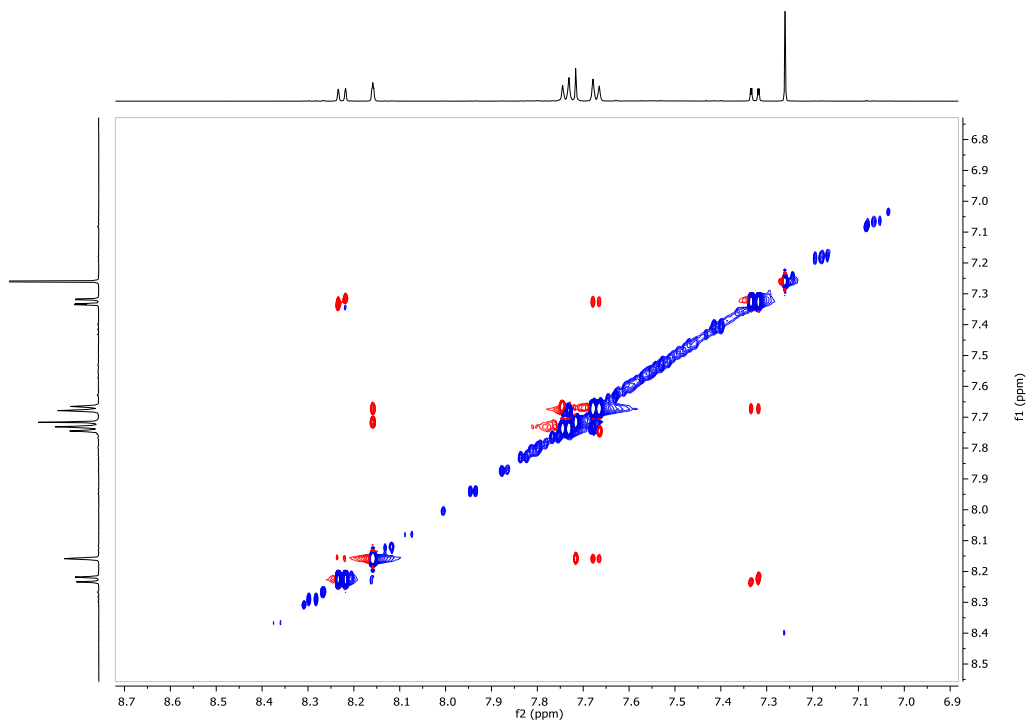
Compound **16**: HSQC (¹H NMR 600 MHz, CDCl₃ ; ¹³C NMR 151 MHz, CDCl₃).
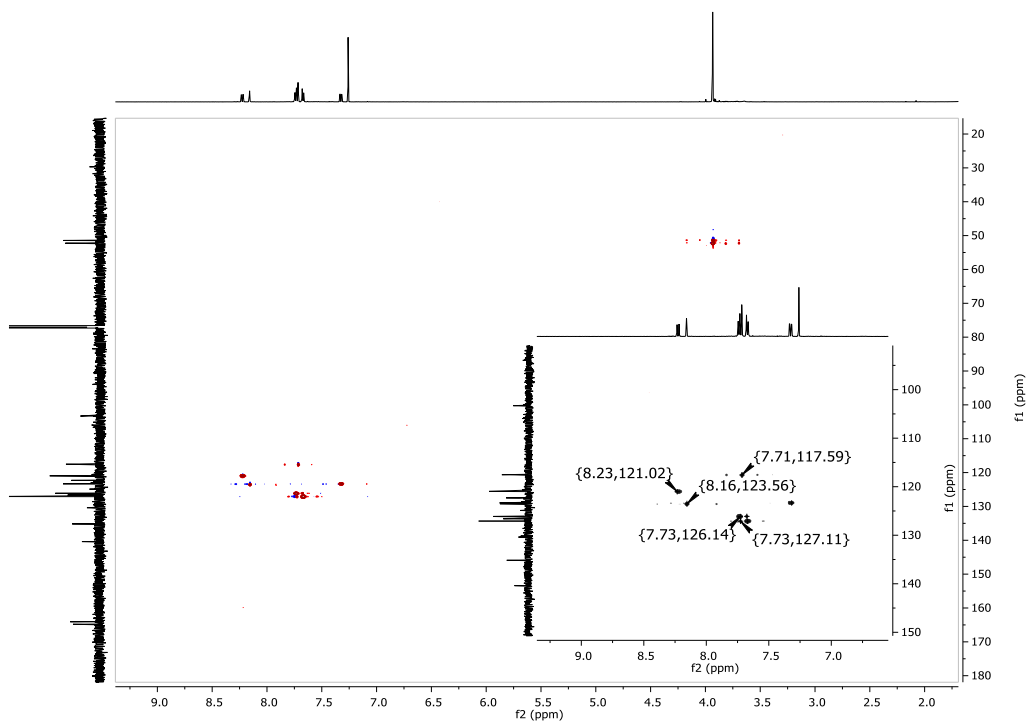
Compound **16**: HMBC (^{1}H NMR 600 MHz, CDCl$_3$; ^{13}C NMR 151 MHz, CDCl$_3$).
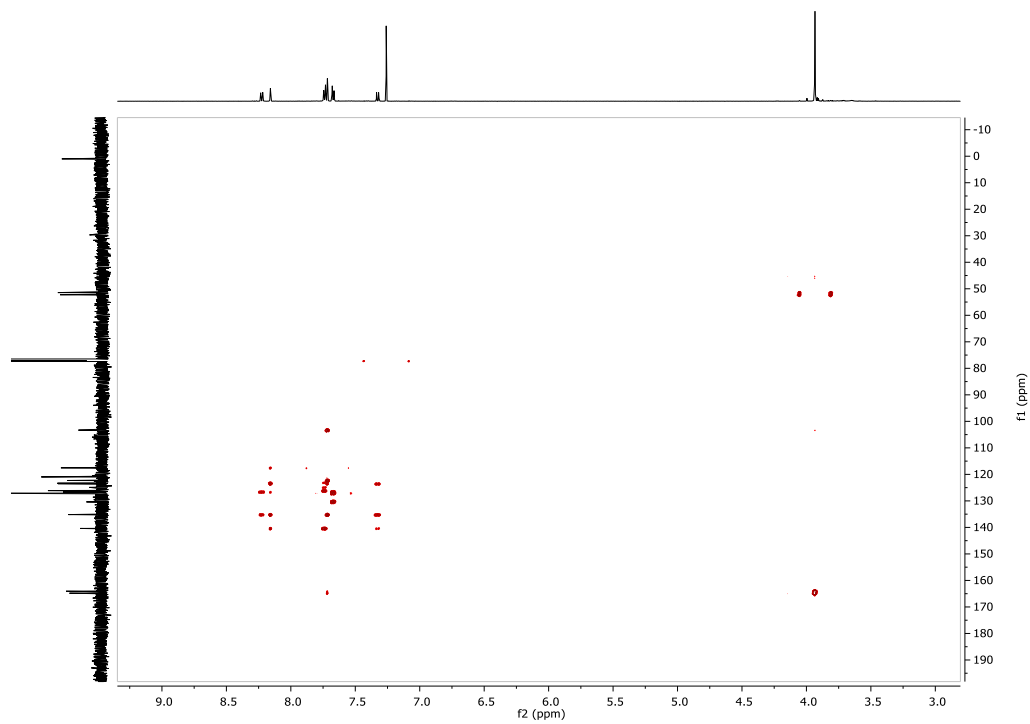
Compound **17:** ^{1}H NMR (600 MHz, CDCl$_3$)**.**
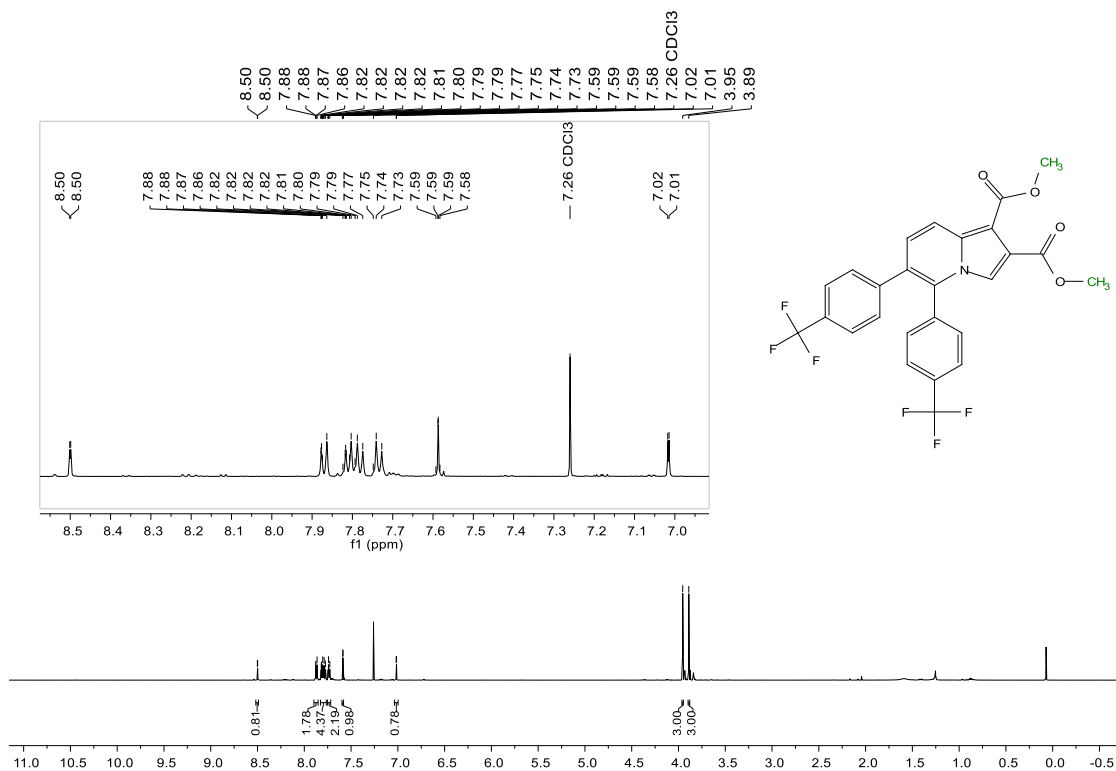
Compound **17:** ^{13}C NMR (151 MHz, CDCl$_3$)**.**
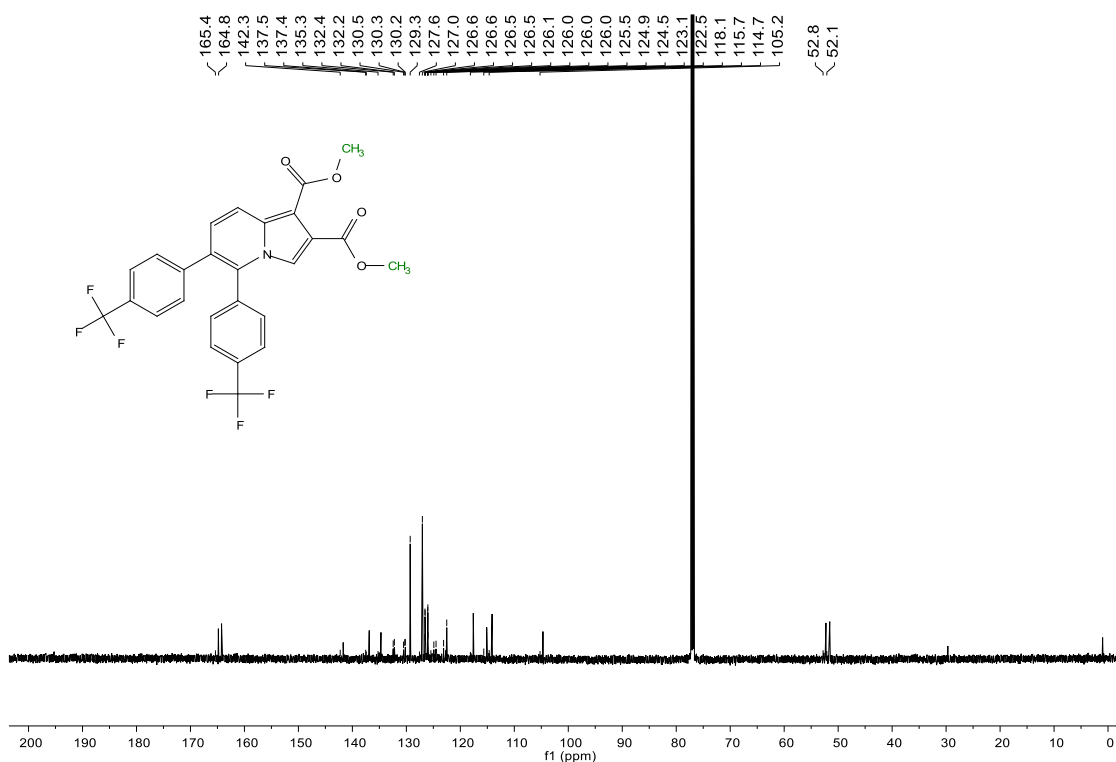
Compound **17**: NOESY (^{1}H NMR 600 MHz, CDCl$_3$; ^{13}C NMR 151 MHz, CDCl$_3$).
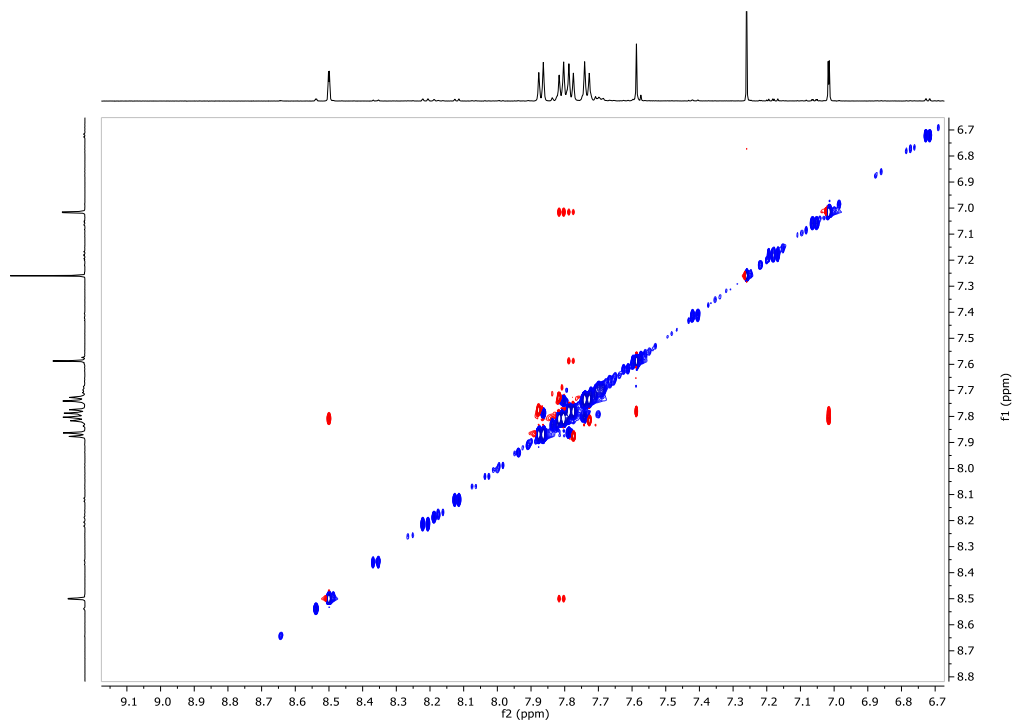
Compound **17**: HSQC (^{1}H NMR 600 MHz, CDCl$_3$; ^{13}C NMR 151 MHz, CDCl$_3$).
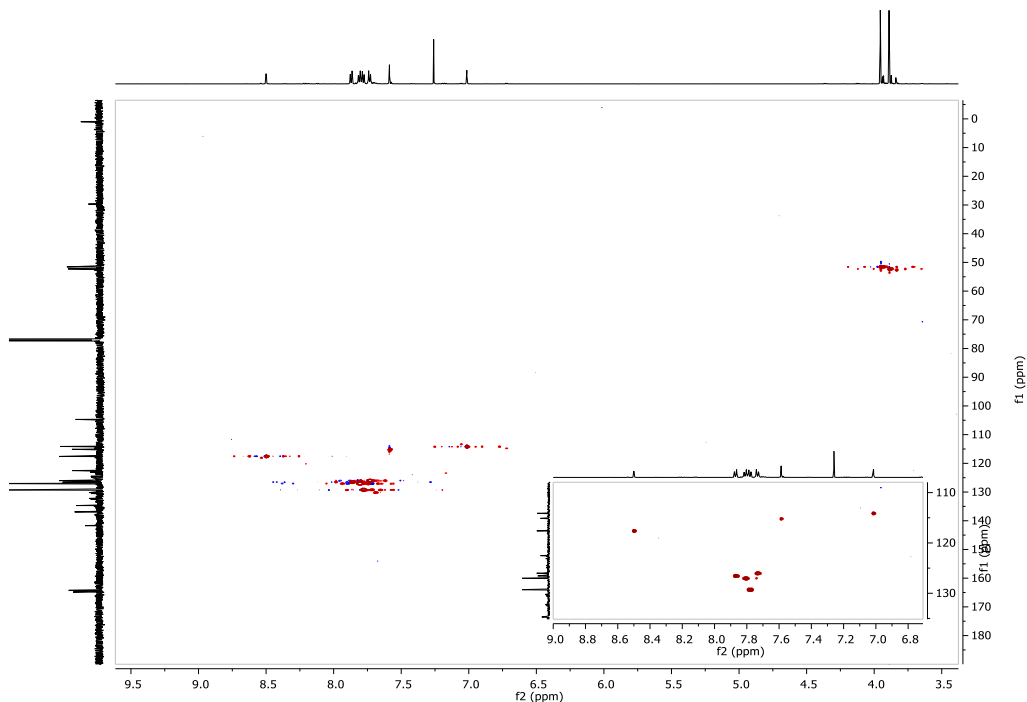
Compound **17**: HMBC (^{1}H NMR 600 MHz, CDCl$_3$; ^{13}C NMR 151 MHz, CDCl$_3$).